THE USE OF REMOTE SENSING AND GIS IN THE IDENTIFICATION AND VULNERABILITY DETECTION OF COASTAL EROSION AS A HAZARD IN FALSE BAY, SOUTH AFRICA

by

Kerry Lee Callaghan

Thesis presented in fulfilment of the requirements for the degree of Master of Science in the Faculty of Science at Stellenbosch University.

Supervisor: Dr JN Kemp

April 2014

DECLARATION

By submitting this thesis electronically, I declare that the entirety of the work contained therein is my own, original work, that I am the sole author thereof (save to the extent explicitly otherwise stated), that reproduction and publication thereof by Stellenbosch University will not infringe any third party rights and that I have not previously in its entirety or in part submitted it for obtaining any qualification.

April 2014

ABSTRACT

Coastal erosion is a worldwide hazard of which the consequences can only be mitigated via thorough and efficient monitoring of erosion and vulnerability to erosion. This study aimed to establish the accuracy, efficacy and efficiency of various remote sensing techniques for the detection and monitoring of coastal erosion and vulnerability occurring in False Bay, South Africa. There is a need to monitor the erosion in this area as well as to determine the most effective techniques for monitoring the erosion in False Bay and other similar environments in the future. This study provides an assessment of the usefulness of different data sources and techniques for change detection in the coastal environment.

The data sources used were Landsat TM/ETM+ imagery and aerial photographs. Image differencing, tasselled cap transformations, vegetation index differencing, Boolean change detection, and post-classification change detection were all performed on the Landsat imagery. The aerial photographs were assessed using the Digital Shoreline Analysis System (DSAS) add-on for ArcGIS which determines statistical differences in the shoreline position as digitised in vector format.

The results showed that while the resolution of the Landsat imagery was not sufficient to analyse erosion along the beach itself, the larger area covered by the satellite images enabled vulnerability indicators to be seen. Notably, the post-classification change detection indicated consistent increases in built-up areas, while sand dune, beach, and sand (not beach) all decreased. NDVI differencing showed consistent decreases in NDVI indicating decreasing plant health and density. The results of image differencing with both band 4 and the brightness band led to conclusions that vegetation health was decreasing while reflective surfaces such as bare sand and roads were increasing. All of these indicate an increased vulnerability to coastal erosion. The Boolean change detection method was found not to be useful in this case.

Aerial photographs were studied on four focus areas: Bayview Heights, Macassar Beach, Strand, and Pringle Bay. The results showed erosion at all four areas, with Strand experiencing only erosion (no accretion) at an average of 53 cm erosion per year. Erosion at Macassar Beach and Pringle Bay was also severe, with Bayview Heights being the least severe and showing a combination of erosion and accretion. The higher resolution available on the aerial photographs was vital to view changes on the beach itself.

In future studies requiring assessment of changes in the position or condition of the beach itself, aerial photographs or high resolution satellite data should be used. Studies of vulnerability extending over the entire coastal zone may make use of Landsat TM images.

Post-classification change detection provides powerful change direction information and can indicate the percentage of area change from one class to another. However, image differencing and vegetation index differencing are much faster to perform and can provide information about general trends in the changes occurring. Therefore post-classification change detection might be used in areas of high and rapid change while image differencing and vegetation index differencing can be useful to cover vast areas where little change is expected.

Keywords

Coastal erosion, vulnerability, Landsat TM, aerial photographs, change detection, post-classification change detection, image differencing, NDVI differencing, digital shoreline analysis system.

OPSOMMING

Kus-erosie is ‘n wêreldwye gevaar waarvan die gevolge slegs deur deeglike en doeltreffende monitering van erosie en kwesbaarheid vir erosie verminder kan word. Hierdie studie poog om die akkuraatheid, doeltreffendheid en effektiwiteit van verskillende afstandswaarneming tegnieke vas te stel vir die opsporing en monitering van kus-erosie en kwesbaarheid in Valsbaai, Suid Afrika. Daar is ‘n behoefte aan die monitering van erosie in hierdie area, sowel as om die mees doeltreffende tegnieke van die monitering hiervan in Valsbaai en ander soortgelyke omgewings in die toekoms te bepaal. Hierdie studie bied ‘n evaluering van die nut van verskillende data-bronne en tegnieke vir die opsporing van verandering in ‘n kusomgewing.

Die data-bronne wat gebruik is, is Landsat TM/ETM+ beelde asook lugfoto’s. Beeld differensievorming, “tasselled cap” transformasies, plantegroei indeks differensievorming, Boolse verandering en post-klassifikasie verandering is toegepas op die Landsat beelde. Die lugfotos is ge-evalueer deur die Digitale Kuslyn Analise Stelsel (Digital Shoreline Analysis System – DSAS). DSAS is ‘n bykomstige sagteware vir ArcGIS wat statistiese verskille in gedigitaliseerde kuslyn posisie bepaal.

Die resultate toon dat terwyl die resolusie van die Landsat beelde nie voldoende was om strand-erosie self te analiseer, die groter area wat deur die satellietbeelde gedek word toegelaat het om kwesbaarheid aanwysers te ontleed. Spesifiek die post-klassifikasie verandering het aangedui dat konsekwente toenames in beboude areas voorkom, terwyl afnames in sandduine, strand en sand-areas voorgekom het. NDVI differensievorming het konsekwente afnames in NDVI getoon, wat dui op afnames in die gesondheid en digtheid van plantegroei. Die resultate van die beeld differensievorming met beide Landsat Band 4 en die helderheid-band het gelei tot die gevolgtrekking dat die gesondheid van plantegroei afgeneem het, terwyl reflektiewe oppervlaktes soos oop sand en paaie aan die toeneem is. Al hierdie resultate dui op die verhoogde kwesbaarheid vir kus erosie. Die Boolse verandering metode is bevind om nie van nut te wees in hierdie geval nie.

Lugfoto’s van vier fokus-areas is bestudeer: Bayview Heights, Macassar Strand, Strand en Pringlebaai. Resultate van die DSAS analise het gevind dat oorwegend erosie by al vier areas plaasvind, met Strand die enigste area wat slegs erosie (geen aanwas) ervaar teen ‘n gemiddelde koers van 0.53 m per jaar. Erosie by Macassar Strand en Pringlebaai was ook ernstig, terwyl Bayview Heights die minste erosie ervaar het, met ‘n kombinasie van erosie en aanwas. Die hoër resolusie beskikbaar deur die lugfoto’s was noodsaaklik om veranderinge in strand areas waar te neem.

In toekomstige studies wat die assessering van verandering in die posisie of toestand van strande noodsaak behoort lugfotos of hoë-resolusie satellietbeeld data gebruik te word. Studies oor die kwesbaarheid van ‘n hele kusstreek kan wel gebruik maak van Landsat data. Post-klassifikasie verandering bied kragtige informasie oor die rigting van verandering en kan die persentasie van verandering van een klas na ‘n ander aandui. Beeld en NDVI differensievorming is egter veel vinniger om uit te voer en kan informasie rakende die algemene tendense in verandering lewer. Post-klassifikasie verandering kan dus gebruik word in gebiede van vinnige en beduidende verandering plaasvind, terwyl beeld en NDVI differensievorming nuttig kan wees om groot areas te dek waar min verandering verwag word.

Trefwoorde

Kus-erosie, kwesbaarheid, Landsat, lugfoto’s, verandering opsporing, post-klassifikasie verandering, beeld differensievorming, NDVI differensievorming, digitale kuslyn analise stelsel.

ACKNOWLEDGEMENTS

First and foremost, thanks go to Dr Jeanine Engelbrecht, who provided support throughout the completion of this project, and especially during the process of writing this thesis. Jeanine volunteered to read through all of my work and the feedback she provided was invaluable.

Secondly, I would like to thank by boyfriend Chris for providing support for me through two years of working on this project. He listened to all of the issues I had during processing stages and was supportive and encouraging throughout tedious hours of reading and writing up.

Finally, thanks go to the Department of Science and Technology and the Council for Geoscience for providing the funding needed for this research.

CONTENTS

LIST OF TABLES

LIST OF FIGURES

LIST OF APPENDICES

LIST OF ACRONYMS AND ABBREVIATIONS

ARVI: Atmospherically resistant vegetation index

ATCOR: Atmospheric Correction

AVHRR: Advanced Very High Resolution Radiometer

CAM: Coastal Area Management

cm: centimetres

DEM: Digital Elevation Model

DN: Digital Number

DSAS: Digital Shoreline Analysis System

ECI: Confidence interval of end point rate

ENVI: Environment for Visualising Images

EPR: End point rate

EROS: Earth Resources Observation and Science Center

ESP: Estimation of Scale Parameter

ETM+: Enhanced Thematic Mapper Plus

GEOBIA: Geographic object-based image analysis

GIS: Geographic Information System

km: kilometres

LANDSAT: Land Remote Sensing Satellite System

LCI: Confidence interval of linear regression rate

LMS: Least median of squares

LRR: Linear regression rate

LR2: R^2 of linear regression rate

LSE: Standard error of linear regression rate

m: metres

MATLAB: Matrix Laboratory

mm: millimetres

MNDVI: Modified normalised difference vegetation index

MSS: Multispectral Scanner

NDVI: Normalised difference vegetation index

NGI: National Geo-spatial Information

NN: Neural Networks

NOAA: National Oceanic and Atmospheric Administration

NSM: Net shoreline movement

RGB: Red, green and blue colour composite

ROI: Region of Interest

SANSA: South African National Space Agency

SAR: Synthetic Aperture Radar

SARVI: Soil and atmospherically resistant vegetation index

SAVI: Soil-adjusted vegetation index

SCE: Shoreline change envelope

SUDEM: Stellenbosch University Digital Elevation Model

SVM: Support Vector Machines

TM: Thematic Mapper

USGS: United States Geological Survey

WCI: Confidence interval of weighted linear regression rate

WLR: Weighted linear regression rate

WR2: R^2 of weighted linear regression rate

WSE: Standard error of weighted linear regression rate

1. INTRODUCTION

1.1. Background to the study

Coastal erosion is a major hazard in many parts of the world. Coastal erosion poses a risk since it may result in damage to infrastructure as well as limiting the land area which may be used for urban or industrial purposes. Various forces such as wind, waves and currents as well as catastrophic events such as storms cause constant reshaping of the coastline and may contribute to the occurrence of coastal erosion (Unterner et al., 2011). Locally, these forces are influenced by many factors, including tidal range, wave height, coastal slope, geomorphology, and geology (Unterner et al., 2011).

Throughout the world, shoreline areas are associated with an increasing concentration of human population and construction (Small and Nicholls, 2003). In South Africa, as much as 40% of the population lives within 100 km of the coast (Department of Environmental Affairs and Tourism and Council for Scientific and Industrial Research, 2005). The global trend towards coastline degradation is often associated with urbanisation and anthropogenic effects (Unterner et al., 2011). Anthropogenic effects may exacerbate natural processes which would increase the vulnerability of the coastal zone (Small and Nicholls, 2003). The increasing population and commercial activities in the coastal zone result in increased development-related impacts, including increased pollution in the coastal zone, habitat loss, coastal erosion, and vulnerability to coastal hazards (Huang and Fu, 2002). Since vulnerability refers to the degree of loss or damage arising from a hazardous event (Mahendra et al., 2011), the increasing coastal population also increases human vulnerability and susceptibility to experiencing the effects of coastal erosion.

The main risk associated with coastal erosion is damage to infrastructure. Roads and other structures which have been built in vulnerable areas, close to the beach or even on the beach, are particularly vulnerable to damage. Since South Africa's coastline stretches some 3000 km (Unterner et al., 2011), coastal erosion is a particularly relevant hazard. In some cases, attempts to rectify or alleviate the situation only exacerbate the problem due to various factors being overlooked. For example, construction of a seawall may increase beach erosion on adjacent beaches, resulting in further seawalls being built to mitigate the effects of the first one (Hayashi, 1987). While properly constructed seawalls have little impact on cross-shore sediment processes, in cases where seawalls interrupt longshore processes, they are likely to damage neighbouring beaches. Jetties and long groins are also known to cause erosion on downdrift shores by blocking longshore sediment transport (Kraus, 1988). Furthermore a lack of understanding of the complexity of the parameters

leading to erosion and the areas that are the most vulnerable to future erosion adds to the inability to mitigate the problem.

Sea level rise may also have the same effects as erosion, as well as causing an increase in erosion rates since a rise in sea level reduces coastal land area. Over the last 100 years, global sea level rose by 1.0-2.5 mm per year, and projections show that it will continue to rise (Klein and Nicholls, 1999). However, when assessing the impacts of sea level rise, it is the local change in relative sea level that matters, rather than the global average. This is the level of the sea relative to the land within the specific study area (Klein and Nicholls, 1999).

All of these factors together create a need to monitor coastal erosion. Only through the monitoring and assessment of this hazard can preparations be made to protect infrastructure as well as to protect the coastal environment itself.

1.2. **Research Problem**

Over the past several years, there has been an increase in the use of remote sensing for the study of the phenomena underlying natural hazards, including coastal erosion. The use of remotely sensed data can lead to conclusions which may aid in risk mitigation and disaster response planning (Tralli et al., 2005). There is a need for the performance of various change detection techniques in different environments to be evaluated quantitatively. Without such evaluations, future researchers may not be able to achieve optimal results while monitoring changes in a specific environment due to a lack of knowledge about tested change detection procedures (Singh, 1989). Because a variety of complex factors are at play at any specific study area, different authors often arrive at different conclusions about which change detection techniques are most effective, and in practice it is challenging to select a suitable algorithm for a specific change detection project (Lu et al., 2004).

Past studies of coastal vulnerability in South Africa (e.g. Palmer et al., 2011; Unterner et al., 2011) have utilised vulnerability parameters such as tidal range, wave height, geology, beach width, and more as measured on Google Earth images and ortho-photographs in order to determine a vulnerability index for the coastline. These studies did not make use of change detection in order to determine where erosion was actually occurring, but rather assessed factors which may objectively make the region more vulnerable to erosion at a single time. There is therefore a need to assess the erosion which is occurring along the South African coastline via change detection. By testing various data sources and techniques along the coast within False Bay, the most appropriate techniques for future assessments of the remainder of the South African coastline can be determined.

1.3. **Project aims and Goals**

This project intends to establish the accuracy, efficacy and efficiency of various remote sensing techniques for the detection and monitoring of coastal erosion occurring in the False Bay region. The main focus of the project is the analysis of Landsat TM and ETM+ imagery using different processing and analysis techniques to establish which are the most effective for detection, monitoring, and assessment of coastal erosion occurring in False Bay, South Africa. Aerial photographs were utilised on smaller focus areas and the two data sources are also compared. Thus, the project aims to assess the usefulness of various remote sensing techniques as a medium to obtain information about coastal erosion. This project further aims to assess coastal erosion over a period of years in order to determine longer term change as opposed to just seasonal changes to the coastline. The satellite images cover a period of 26 years while the aerial photographs cover a period of 66 years. Use of remotely sensed data will allow for the assessment of coastal erosion over a period of several years, enabling the creation of an historical assessment of the erosion that has occurred. The resulting information can be used to assess which regions are the most vulnerable to future coastal erosion.

1.3.1. Research aim

The aim of this study is to determine which of several remote sensing techniques and data sources may most effectively help us to detect, monitor and assess coastal erosion in False Bay, South Africa; as well as to detect coastal erosion and vulnerability changes in False Bay.

1.3.2. Research objectives

The research objectives for the study were as follows:

- Classify Landsat 5 TM and Landsat 7 ETM+ images using an object-based classification.
- Perform an accuracy assessment of the classification.
- Use various change detection techniques on the satellite images over the entire time period available (1985 to 2011), utilising both the classified images (post-classification change detection) and unclassified images (image differencing; NDVI differencing; Boolean change detection).

- Select focus regions for further study using the Digital Shoreline Analysis System on aerial photographs.
- Assess the results to see if areas of increased vulnerability can be detected and how this corresponds with results on aerial photograph study as well as field observations.
- Evaluate which of the techniques allowed the most accurate and efficient observation of coastal erosion.

1.4. Description of the study area

The study area is the coastline of False Bay (Figure 1), located at the south-western tip of South Africa, in the Western Cape Province. The green zones shown indicate focus areas which were studied in more detail on aerial photographs, discussed in Section 3.7. The coastline of the study areais about 130 km long, stretching from Cape Point in the west, along the coastline, to Cape Hangklip in the east. It is southern Africa's largest true bay (Clark et al., 1996). The study area extends a few kilometres inland since coastal vulnerability extends across the entire coastal zone, not just beach or cliff areas. The study region extends around 8 to 12 kilometres from the shore. It is challenging to define exactly which areas constitute the 'coastal zone'. However, Small and Nicholls (2003) defined those regions which are within 100 horizontal kilometres of the coastline and 100 vertical metres of sea level to be the 'near-coastal zone'. This study does not extend that far inland as the focus is on the immediate coastal zone rather than the near-coastal zone. However, the study does extend several kilometres from the shoreline since it is recognised that changes near to the shore can have a direct impact on shoreline processes including coastal erosion and vulnerability to erosion. The northern part of the study area is relatively flat, comprising the Cape Flats, while to the east and the west it is more mountainous, featuring the Hottentots Holland mountains and the Peninsula mountains, respectively (Harrison, 1998).

The climate in False Bay is a Mediterranean-type climate, with cold, wet winters and hot, dry summers (Clark et al., 1996). Average annual rainfall is 500-1000 mm, most of which falls during the winter months (Harrison, 1998).

False Bay falls within the influence of the south-eastern Atlantic Ocean (Harrison, 1998). In the mouth of the bay, the water depth reaches around 80 m, sloping steeply upwards towards the rockier western and eastern shores and gently upwards towards the northern sandy beaches (Clark et al., 1996). The tidal ranges in the study region are relatively modest, with a mean spring range of 1.48 m (Clark et al., 1996). The bay also experiences localised wind-induced upwelling, particularly off Cape Hangklip, and to a lesser degree off Gordon's Bay (Harrison, 1998).

A variety of beach types can be found in this region, from cliffs along the Cape Peninsula to sandy beaches along the Cape Flats, providing a large variation in the susceptibility to erosion. Much of the region is densely populated – especially the northern and north-eastern parts of the study area. The region is also a popular tourist zone, meaning that anthropogenic impacts are also likely to play an important role in the vulnerability of the coastline.

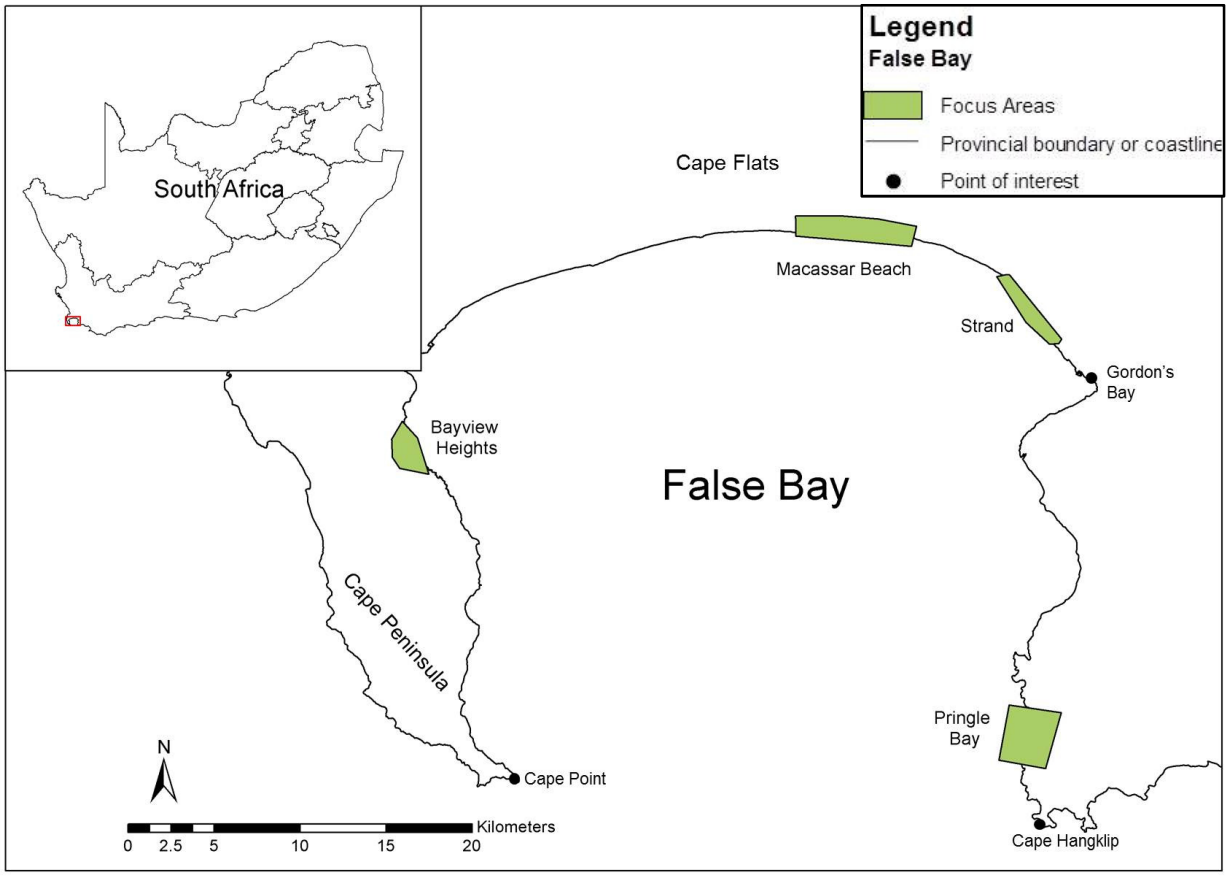

Figure 1: The study area – False Bay, South Africa.

This document is structured in six chapters. This, the first chapter, provided an outline of the research problem and the steps taken during the research process along with an introduction to the study area. In Chapter 2, a review of past literature regarding remote sensing in coastal erosion is given. Chapter 3 presents the methods used during this study along with further technical details of each step in the methodology. The results obtained are presented in Chapter 4. Chapter 5 gives a discussion of these results and Chapter 6 provides a summary and conclusions.

2. LITERATURE REVIEW AND THEORY

While little work has been done regarding coastal erosion in False Bay, many studies have been performed addressing coastal erosion in different areas, and assessing various remote sensing techniques. A summary of some of the pertinent literature is supplied in this chapter.

2.1. Coastal erosion as a hazard

Coastal erosion is a hazard which causes damage to both human infrastructure and natural ecosystems throughout the world. An assessment of the areas that are most vulnerable to coastal erosion can provide forewarning and allow measures to be taken to avoid damages. The factors influencing coastal erosion include both natural processes, such as waves, tides, currents, and sea level change (Phillips, 2008), and human influences, such as industrialisation near the coast, which often aggravates the situation (Siripong, 2010; Smith and Abdel-Kader, 1988). These inter-related factors, both natural and anthropogenic, are all potential causes of coastal change (Thampanya et al., 2006).

Based on various factors, each specific study site will be either more or less vulnerable to the hazard of coastal erosion. A system which is highly vulnerable will retain the erosion effects for a long time, while a system with a low vulnerability will soon return to a natural balance (Rust and Illenberger, 1996). Areas adjacent to shorelines are associated with large and growing concentrations of human population, settlements, and socioeconomic activities (Small and Nicholls, 2003). The implication of this is a high exposure of settlements and man-made structures to coastal hazards, as well as significant anthropogenic effects on natural processes in these regions (Small and Nicholls, 2003). While a coastal location does provide many benefits, people in these regions also risk exposure to hazards including saltwater intrusion, subsidence, tsunamis, floods, and, of course, coastal erosion (Small and Nicholls, 2003).

Coastal lands may also be lost through sea level rise. The global sea level has risen at a rate of approximately 1.8 ± 0.3 mm per year from 1950 to 2000, although the rate varies widely by location (Church et al., 2004 and 2006, in Ford, 2013).

Various previous studies have addressed coastal erosion and its associated issues at international locations (e.g. Phillips, 2008; Smith and Abdel-Kader, 1988;Thampanya et al., 2006). Such studies have focused on various different aspects of the issue. These include the creation of coastal vulnerability indices based on predefined criteria (e.g. Boruff et al., 2005; Palmer et al., 2011; Unterner et al., 2011; Zhang et al., 2001;); studies investigating

various erosion criteria using remotely sensed imagery (e.g. Huang and Fu, 2002; Siripong, 2010); statistical analysis of rates of change and other factors (e.g. Thampanya et al., 2006); in situ studies of the causes and effects of erosion; and creation of numerical models for erosion (e.g. Hanson, 1988).

Some studies have also had a specific focus on the South African coastline. A study by Palmer et al. (2011) assessed the Kwazulu-Natal coastline to determine the vulnerability to erosion. They focussed on the creation of a coastal vulnerability index by dividing the region into 50 m by 50 m cells, and rating each cell in terms of its degree of vulnerability, based on a number of factors such as beach width. A similar study was performed by Unterner et al. (2011), who extended the use of a coastal vulnerability index to the whole South African coastline. Their findings show a considerable variation in the degree of erosion vulnerability within False Bay.

2.2. **Remote sensing for the assessment of coastal erosion**

Remote sensing plays an important role in the study of coastal erosion by allowing the identification of regions which may be at risk. Remote sensing is an attractive data source for assessment of land cover conditions and changes in these conditions over time. This is due to the fact that it provides a map-like, spatially continuous, and consistent representation of the study area, which is available at a range of spatial scales and dates (Foody, 2002). The use of remotely sensed data allows for the investigation of large areas, providing an efficient way to extract information and making it possible to reach restricted areas (Livingstone et al., 1999; Smith and Abdel-Kader, 1988). In addition, remote sensing can be especially useful for long-term monitoring of change, since it provides an historical archive of data, allowing studies initiated in the present day to assess changes which have occurred years ago. Data in the same region can be collected over long periods of time, enabling a long study period to be selected (Livingstone et al., 1999). The use of digital imagery provides accurate data which is standardised over large areas and provides a variety of potential spatial and spectral resolutions (Althausen et al., 2003).

Many past studies have utilised remote sensing for the assessment of coastal erosion and vulnerability. Thampanya et al. (2006) combined the use of Landsat TM satellite data and aerial photographs to study coastal erosion in Southern Thailand over a period of 30 years. They found that their study site was experiencing overall net coastal erosion and that the presence of mangroves was associated with the remaining areas of accretion. Non-vegetated areas experienced considerable erosion.

Ford (2013) studied shoreline erosion on the Wotje Atoll in the Republic of Marshall Islands and utilised aerial photographs and high resolution satellite imagery to digitise the edge of the vegetation as a proxy for the shoreline position. The study made use of the DSAS (digital shoreline analysis system) software (Thieler et al., 2009) to calculate statistics, and found that while a combination of accretion and erosion occurred, their study area experienced net accretion. They also found that there may have been a more recent shift towards erosion.

A study by Althausen et al. (2003) used Landsat TM and MSS images to study a region in Abu Dhabi. They used a binary mask to separate 'upland' (algal mats and surface features inland) and 'bathymetric' (shallow water) regions. They utilised iterative statistical algorithms with band ratios, vegetation indices, and principal components analysis to analyse the data. Principal components analysis was used for the bathymetric region while band ratioing was used to help classify the upland region. While they found this method to be useful to assist in classification, they did not perform any accuracy assessment and instead assumed that the accuracy of the classification should be high since the findings appeared similar to other studies in the Arabian Gulf region.

A study by Kwarteng and Al-Ajmi (1996) used Landsat TM imagery to study vegetation change in Kuwait and made use of NDVI with an automatic change detection procedure to map vegetation differences between two dates. They used the NDVI with a selective principal components analysis technique. They found that the NDVI increased over their 5-year study period, indicating increasing biomass during that period. They found that the use of Landsat TM data was effective in mapping vegetation changes in arid environments.

A Chinese program using remote sensing for coastal area management (CAM) was implemented as early as the 1970s (Huang and Fu, 2002). It makes use of various satellites, including Landsat MSS and TM, as well as ERS-1/2, JERS-1, SAR, NOAA AVHRR, SeaWiFS, and Fenyun-1A and 1B (which are Chinese satellites) for the project (Huang and Fu, 2002). These are used to map coastal resources such as mangroves, coral reefs, wetlands, and sandbanks. The data is also used to monitor coastal environmental change and hazards, as well as the study of coastal processes including sediment dynamics (Huang and Fu, 2002). Their findings include the observation that the Yellow River Delta is expanding while the river mouth moves from northeast to southeast and seaward at a rate of 3 km per year (Huang and Fu, 2002).

Ford (2013) identifies two main approaches used when assessing shoreline change: field-based methods used to establish shore-perpendicular profiles which are repeatedly surveyed, and the analysis of a time series of remotely sensed data. While field-based

surveys provide a detailed analysis, their spatial coverage is often limited. A typical approach to mapping shoreline change is the use of vectorised shorelines in calculation of rates of change (Ford, 2013).

2.3. **Remote sensing framework**

2.3.1. Data sources

One of the most important uses of digital remote sensing data is detection of land cover changes over time (Mouat et al., 1993). Remotely sensed data is commonly used for classification of land use and land cover since it provides the ability to produce map-like images, which are more intuitive to interpret than tables and figures. These classifications can also be used for change detection. The many advantages of using remotely sensed data for change detection include repetitive data acquisition and a digital format for computer processing (Lu et al., 2004). Use of satellite remote sensing allows routine observation of the coastal area, providing information about conditions and changes over time (Huang and Fu, 2002). In many cases, even a visual examination of the remotely sensed data can provide invaluable information about the study area (e.g. Ulbricht and Heckendorff, 1988).

Various data sources may be helpful when studying complex, dynamic coastal processes. These include aerial photographs, satellite images, ground surveys, historical maps, and ground-based photographs (Livingstone et al., 1999). Each study makes use of different data sources according to their needs and to availability of the data.

One popular remotely sensed data source which has been used in erosion detection and other change detection studies throughout the world is Landsat TM data (e.g. Althausen et al., 2003; Hayes and Sader, 2001; Kwarteng and Al-Ajmi, 1996; Smith and Abdel-Kader, 1988; Thampanya et al., 2006; van der Werff and van der Meer, 2008; Zhang et al., 2002, and many others). Landsat imagery is seen as invaluable in the monitoring of environmental change and the historical archive which it provides gives a unique data source for change detection (Woodcock et al., 2001).

This study utilised Landsat TM imagery and aerial photographs, and data acquisition is detailed in Section 3.1.

2.3.2. Study site parameters

A challenge faced in a coastal erosion study is the definition of exactly which areas constitute the 'coastal zone' as well as the exact location of the shoreline. Although South African studies by Palmer et al. (2011) and Unterner et al. (2011) focussed on blocks of only 50 by 50 metres in determining coastal erosion vulnerability, influences from much further inland can have an impact on the vulnerability to coastal erosion. Regions within as much as 100 horizontal kilometres of the coastline and 100 vertical metres above sea level were defined by Small and Nicholls (2003) to be the near-coastal zone. While the direct impact of coastal hazards may not extend through the entire region of the 'near-coastal zone', indirect impacts may well extend further inland (Small and Nicholls, 2003).

The shoreline itself can also be difficult to isolate. The location of the shoreline is vital to this study since it can provide information regarding shoreline location and orientation relative to adjacent structures, beach width and volume information, and – most importantly – can be used to quantify historical rates of change (Boak and Turner, 2005). The shoreline can ideally be defined as the physical interface between land and water, however, this is difficult to apply in practice (Boak and Turner, 2005).

The shoreline position is dependent on the time at which it is measured, and wave, tidal, and weather conditions all have a significant impact on the instantaneous shoreline position (Boak and Turner, 2005). For practical purposes, a shoreline indicator can be used. This is a feature which is used as a proxy to represent the 'true' shoreline position (Boak and Turner, 2005). These indicators can include the vegetation line, high water line, low water line, instantaneous water line, or the wet/dry line (Boak and Turner, 2005; Thieler et al., 2009).

The high water line, while commonly used as a shoreline indicator, is often not clearly visible on remotely sensed images. The wet-dry line is more clearly visible, but is affected by the wave and wind conditions at the time – though not as sensitive to tidal stage as the instantaneous run-up limit (Boak and Turner, 2005). While many indicators do not take into account the tide and wave conditions or seasonal effects, in practice, the decision as to which shoreline indicator to use is usually determined by data availability (Boak and Turner, 2005). Where available, aerial photography is the most common data source for determining past shoreline positions (Boak and Turner, 2005).

Once a shoreline indicator has been selected, it must be detected within the available data source. Most commonly, for a visibly discernable shoreline feature, manual visual interpretation is used. A disadvantage of this is the inherent subjectivity involved (Boak and Turner, 2005). While more objective shoreline detection is now possible for tidal datum

shoreline indicators, these techniques have only limited applicability to historical data sets (Boak and Turner, 2005).

In this study, the wet-dry line was used as a shoreline indicator in the study of aerial photographs, as detailed in Section 3.7.

2.3.3. Classification

Classification of remotely sensed data can provide a host of information about the land cover and land use within the area, as well as allowing for the use of post-classification change detection to observe changes which occur within the area.

The majority of earlier classification techniques were based solely on spectral information at a pixel level. In recent years, object-based classifications which incorporate spatial information have been gaining popularity (van der Werff and van der Meer, 2008). A review paper by Blaschke (2010) found that an increasing number of empirical studies in peer-reviewed journals have shown that object-based image analysis provides improvements over per-pixel analysis. In addition, the launch of very high resolution satellites such as IKONOS and Quickbird since 2000 result in a huge volume of data and object-based image analysis is one way to deal with this challenge (Blaschke, 2010).

A study by Kamagata et al. (2006) compared two different types of pixel-based classifications with an object-based classification for vegetation mapping using IKONOS imagery. They found that the object-based classification provided the most accurate result.

Various studies have shown that an object-based approach provides more accurate classifications than a pixel-based approach (e.g. Drăguţ et al., 2010;Kamagata et al., 2006; Sun et al., 2004). Although in many cases per-pixel classifications may provide adequate information, the data quality may be improved by making use of spatial information (Blaschke, 2003). The information available within an image is contained not only in individual pixels, but also in the objects which are built up by the pixels and their relationships to one another (Blaschke, 2003). The use of an object-based approach allows incorporation of this contextual data along with texture and shape into the classification (Blaschke, 2003; Darwish et al., 2003). This is especially useful when different classes within an image may have a similar spectral signature (van der Werff and van der Meer, 2008), or when pixels comprising a single real-world object are not spectrally homogeneous (Ryherd and Woodcock, 1996). A major advantage of incorporating shape measures into the classification is that the spatial information is not solely subjectively interpreted by the user,

but is measured automatically and without bias by the software (van der Werff and van der Meer, 2008).

Ryherd and Woodcock (1996) studied the usefulness of texture data and segmentation of data for image classification and found that in general, segmentation was more effective when combining both spectral and texture data, rather than using either one of the two on its own. While the addition of texture did not always make a huge improvement in results, it did not worsen the results and in many cases it did provide a major improvement. Their study also found that the use of texture alone – without spectral data – provided poor results. They also state that textural information is often important in discriminating man-made landscapes.

The steps used in an object-based classification along with the specific methods employed in this study are given in Section 3.3.

2.3.4. Accuracy assessment

Once the classification step has been completed, an accuracy assessment is vital. This allows an assessment of how well the classification represents reality, which is important to report to the end user. The accuracy assessment contributes important data quality information to the user (Stehman, 1997). The results of the accuracy assessment can be represented in various ways, but the generally accepted reporting method is an error matrix, which is recognised as an effective descriptive tool for organisation and presentation of the accuracy assessment information (Congalton, 1991; Stehman, 1997).

An important part of the accuracy assessment is using an appropriate method to select samples for the assessment. Congalton (1991) noted that the selection of a proper sampling scheme is a critical step during any accuracy assessment and recommends a stratified sampling scheme where the samples are stratified according to which class they have been classified into and then randomly selected from within each class. Congalton (1991) suggests compromising between statistically sound and practically attainable sample sizes by selecting a minimum of 50 samples per class, increasing this to 75 or 100 for classifications with a large number of classes. The number of samples should also be adjusted based on the variability found within each individual class (Congalton, 1991).

Details of accuracy assessments and the steps followed in this study are given in Section 3.4.

2.3.5. Other transformations

The assessment of the health and productivity of vegetation and how it changes over time is important in studies of coastal erosion. Vegetation index differencing is a useful method for detection of vegetation change (e.g. Jano et al., 1998) and is very important in coastal erosion studies, since the loss of vegetation may result in enhanced erosion while vegetation growth may aid accretion (Thampanya et al., 2006). Use of vegetation index differencing emphasises differences in different features and reduces impacts of topographic effects, but it can enhance random noise (Lu et al., 2004).

Information on the health and productivity of vegetation can be derived through the calculation of vegetation descriptors including vegetation indices and spectral transformations. One popular vegetation index is the NDVI (Normalised Difference Vegetation Index), which is correlated with fractional vegetation cover, vegetation condition, and biomass (Carlson and Ripley, 1997). In a comparison of several different vegetation indices by Lyon et al. (1998), it was found that the NDVI provided results which appeared most accurate based on their visual interpretations of the imagery and field work. They also found that NDVI was least affected by topography. The NDVI has been the most widely used index in global vegetation studies (Huete et al., 1997). Studies have shown a qualitative correspondence of differences in NDVI with observed or recognised variations in vegetation growth (Huete et al., 1997).

Various other vegetation indices are also available, including SAVI (soil adjusted vegetation index); ARVI (atmospherically resistant vegetation index); SARVI (soil and atmospherically resistant vegetation index); and MNDVI (modified normalised difference vegetation index) (Huete et al., 1997). SARVI and SAVI were found to have increased sensitivity in densely vegetated areas, while the NDVI was most sensitive to red reflectance variations and could be useful in green cover studies (Huete et al., 1997).

Another transformation which can be useful in change detection studies is the tasselled cap transformation. The tasselled cap transformation can help to reduce data redundancy between bands and emphasise different information (Lu et al., 2004). The first three bands of a tasselled cap transformation provide information on the main components of natural surfaces. These bands are known as the brightness, greenness, and wetness components. The brightness component is designed to capture the main trend of variation in soil reflectance which is sensitive to changes in biological factors. The greenness component, like the NDVI, is related to the amount of healthy green vegetation. The wetness component responds to canopy and soil moisture.Various studies have found different bands (brightness, greenness, wetness) of the tasselled cap transformation to be the most

appropriate. Fung and LeDrew (1987)(in Lu et al., 2004), found that the greenness and brightness layers used in image differencing were most appropriate for detecting land-cover changes from multi-sensor data. Fung (1990) found that image differencing in the near-infrared band and in the greenness band resulting from a tasselled cap transformation were useful for detection of crop type change and changes between vegetative features and bare soil, while use of the brightness band was efficient in detection of rural-to-urban land cover change. Coppin and Bauer (1994) found that changes in brightness and greenness were most useful for identification of important forest canopy change features. On the other hand, Woodcock (1996)(in Lu et al.,2004), found that changes in the wetness band were the most reliable indicators of forest change.

In this study, the NDVI is used for vegetation index differencing and the brightness band resulting from a tasselled cap transformation is used in image differencing. The transformations are detailed in Section 3.5 and the change detection using them is detailed in Sections 3.6.2 and 3.6.3.

2.3.6. Change detection

Multi-temporal imagery can be used for assessing changes which have occurred over time. Change detection is the process of identifying changes which have occurred by assessing differences in the state of an object or phenomenon by observing it at different times (Hayes and Sader, 2001; Lu et al., 2004; Ridd and Liu, 1998;). The basis of change detection using remotely sensed data is that changes in the real world will result in changes in reflectance values or textures observable on the remotely sensed images (Lu et al., 2004).

Various techniques are available for detection of land cover changes from multi-temporal remote sensing data sets (Hayes and Sader, 2001). Although many authors and studies have compared change detection techniques, there is much debate as to which is the best. In general, it can be concluded that no single method is suitable for all cases, and the success of the methods selected are largely dependent on the skill and knowledge of the analyst performing the change detection (Lu et al., 2004).

Either classified or unclassified images may be used to implement different types of change detection. On unclassified images, techniques include image differencing, image ratioing, vegetation index differencing, and background subtraction, all of which require selection of thresholds to determine changed areas (Lu et al., 2004). These techniques are simple, easy to implement and interpret, but they cannot provide complete matrices of change information (Lu et al., 2004). Use of the tasselled cap transformation reduces data redundancy between

bands and emphasises different information. However, it can be difficult to interpret and cannot provide a complete change matrix (Lu et al., 2004). On classified images, post-classification change detection can be performed. This minimises impacts of atmospheric and environmental differences and also provides a complete matrix of change information, however, it requires considerable time and expertise to perform (Lu et al., 2004).

A study by Zhang et al. (2002) addressed the change in urban and rural land use in and around Beijing on Landsat TM images. They used both post-classification change detection and image differencing. They found that the results from post-classification change detection were more useful, and less sensitive to registration errors. They also noted that it was possible to integrate the interpreter's knowledge into the classification procedure. The disadvantage of post-classification change detection is that image classification is a time-consuming process.

Details of these techniques and the methods used in this study are given in Section 3.6.

2.4. **Conclusions**

Past studies have used and compared a variety of different techniques, however, the most appropriate technique to use depends on the specific objectives, study area, and data available. One aspect on which there is broad agreement in the scientific community is that object-based classifications provide better results than pixel-based classifications. The use of Landsat TM imagery is also popular and generally found effective. Even though there is a host of other imagery options available, use of Landsat TM images and aerial photographs can make the techniques used more repeatable for future studies since these are easily available, free for research purposes, and have a good historical availability.

Of the many vegetation indices available, the most appropriate index to use also depends on the study site and objectives, but NDVI is widely used and accepted as a good vegetation index. With respect to the tasselled cap transformation, there is no agreement on the best band to use in image differencing, though most studies recommend either the brightness or the greenness band.

The best change detection methods to use remain an unanswered question and are highly dependent on the study parameters. Post-classification change detection has the advantage of providing a complete change matrix. Other popular and useful methods include image differencing and vegetation index differencing.

The next chapter details the techniques and methods used in this study.

3. MATERIALS AND METHODS

This chapter provides details on the methods used during this study and gives a discussion of the technical aspects of each step performed. Figure 2gives an overview of all the steps performed and each step is discussed in detail within this chapter.

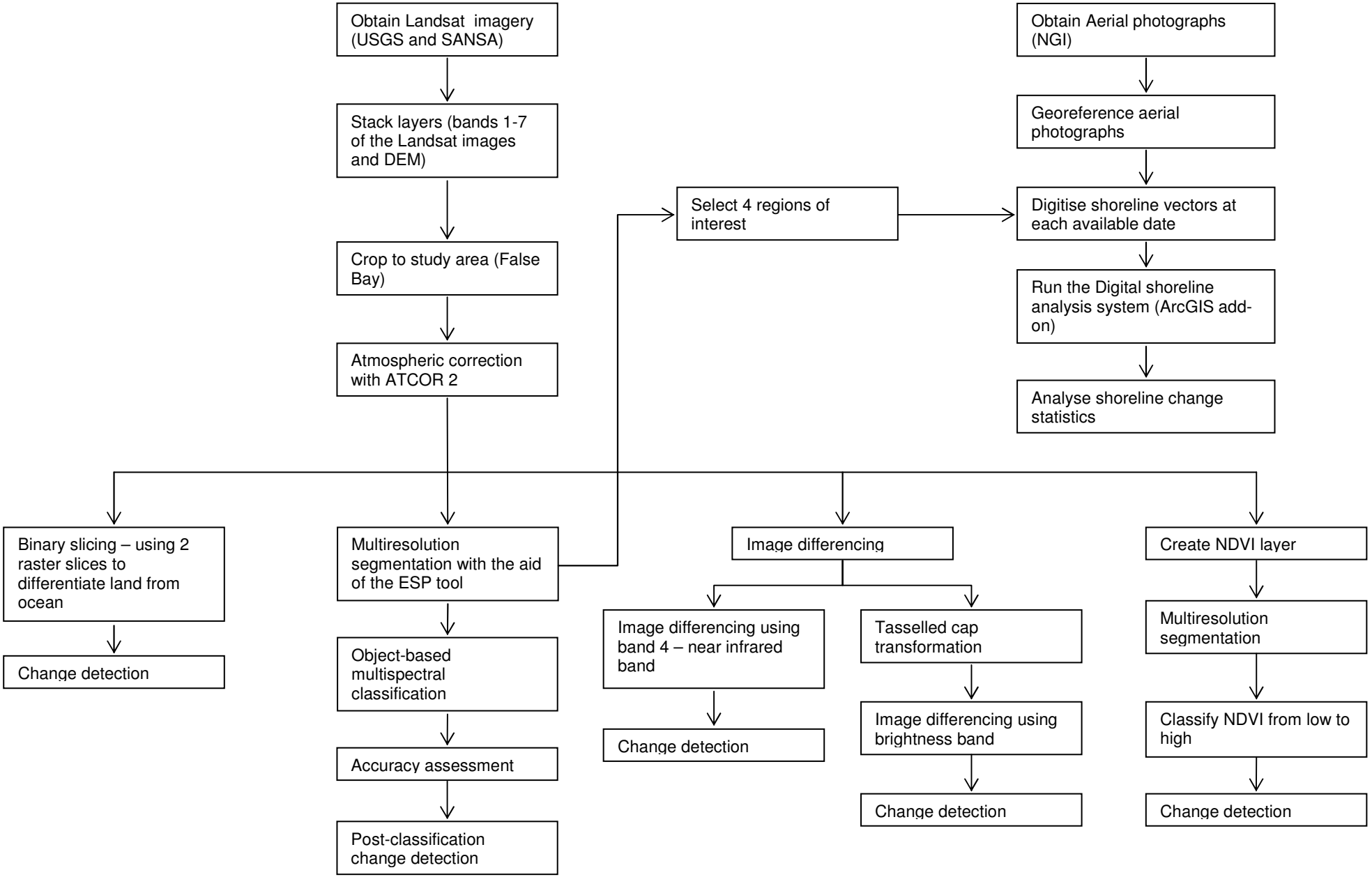

Figure 2: An outline of the methods used during this study. Each step is discussed in detail in this chapter (Chapter 3).

3.1. Data Acquisition

This project utilised Landsat 5 TM and Landsat 7 ETM+ imagery as well as aerial photographs. Both data sources provided different advantages. Landsat imagery was available at more consistent time intervals and could be selected in the same seasons at regular intervals. Aerial photographs provided both higher resolution data for the study area, and provided data over a longer time period from before Landsat imagery became available. A digital elevation model (DEM) has also been used to provide some elevation information. The DEM used was the SUDEM (Stellenbosch University Digital Elevation Model), a high resolution model with a resolution of 5 m (Van Niekerk, 2012). The model was resampled to 30 m resolution for use with the Landsat imagery.

The Landsat 5 TM and Landsat 7 ETM+ images were obtained from the United States Geological Survey (USGS) Earth Resources Observation and Science Center (EROS) at http://glovis.usgs.gov, where available. Further Landsat images were obtained from the South African National Space Agency (SANSA) at http://www.sansa.org.za. Figure 3 shows an example of one of the Landsat images as it was obtained, before any processing was performed. The dates selected as well as the data source are shown in Table 1.

Table 1: The Landsat images used. The Path/Row number for all acquisitions was 175/84.

Acquisition Date	Satellite	Obtained from
1985/05/11	Landsat 5 TM	Glovis (USGS)
1991/05/28	Landsat 5 TM	SANSA
1996/05/25	Landsat 5 TM	SANSA
2001/05/15	Landsat 7 ETM+	Glovis (USGS)
2006/04/19	Landsat 5 TM	SANSA
2011/04/17	Landsat 5 TM	Glovis (USGS)

Landsat 5 TM and Landsat 7 ETM+ images were available at many dates from 1985 to the present. Since the study aimed to address longer-term erosion rather than short-term and seasonal erosion, six Landsat images were selected at 5- and 6-year intervals, spanning a total of 26 years. This time spacing allowed the study to stretch over as long a period as possible while still viewing progress at moderate intervals. Several factors were incorporated into selection of the images. Firstly, images with minimal cloud cover were selected. All images were taken during the autumn season, in the months of April or May, since this was the time at which most images with a low cloud cover were available in the required years. This also avoids seasonal change affecting the results and resulting in misinterpretation of the erosion occurring. In addition, use of images from April and May allowed image usage from the latest as well as the earliest available years.

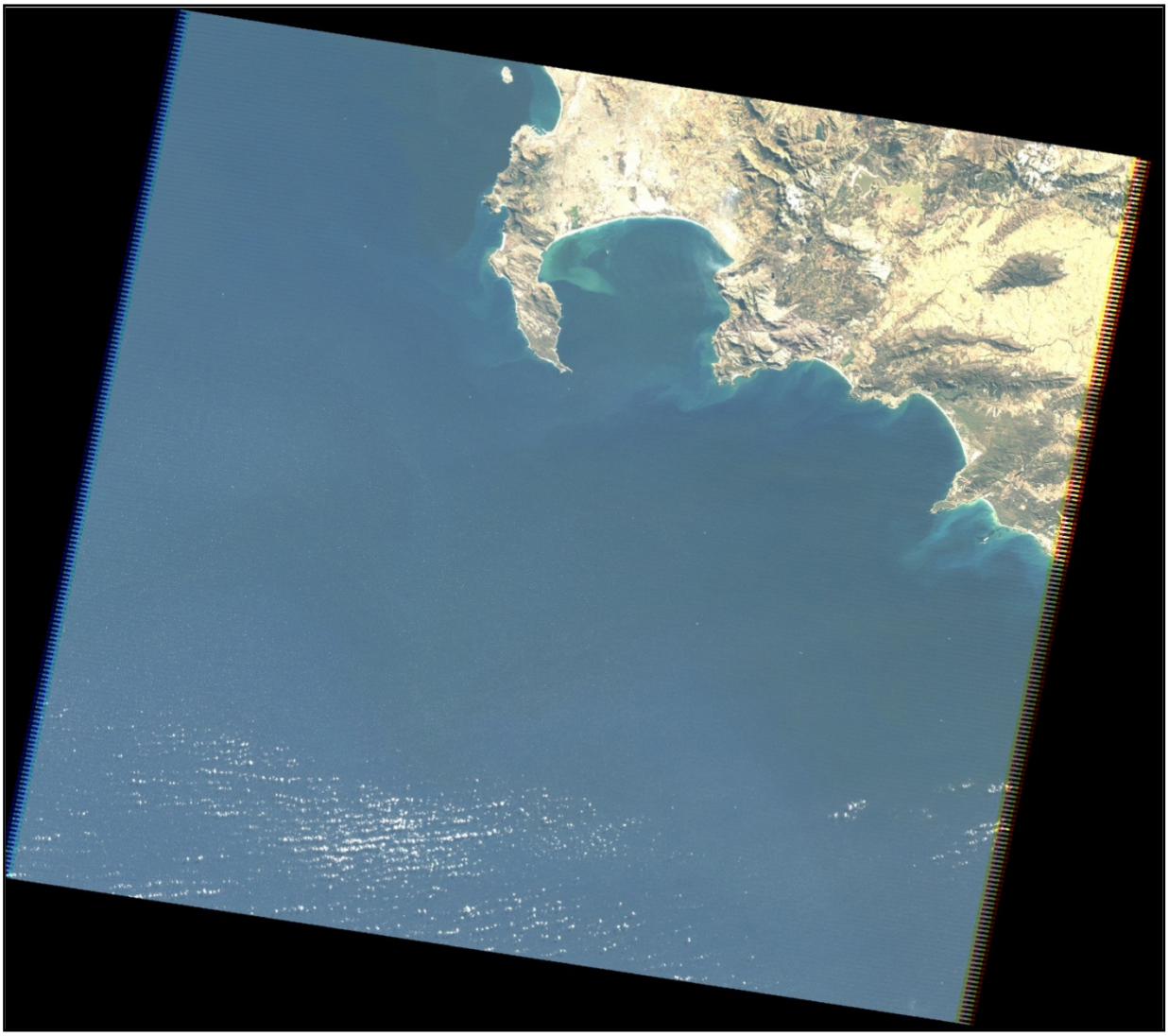

Figure 3: The original Landsat image for 2011.

The aerial photographs used were obtained from National Geo-spatial Information (NGI), a part of the Department of Rural Development and Land Reform. The aerial photographs were available over a long time period, from 1944 to 2010. However, at many dates they are available over only a portion of the study area. The dates at which they are available are sporadic and during different seasons, meaning seasonal changes will influence the results. Spatial and spectral resolutions vary greatly from one image set to another. The dates and scales of the aerial photographs used are given in Table 2.

Table 2: Details of the aerial photographs utilised.

Date	Scale (as supplied)	Pixel size (metres)	Job Number	Areas Covered
2010	not supplied	0.5	307	All
03-2009	not supplied	0.125	W27A; W27B; W58b; W58d; W17A; W17B; W17C; W17D	Bayview; Macassar; Strand
2008	not supplied	0.5	19	Bayview; Macassar; Strand
09-11-2000	1:50000	4.64	1033	All
07-06-1999	1:30000	3.1	498_367	Macassar; Strand
09-09-1989	1:110000	9.63	929	Bayview; Pringle Bay
28-07-1989	1:30000	2.74	498_249	Macassar; Strand
27-05-1989	1:30000	2.94	498_253	Bayview
26-01-1989	1:50000	7.17	919	Bayview
25-08-1988	1:50000	5.3	919	Strand; Pringle Bay
17-04-1983	1:30000	3.14	198_188	Macassar
09-03-1980	1:30000	3.09	498_146	Pringle Bay
27-04-1978	1:30000	2.93	498_98	Strand
04-10-1977	1:60000	7.7	786	Bayview
27-09-1977	1:20000	1.87	794	Strand
27-03-1977	1:50000	4.76	786	Macassar; Strand; Pringle Bay
23-04-1976	1:30000	2.92	498_73	Bayview
12-05-1971	1:30000	2.71	498_19	Macassar; Strand
21-10-1968	1:20000	1.82	620	Bayview
01-04-1968	1:20000	1.8	620	Macassar
26-01-1967	1:36000	3.57	534	Macassar
10-12-1966	1:36000	3.6	534	Strand
31-10-1961	1:36000	4.02	461	Pringle Bay
10-1958	Various	3.38	424_004	Bayview
11-1953	1:36000	3.24	335	Strand
1945	1:8400	0.77	203B	Bayview
1944	1:18000	1.64	61	Bayview; Macassar; Strand

3.2. **Pre-processing**

The first processing step for the Landsat imagery was to stack the layers (bands) of each image in the ENVI software, allowing later processing to be correctly performed on all data layers for each image. Next, the images were cropped. Cropping the images allowed unnecessary data comprising open sea and far inland regions to be excluded from later steps, drastically cutting down on processing time. Images were cropped to include the whole of False Bay, including enough of the surrounding areas to include directly interacting factors and provide some context. The original extent of the data is shown in Figure 3, while the clipped version is given in Figure 4. This was also done using the ENVI software, by creating a region of interest (ROI) and then subsetting the data via the ROI.

Following the image cropping, the images were atmospherically corrected. Atmospheric correction is an important step when performing various change detection algorithms in order to make the images more directly comparable (McGovern et al., 2002). Atmospheric correction can be either absolute, where the actual surface reflectance of the image pixels are determined, or relative, where the images being used are corrected relative to each other so that the same digital number in each image represents the same reflectance (Song et al., 2001).

The process of atmospheric correction is intended to remove atmospheric effects from the imagery, allowing direct comparisons from one image to another without the external factors, including atmospheric haze, influencing the results. Haze is caused by the scattering of electromagnetic waves and increases the overall radiance of an image while reducing image contrast (Kwarteng and Al-Ajmi, 1996). Atmospheric aerosols increase the apparent reflectance of dark objects while reducing the apparent reflectance of bright objects in an image through scattering, resulting in a loss of information within the image (Song et al., 2001). An atmospheric correction, while unable to recover the information lost by scattering and haze, can reduce the error in estimating the surface reflectance, or can set a multi-temporal dataset (as used in this project) to a common radiometric scale (Song et al., 2001).

While it is possible to perform certain types of change detection without an atmospheric correction being necessary (for example, post-classification change detection), it is necessary for certain methods, including cases where NDVI is used (Song et al., 2001). Atmospheric correction was therefore performed to ensure radiometric compatibility of the scenes used in this project. Since the images were selected during the same season, the worst atmospheric effects were reduced, however, daily atmospheric variability could still affect the acquired scenes (McGovern et al., 2002).

One of the most popular atmospheric correction algorithms available is theATCOR module. The ATCOR module has been used for atmospheric correction of Landsat TM imagery in various previous change detection projects (e.g. Kwarteng and Al-Ajmi, 1996). The ATCOR 2 algorithm converts digital numbers (DN) into at-sensor radiance by using a calibration file based on gain and offset values obtained from the imagery's metadata (Balthazar et al., 2012). Once the DNs have been converted to at-sensor radiance, atmospheric disturbances have to be removed in order to obtain surface reflectance values (Balthazar et al., 2012).

The ATCOR 2 atmospheric correction algorithm was implemented in this project using the PCI Geomatica software. An example of the results of the image pre-processing, including the atmospheric correction, is shown in Figure 4. This includes the uncorrected image in Figure 4 (a), where haze is visible on the scene. The effect of haze is visibly minimised in the atmospherically corrected image depicted in Figure 4 (b). The removal of bluish atmospheric haze in this figure should be noted.

The ATCOR module calls for several values to be provided and then performs the remainder of the correction automatically. The values which have to be provided include the average elevation (28.57 m), the sensor type (Landsat 5 TM or Landsat 7 ETM+), the condition and thermal atmospheric definition (fall/spring), solar zenith, and calibration information. ATCOR then uses preset lookup tables containing altitude profiles of pressure, temperature, humidity, and aerosol type that are used to calculate the necessary radiation components as well as molecular and particulate absorption, emission, and scattering (Balthazar et al., 2012).

The Landsat imagery obtained from SANSA presented some problems during the ATCOR 2 process, since in some cases the metadata files reported the solar elevation angle but labelled it as the solar zenith angle. Once the correct values were established, however, atmospheric correction could be performed correctly.

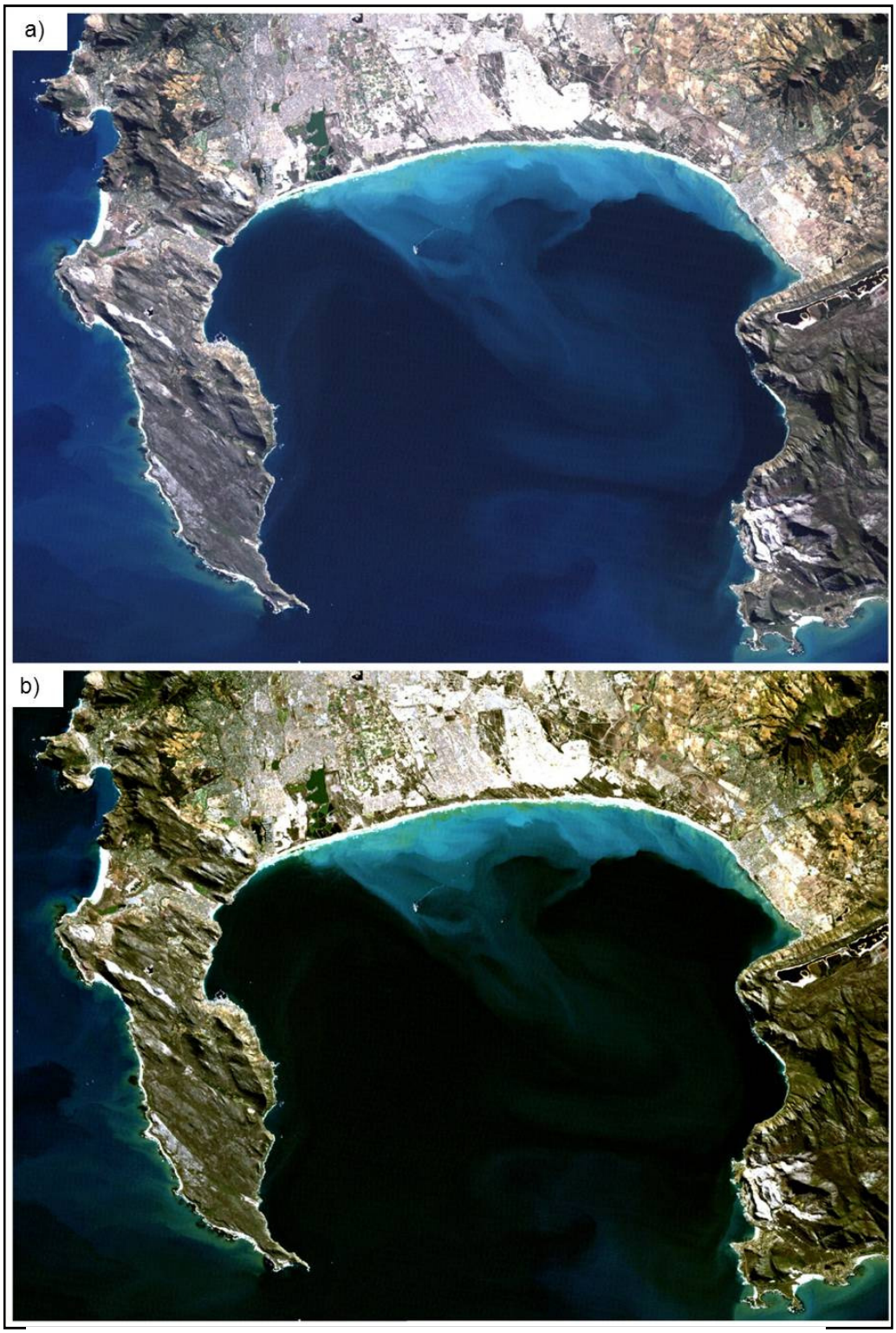

Figure 4: a) the original 2006 Landsat true colour image and b) the image after the atmospheric correction (ATCOR 2) had been performed.

In the case of the aerial photographs, the only pre-processing necessary was georeferencing. The photographs for the four focus areas were georeferenced using the spline function in ArcGIS. Since the 2008 and 2010 photographs were already georeferenced when they were obtained, the earlier photographs were georeferenced in reference to these. Further pre-processing such as atmospheric corrections was not necessary since digital change detection was not being performed on the aerial photographs.

3.3. **Multispectral object-based image classification**

3.3.1. Segmentation

Object-based image classification comprises two main steps: image segmentation, and classification of the objects obtained through segmentation. Both steps were performed using the Definiens Developer software (previously known as eCognition) for this study.

Segmentation of images through the aggregation of pixels is the first step of any geographic object-based image analysis (GEOBIA) (Drăguţ et al., 2010). Image segmentation was defined by Ryherd and Woodcock (1996) as the process of dividing digital images into spatially cohesive units. The resulting segments should be representative of discrete objects within the image, where each of these discrete objects is relatively spectrally and spatially homogeneous (Drăguţ et al., 2010).

When a human observer or analyst looks at an image, the human mind automatically segments the image into recognisable objects (Ryherd and Woodcock, 1996). This means that representation of the image in terms of such objects much better satisfies human understanding than a basic pixel-based approach (Drăguţ et al., 2010). However, it is complex to effectively segment images using computer software (Ryherd and Woodcock, 1996).

Segmentation of remotely sensed imagery can make image interpretation easier by highlighting specific objects within the image (Ryherd and Woodcock, 1996). Not only spectral information, but also spatial information may be applied in this step, which is useful for successful segmentation (van der Werff and can der Meer, 2008). Spatial information has been successfully applied during classification in various different studies (e.g. Frohn et al., 2005; Segl et al., 2003; Silva and Bigg, 2004; van der Werff and van der Meer, 2008). There is a degree of generalisation associated with the application of a segmentation algorithm (Blaschke, 2003), however, such generalisation is usually required in order to simplify the study region for effective investigation.

In the Definiens Developer software, various types of segmentation are available, including chessboard segmentation, quadtree based segmentation, contrast split segmentation, spectral difference segmentation, multiresolution segmentation, multi-threshold segmentation, and contrast filter segmentation. Multiresolution segmentation is performed by creating single-pixel objects which are gradually merged into larger objects (Drăguţ et al., 2010). In other words, it is a region-based bottom-up region-merging technique (Darwish et al., 2003). It works by considering each pixel a separate object and then merging them to form bigger segments (Darwish et al., 2003). The segments are optimised in order to minimise the internal heterogeneity of each segment, and the growth of the segments will cease once the segment will exceed a predefined heterogeneity threshold (Drăguţ et al., 2010), specified by the user-defined scale parameter. A higher scale value results in larger and more heterogeneous objects (Drăguţ et al., 2010). The heterogeneity is further defined both in terms of colour (spectral values) and shape (spatial values) of the object (Drăguţ et al., 2010), which are weighted by the user. The multiresolution segmentation algorithm within Definiens Developer has been used by various scholars (e.g. Darwish et al., 2003;Ngcofe and Minnaar, 2012; Sun et al., 2004) and was the algorithm used for this study.

When conducted at appropriate scales, segmentation can increase classification accuracy, however, selection of the appropriate scale can be difficult and is often dependent on trial-and-error methods (Drăguţ et al., 2010), which are both time-consuming and subjective. Some authors, such as Darwish et al. (2003), have performed segmentations at several different scales and then performed a statistical analysis on the results in order to determine which was the most effective. However, this method is not only very time consuming, but it is also only capable of assessing a few of the available scale options. Drăguţ et al. (2010) have created an estimation of scale parameter (ESP) tool in order to expedite this process. The ESP tool is intended to improve and speed up scale parameter estimation for a multiresolution segmentation (Drăguţ et al., 2010).

Details on the working of the ESP tool can be found in Drăguţ et al., (2010). The ESP tool allows for specification of a starting scale parameter, step size between increasing scale parameters, the option of whether or not to use an object hierarchy during segmentation, the number of scales to be tested, and the shape and compactness weightings to be used during the segmentation (Drăguţ et al., 2010). The tool utilises the local variance within an image to identify the most suitable range of scale parameters at which to conduct image segmentation within Definiens Developer (Drăguţ et al., 2010). By iteratively segmenting the image at different scales, the change in local variance at each scale is determined. The tool is capable of analysing only a single layer of image data and outputs a graph for user interpretation (Drăguţ et al., 2010). The graph shows both the local variance and the rate of

change of local variance, making interpretation easier since a peak in the rate of change indicates an object level at which the image can be appropriately segmented (Drăguţ et al., 2010). This enables the user to select a few appropriate segmentation scales. A visual interpretation of the resultant scales is often the most useful method for determining which will be the most useful for the specific project. The human eye is seen as an experienced, strong source during evaluation of segmentation (Baatz and Schäpe, 2000).

For multiresolution segmentation in Definiens Developer, not only the scale value, but also the shape and compactness parameters must be defined by the user. The shape parameter is a weighting of how much the segmentation should take the shape versus the colour (spectral characteristics) into account. The value ranges from 0 to 1, where a value of 0 would mean only the colour is taken into account while at values greater than 0, shape is increasingly considered. The compactness parameter refers to the shape portion, and sets how compact the segments should be. If the compactness is weighted low, the segments have a high smoothness factor and objects with a more linear shape are favoured, while higher compactness values will result in more compact objects. Chitade and Katiya (2010) (In Ngcofe and Minnaar, 2012), recommend that where possible, high colour values should be used, since spectral information has high discriminative power in imagery data.

For this study, the segmentation was performed in Definiens Developer, with the help of the ESP tool. The ESP tool assessed all possible scale values from 1 to 250 for one of the Landsat images. This scale value is a unitless value providing a heterogeneity threshold for the segments, thus influencing the size of the segments. The shape and compactness values had to be supplied to the ESP tool. These were both set to a value of 0.3. As discussed above, high colour values are often useful since spectral information provides considerable discriminative power between classes. However, it is also vital to include spatial information since this has been shown to improve classifications as discussed in section 2.3.3. Therefore the shape value was set to 0.3 – a strong focus on colour, but still incorporating shape. The compactness value was also set to 0.3, where objects with a more linear shape would be favoured somewhat, since vital classes in this classification such as beach and shallow coastal (discussed in section 3.3.2) tend to have a linear shape. In addition, segmentations with higher shape and compactness values were tested, and a visual assessment showed that these values produced a better result.

The output of the ESP tool can be seen in Figure 5. By zooming in on the rate of change line of the graph, it was possible to distinguish the most significant peaks. The first, or threshold peak, was located at a scale of 18. Other significant peaks could be seen at scales of 80, 93, 116, 176, and 234. Many smaller peaks were visible in between these, however the

indicated peaks were the most significant. The recommended scales identified through the ESP tool were then subjected to a visual assessment to determine which would be best for the purposes of this project. Upon initial visual assessment, a scale of 80 seemed most appropriate. This segmentation is shown in Figure 6. When viewing this scale of segmentation over the entire study region, the segmentation appeared effective. However, once classification was initiated, it became clear that this scale value caused many portions of classes which were intended to be separately classified to be contained within the same objects. This is indicated in Figure 7. Viewing the segmentation at a larger scale revealed that it did not provide enough detail. Therefore, a smaller scale of 18 was selected as indicated by the ESP tool results. The segmentation can be viewed in Figure 8 and Figure 9. Figure 8: The segmentation at a scale of 18.shows how the segments appear small when viewing the entire study area, however Figure 9: At a larger scale, it is possible to see how the scale value of 18 allows the separate classes to be captured more precisely.reveals that it showed the necessary amount of detail. This scale was utilised for all the images for consistency.

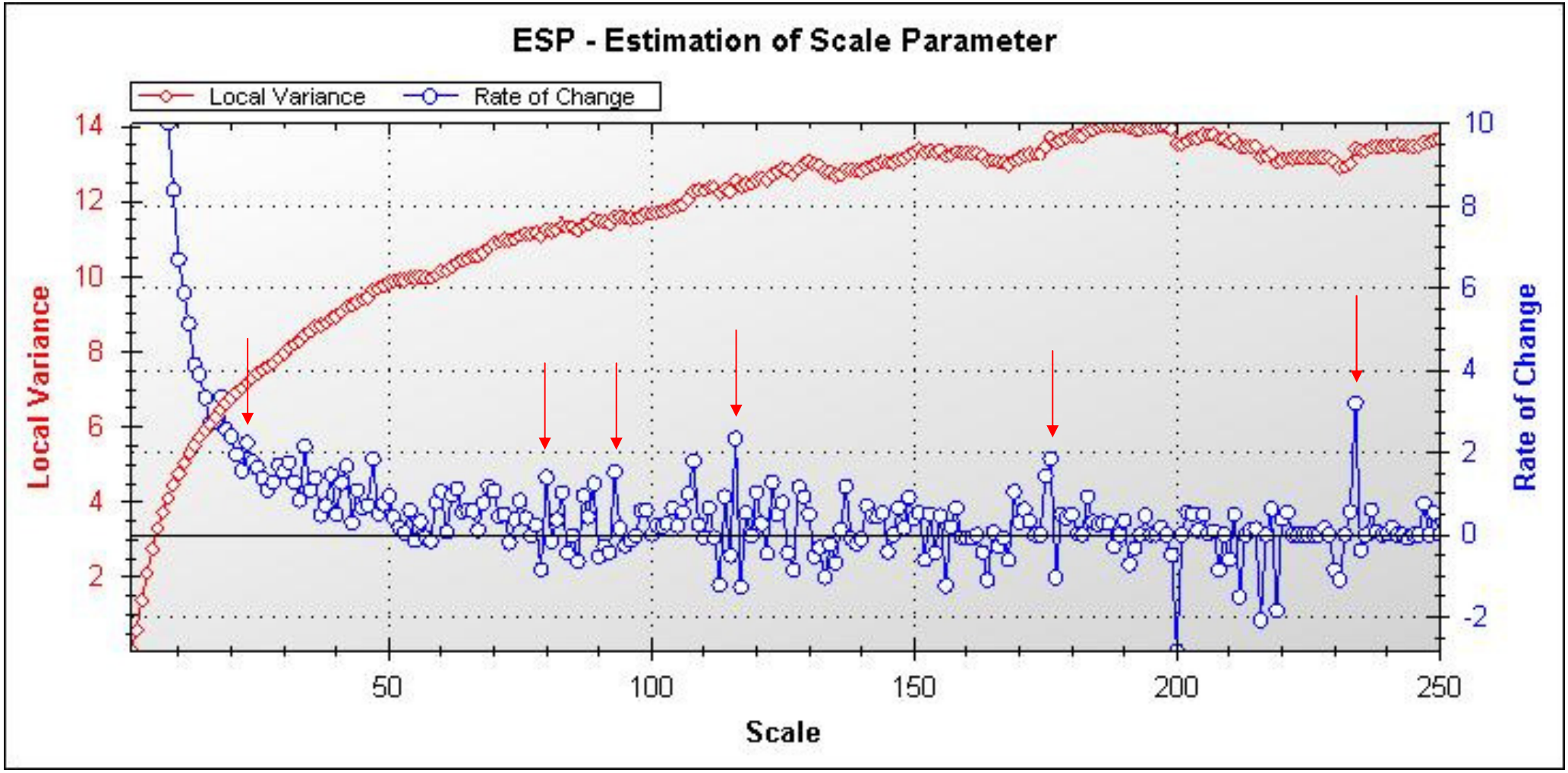

Figure 5: Results of the ESP tool providing recommended scales. Several of the peaks are indicated with arrows. The first (threshold) peak is more easily identified when the graph is zoomed in.

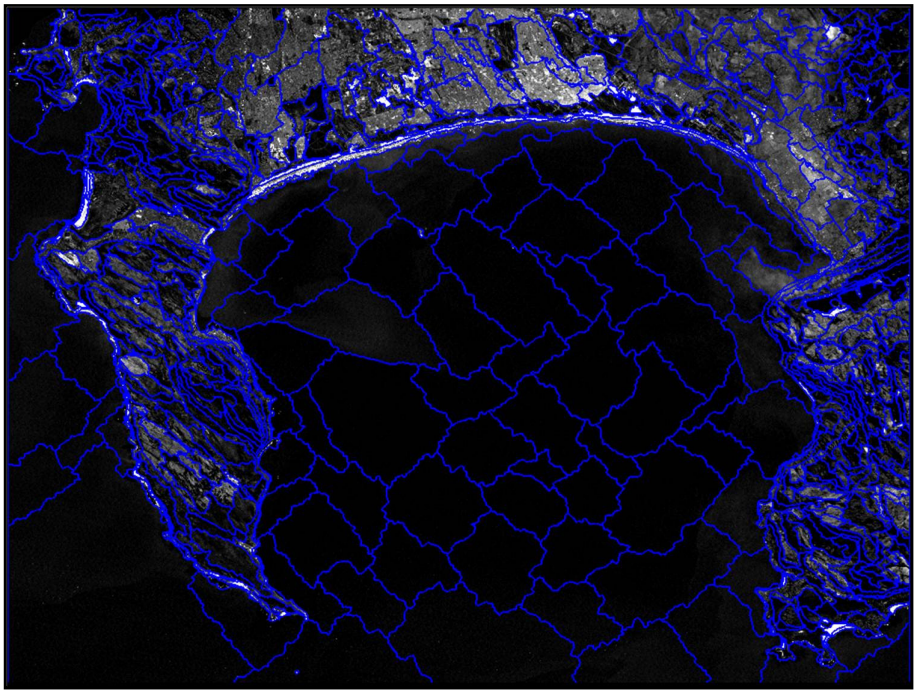

Figure 6: An example of the segmentation with a scale value of 80.

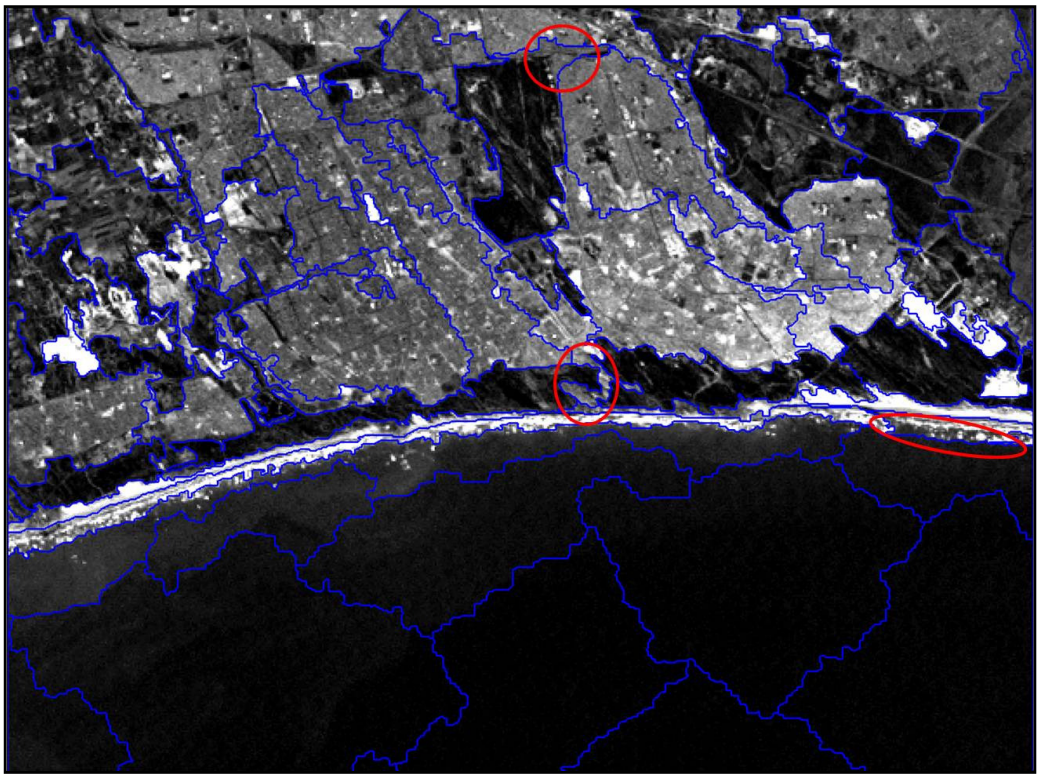

Figure 7: The segmentation at scale 80 shown at a larger scale. Several problem areas are circled. These show where built-up was grouped with natural and sand dune areas, as well as where shallow coastal was grouped with ocean.

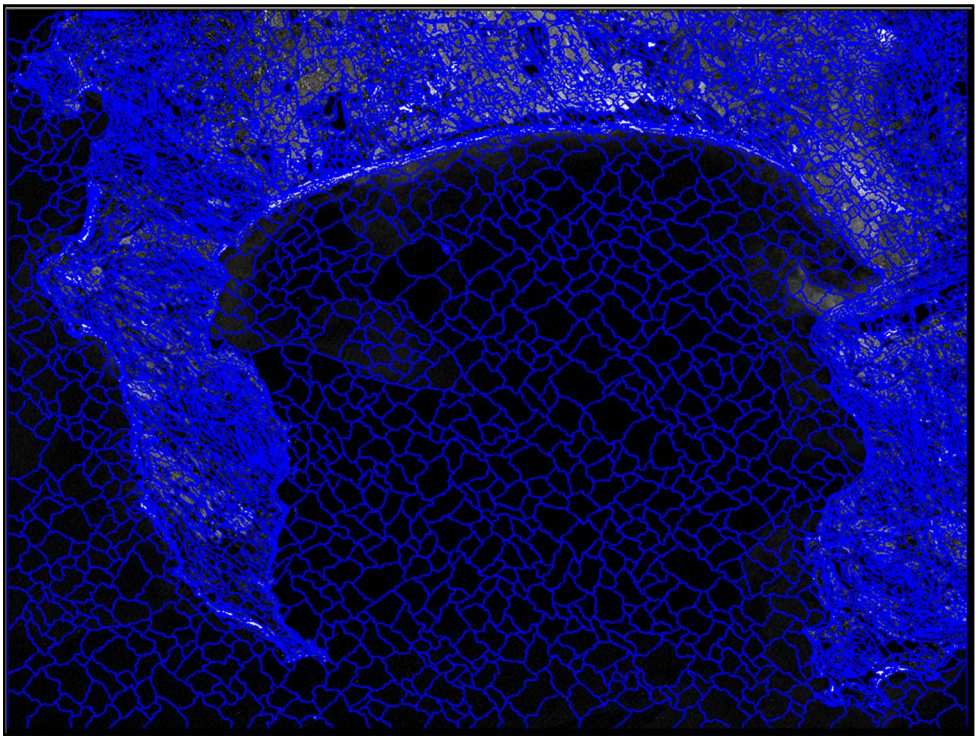

Figure 8: The segmentation at a scale of 18.

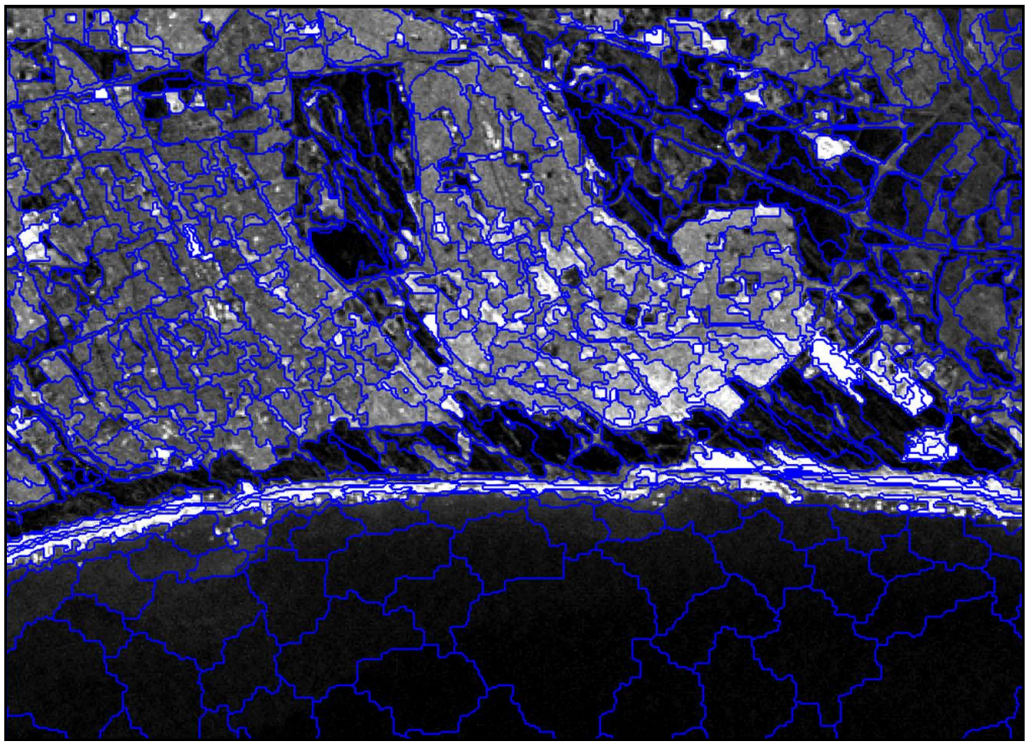

Figure 9: At a larger scale, it is possible to see how the scale value of 18 allows the separate classes to be captured more precisely.

3.3.2. Classification

Once the vital step of segmentation has been completed, image classification may be initiated. A supervised classification involves pre-defining the classes which will be used and giving the software certain parameters for these classes. The use of artificial neural networks during the classification step is very useful since they have the ability to learn by example and generalise (Foody and Arora, 1997). Training data samples would be selected for each class in order to allow the neural network to learn what the class parameters are. One vital assumption made at this time is that the training data used for a supervised classification provides a representation of the classes of interest (Chen and Stow, 2002). Selection of training samples for the classification can often be difficult, particularly in the case of historical data (Lu et al., 2004). The aim of the training stage in a supervised classification is to derive a representative sample of each class. The quality of such training data will have a significant effect on classification accuracy (Chen and Stow, 2002). In cases when there is little knowledge to describe the different features to be used, this method is much more effective than a rule-based approach (Sun et al., 2004).

Recent studies (e.g. Myburgh and van Niekerk, 2013) have shown that Support Vector Machines (SVM) produce superior classification results to neural networks (NN). However, neural networks were utilised for this study since this was the only supervised classifier supported by Definiens at the time of image processing. SVM has since also been added to the Definiens environment as a potential supervised classifier.

A study by Foody and Arora (1997) found that classification accuracy increased with the size of the training set, however, the increase was not linear. There were drastic increases in accuracy from a small to a medium training set size, but as the training set size increased further, the accuracy payoff became less significant. Their findings indicated that beyond a certain training set size, the addition of further training data may not significantly increase classification accuracy.

In this study, image classification was performed in Definiens Developer using the segmented images as discussed in section 3.3.1. Image classification was achieved by a supervised approach using the neural networks classifier, which involves selection of samples for each class as training data. Samples from each class were selected, then the classification algorithm was executed, enabling visualisation of the resulting classification. The classification was iteratively improved by selecting some segments which had been incorrectly classified, placing them within the correct class, and rerunning the classification (e.g. Sun et al., 2004). In accordance with the findings of the study by Foody and Arora (1997) discussed above, training samples were added iteratively until the accuracy appeared

good according to a visual assessment and the addition of further samples did not appear to result in a significant improvement.

This study made use of a new classification scheme, rather than using the classes from accepted schemes (e.g. Department of Rural Development and Land Reform, 2013; Lück et al., 2010). The class scheme used in this study was based on the requirement to view changes in certain specific features. The scheme was based on visual inspection of the imagery, and the abundance of certain land cover types within the study area. The following classes were created: ocean, shallow coastal, beach, built-up, natural, mountain, mountain shadow, dams, cultivated, sand (not beach), and sand dune. All completed classifications are shown in Section 4.1. The shallow coastal class refers to those areas currently covered by waves; where the beach is visible through a shallow ocean covering; underwater sediment plumes and phytoplankton blooms. The other classes are self-explanatory.

As with other classification algorithms, the accuracy of the resulting classification is a function of a wide range of factors (Foody and Arora, 1997). All classifications provide only a generalisation of the real world, and therefore, contain inherent error (Foody, 2002). It is therefore important to assess and express the quality and accuracy of any classification (Foody, 2002). A discussion of the accuracy assessment used for this study is given in Section 3.4.

3.4. **Accuracy assessment**

Together with the object-based multispectral classification, an accuracy assessment was performed in order to show how successful the classification was. An accuracy assessment is usually performed by selection of reference samples at various locations, and the comparison of these to the classified image (Stehman, 1997).

Various important factors are at play when selecting the samples to be used for an accuracy assessment. In some studies, testing is done on the same samples which were used for training, which results in overestimates of classification accuracy (Congalton, 1991). The reference samples should rather be selected separately and independently of the training data (Stehman, 1997). Recommendations for the sampling scheme and sample size are given in Section 2.3.4.

A weakness which is still found in any accuracy assessment is the fact that there is generally an assumption that the reference data used is itself an accurate representation of reality (Foody, 2002). In many cases, the samples are assessed with reference to

photointerpretation (Congalton, 1991). This makes the assumption that the photointerpretation is absolutely correct, which is rarely the case (Congalton, 1991). However, in many cases collection of ground reference data can be difficult or even impossible, and the assumption that photointerpretation is correct provides a manner of performing the accuracy assessment (Congalton, 1991). It is rarely the case that any form of reference data is completely accurate, since the reference data is also merely a subjective interpretation of reality, and may contain error of its own. The accuracy assessment reflects only the degree of agreement to this reference data, and not directly to the real world (Foody, 2002). This can lead to poor assessments of the classification (Congalton, 1991).

The results of the accuracy assessment can be represented in various ways, but the generally accepted reporting method is an error matrix. This is recognised as an effective descriptive tool for organisation and presentation of the accuracy assessment information and is used and recommended by many different authors (Congalton, 1991; Darwish et al., 2003;Stehman, 1997). The error matrix is a table describing the mapped class label against the reference data class for sample cases and it describes the classification accuracy and characterises errors (Congalton, 1991; Foody, 2002). This is a considerably better method of accuracy reporting than was used in many earlier studies, which often reported only a single number, which may not even have been site-specific – if accuracy was reported at all (Congalton, 1991). An error matrix effectively represents the accuracy of each category along with both the commission and omission errors present in the classification (Congalton, 1991).

Various different measures of accuracy may be derived from the error matrix. One of the most popular measures is the percentage of cases which are allocated to the correct class, reported in the form of the user's or producer's accuracy (Foody, 2002). These are ideal for describing the accuracy of a final map product (Stehman, 1997). Further details of these measures and of accuracy assessments are given in Congalton, 1991; Congalton and Green, 2008;Foody, 2002; and Stehman, 1997.

In this study, aerial photographs were used as reference data to identify the classes at reference locations. The photographs were used at dates as near as possible to each of the relevant Landsat imagery dates. As mentioned above, a disadvantage of using aerial photographs for validation is the assumption that the photointerpretation is 100% correct (Congalton, 1991), however, it was the best method in order to provide some form of reference data for images which are, in some cases, decades old.

The samples were selected in Definiens Developer, which then has the capability to compare the samples to the classified image in order to determine the accuracy of the image.

As discussed in section 2.3.4, samples were selected using a stratified random sampling method. The segments were stratified according to which class they had been classified into. Segments were then randomly selected from within each class. 75 samples were selected from each class, except the cultivated, built-up, natural, and mountain classes. For these classes, 100 samples were selected per class, due to the higher variability and greater size of these classes. The reference samples were selected after classification in order to use the stratified random sampling method.

The process was repeated independently for all 6 classifications. This means that for each image, the results of each classification were taken, the segments were classified according to class, and samples were selected. The samples selected specific to that image were then used for the accuracy assessment.

The results of the accuracy assessment are discussed in section 4.1 and the error matrices are given in Appendix B.

3.5. **Other classifications and transformations**

In addition to the image classification, additional image transformations were performed to extract meaningful information from the satellite imagery.

3.5.1. NDVI

A vegetation index was used in order to observe changes in vegetation, which is useful for determining vulnerability to erosion and observing dune changes. The NDVI was selected, and is discussed in section 2.3.5. The formula for the NDVI (as taken from Carlson and Ripley, 1997) is as follows:

$$NDVI = \frac{(\alpha_{nir} - \alpha_{vis})}{(\alpha_{nir} + \alpha_{vis})}$$

Where α_{nir} represents the near infrared band (band 4 of Landsat TM data), and α_{vis} represents the red band (band 3 of Landsat TM data).

For this study, an NDVI layer was created using this formula for each image in the ENVI software. The NDVI layers were then segmented in Definiens Developer, based on a clustering method used by Hayes and Sader (2001), who classified NDVI from low to high

prior to change detection. After segmentation, the NDVI layers were also classified from low to high.

3.5.2. Tasselled Cap

Another transformation that was performed was a tasselled cap transformation for all the images. This transformation is discussed in section 2.3.5. It was performed using the ENVI software. It transformed the data into three new spectral layers – brightness, wetness and greenness. This allowed data from several bands to be incorporated into a single layer, which was useful for image differencing since it provided more information than traditional image differencing. Further details on the tasselled cap transformation can be found in Huang et al., 2002.

3.5.3. Raster colour slices

A third transformation performed was creation of raster colour slices. This was done in an attempt to define the coastline through binary slicing by splitting the image into two classes at a single reflectance value.ENVI was once again used for this step. The colour slices were created using the near-infrared band, band 4, since this shows a distinctive difference between land and water, with ocean having low values and land having higher values. The image was split into anocean class with values from 0-4% reflectance and aland class with values from 4-100% reflectance. The same values were used through all 6 images for consistency. These values were selected by visual inspection. The raster slices were created at different values and the results were narrowed down by visual inspection to those that appeared the most accurate, until these values were selected.

3.6. **Change detection techniques**

Several change detection techniques have been identified and applied in literature (e.g. Byrne et al, 1980; Hayes and Sader, 2001; Jano et al., 1998; Lyon et al., 1998; Ward et al., 2000; Yang and Lo, 2002;Zhang et al, 2002;and many others). This study aims to assess techniques which are appropriate for detecting change in beach and coastal zones. Based on their applicability to this study and the data used, the following change detection techniques were selected for use in this study: single-band image differencing; tasselled cap

differencing; Boolean change detection; vegetation index differencing; and post-classification change detection.

The accuracy of any conclusions drawn during change detection is bounded by the pixel size of the imagery used. As stated by Smith and Abdel-Kader (1988), although in situ observations may show that an area is eroding or changing, this will be reported as unchanged if the erosion has been less than the size of a pixel cell.

3.6.1. Image differencing

One of the most commonly used techniques is image differencing. Image differencing involves the subtraction of a band of one image at a scene with the same band of another image at the same scene, with some time difference between them. Image differencing is easy to implement, but it is not capable of providing a complete matrix of change information (Lu et al., 2004). Values in the change image which are near zero represent no change, while those which are positive or negative represent changes between the two images. An advantage of this method is that it is simple to perform and relatively easy to interpret. One challenge that may be encountered is the selection of the threshold between real and spurious change (Hayes and Sader, 2001).

Image differencing has been found useful in a variety of geographical environments and is the most widely used technique (e.g. Chavez and Mackinnon, 1994, in Lu et al., 2004; Jensen and Toll, 1982, in Lu et al., 2004;Nelson, 1983, in Lu et al., 2004;Pilon et al., 1988, in Lu et al., 2004;Prakash and Gupta, 1998, in Lu et al., 2004;Ridd and Liu, 1998, in Lu et al., 2004;Singh, 1989). This method compares the changes between the images on a pixel-by-pixel basis.

In this study, image differencing was performed using the ENVI software. The near-infrared bands (band 4) of the images were used. In several studies, the red band (band 3) has found to perform exceptionally during image differencing (e.g. Chavez and Mackinnon, 1994, in Lu et al., 2004; Jenson and Toll, 1982,in Lu et al., 2004; Pilon et al., 1988, in Lu et al., 2004). However, in this case, band 4 was selected since change along the shoreline was of particular interest. Since band 4 shows a high contrast between water and land, it was the most appropriate choice for image differencing.

For this and the two differencing techniques to follow, six difference images were created, with dates as follows:

Image 1: 1991/05/28 – 1985/05/11 (72 months apart)

Image 2: 1996/05/25 – 1991/05/28 (60 months apart)

Image 3: 2001/05/15 – 1996/05/25 (60 months apart)

Image 4: 2006/04/19 – 2001/05/15 (59 months apart)

Image 5: 2011/04/17 – 2006/04/19 (60 months apart)

Image 6: 2011/04/17 – 1985/05/11 (311 months apart)

ENVI's image change workflow was used to perform image differencing. The two dates were selected for image differencing and band 4 was selected. Thresholding was applied and the Otsu's method for auto-thresholding was selected. Automatic smoothing was then enabled at a window size of 5 pixelsto lessen the noise and salt-and-pepper effect often seen when utilising this method. Aggregation was not enabled. The change class image was then exported.

The results of the band 4 image differencing are given in Section 4.4.

3.6.2. Tasselled cap differencing

The tasselled cap transformation was discussed in Section 2.3.5.One disadvantage of simple image differencing is that is only allows for one band of information to be processed at a time (Hayes and Sader, 2001). One way of obtaining more information from image differencing is by first transforming the data so that information from multiple bands may be combined. The tasselled cap transformation was used to achieve this. It converts the original bands of the Landsat TM image into brightness, wetness and greenness bands. The tasselled cap transformation in this study was discussed in section 3.5.2.

In this study, the brightness band was used during image differencing. As discussed in section 2.3.5, various different studies have found that different bands (brightness, greenness, or wetness) of the tasselled cap transformation were the most useful for their study. There is no straightforward way to select the best band to use. It was decided to use the brightness band since this has been successful in land-cover studies using multi-temporal images (Fung and LeDrew, 1987) and because the author felt it would be the most able to show changes across a variety of classes, from natural to built-up to beach areas.

Differencing was again performed between all images of successive dates, as well as between the first (1985) and the last (2011) image, yielding six brightness difference images in total.

The results of the brightness band image differencing are given in Section 4.4.

3.6.3. Vegetation Index Differencing

Certain methods focus on specific parameters in the real world for different aspects of a study. For example, the study of vegetation changes has a direct application to erosion and erosivity since vegetation loss generally results in increased erosion (Kwarteng and Al-Ajmi, 1996). A popular method of estimating vegetation parameters is use of the Normalised Difference Vegetation Index (NDVI) (Ramsey et al., 2004). Use of such vegetation indices may also provide more specific information than is available in the individual bands. Vegetation indices were discussed in more detail in Section 2.3.5.

Spectral differences can provide data about the health, extent, and changes occurring in a plant community (Mouat et al., 1993). A technique used by Hayes and Sader (2001), called RGB-NDVI, involves the use of an NDVI layer for each image, which is clustered into groups from low to high NDVI. An automated classification is performed and the interpreter can label change and no-change categories. Changes in NDVI levels over time can be observed. Hayes and Sader (2001) found that use of this method provided better results than simple NDVI differencing. They also suggest that NDVI changes may be interpreted through use of colour additive theory. By simultaneously projecting the NDVI from three different dates as the red, green, and blue layers of an image, major changes in NDVI between dates will appear in combinations of the primary (RGB) colours (Hayes and Sader, 2001). Knowing which date of NDVI is coupled with which display colour, the analyst can visually interpret the magnitude and direction of vegetation change (Hayes and Sader, 2001).

The production of the NDVI images for this study was discussed in Section 3.5.1. For this study, the NDVI images were segmented at a scale of 18 and classed from low to high, as discussed above in the methodology by Hayes and Sader (2001). A rule-based approach was used to class the NDVI in steps of 0.1. Rather than using the visual assessment RGB method used by Hayes and Sader (2001), a more objective change detection technique was selected for this study. The segmented layers were imported into ArcGIS, where a pairwise union was used to show the change in NDVI at each segment between successive image dates. The union command used in ArcGIS results in the combination of image data from

both dates in a single layer, with the attribute table containing the fields indicating the NDVI at both dates. A new field was created and populated with the change in values (e.g. change from 0.5-0.6 to 0.3-0.4, and so forth). The images were then coloured according to the amount of increase or increase in NDVI. This provided information about whether the NDVIhad increased or decreased in each segment. This method was essentially vegetation index differencing, performed on a segmented image rather than the original pixels.

The results of the vegetation index differencing are given in Section 4.5.

3.6.4. Boolean Change detection

Boolean change detection was performed via binary slicing on all the images. The creation of the raster colour slices was detailed in section 3.5.3. This method can be useful to define the coastline, allowing changes in the coastline shape and position to be assessed.

Although this method creates raster colour slices, ENVI is able to output the result in both raster and vector form. The vector images were imported to ArcGIS where a union was created between each two adjacent dates as well as between the first and last dates. The attribute table then included the values at each location at both dates. A new field was populated to show the change between the dates (e.g. 0-4% to 4-100%). This made it possible to see which regions had remained the same, and which had changed from ‘land’ to ‘sea’ and vice versa.

The results of this method are shown in Section 4.6.

3.6.5. Post-classification change detection

All of the above methods of change detection are performed using unclassified data. An alternative is the use of post-classification change detection. The major advantage of this method is the ability to provide a matrix of change information showing which classes have changed to what (Lu et al., 2004). The external impact from atmospheric and other factors between multi-temporal images is also reduced (Lu et al., 2004), although atmospheric correction had already been performed for this study. The main disadvantage of this method is that it is time-consuming to perform (Lu et al. 2004). Studies by Mas (1997; 1999) compared six different change detection methods and found that post-classification change detection was the most accurate.

Image classification was discussed in Section 3.3. In this study, post-classification change detection was performed on the results of this classification. This method shows both the areas where change has occurred, as well as the nature of the change, for example beach to shallow coastal, cultivated to built-up, and so forth. The classified images were imported into ArcGIS where a union at two dates was used to identify the change which had occurred between them. This was performed at the same time gaps listed under Section 3.6.1, i.e. between each two successive dates as well as between the first and last dates.

The results of the post-classification change detection are given in Section 4.3.

3.7. Digital shoreline analysis system

In order to provide a detailed analysis of changes in beach width and position, the Digital Shoreline Analysis System (DSAS) was used. This is a freely available software application for use as an add-on within the ArcGIS software. It is capable of computing various rate-of-change statistics when supplied with a time series of image-derived vector data (Thieler et al., 2009).

Aerial photographs were used for the Digital Shoreline Analysis System. The higher spatial resolution and longer history available with aerial photography was exploited in order to focus on the changes specific to beach environments and beach position. One challenge faced while using multi-temporal aerial photography was the changing image resolution between jobs. It was decided not to resample the photographs to the coarsest resolution since it was possible to specify a different measure of accuracy for each image into the digital shoreline analysis, meaning that the information included in an image with a better resolution had a positive effect on the accuracy of the results.

It is important to note that aerial photographs were not captured at frequent intervals as is the case of Landsat scenes. Therefore, the available aerial photographs were captured at different seasons meaning that seasonal changes would affect the results. Consequently, direct comparison between images was not always relevant. These variables need to be taken into account when interpreting the results of multi-temporal aerial image analysis.

The input data for DSAS is a feature class within a personal geodatabase containing all the shoreline data from the different years to be analysed. The shoreline positions were manually digitised and placed in the feature class together with information on the date for which the shoreline position was recorded. All shoreline vectors should be referenced to the same feature before using DSAS (Thieler et al., 2009). As discussed in Section 2.3.2,

several different indicators may be used to determine the shoreline position. In this case, the wet/dry line was used, since indicators like the high water line were indistinguishable on the available imagery.

Additional data including the date, positional uncertainty, and the dates on which the transects were created were also entered for each shoreline vector. The date for each vector is necessary to determine all the rate of change statistics. The positional uncertainty is necessary since the calculated rates of change as provided by DSAS are only as reliable as the shoreline data with which it is provided. The uncertainty as provided is incorporated into the calculations (Thieler et al., 2009). Romine et al. (2009) identified potential sources of uncertainty in shoreline position interpreted from aerial photographs as pixel error, rectification error, seasonal error, and tidal fluctuation error.

For this study, all dates were entered as accurately as they were known. In most cases, the exact date was known. In cases where only the month was known, the date was set as the 15th of that month. In cases where only the year was known, the date was set as the 1st of July of that year. For the uncertainty field, the measured pixel size was entered. This was based on the assumption that the shoreline could be digitised with an accuracy of up to one pixel. The sources of error listed above also limit the accuracy of the results, but are more difficult to quantify.

The DSAS tool requires that a baseline be defined alongside the shoreline vectors. The baseline is essentially the reference position based on which change vectors are identified. The DSAS algorithm then works by casting transects perpendicular from the baseline to intersect the shoreline vectors at different dates. An example of the shoreline vectors digitised for each date, baseline, and transects produced by the tool is shown in Figure 10. The points of intersection of the transects with the shoreline position vectors provide both location and date information which are then used to calculate the rates of change (Thieler et al., 2009). Ideally, the transects should be cast perpendicular to the general trend of the shorelines, so that shoreline change rates describe the area immediately seaward of the current shoreline (Thieler et al., 2009). The transect spacing for this project was selected as 20 m in order to show change along the entire study region. The transect casting was smoothed for 10 m in order to accommodate sudden changes in the angle of the baseline. This means that a supplemental baseline was temporarily created 10 m to each side of each transect position in order to determine the orientation of the transect at curved sections along the baseline.

Once all of the abovementioned necessary data had been input, the DSAS toolbar was used to calculate change statistics. For each transect, the closest intersection with shoreline

vectors was selected for use in statistical calculations. DSAS runs the statistical calculations automatically via MATLAB (Thieler et al., 2009).

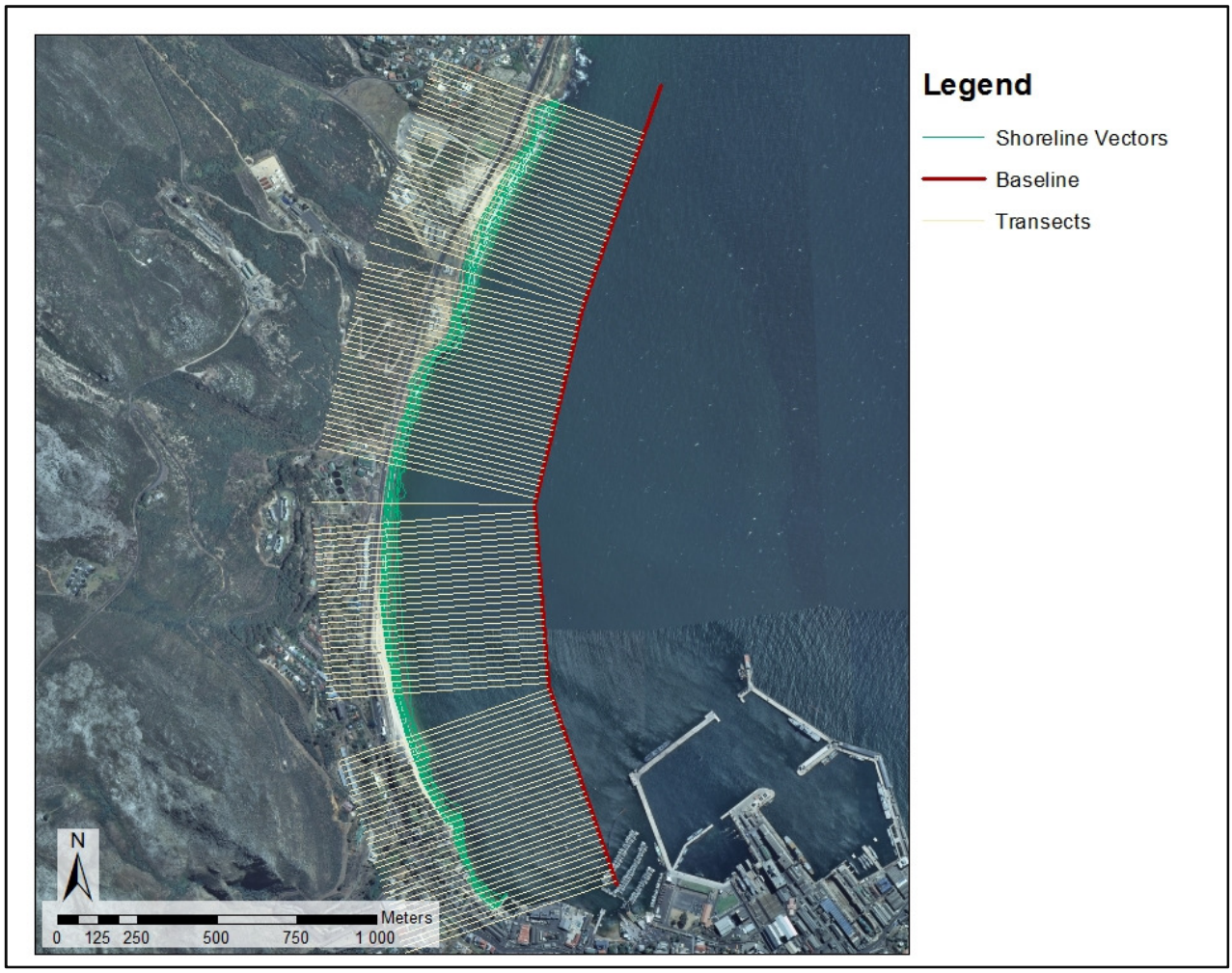

Figure 10: The DSAS setup at Bayview Heights. The aerial photograph is from 2010.

The statistics calculated were based on measured differences between shoreline positions through time and are measured in metres of change along transects per year (Thieler et al., 2009). The following statistics are reported:

- Shoreline change envelope. This reports the total change in shoreline position from the shoreline closest to the baseline to the shoreline farthest from the baseline, no matter which dates the shoreline positions represent. The change envelope is given as a distance in metres as opposed to a rate of change (Theiler et al., 2009).

- Net shoreline movement. This reports the overall change in shoreline position from the first date to the last date supplied. The change is again measured as a distance in metres rather than a rate (Theiler et al., 2009)

- End point rate. As with the net shoreline movement, the end point rate uses the shoreline positions at the first and last dates. However, the end point rate reports the rate of change in metres per year as opposed to just the distance (Theiler et al., 2009). The confidence of the end point rate is also supplied.

- Linear regression rate. This is a measure of the rate of change of shoreline position in metres per year. It is determined by fitting a least-squares regression line to all the shoreline points for a particular transect such that the sum of the squared residuals is minimised (Theiler et al, 2009). This statistic uses all data, unlike the above measures which only include the first and last dates and thus miss cyclical trends. While this is a useful and widely accepted method, it can be susceptible to outlier effects and can underestimate the rate of change relative to other statistics (Theiler et al., 2009). The standard error, confidence interval, and R-squared are also supplied.

- Weighted linear regression rate. Again, this is a measure of the rate of change of shoreline position in metres per year.It is calculated in the same way as the linear regression rate, except that greater emphasis is placed on data with a better positional certainty (i.e. data with a smaller pixel size) (Theiler et al., 2009). The standard error, confidence interval, and R-squared are also supplied.

- Least median of squares. This is another measure of the rate of change of shoreline position in metres per year.It is calculated in the same way as linear regression, except that the median of the squared residuals is used rather than the mean. This is a more robust method, minimising the effect of outliers (Theiler et al., 2009).

A confidence interval of 95% for the statistics was selected. The outputs of the calculations are given in Appendix A. Figures illustrating all of these measures are given in Section 4.7.

4. RESULTS

This chapter gives the results obtained by all the methods used as described in Chapter 3. The results of the object-based classification are given in Section 4.1 with the accuracy assessment of this classification in Section 4.2. The remainder of the chapter supplies the results of the various change detection techniques used. Post-classification change detection results are shown in Section 4.3. Image differencing both of band 4 and of the brightness band is shown in Section 4.4. Change detection using the NDVI is given in Section 4.5 and the results of the binary slicing method are given in Section 4.6. The results of the shoreline position change detection on aerial photographs at the four focus areas are given in section 4.7.

4.1. Classification results

The steps taken during image classification are given in Section 3.3. The results of this classification are useful in supplying context for the study, allowing the end-user a faster overview of the contents of the study area, as well as making post-classification change detection possible.

Eleven classes were used for the classification: beach; built-up; cultivated; dams; mountain; mountain shadow; natural; ocean; sand (not beach); sand dune; and shallow coastal. Although some of these classes may not be directly relevant to the study – for example, the differentiation between mountain and mountain shadow is not relevant to coastal erosion – it was necessary for the ease of classification between classes which visually appear vastly different. These classes were combined during later processing and interpretation steps where necessary. The percentage of the study area classified into each class for each study year is given in Table 3. The Landsat 5 TM/Landsat 7 ETM+ images spanning all six dates from 1985 to 2011 were separately classified and are shown in Figure 11.

Table 3*:* The percentage of the study area classified into each class for each study year. Mountain and mountain shadow were joined to form a single class in this table.

	Beach	Built-up	Cultivated	Dams	Mountain	Natural	Ocean	Sand (not beach)	Sand dune	Shallow coastal	Total
1985	0.52	6.83	6.85	0.55	12.43	7.71	60.60	0.73	3.22	0.55	100
1991	0.40	7.45	9.25	0.52	12.63	5.32	60.50	0.64	2.76	0.55	100
1996	0.35	8.01	7.89	0.63	12.24	5.49	60.67	0.57	3.65	0.48	100
2001	0.46	9.57	5.88	0.56	12.24	5.98	60.38	0.54	3.47	0.92	100
2006	0.41	9.12	8.06	0.51	11.44	5.89	60.46	0.59	2.76	0.76	100
2011	0.49	9.59	5.75	0.52	12.55	7.41	60.11	0.56	2.06	0.96	100

Since this was an object-based classification, one challenge faced was that some segments represented more than one land cover class, although most covered only one class. In

cases where more than one class was included, it was attempted to classify the sample into that class which covered the largest area within the segment.

The classified images clearly show a gradual increase in built-up regions over the years. This is the most noticeable change, as regions which were initially natural, cultivated, sand (not beach) or sand dune gradually change to built-up. Large decreases in sand (not beach) and sand dune classes are also seen. In the region of greatest urban expansion in the image, the central northern region, gradual change can be seen from one image to the next as sand dune changes first to sand (not beach) and then to built-up. Various other changes take place at a smaller scale.

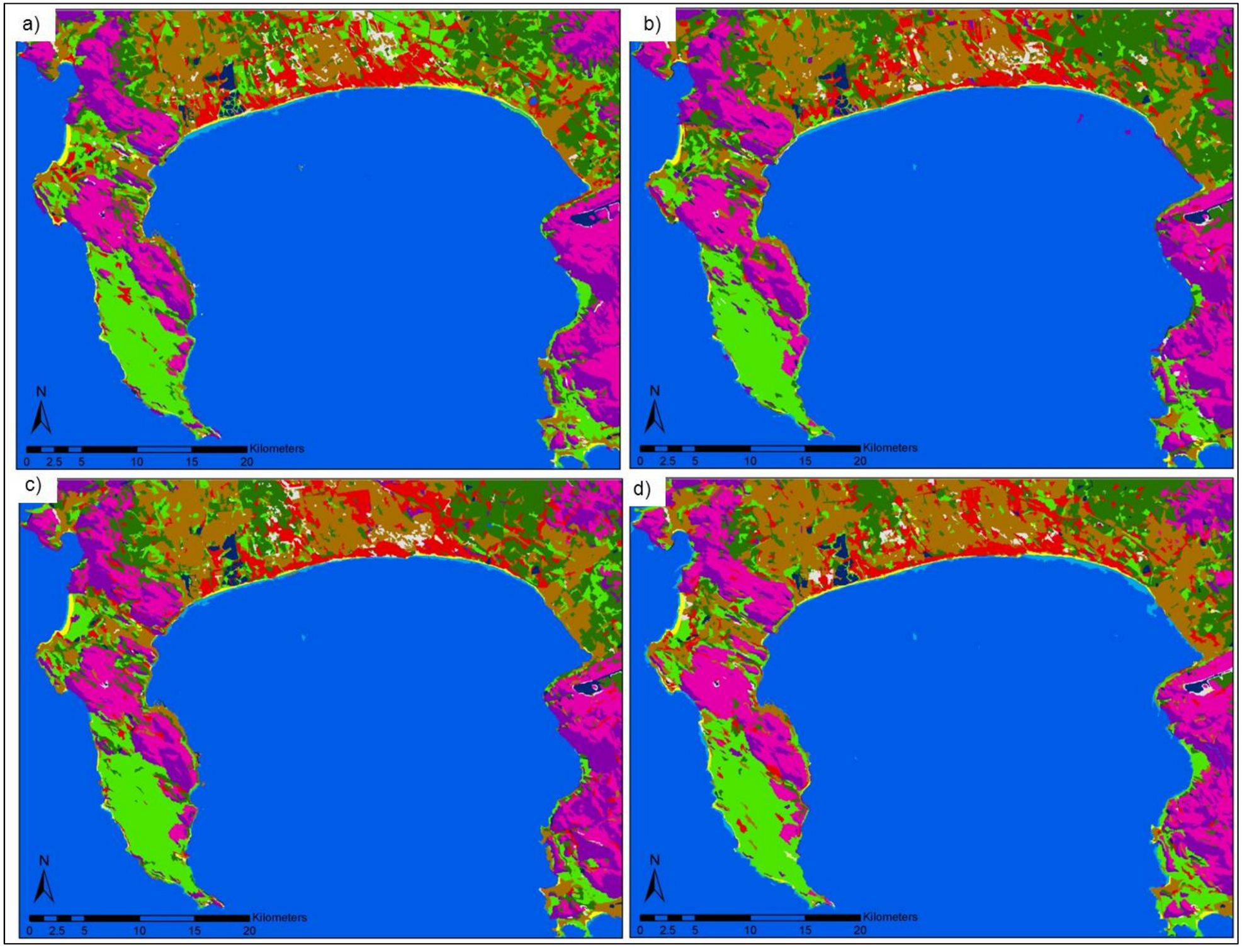

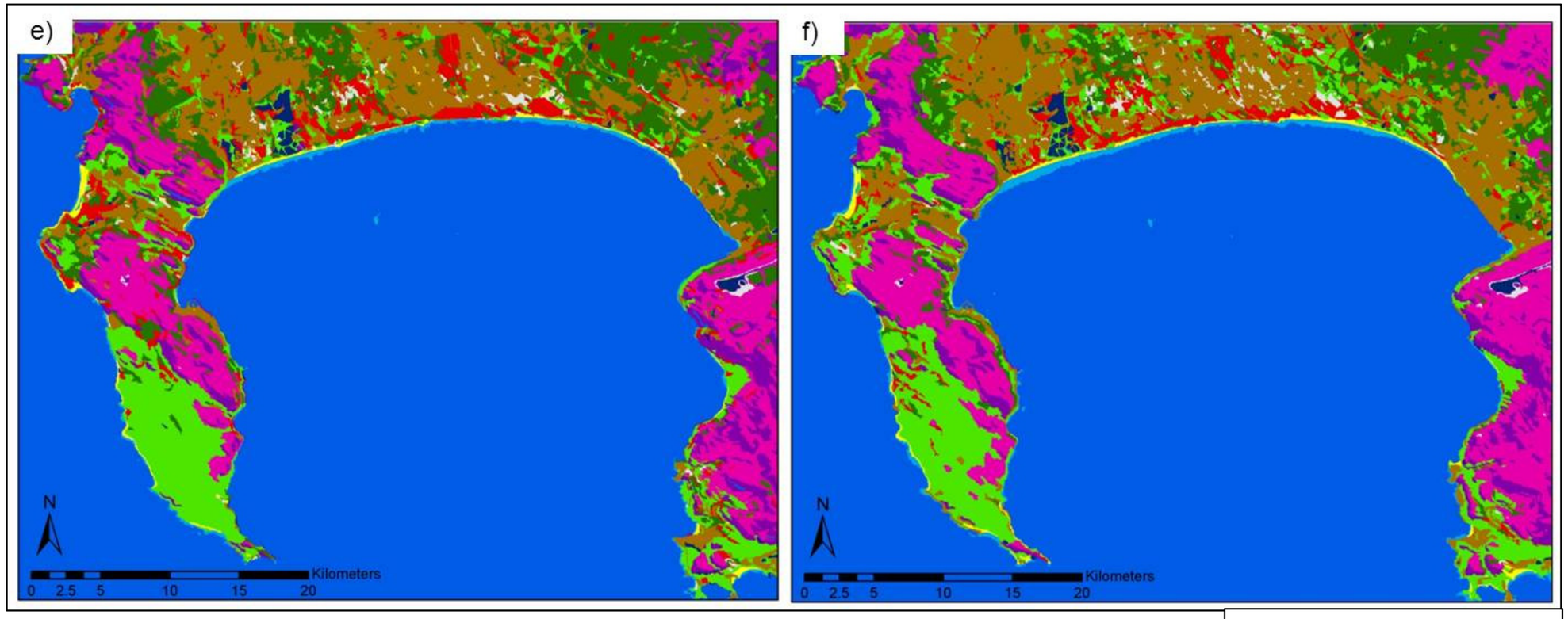

Figure 11: The object-based classifications based on the Landsat TM images for all dates used in this study. a) the 1985 classification; b) the 1991 classification; c) the 1996 classification; d) the 2001 classification; e) the 2006 classification; f) the 2011 classification.

4.2. Accuracy assessment

Once the classification was completed, an accuracy assessment was also performed as described in Section 3.4. The accuracy is presented in the form of error matrices, which are efficient and useful reporting tools. The full error matrices are given in Appendix B. One of the easiest to determine yet most useful statistics obtainable from such a matrix is the overall accuracy. All the classifications performed had a high overall accuracy of over 85%. The accuracies of the individual classes, however, were more variable. Certain classes had exceptionally high accuracies, notably the ocean class, which had both user's and producer's accuracies of over 97% in every case and averaged over 99%. This high accuracy was achievable due to the unique nature of the ocean class, making it more easily distinguishable from the other classes. The few errors which did occur in this class included ocean being classified as dams or as shallow coastal (producer's errors); and mountain shadow being classified as ocean (user's error).

Other classes appeared more similar with considerable spectral overlap in some cases, and hence there were considerably more errors. The next best classified class was the shallow coastal class. The average accuracy for this class was 90.9% and it was over 90% in almost all cases. It had a considerably lower accuracy in only one case, in the user's accuracy for 2001 where it was 63.1%. This was due to a higher amount of ocean segments being classified as shallow coastal within this year, and was the only large discrepancy in the user's accuracy in any year, although there were also cases of beach, natural, ocean, built-up, and mountain shadow being classified as shallow coastal in small amounts. The most common producer's error was shallow coastal regions being classified as beach.

The dams class was well classified with an average accuracy of 88.9% and in a few cases reached 100% producer's accuracy. The user's accuracies were not quite as high and the lowest was 67.6% in 1991. While the dams class had an exceptionally high producer's accuracy, the most common producer's accuracy errors were misclassifications of dam as ocean or natural. There were user's errors in this class where mountain shadow regions were classified as dams. To a lesser extent, ocean and natural classes were also notable in being classified as dams.

Both mountain and mountain shadow classes had a fairly consistently high accuracy. Both user's and producer's accuracy for these were over 74% in all cases except for the producer's accuracy in 1996, where mountain dipped to 66.3% and mountain shadow to 68.8% accuracy. The average accuracy for the mountain class was 83.5% and for mountain shadow was 79.8%. In most cases, their accuracies were over 80%. The most common

producer's errors for mountain were misclassifications as mountain shadow and cultivated. In some cases, mountain was also misclassified as sand dune. The most significant user's errors were cultivated regions being classified as mountain. Mountain shadow regions were also sometimes classified as mountain. Misclassifications between the mountain and mountain shadow classes are however of very little importance for this study, and the main reason they were kept as separate classes was for ease of classification. Once again, part of the producer's error in the mountain shadow class was explained by misclassification to mountain; however the most significant errors were misclassifications to the spectrally similar dams class. User's errors typically involved the mountain, cultivated, and natural classes.

The important beach class was well classified, with the lowest accuracy being the user's accuracy in 1985 at 74.8%. The accuracy was well over 80% in most cases and reached 95.8% for the producer's accuracy in 2001. The average accuracy was 86.1%. The most common producer's error for the beach class was misclassification to the sand (not beach) class. Misclassification to shallow coastal also occurred. Sand (not beach) and shallow coastal being classified as beach explained the most common user's errors as well, although confusion with natural and built-up classes also occurred.

The remaining five classes were the least accurately classified, although their accuracies were still adequate. Natural had an average accuracy of 75% and ranged from 62.98% to 91.8%. Its most common producer's errors were misclassifications to cultivated, built-up, and sand dunes, although there was also a small amount of confusion with mountain shadow, beach, dams, sand (not beach) and shallow coastal. User's accuracy errors were similarly the most common in cultivated, built-up and sand dunes being classified as natural.

The built-up class had an average accuracy of 77.3% and ranged from 69.9% to 83.5% accurate. Once again, there was confusion between several classes in both user's and producer's accuracy, most significantly natural, cultivated, sand dune, and sand (not beach).

Sand (not beach) had an average accuracy of 76.96%. In one case, the user's accuracy fell to 55.4% (in 2006), however, in most cases the accuracy was over 75%. The main classes involved in both user's and producer's errors were beach, built-up, and sand dune.

The cultivated class had an average accuracy of 67.9% with a range from 56.0% to 84.7%. Again, several classes were involved in the errors for the cultivated class, most notably mountain, mountain shadow, natural, built-up, and sand dune.

The least accurately classified class was the sand dune class. It had an average accuracy of 65.9% and ranged from 48.2% to 89.3%. This was also the greatest range of different accuracies. The lowest producer's accuracy was 66.3%, with most being over 75%, while the user's accuracies were lower. The greatest proportions of producer's error for this class came from misclassifications to natural and built-up. The user's accuracy was lower and stemmed most significantly from misclassifications form the natural, cultivated, and built-up classes.

4.3. Post-classification change detection

The main advantage in performing image classification in a change detection study is the ability to visually see which classes have been subject to the most significant change. Therefore, the classified images shown in Section 4.1 were used for post-classification change detection. The steps taken for post-classification change detection are given in Section 3.6.5. When looking at all 11 classes used in the classification, a large amount of change can be seen between images. Naturally, some of this change can be explained by classification errors in one or other image, resulting in false change from a misclassification to the actual class. This would result in an overestimation of the actual change taking place. However, the change images still provide useful information and a valuable overview of the change in the study region. Focussed study on specific areas allows the correct change shown to be extremely useful.

Table 4 shows the percentage increase and decrease in each of the classes taken as individual classes. This shows that some changes which appear small over the total image are actually large within the individual class. For example, the built-up class had an overall increase of over 40% from its original extent. The changing percentage classified as each class is also shown graphically in Figure 12, Figure 13, and Figure 14.Images showing the total change in all classes from year to yearare given in Appendix D.

Table 4*:* The changes in area of each class shown as a percentage of that specific class. The percentage change is calculated from the previous date (i.e. from 1985 to 1991, then from 1991 to 1996, etc). The bottom row shows the total percentage change per class from 1985 to 2011.

	Beach	Built-up	Cultivated	Dams	Mountain	Natural	Ocean	Sand (not beach)	Sand dune	Shallow coastal
1985	0.00	0.00	0.00	0.00	0.00	0.00	0.00	0.00	0.00	0.00
1991	-23.35	9.02	35.07	-6.78	1.64	-31.05	-0.18	-13.09	-14.12	-1.51
1996	-12.13	7.64	-14.69	22.45	-3.10	3.25	0.29	-9.97	32.21	-11.36
2001	31.48	19.42	-25.47	-11.24	-0.04	8.94	-0.48	-5.52	-5.01	89.63
2006	-11.74	-4.72	37.16	-8.76	-6.50	-1.60	0.13	9.22	-20.37	-17.29
2011	20.03	5.20	-28.72	1.49	9.71	25.83	-0.57	-5.01	-25.56	27.02
Total	-6.17	40.46	-16.04	-6.19	0.99	-3.99	-0.81	-23.31	-36.06	73.93

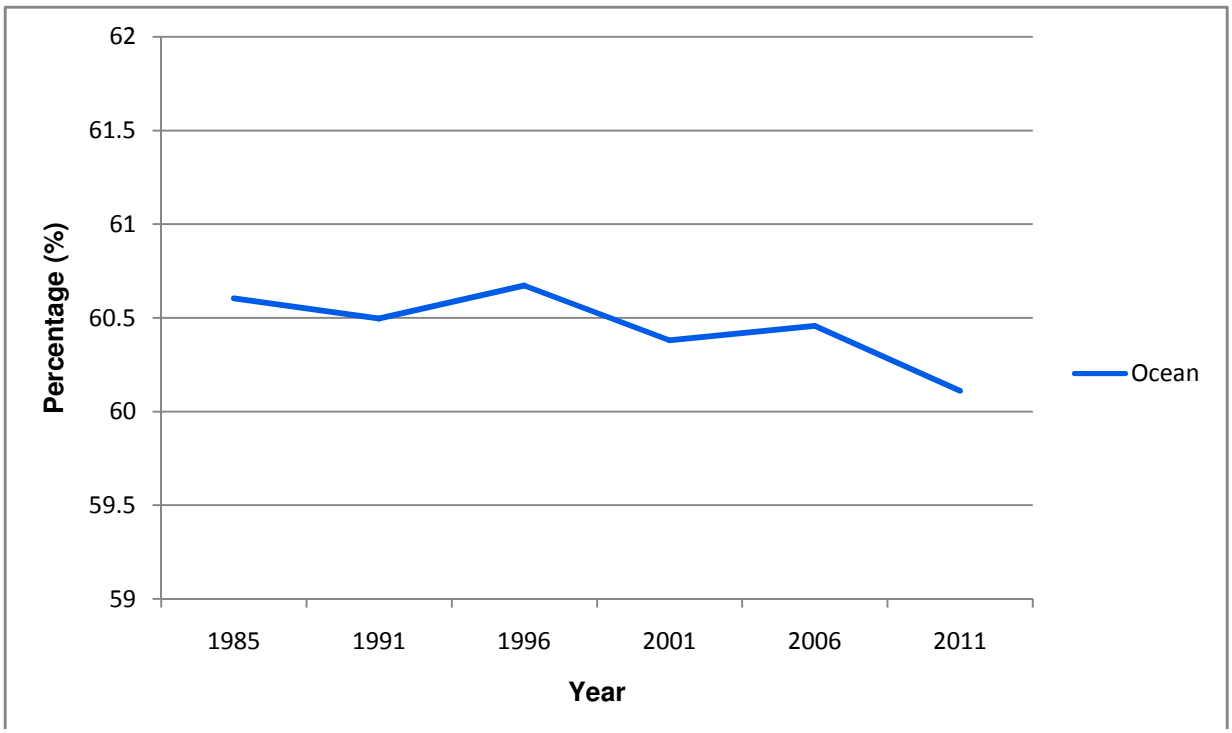

Figure 12: Changes in percentage of the study area classified as ocean over time

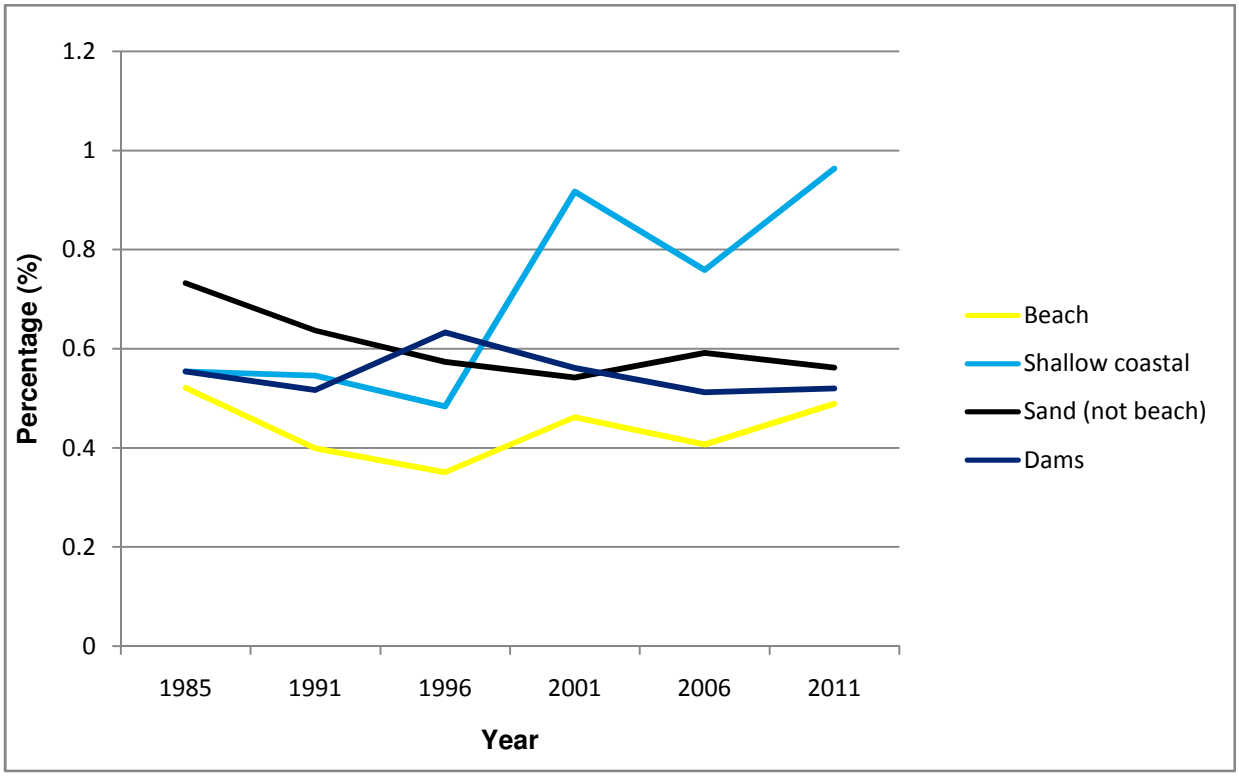

Figure 13: Changes in percentage of the study area classified as beach, shallow coastal, sand (not beach), and dams over time.

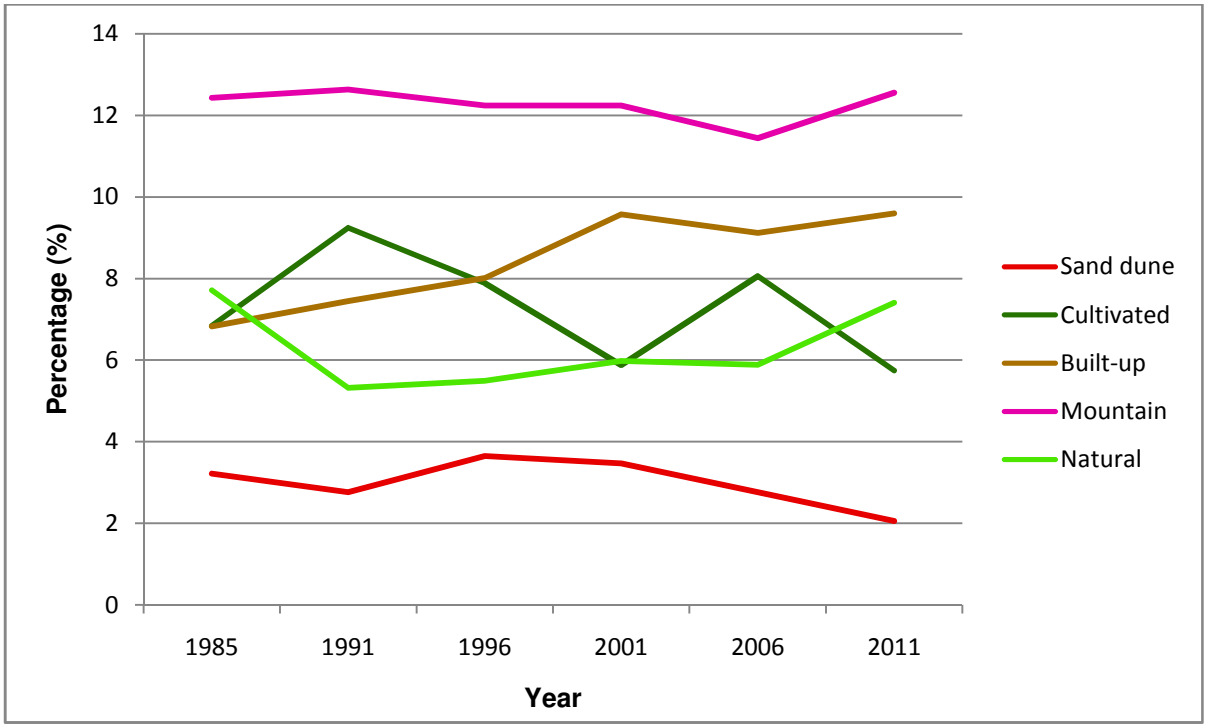

Figure 14: Changes in percentage of the study area classified as sand dune, cultivated, built-up, mountain, and natural over time.

The inclusion of all 11 classes in a single change image such as those shown in Appendix D is somewhat confusing due to the high amount of change which is visible. Large amounts of this change may not be particularly relevant to this study, between classes which were included for ease of classification or to make the classified images easier to interpret (e.g. mountain versus mountain shadow classes). In addition, including all the classes at once makes the important benefit of being able to see from which to which class the change has occurred impossible. Using 121 different colours to show every possible change of class would make it too difficult to distinguish different colours, while the approach used in the images above makes it impossible to see what the original class was. For this reason, the number of classes was reduced by creating an 'other' class including several less important or less relevant classes. In order to still show all the relevant change, several different combinations were selected, showing important classes with a large 'other' class.

The first combination focused on offshore change, showing beach, shallow coastal, and ocean classes in combination with one large 'other' class. This is shown in Figure 15. Naturally, this focused all of the apparent changes onto one thin strip along the coastline. This allowed easier visualisation of changes that have occurred in the beach position. Changes that are seen further inland are likely the result of misclassifications. While the change seen in these images may seem little since it is confined to a narrow zone, the changes in this zone are vital in order to show beach position change as well as change resulting from different tidal heights. Changes are challenging to identify at this scale, though a dark green strip representing change from ocean to shallow coastal can be seen along much of the coastline from Bayview Heights to Strand. An examination of these images at a larger scale when looking at the specific regions of interest later on can provide insights to the differences between each region of interest. Zoomed in images at specific focus areas are given in Section 5.1.1.

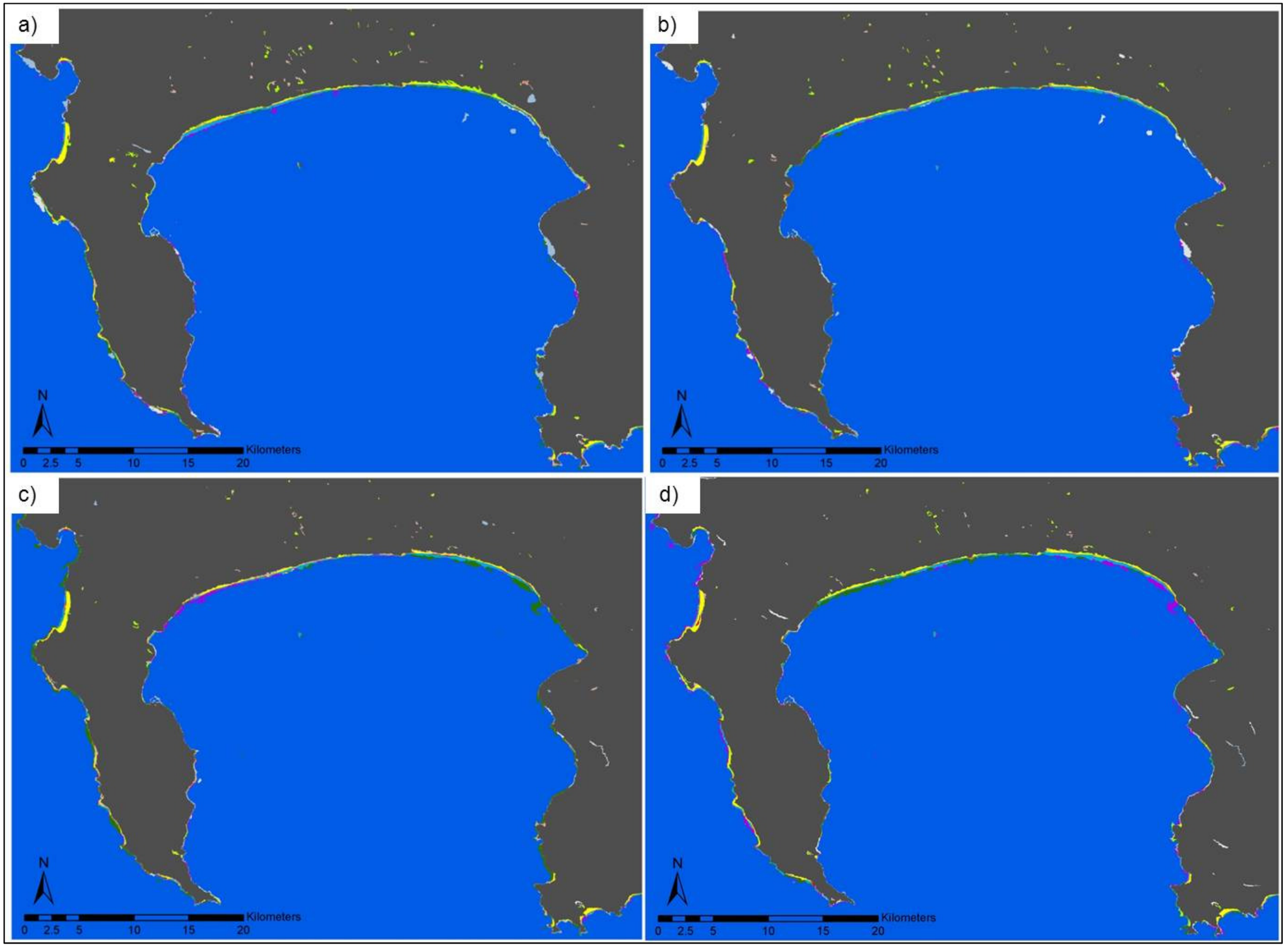

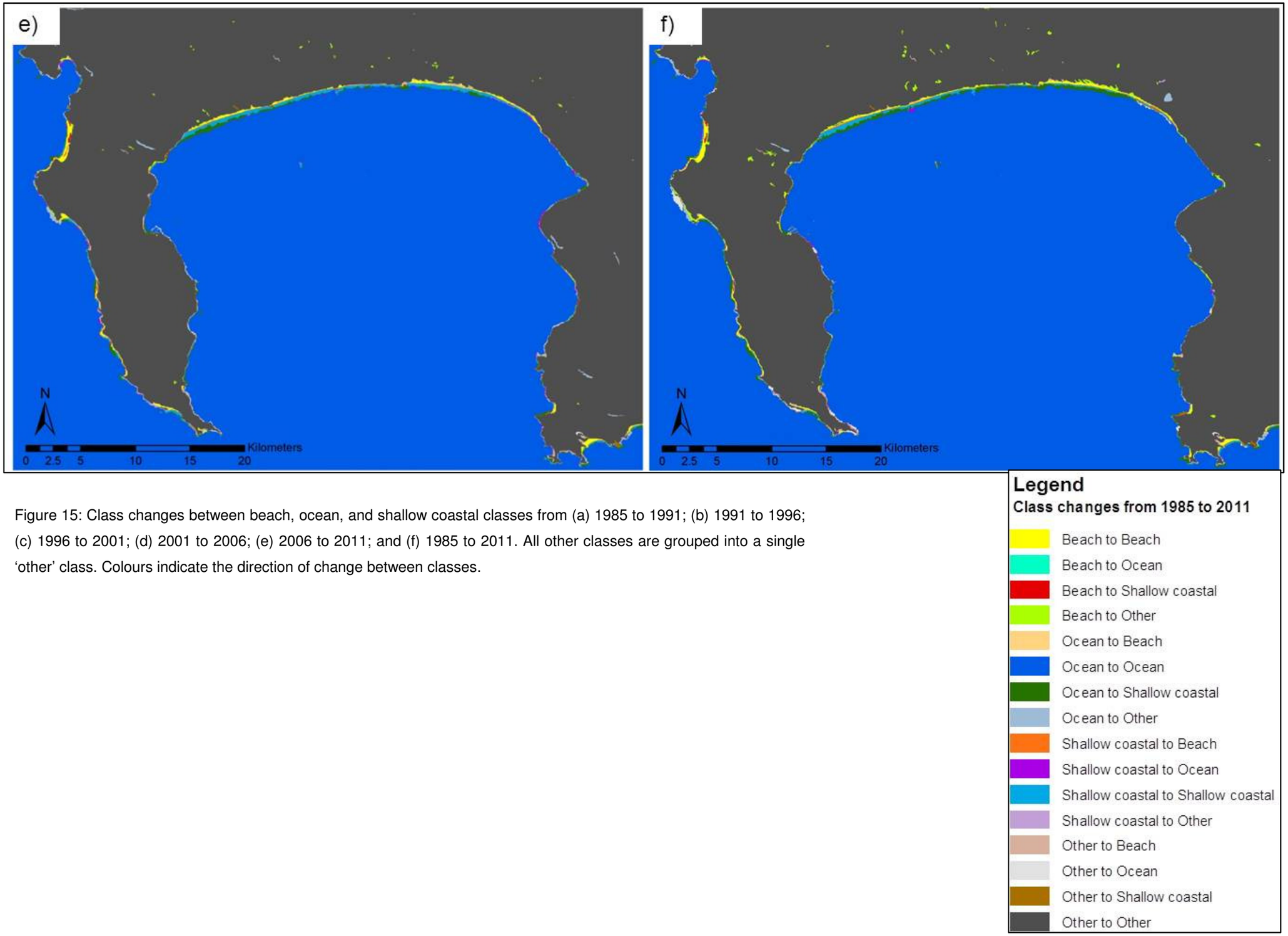

Figure 15: Class changes between beach, ocean, and shallow coastal classes from (a) 1985 to 1991; (b) 1991 to 1996; (c) 1996 to 2001; (d) 2001 to 2006; (e) 2006 to 2011; and (f) 1985 to 2011. All other classes are grouped into a single 'other' class. Colours indicate the direction of change between classes.

The second class combination used examined one of the most important aspects under investigation. It combined beach, dunes, and built-up with an ‘other’ class. The built-up class had the highest visible change throughout the study period due to the rapidly changing and expanding nature of the urban area. This was therefore an important indicator of increases in beach and dune vulnerability, since the urban expansion often came at the cost of removal of natural vegetation. These changes are shown in Figure 16. The most notable change in this class combination was the large red section seen in the central top zone of Figure 16: Class changes between beach, built-up and sand dune classes from (a) 1985 to 1991; (b) 1991 to 1996; (c) 1996 to 2001; (d) 2001 to 2006; (e) 2006 to 2011; and (f) 1985 to 2011. All other classes are grouped into a single ‘other’ class. Colours indicate the direction of change between classes.. This indicates change from sand dune to built-up. Cyan zones across much of the image also indicate changes from other classes to built-up. This provides an indication of the considerable urbanisation occurring in the study area within the study period.

Again, images at a larger scale at specific focus areas are given in Section 5.1.1.

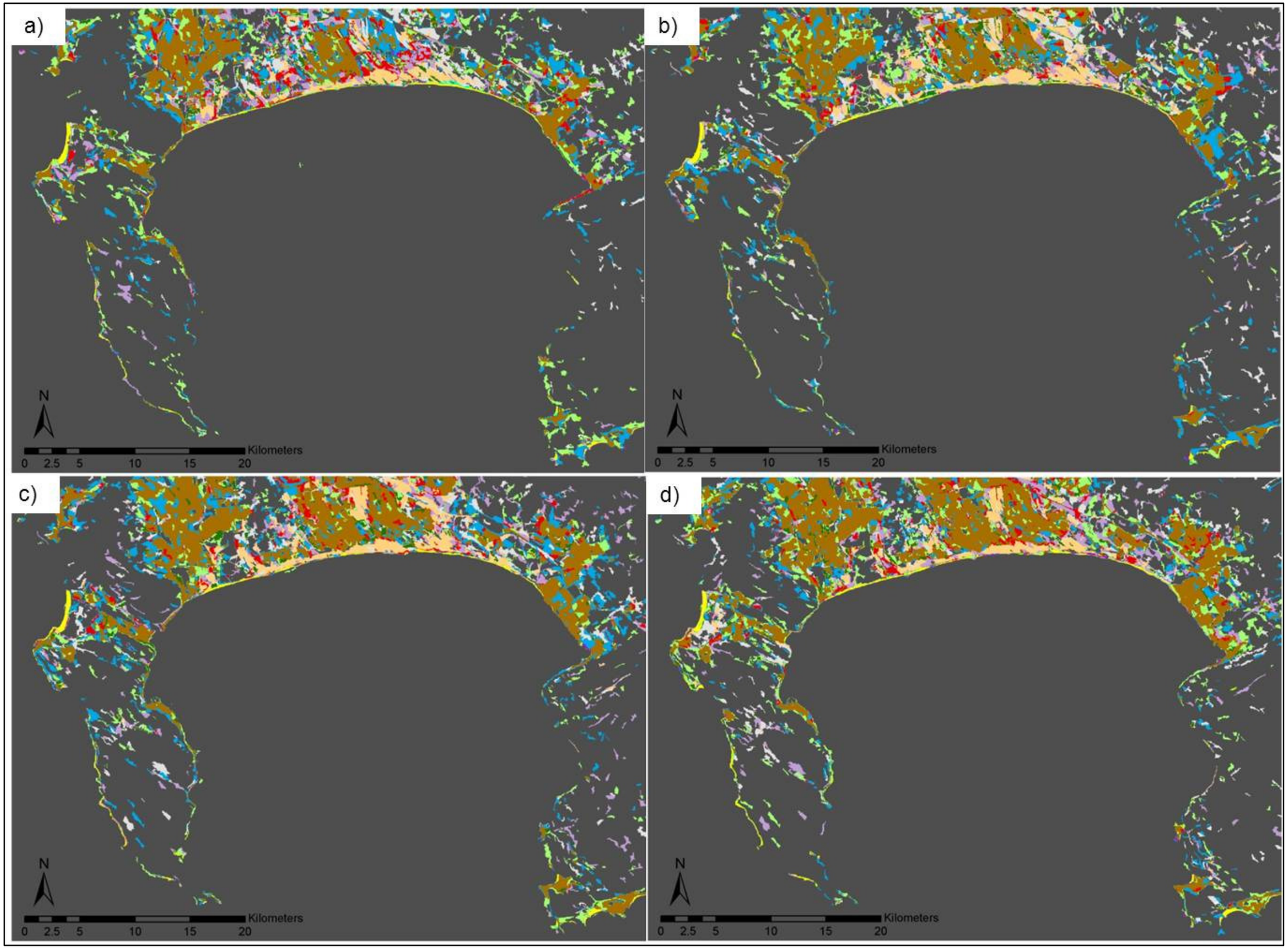

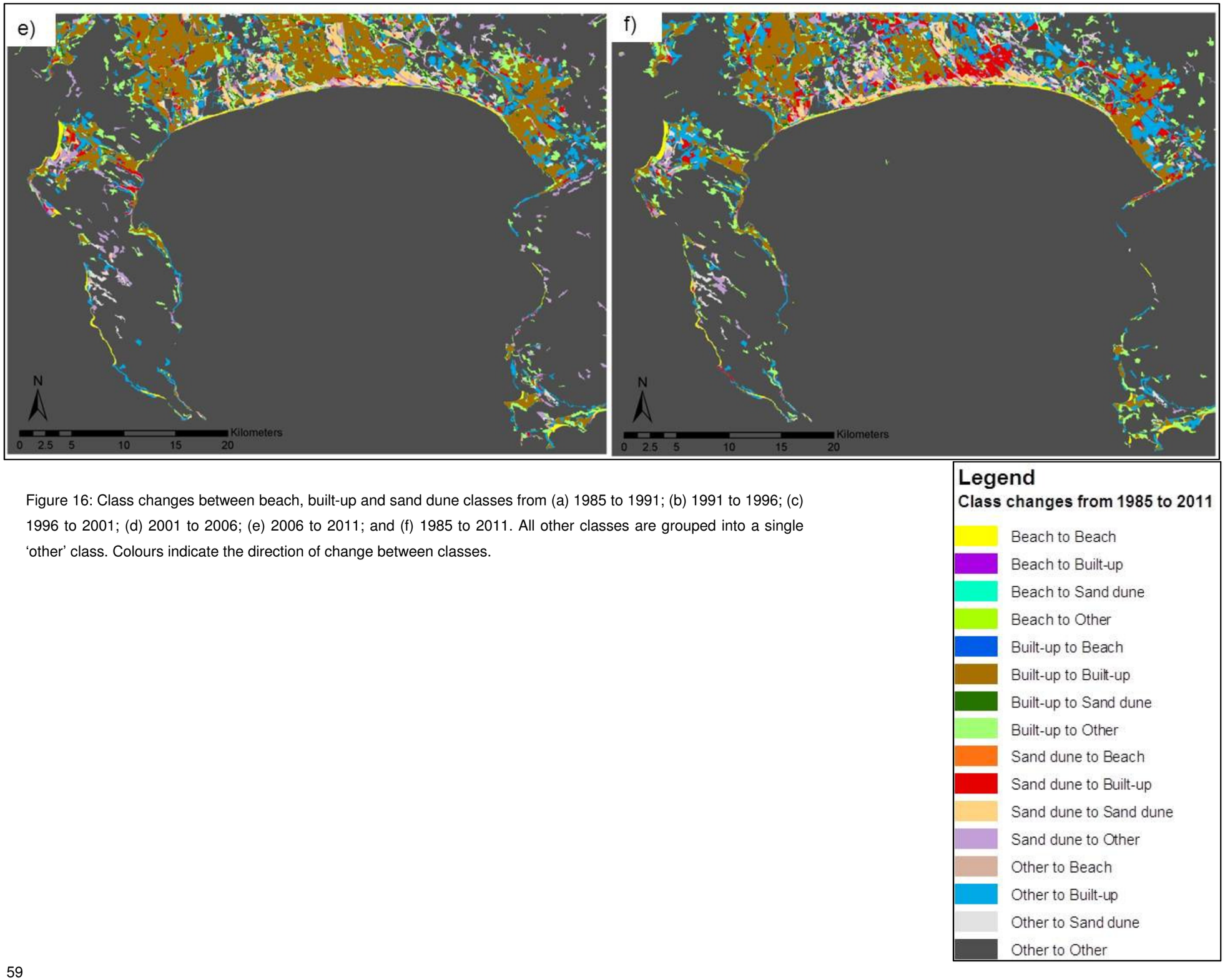

Figure 16: Class changes between beach, built-up and sand dune classes from (a) 1985 to 1991; (b) 1991 to 1996; (c) 1996 to 2001; (d) 2001 to 2006; (e) 2006 to 2011; and (f) 1985 to 2011. All other classes are grouped into a single 'other' class. Colours indicate the direction of change between classes.

The third and final class combination used combined beach, sand dunes, and shallow coastal with an 'other' class. These three classes were used separately in the previous combinations as well, but showing them together helps to emphasise the dynamism of the beach and dune environment. The sand dune class especially underwent considerable change over the study period. These changes are visible in Figure 17. Again, the most notable changes were in the sand dune class. Substantial sections of the sand dune class changed to other classes, shown in light blue.

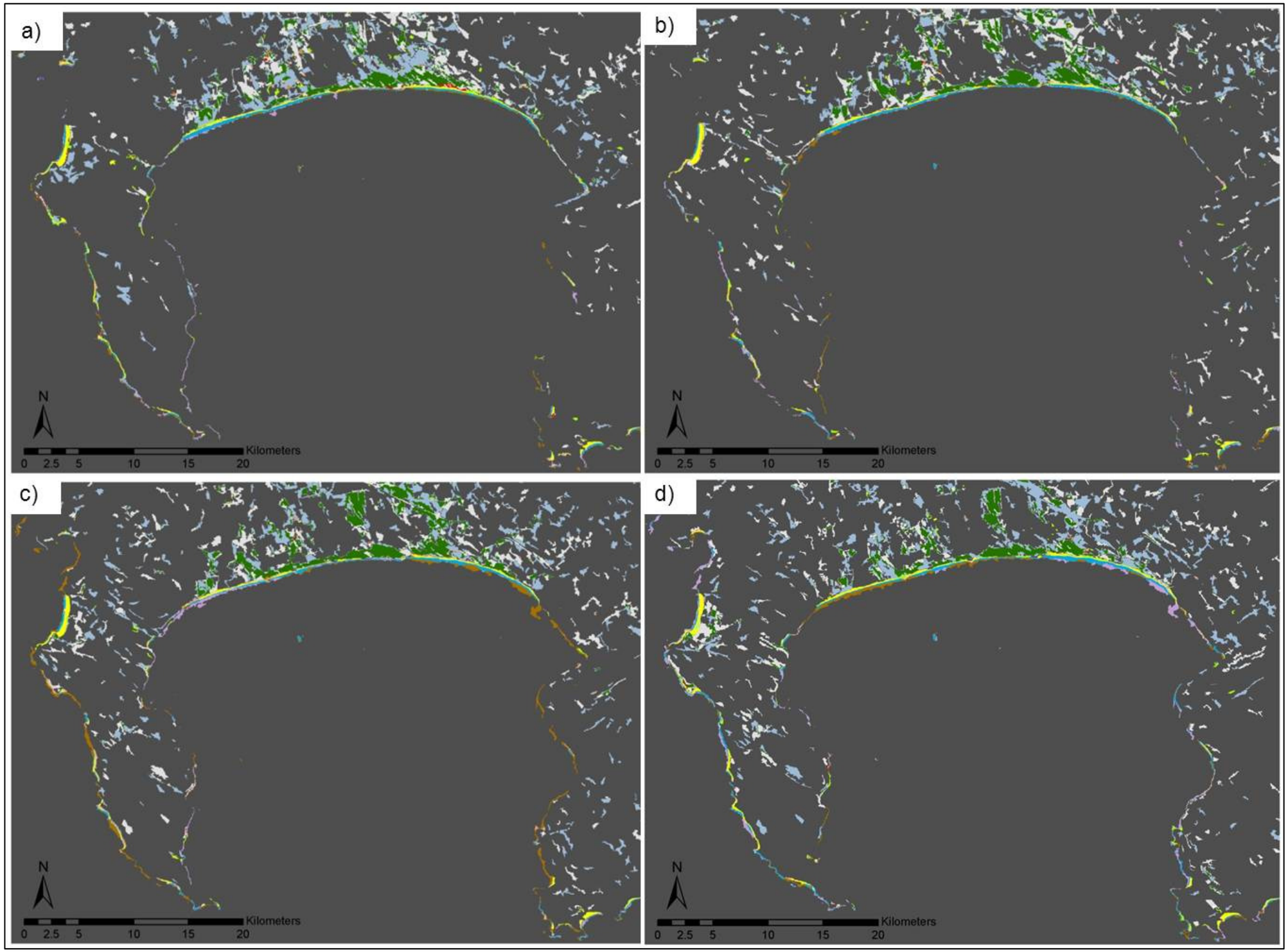

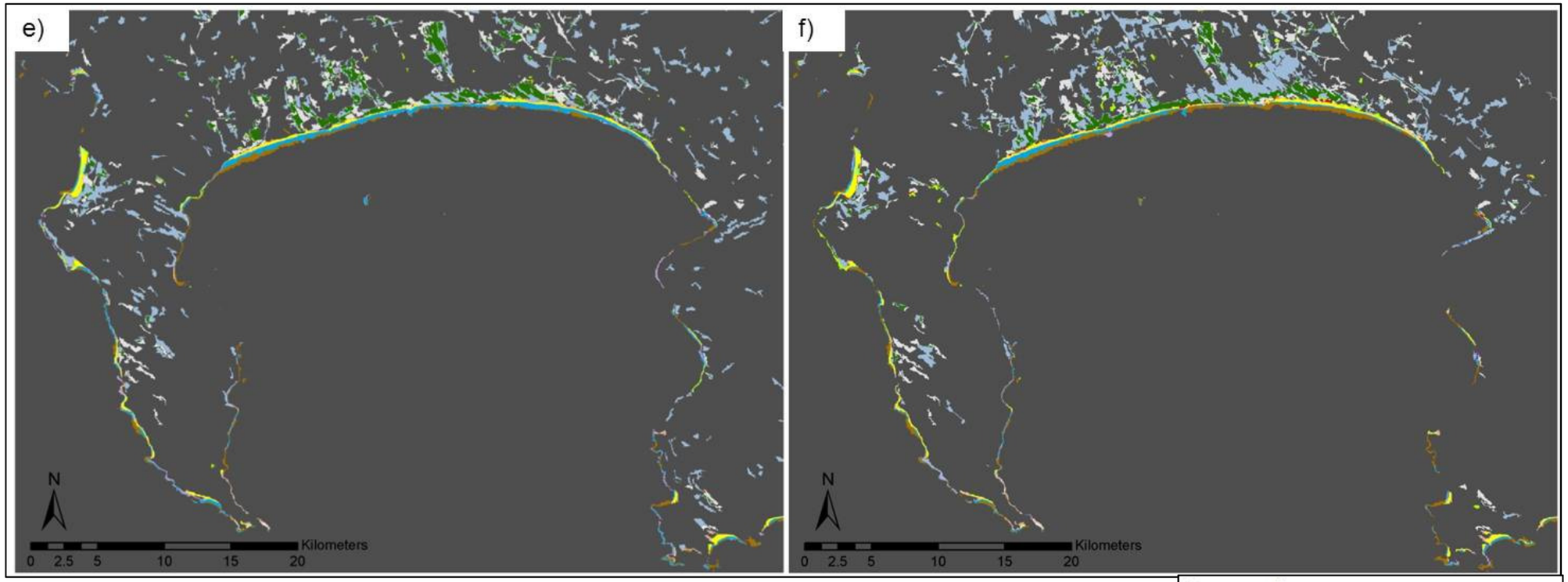

Figure 17: Class changes between beach, sand dune, and shallow coastal classes from (a) 1985 to 1991; (b) 1991 to 1996; (c) 1996 to 2001; (d) 2001 to 2006; (e) 2006 to 2011; and (f) 1985 to 2011. All other classes are grouped into a single ‘other’ class. Colours indicate the direction of change between classes.

4.4. Image differencing

Image differencing is one of the simplest and most commonly used methods of change detection. The steps taken to perform image differencing are given in Section 3.6.1. For this project, image differencing was firstly performed using band 4 (near infrared) of the Landsat TM images. In order to incorporate data from the other bands, a tasselled cap transformation (detailed in Section 3.5.2) was then performed and image differencing was done on the brightness bands, as detailed in Section 3.6.2. The tasselled cap images in RGB as well as the brightness bands alone can be seen in Appendix C.

The difference image resulting from the brightness bands tended to show considerably less change than those using band 4. This could mean that band 4 is more useful at identifying change, but it is likely an indicator that the brightness band is better able to isolate that change which is significant and relevant. The brightness band changes also tended to show more increases while band 4 showed more decreases. Since band 4 is a good indicator of vegetation health, the consistent decreases over the years may be an indicator of vegetation decreasing as the region became increasingly built up. Both types of image differencing for all successive date pairs can be found in Figure 18toFigure 23.

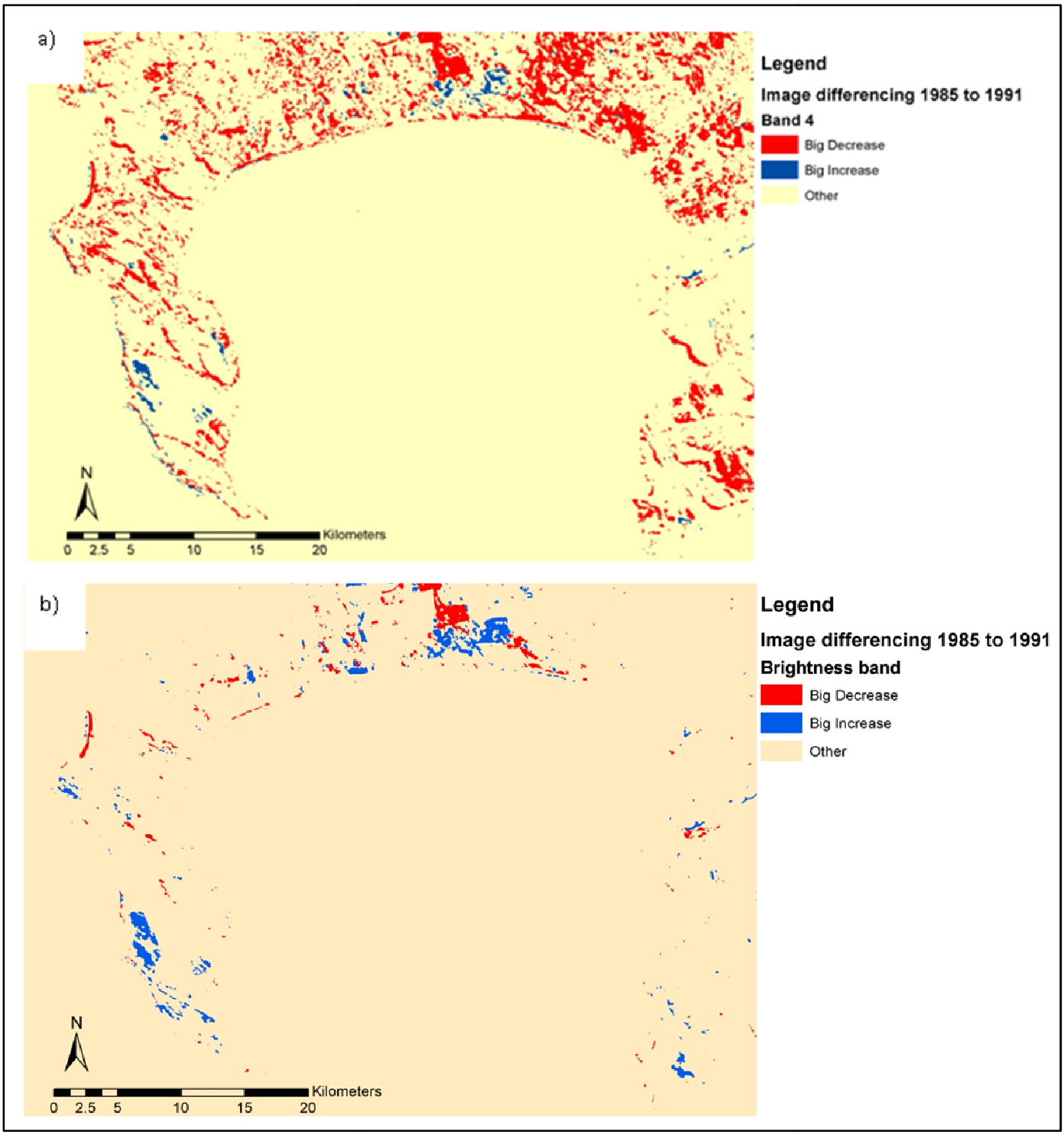

Figure 18: The image differencing results for image change from 1985 to 1991. Depicted is a) image differencing of band 4, and b) image differencing of the brightness band.

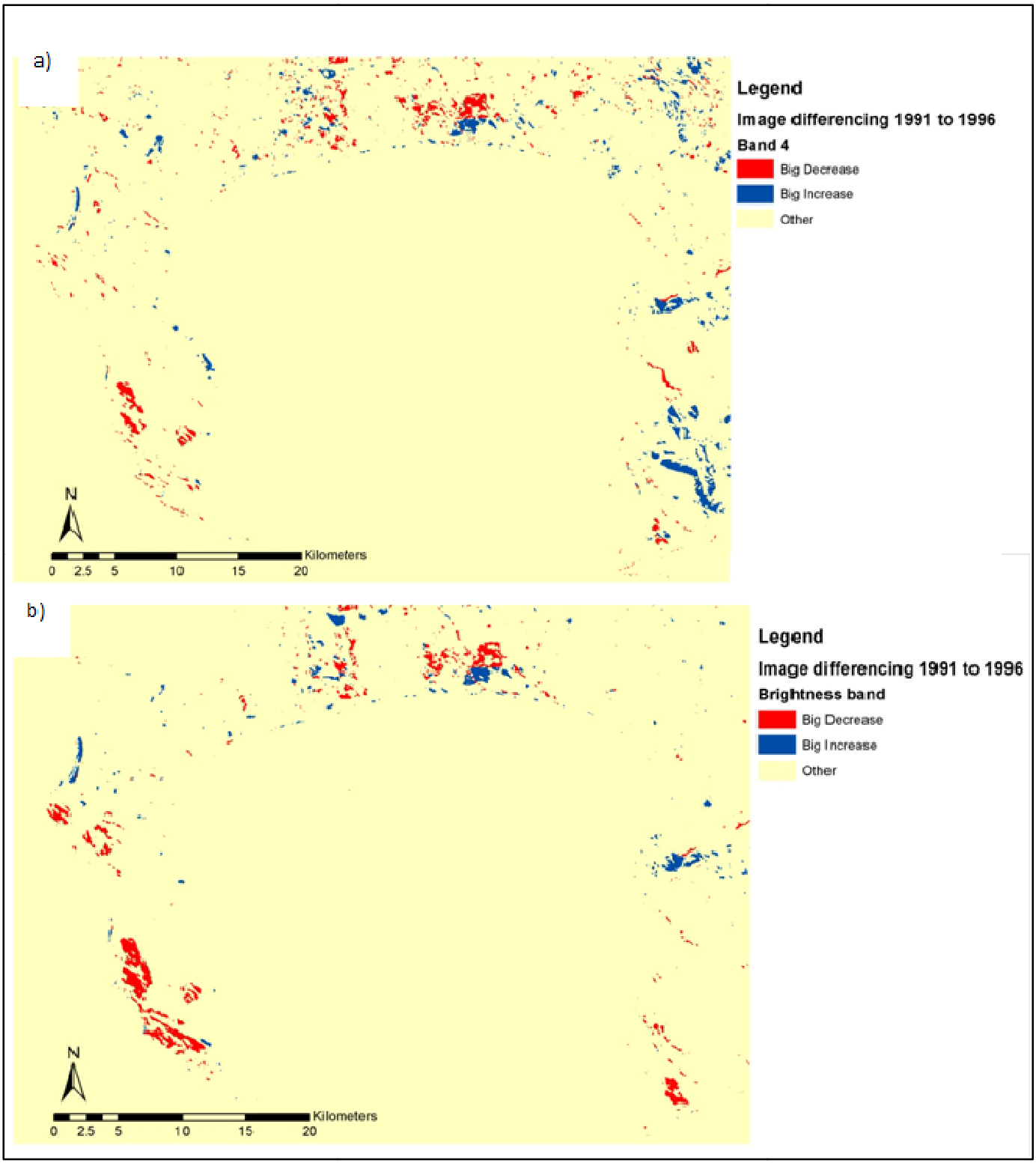

Figure 19: The image differencing results for image change from 1991 to 1996. Depicted is a) image differencing of band 4, and b) image differencing of the brightness band.

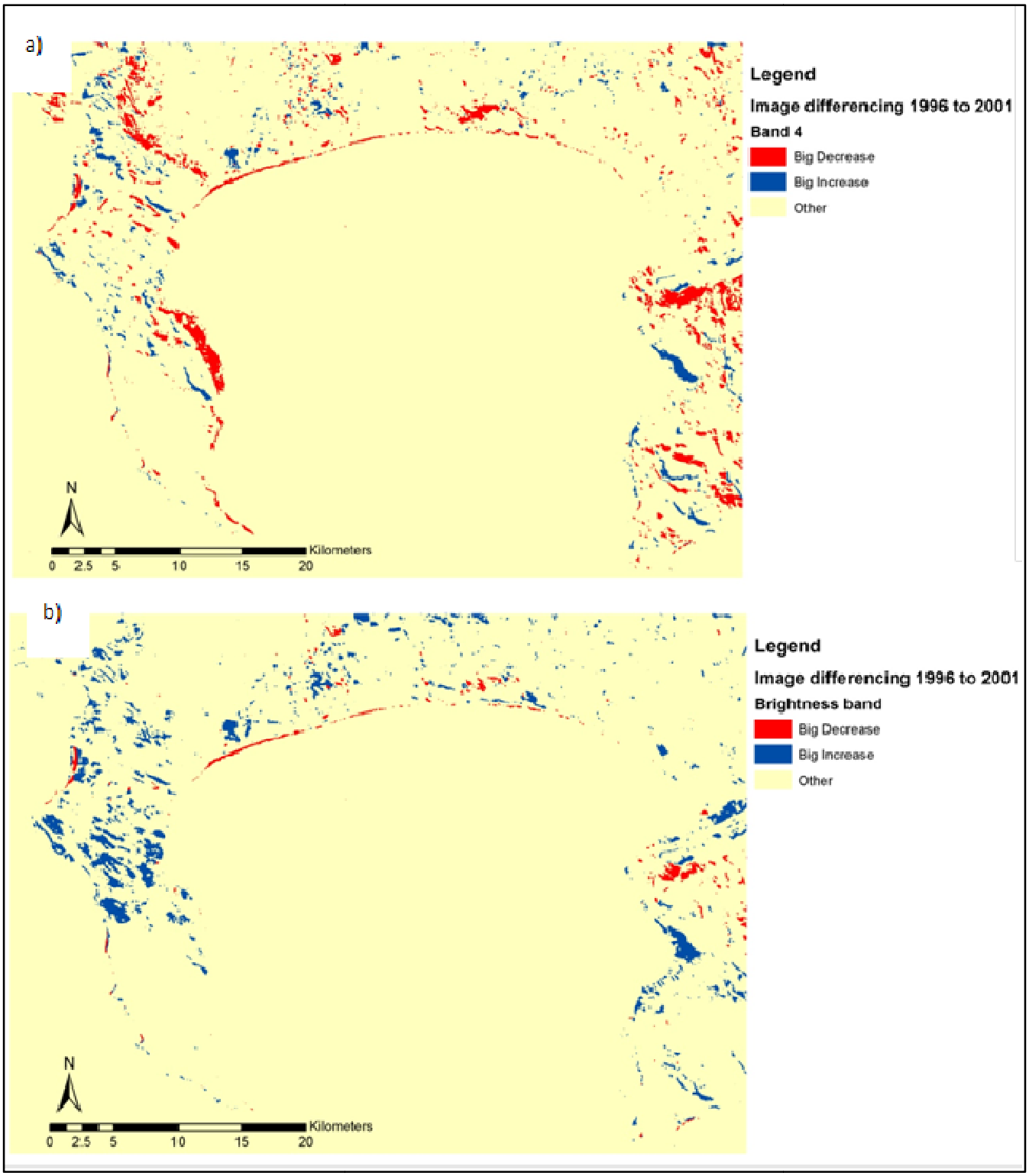

Figure 20: The image differencing results for image change from 1996 to 2001. Depicted is a) image differencing of band 4, and b) image differencing of the brightness band.

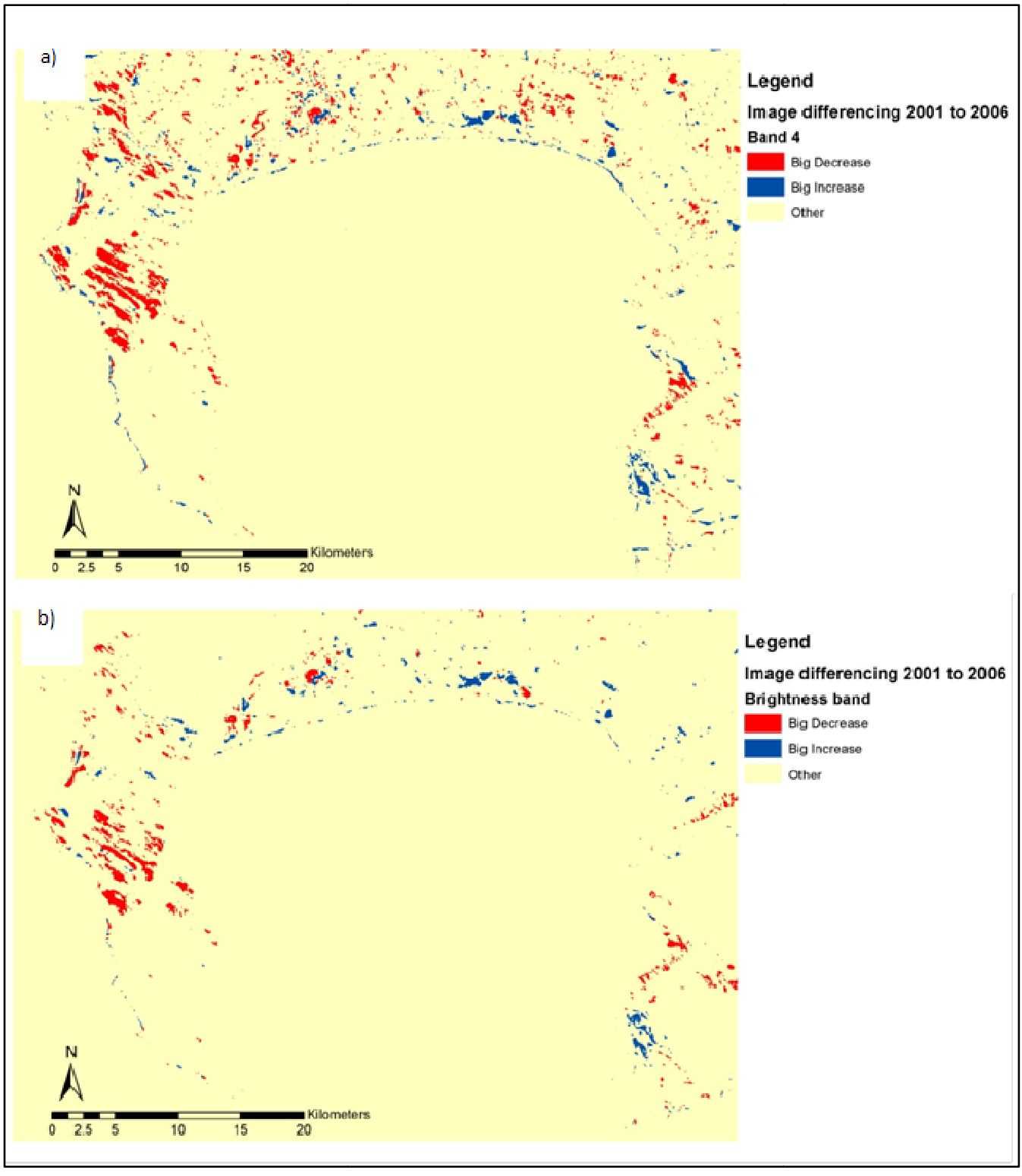

Figure 21: The image differencing results for image change from 2001 to 2006. Depicted is a) image differencing of band 4, and b) image differencing of the brightness band.

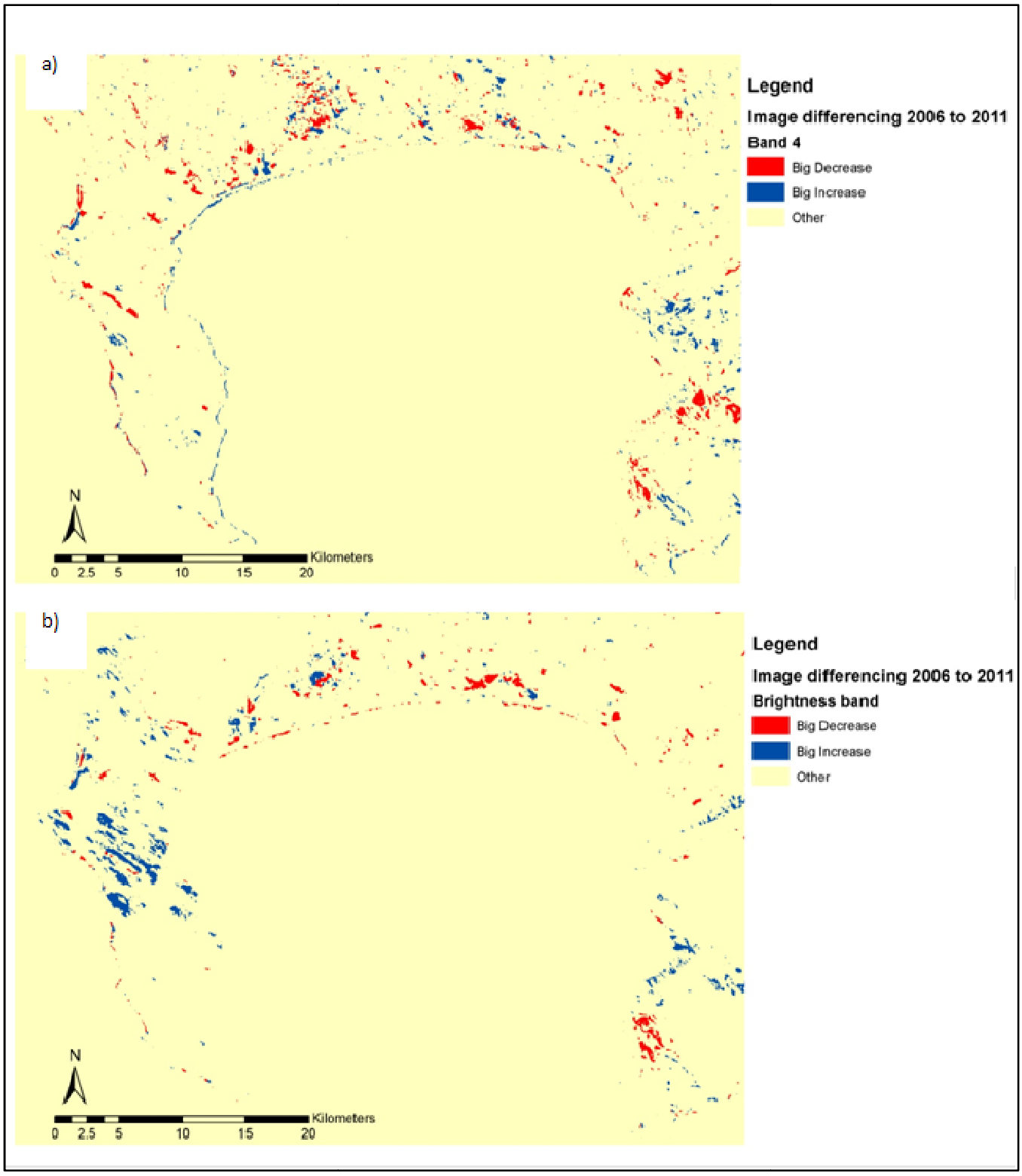

Figure 22: The image differencing results for image change from 2006 to 2011. Depicted is a) image differencing of band 4, and b) image differencing of the brightness band.

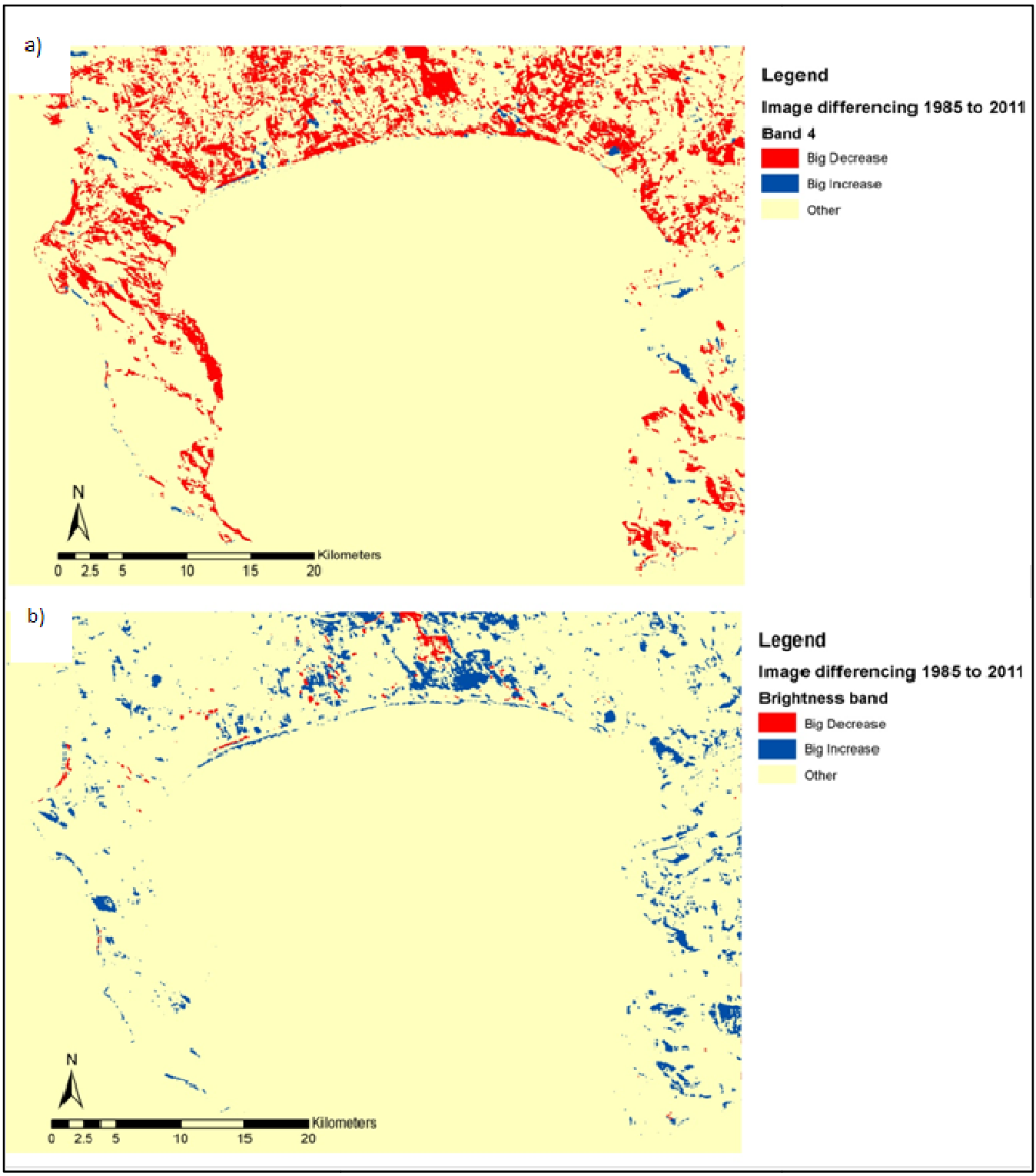

Figure 23: The image differencing results for image change over the entire study period, from 1985 to 2011. Depicted is a) image differencing of band 4, and b) image differencing of the brightness band.

4.5. **Changes in NDVI**

Changes in NDVI were assessed with the aim of focussing on changes in sand dunes. However, NDVI changes are seen throughout the images. The NDVI values at each date are shown in Appendix E. A visual assessment shows that NDVI was highest in 1985 and lowest in 2011. Changes in the NDVI can be seen in Figure 24, Figure 25, Figure 26, Figure 27, Figure 28, and Figure 29. In most years, there is a general decrease in NDVI, although there was a general increase from 1991 to 1996. Drastic decreases in NDVI can be seen when looking over the whole study period (Figure 29). A cropped version of this image showing the NDVI change only in sand dune regions from 1985 to 2011 is given in Section 5.1.1.

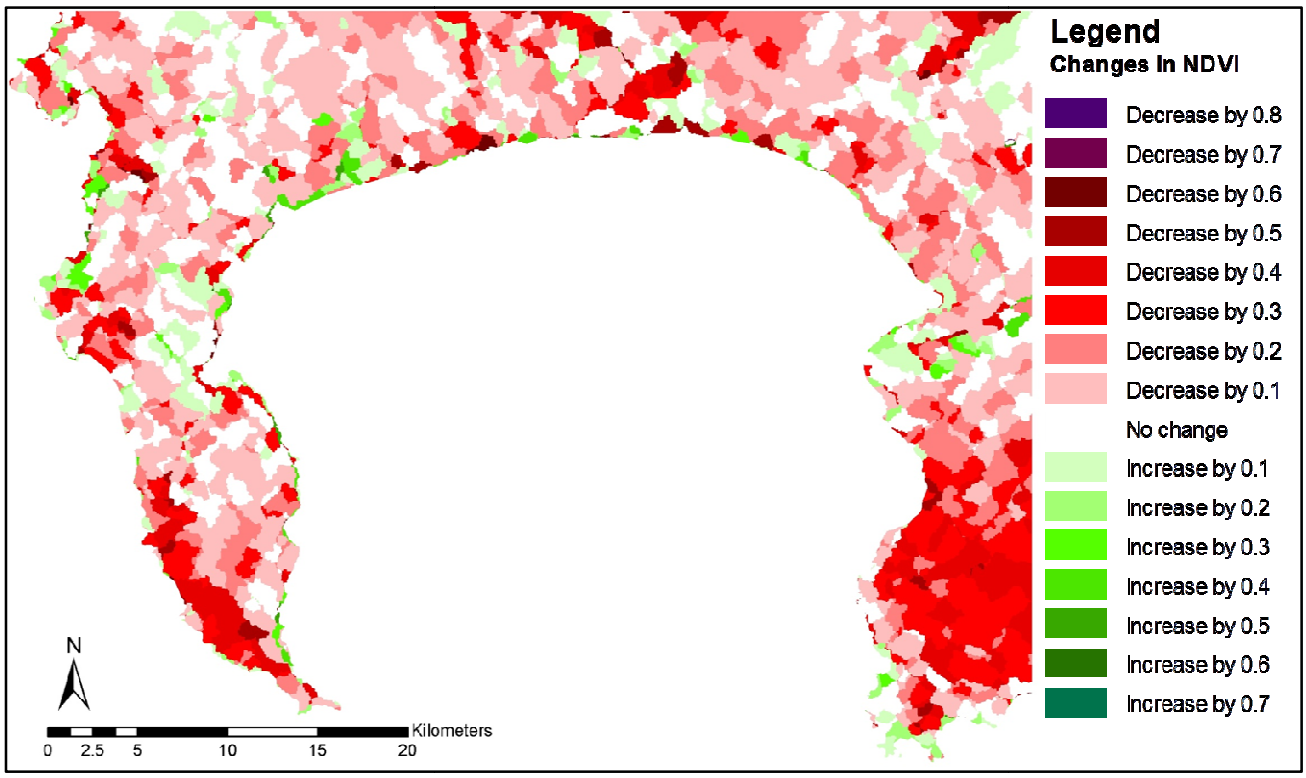

Figure 24: Changes in NDVI from 1985 to 1991.

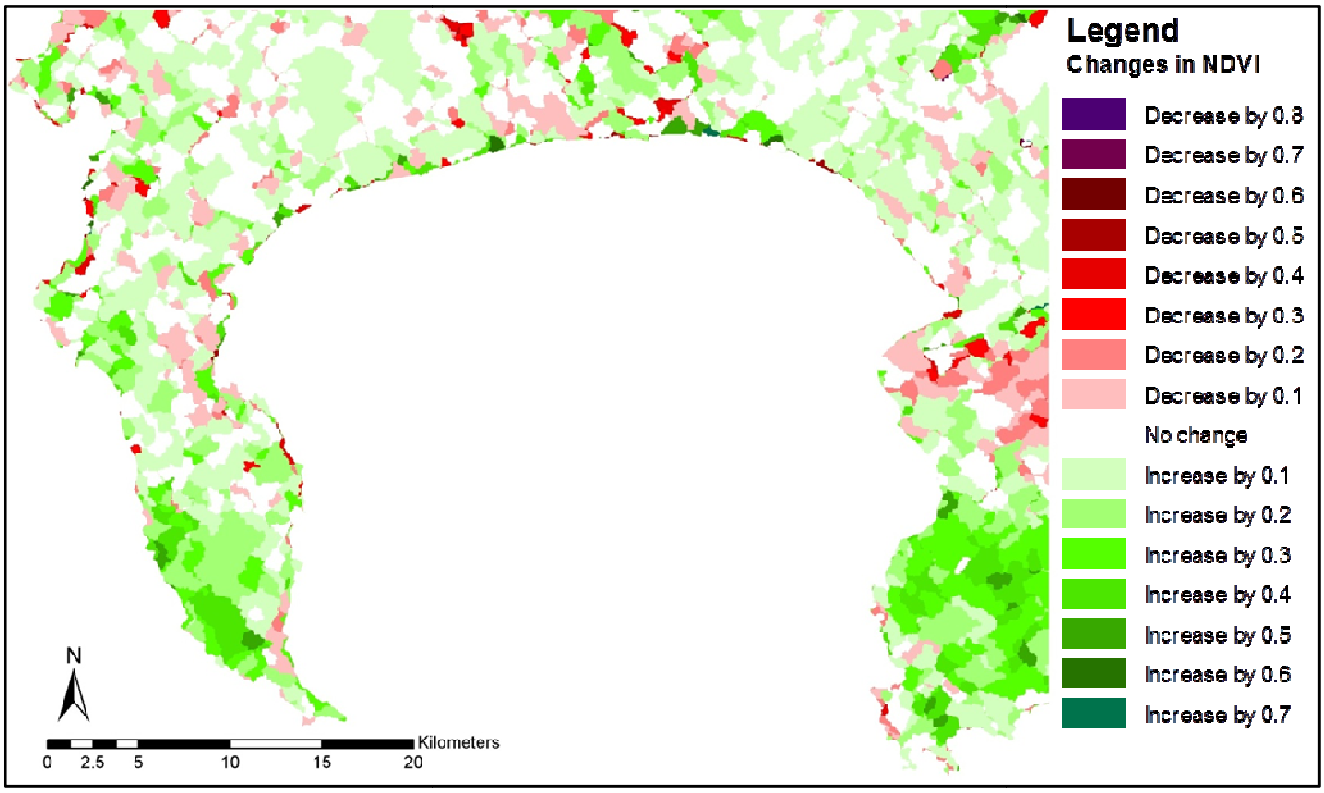

Figure 25: Changes in NDVI from 1991 to 1996.

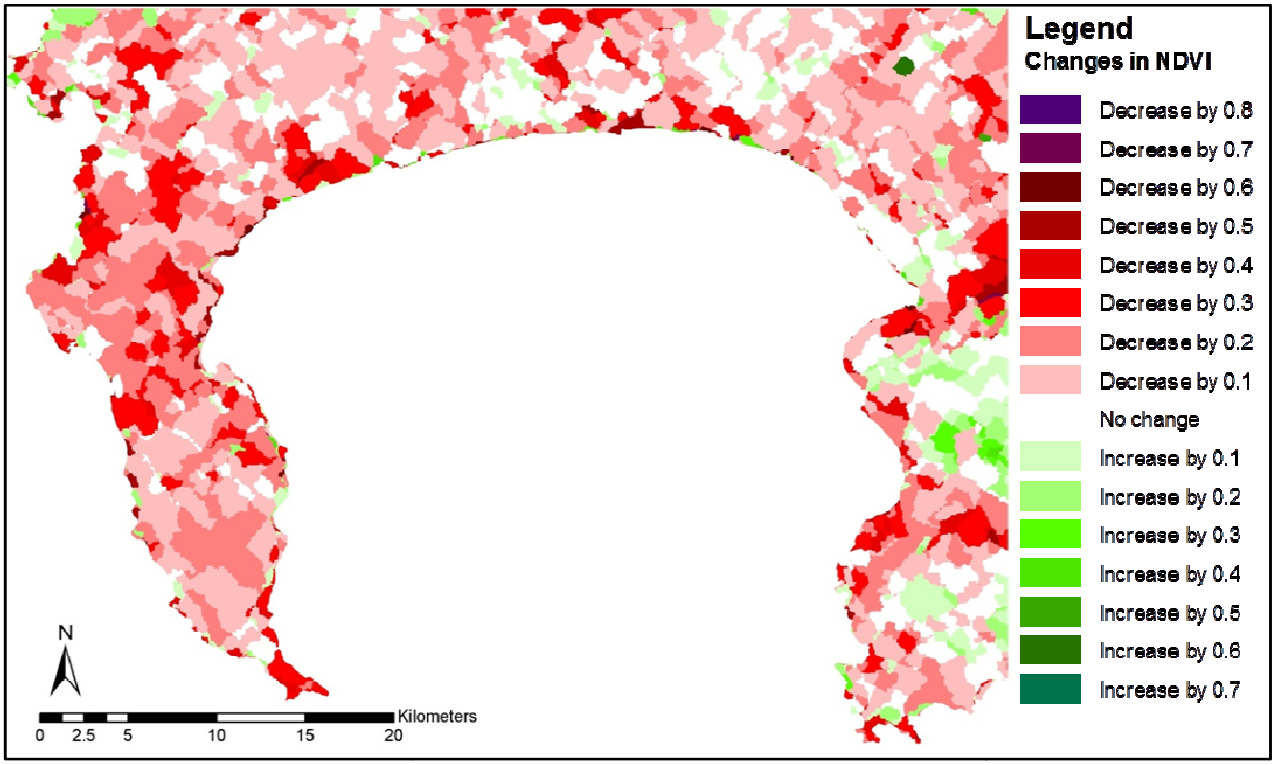

Figure 26: Changes in NDVI from 1996 to 2001.

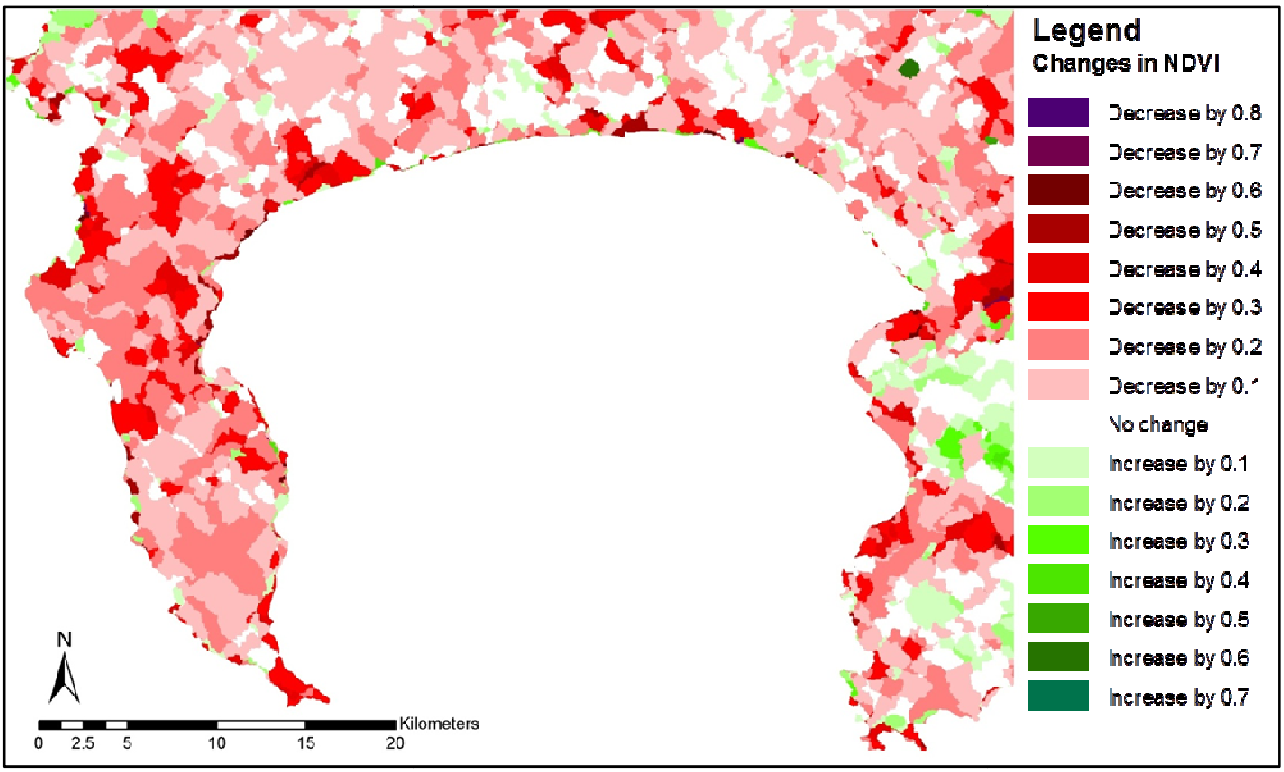

Figure 27: Changes in NDVI from 2001 to 2006.

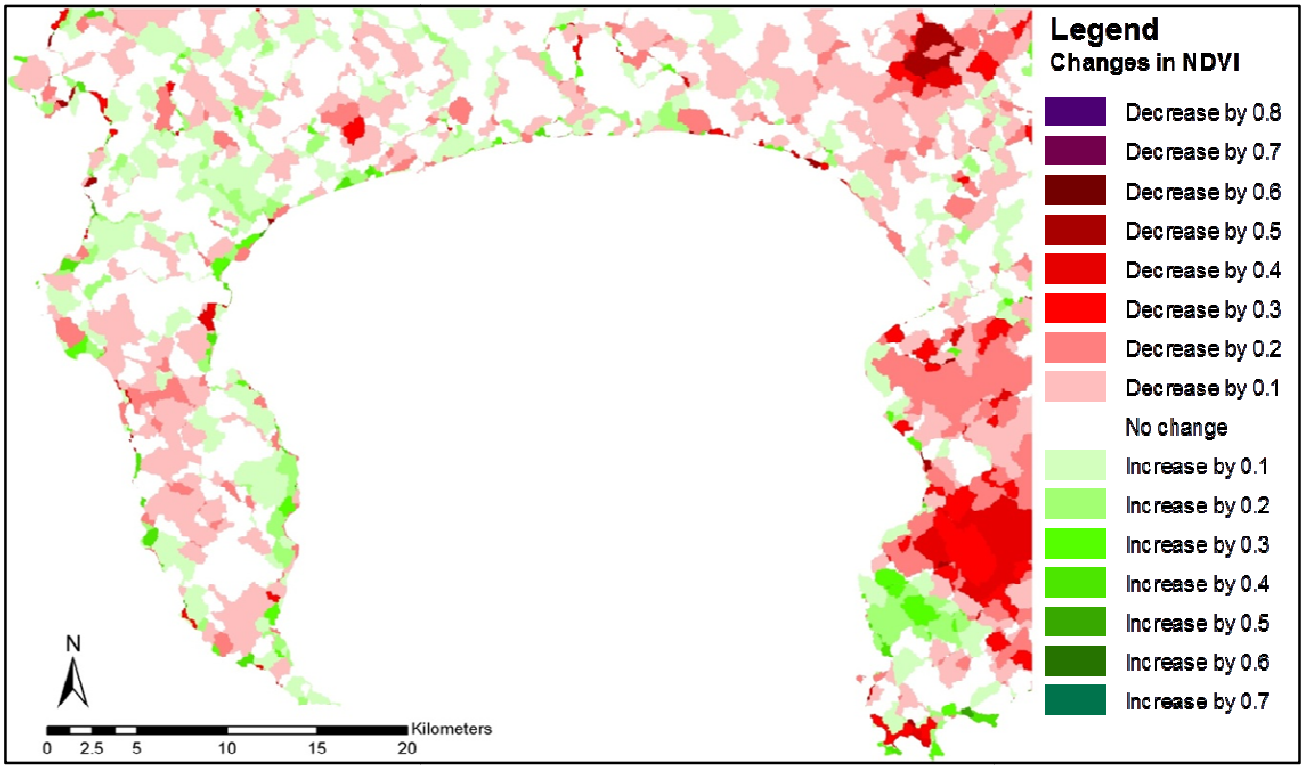

Figure 28: Changes in NDVI from 2006 to 2011.

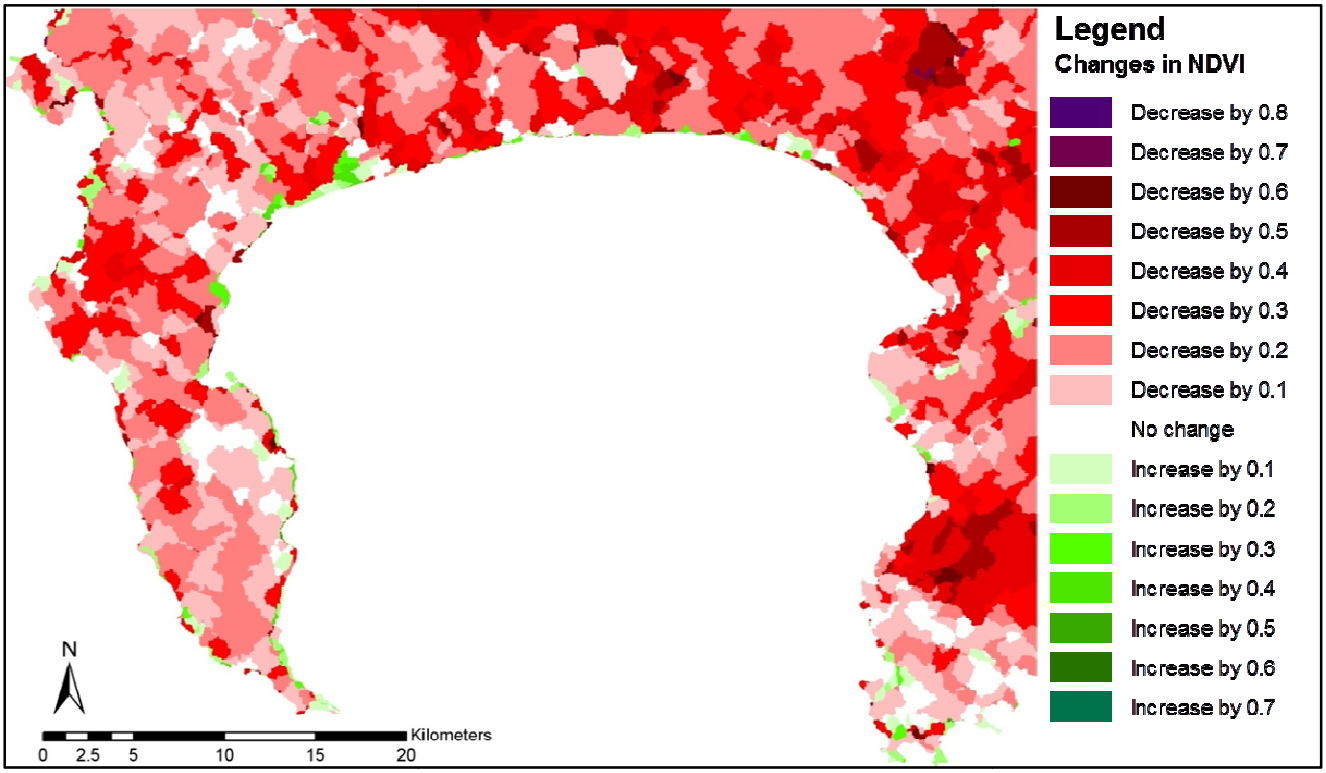

Figure 29: Changes in NDVI over the entire study period, from 1985 to 2011.

4.6. **Binary slicing**

Binary slicing was performed in order to define the coastline and accentuate any changes in shoreline position. The raster colour slices used are shown inAppendix F. They were able to show the shoreline position fairly well, however, errors are visible especially in the eastern portion of Figure 78(f), the image for 2011. This indicates a 'land' area extending into actual ocean just to the south-east of Strand. Such an error provides uncertainty as to how precisely the coastline is defined in other areas. Various dam and mountain shadow zones are also shown in the blue of 'ocean', however these are generally easy to differentiate from the shoreline and are not problematic.

The changes in binary slicing images are shown in Figure 30, Figure 31, Figure 32, Figure 33, Figure 34, and Figure 35. Many of the visible changes are in dam and mountain shadow zones which were spectrally darker in one image than in another. These changes are not relevant. However, there is some change along the coastline, especially in the northern and eastern regions of the images.

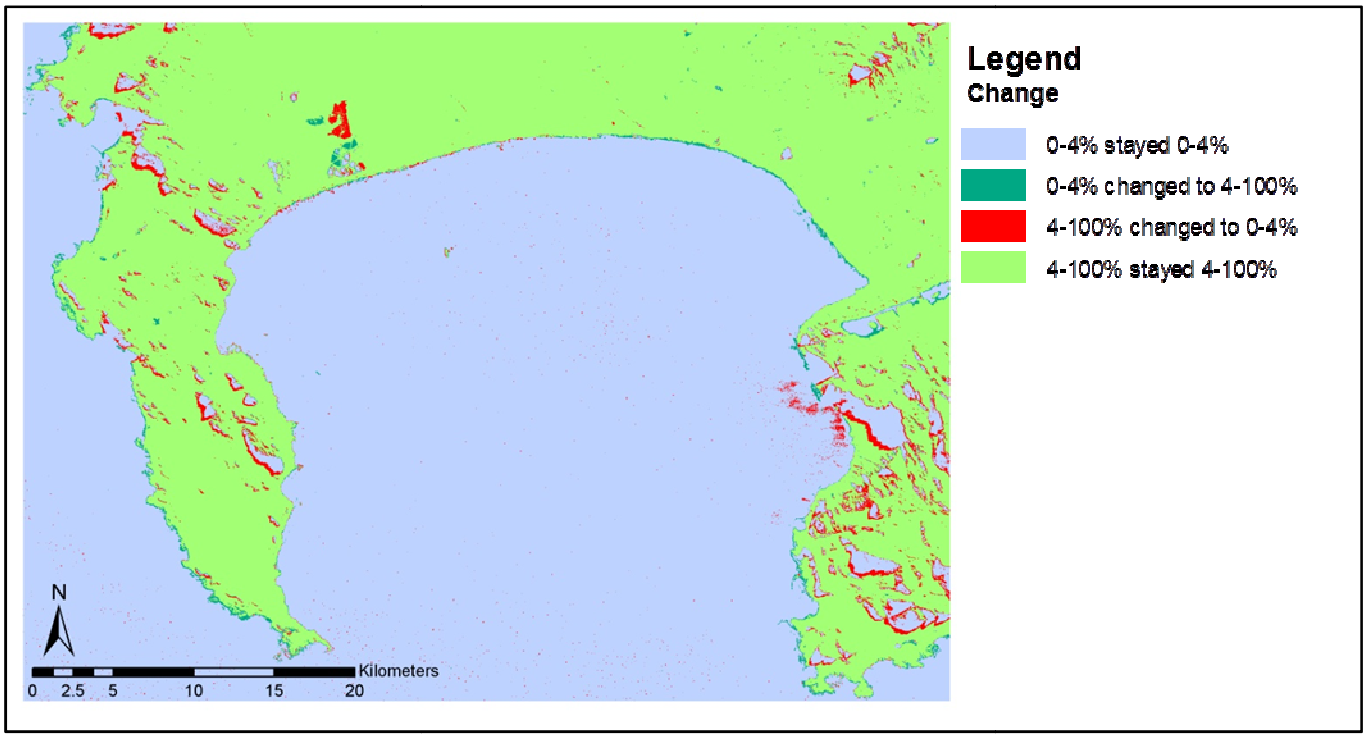

Figure 30: Changes in binary slicing images from 1985 to 1991.

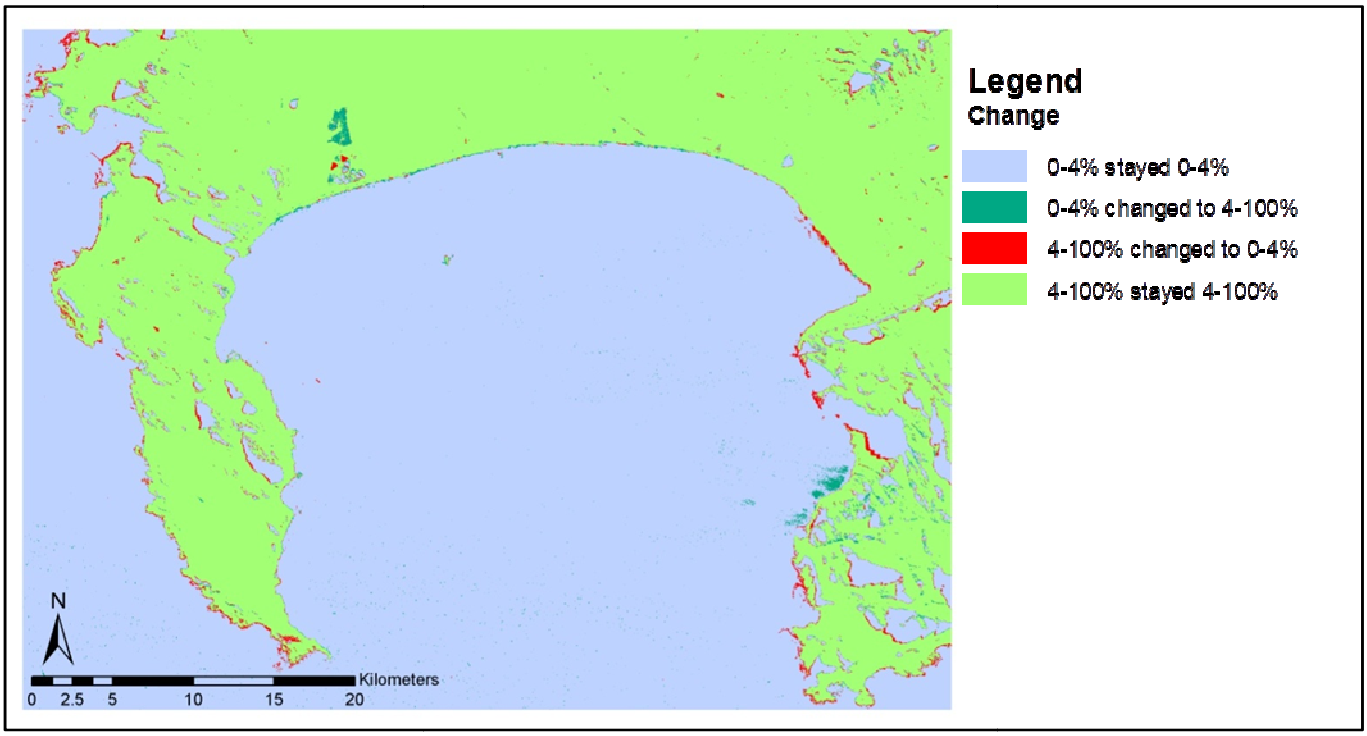

Figure 31: Changes in binary slicing images from 1991 to 1996.

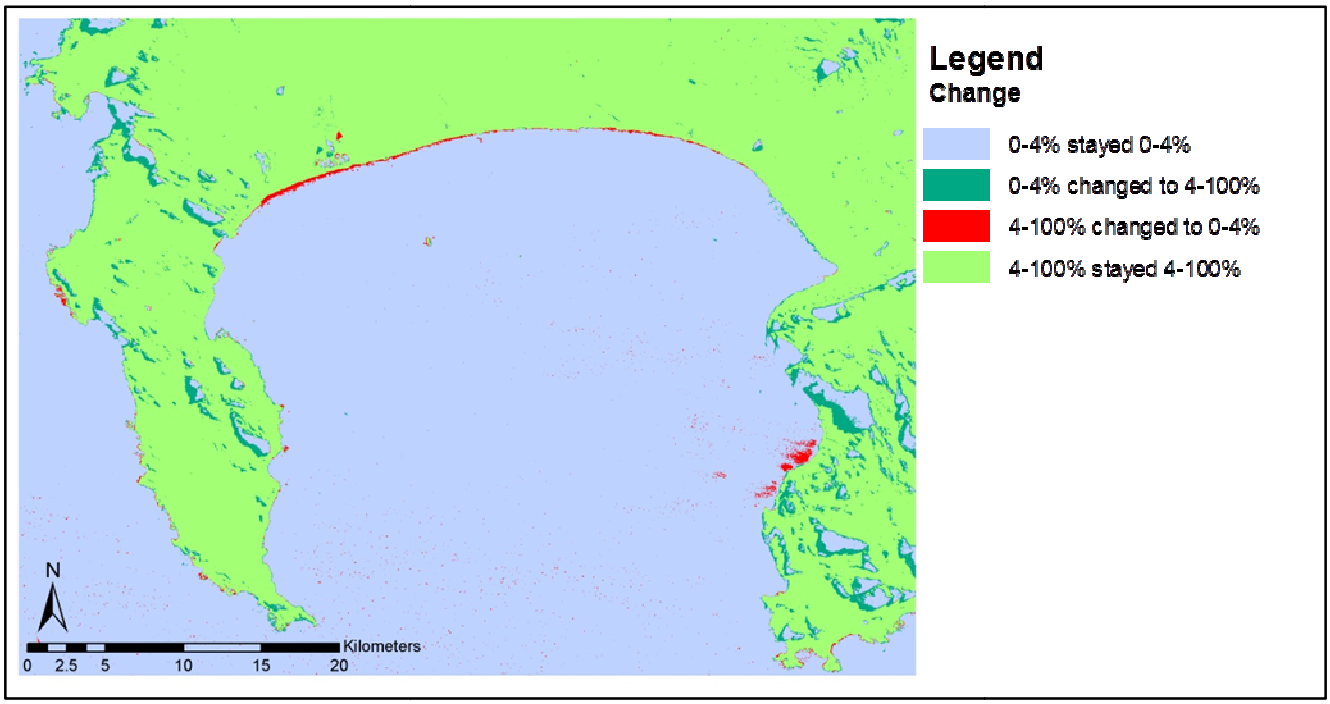

Figure 32: Changes in binary slicing images from 1996 to 2001.

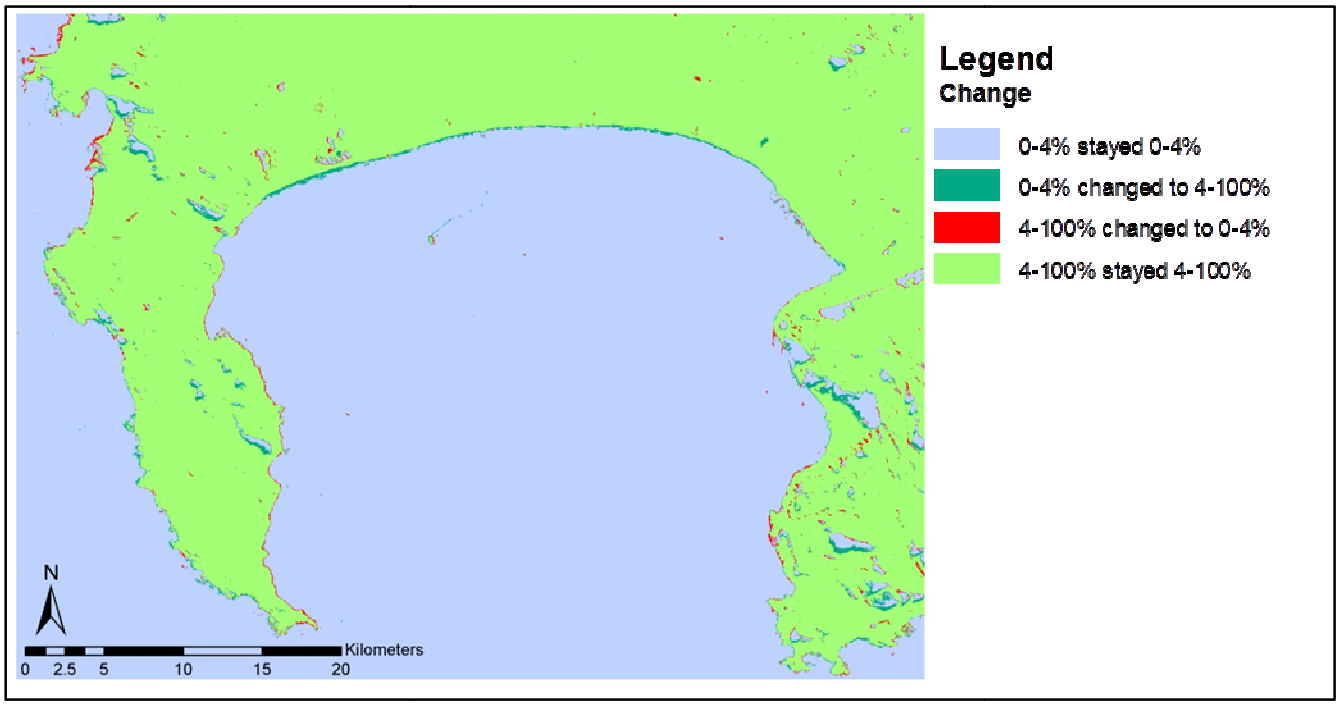

Figure 33: Changes in binary slicing images from 2001 to 2006.

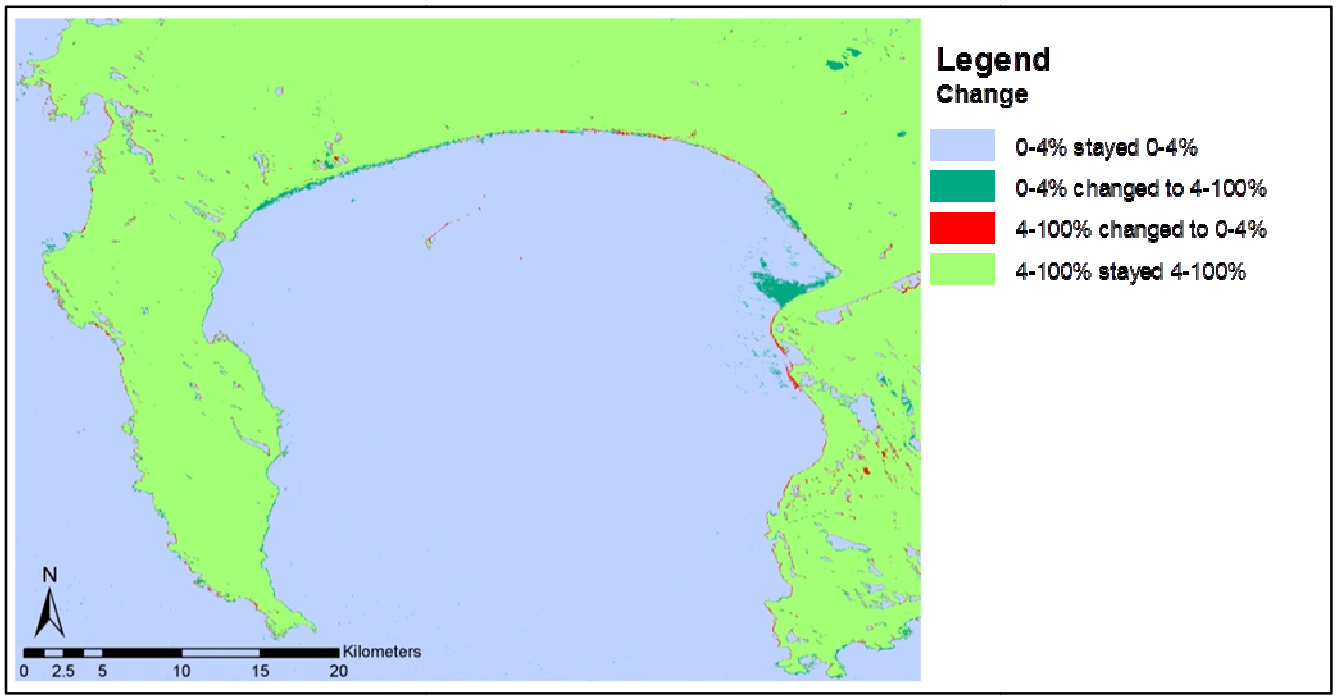

Figure 34: Changes in binary slicing images from 2006 to 2011.

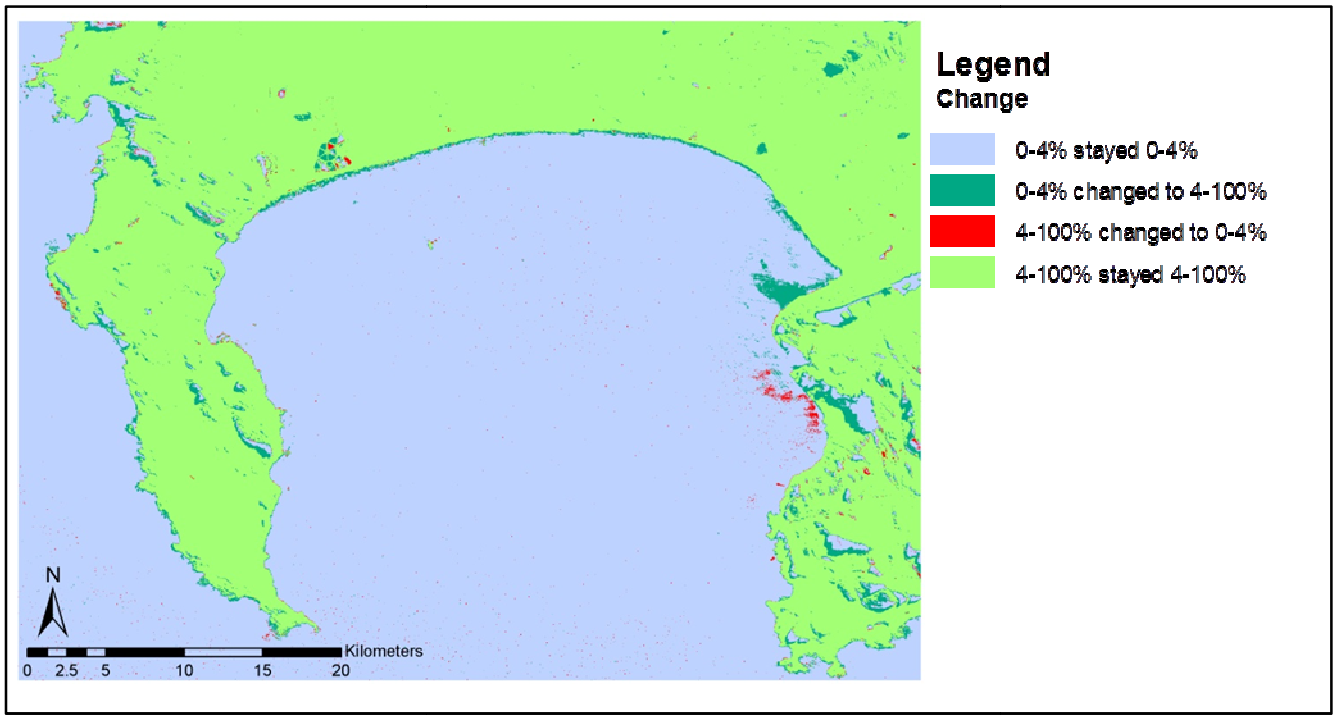

Figure 35: Changes in binary slicing images over the entire study period, from 1985 to 2011.

4.7. **Digital Shoreline Analysis System**

The digital shoreline analysis system (DSAS) is an add-on for ArcGIS designed specifically for use in analysing shoreline change. The steps taken using this tool are given in Section 3.7. This tool was applied to each of the four focus areas selected: Bayview Heights, Macassar Beach, Strand, and Pringle Bay. The tool requires an input of a digitised time series of coastline positions, and then outputs various statistics. The output tables are given in Appendix A. The aerial photographs used in this section are detailed in Table 2.

4.7.1. Bayview Heights

The first focus area addressed was Bayview Heights. The first information output by DSAS is the shoreline change envelope (Figure 36). This shows the overall change in shoreline position that has occurred throughout the study period, including both erosion and accretion. It is a distance measured in metres of change along each transect. This indicates the total change from the most seaward to the most landward point in any year – in other words, it indicates the gross rather than the net change. Importantly, the lengths of the transectsdisplayed in all the DSAS figures belowcorresponds to the size of the shoreline change envelope, while their colours indicate the values of the different parameters.DSAS is equipped to do this automatically.However, the function did not seem to work so in this case it was performed manually by digitising a polygon in the shape of the shoreline change envelope and clipping the transects to this shape. The aerial photographs used as background images for all figures in this section are from 2010.

In Bayview Heights, the shoreline change reaches a maximum of 90.39 m and the minimum change along any of the transects was 8.30 m. This change could be either accretion or erosion, since the shoreline change envelope does not take change direction into account. The average change over all the transects was 49.97 m.

The second set of values supplied is net shoreline movement (Figure 37). Once again, it is given in metres along each transect. This is similar to the shoreline change envelope, however, rather than showing the total from nearest to farthest digitised points along each transect, it indicates the change from the earliest to the latest date (i.e. the net change). For Bayview Heights, this means the change from 1944 to 2010. The net shoreline movement also differentiates between erosion and accretion, with negative values associated with erosion and positive values with accretion.

For Bayview Heights, the net shoreline movement ranges from 26.10 m erosion to 45.47 m accretion. The average change was 0.51 m accretion.

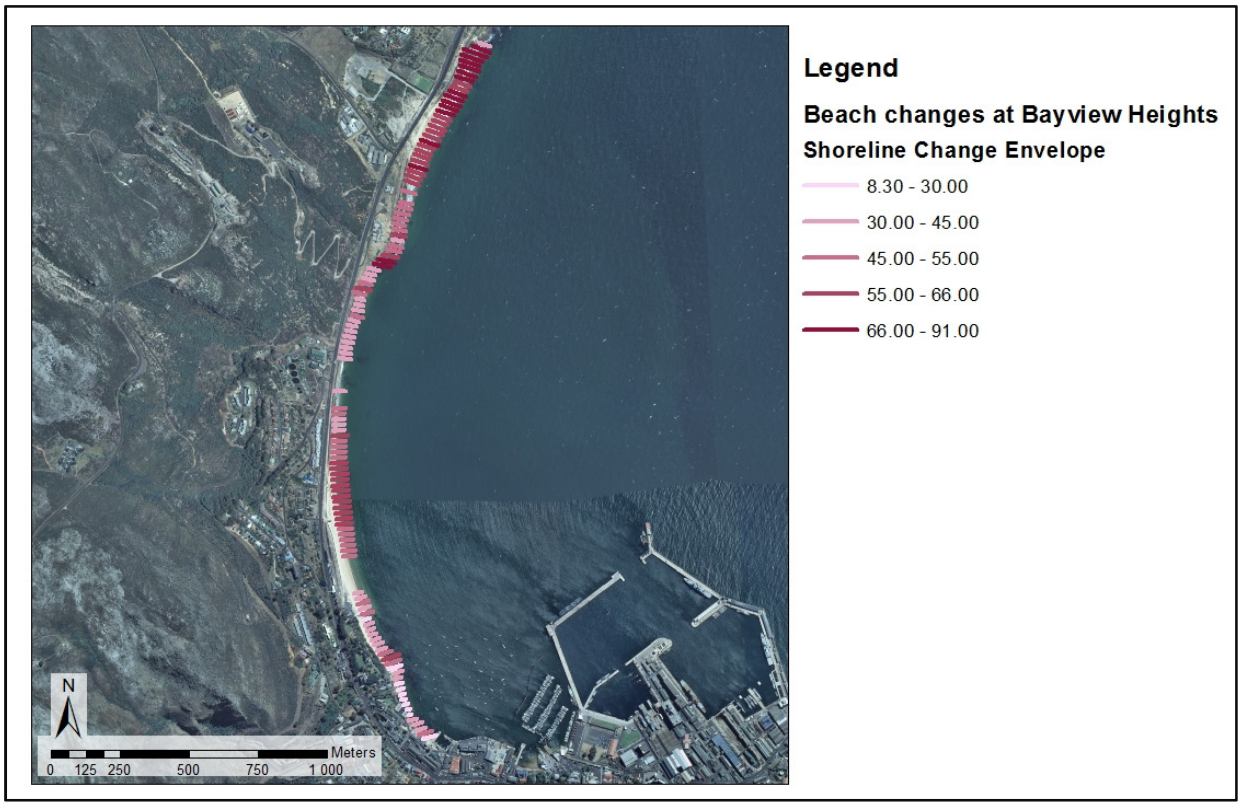

Figure 36: Shoreline Change Envelope in metres at Bayview Heights.

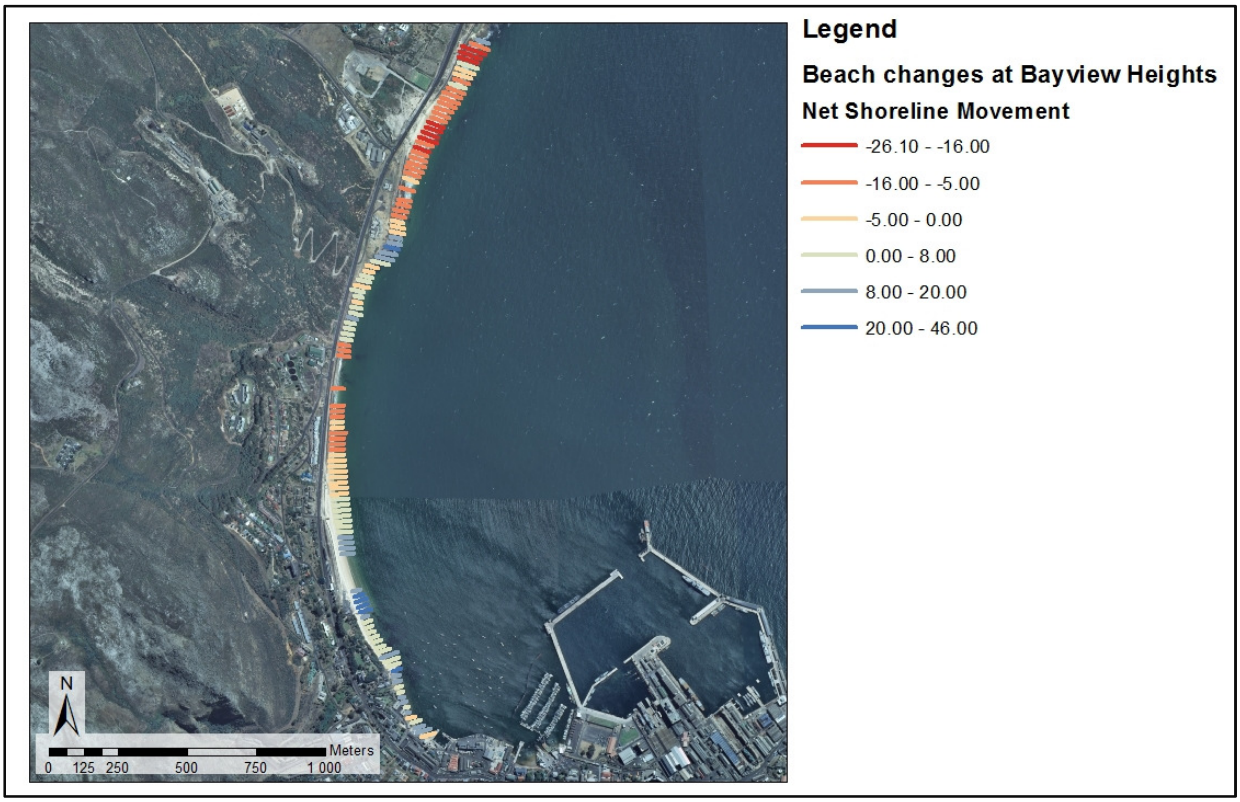

Figure 37: Net shoreline movement in metres at Bayview Heights.

The first calculated rate is the end point rate (Figure 38). This rate, measured in metres of change per year, is calculated by dividing the net shoreline movement by the time elapsed between the oldest and most recent shoreline. Once again, for Bayview Heights, this means from 1944 to 2010. This rate does not take into account anything that occurred in between these two dates, and shows only the rate of the net change.

Since they are based on the same data, Figure 37 and Figure 38 appear similar visually. However, Figure 37 shows the total change in metres while Figure 38 shows the rate of change in metres per year. The erosion/accretion rate for Bayview Heights ranges from 0.40 m erosion per year to 0.69 m accretion per year. Since the erosion and accretion over the different transects balance each other out, the average over the whole area is a mere 0.008 m (0.8 cm) of accretion per year.

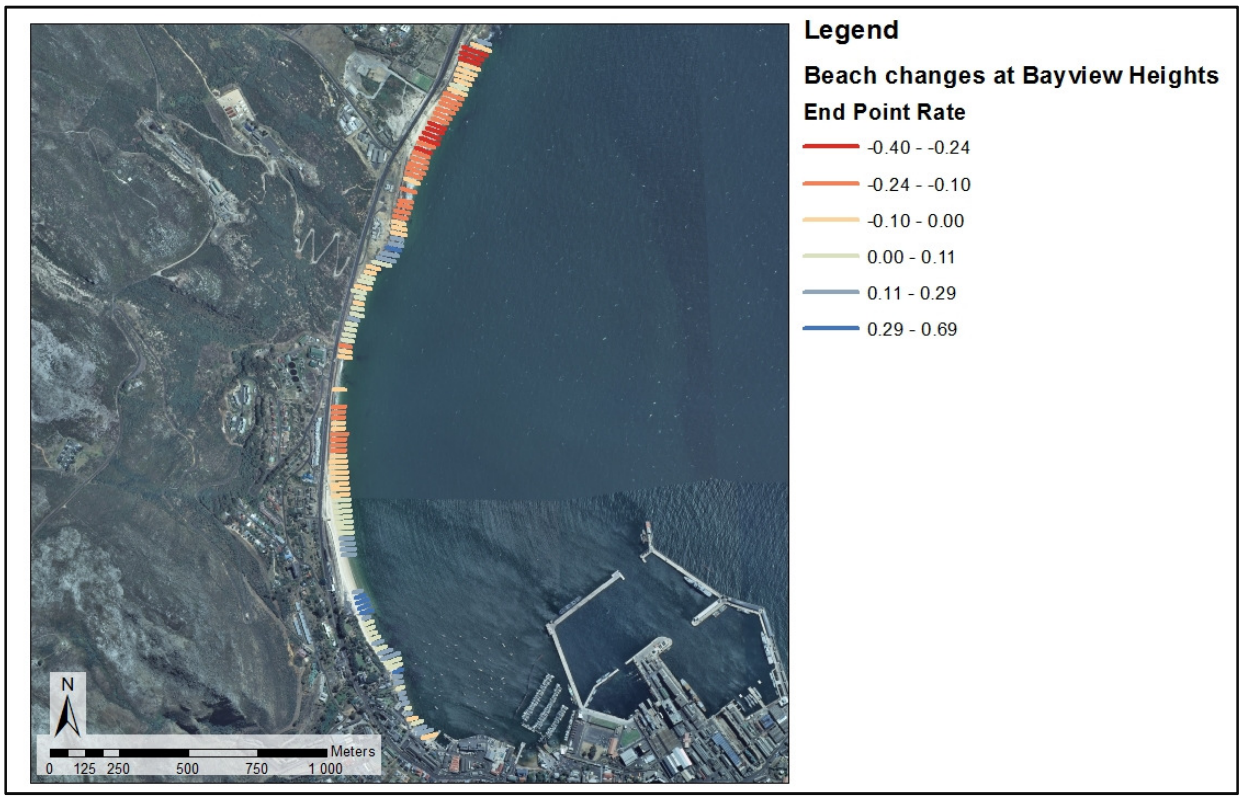

Figure 38: End point rate in metres per year at Bayview Heights.

The next rate calculated was the linear regression rate (Figure 39). This is a well-known and commonly used statistic. Linear regression takes into account all the data available from all years to report the change in shoreline position in metres per year. It can, however, be susceptible to outliers and it can underestimate the rate of change relative to other statistics. The errors associated with this calculation at the selected confidence interval of 95% are shown in the tables in Appendix A.

For Bayview Heights, the linear regression rate ranged from 0.62 m erosion per year to 0.68 m accretion per year. This method shows generally higher erosion compared to the end point rate, with an average of 0.16 m erosion per year.

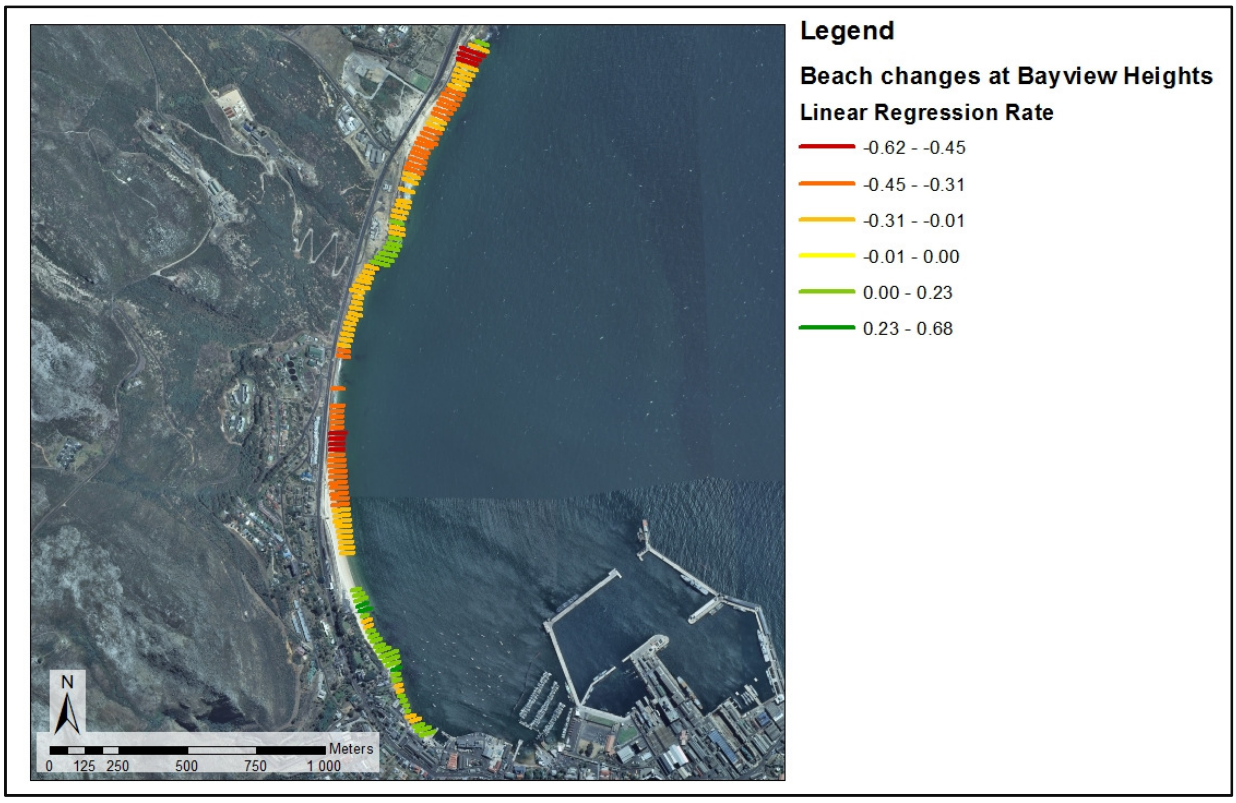

Figure 39: Linear regression rate in metres per year at Bayview Heights.

The weighted linear regression rate was also calculated (Figure 40). This is calculated the same way as the linear regression rate, except that more reliable data are given a higher weighting. In this case, the pixel sizes of the various aerial photographs were used to indicate positional uncertainty, so those with smaller pixel sizes would have been given higher weightings. Again, associated errors are given in Appendix A.

For Bayview Heights, the weighted linear regression method shows even greater erosion, with a range from 0.83 m erosion to 0.67 m accretion and an average of 0.30 m erosion per year.

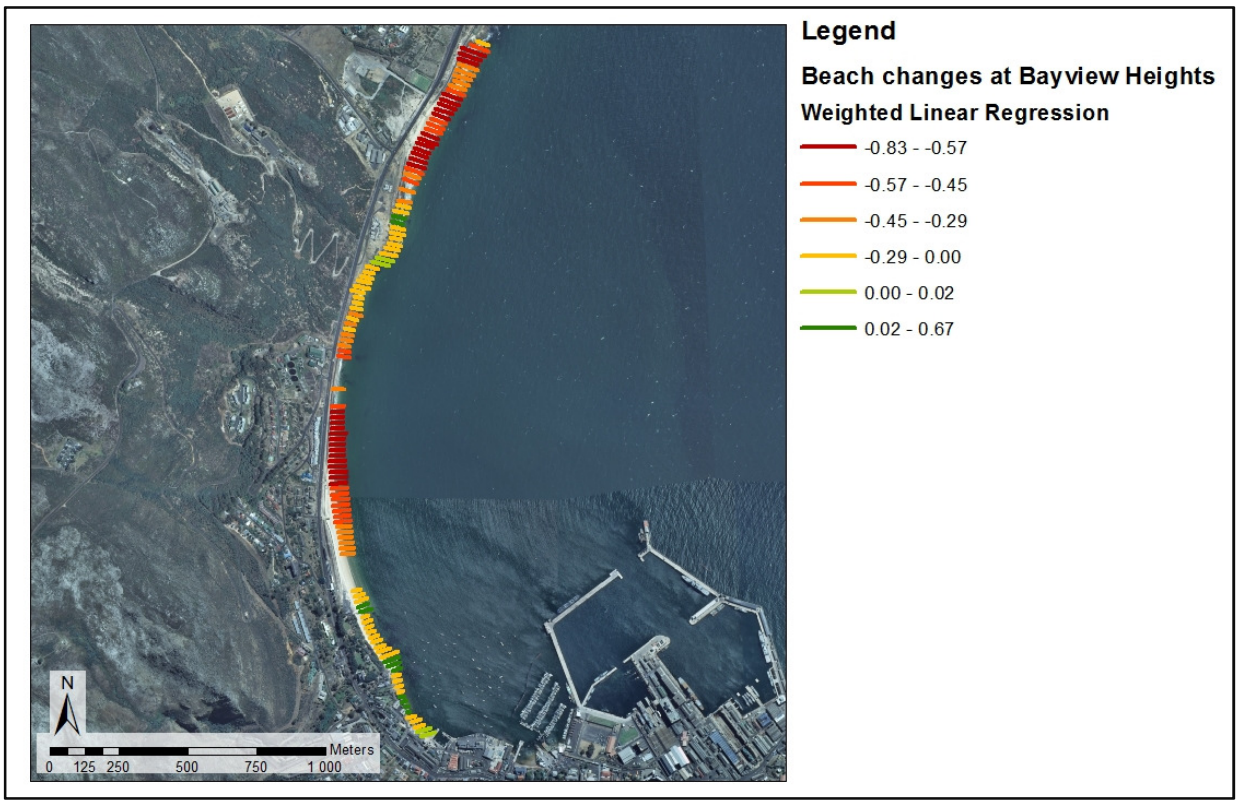

Figure 40: Weighted linear regression rate in metres per year at Bayview Heights.

Finally, the least median of squares was determined. For Bayview Heights, this is visualised in Figure 41. This is determined in a similar way to linear regression, except that where the mean offset of sample data is used for linear regression, the least median of squares method uses the median (rather than the mean) value of the squared residuals. This method minimises the influence of outliers and anomalies on the overall equation.

For Bayview Heights, the least median of squares statistic shows the highest erosion of all, with a range from 1.38 m erosion per year to 0.70 m accretion per year and an average rate of 0.17 m erosion per year.

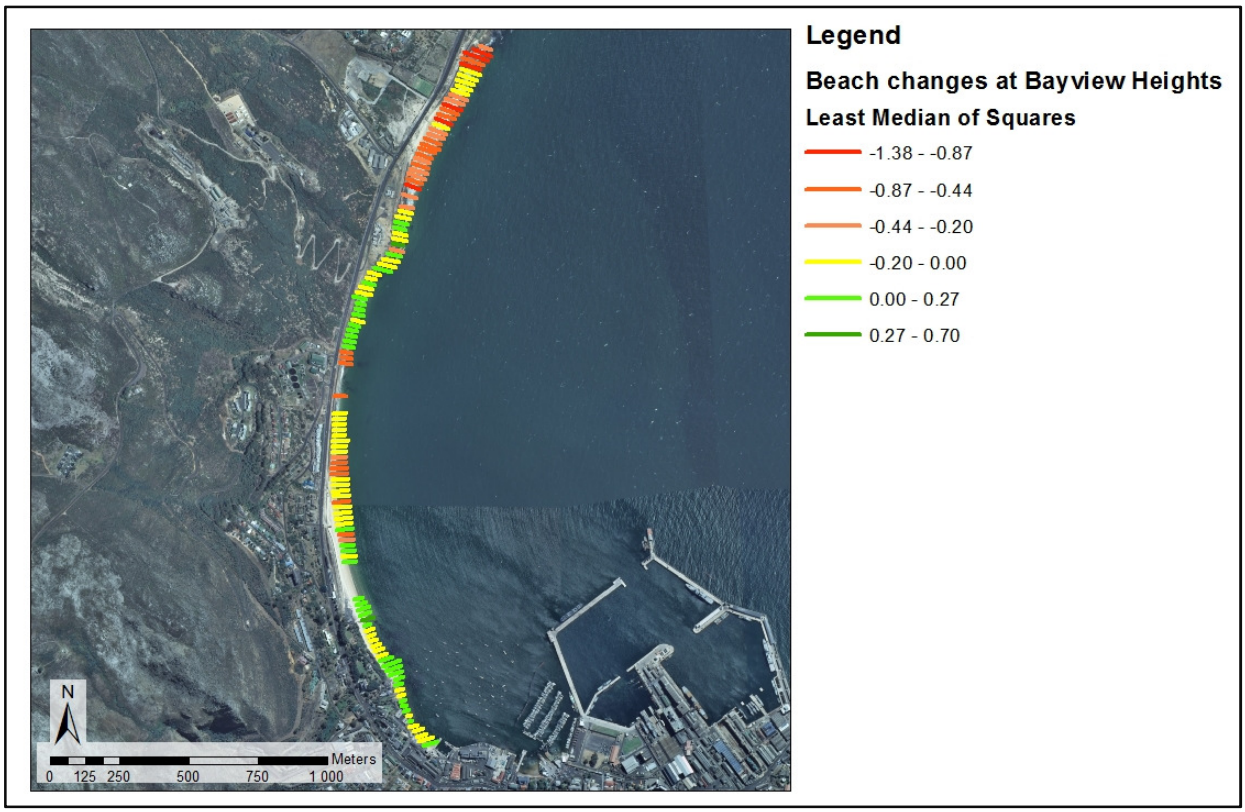

Figure 41: Least median of squares in metres per year at Bayview Heights.

4.7.2. Macassar Beach

The shoreline change envelope for Macassar Beach can be seen in Figure 42. The shoreline change in both erosion and accretion ranges over the study area from 24.59 m to 259.53 m. The average change along all the transects is 91.96 m.

The net shoreline movement (Figure 43) also shows a considerable range, from 73.49 m erosion to 90.47 m accretion. This change also took place from 1944 to 2010. The average net shoreline movement for Macassar Beach is 7.13 m erosion.

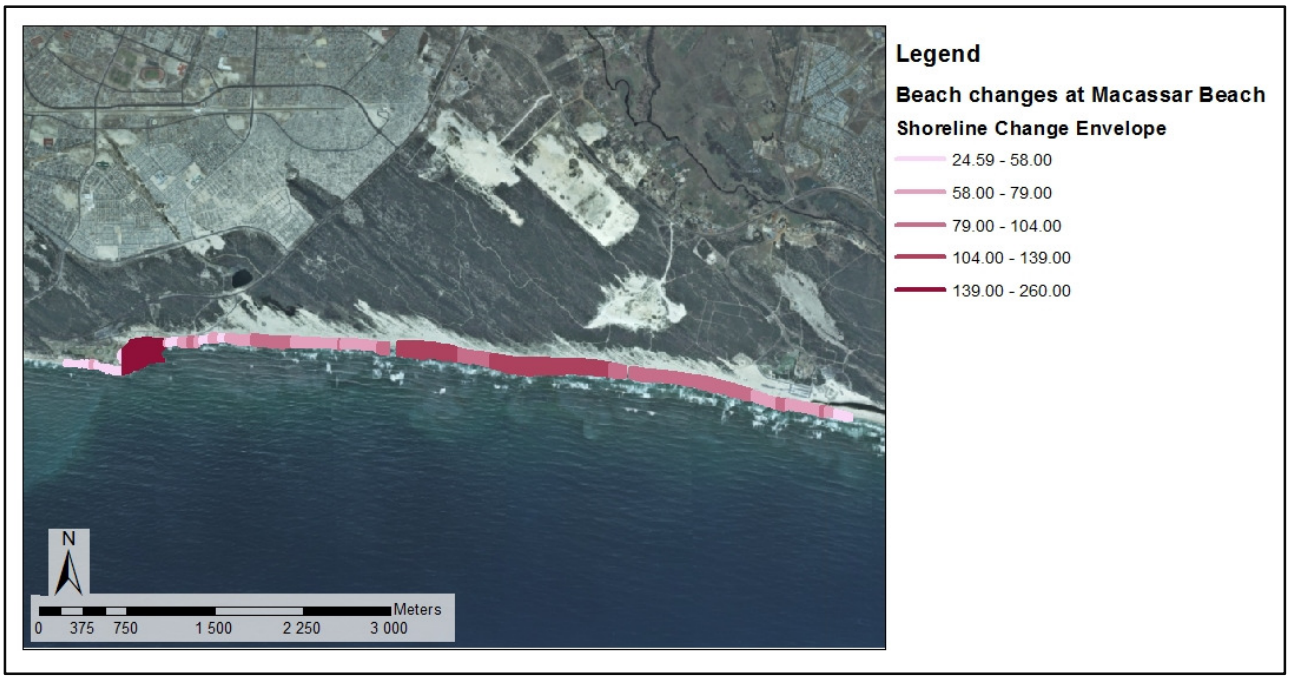

Figure 42: Shoreline change envelope at Macassar Beach.

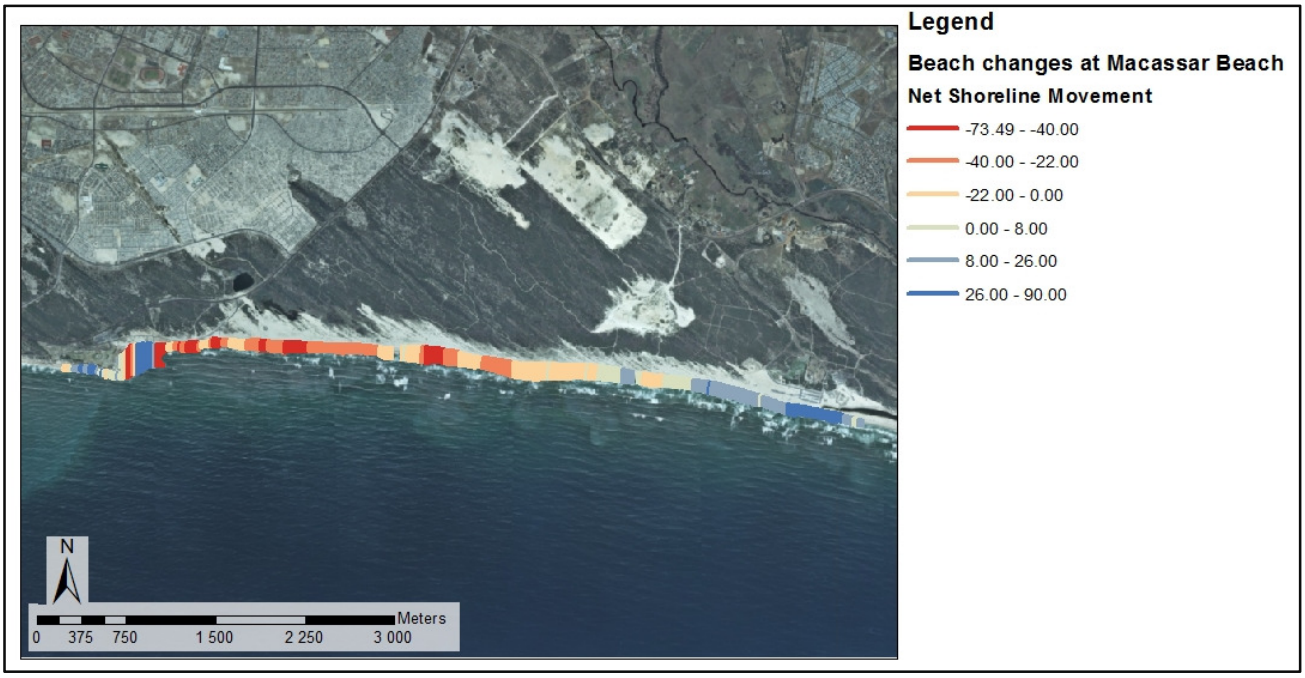

Figure 43: Net shoreline movement at Macassar Beach.

The end point rate at Macassar Beach (Figure 44) shows the rate of change of the beach position from 1944 to 2010. This ranged from 1.11 m erosion per year to 1.37 m accretion per year with an average of 0.11 m erosion per year.

It is important to note, for this as well as the other 3 focus areas, that all rates measured in metres per year (end point rate, linear regression rate, weighted linear regression rate, and least median of squares) provide results which show change of a few metres down to a few centimetres per year. These values are always smaller than the pixel sizes of the worst resolution imagery, and in some cases, even smaller than the pixel size of the best resolution imagery. The pixel sizes range from a smallest pixel size of 0.125 m – which is smaller than many of the measured rates – to 9.63 m for some focus areas (the largest pixel size used at Macassar is 4.76 m). These pixel values have been incorporated into the calculations and error margins are given in the tables in Appendix A, however, it is important to note that the changes occurring on a per year basis cannot be used to make any significant conclusions. However, the total change occurring over a period of years is far greater than the error margin supplied by the pixel size, and so conclusions can be made about the trends in movement.

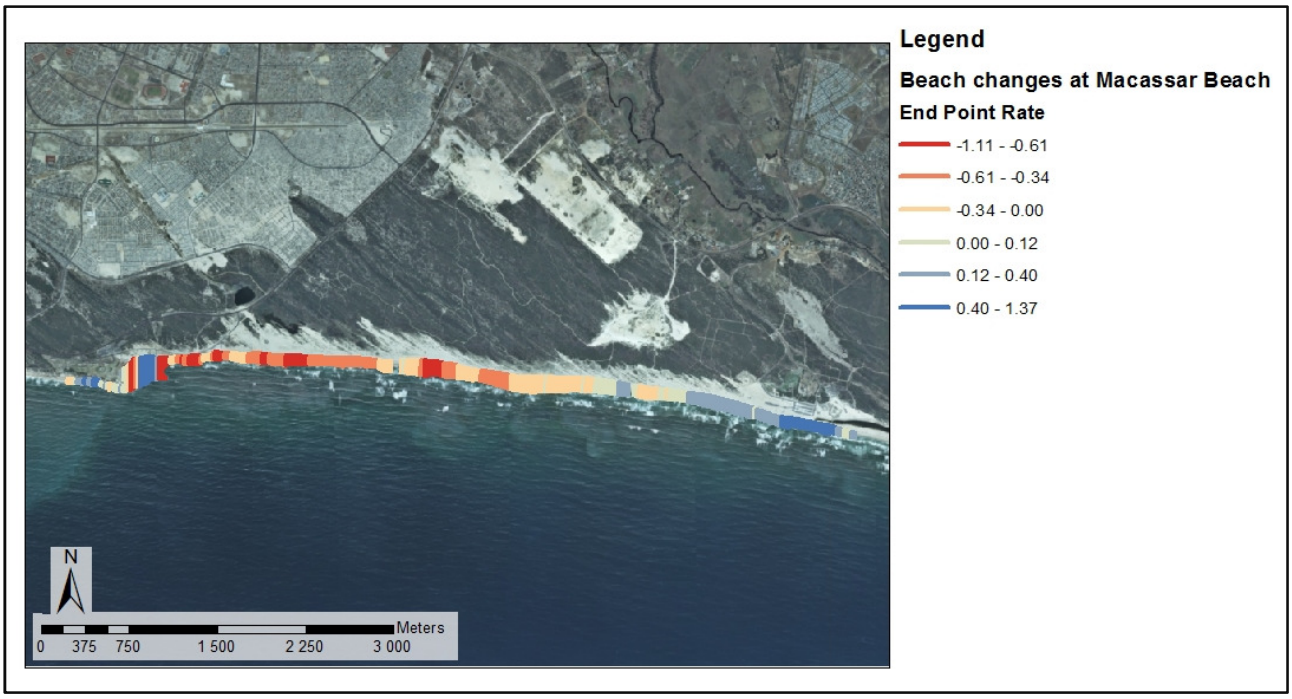

Figure 44: End point rate at Macassar Beach.

The linear regression rate at Macassar Beach (Figure 45) ranges from 0.84 m erosion per year to 2.85 m accretion per year with an average of 0.045 m erosion per year, and the weighted linear regression rate (Figure 46) ranges from 0.89 m erosion per year to 3.29 m accretion per year with an average of 0.04 m erosion per year.

Finally, the least median of squares (Figure 47) ranges from 1.38 m erosion per year to 5.19 m accretion per year with an average of -0.14 m per year, or 14 cm erosion per year.

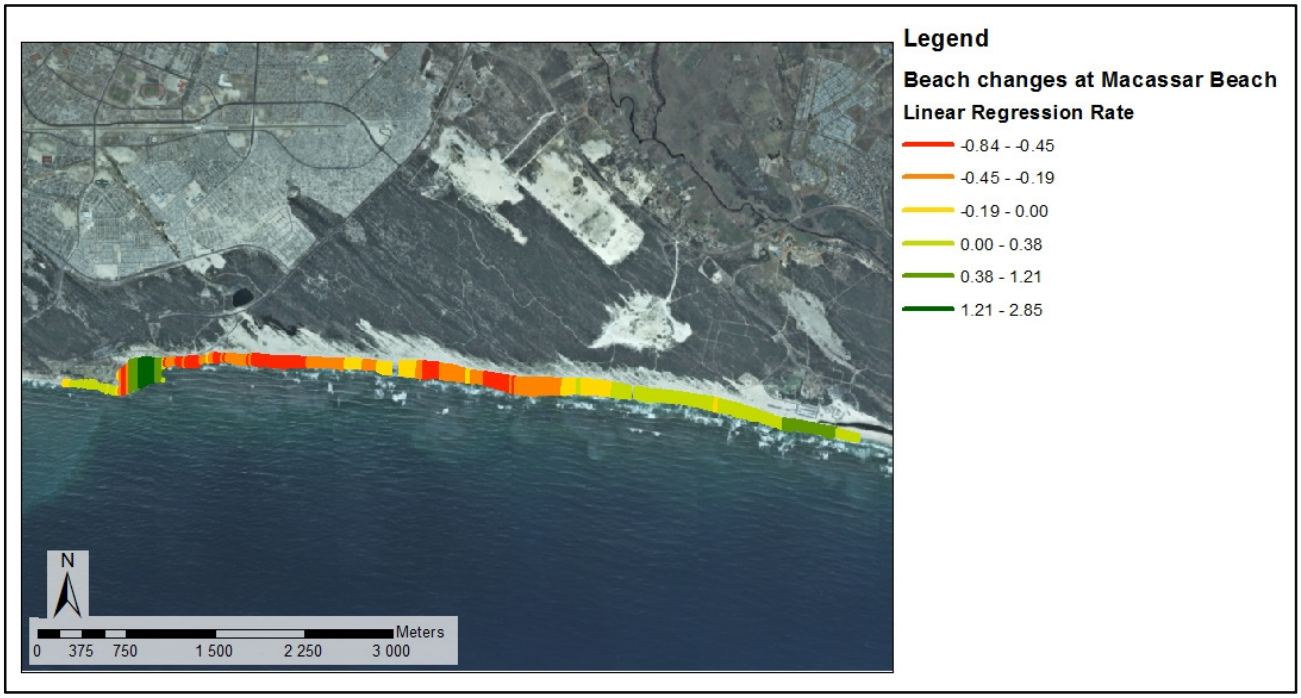

Figure 45: Linear regression rate at Macassar Beach.

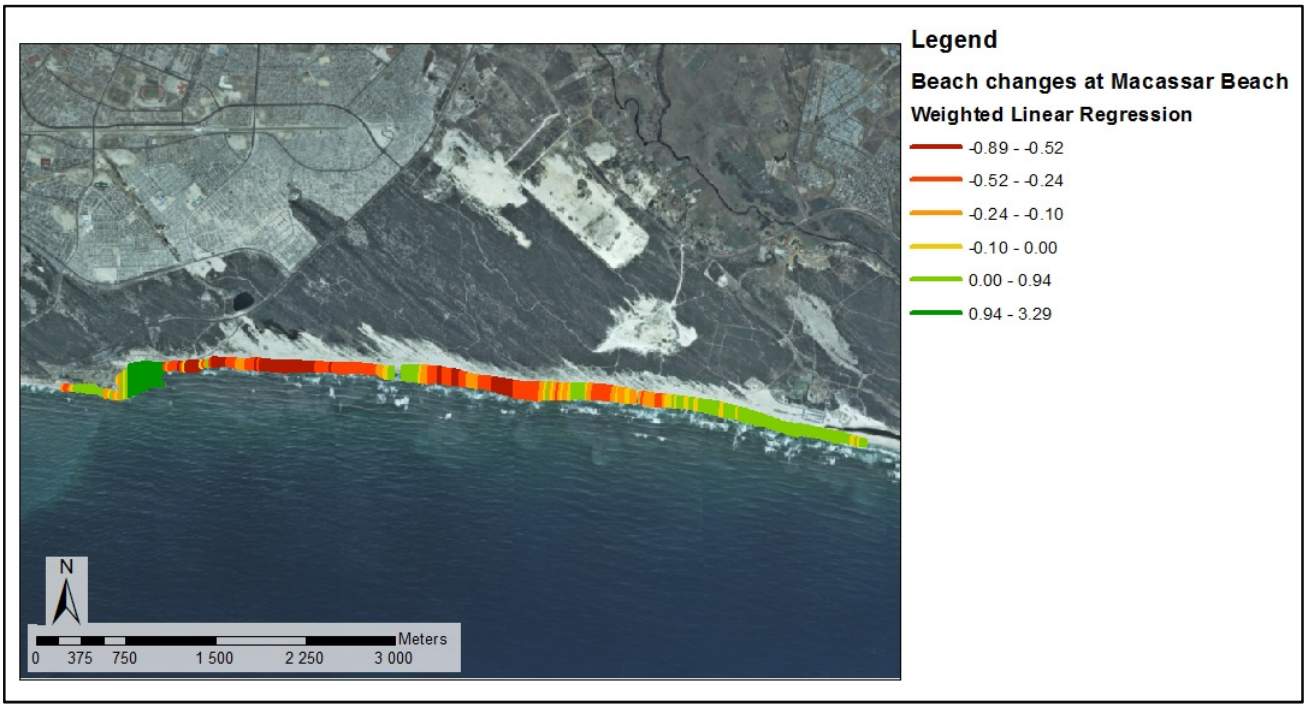

Figure 46: Weighted linear regression rate at Macassar Beach.

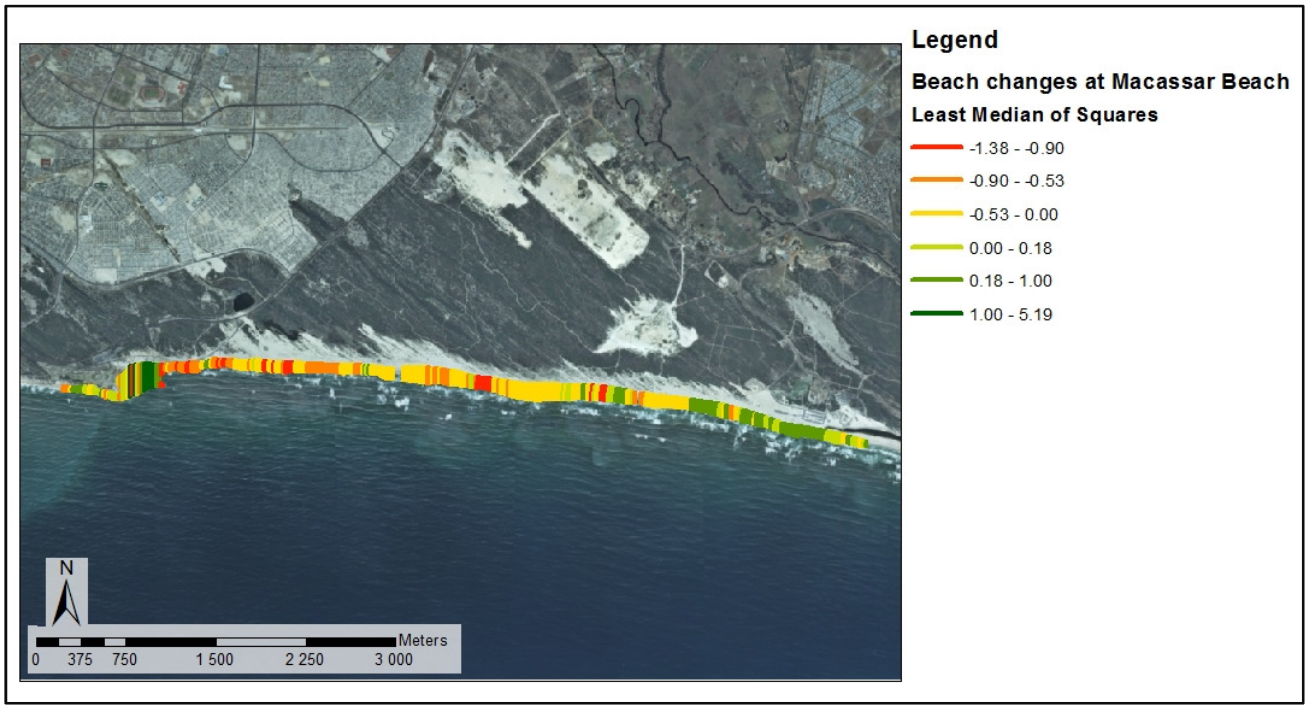

Figure 47: Least median of squares at Macassar Beach.

4.7.3. Strand

The third focus area was Strand. This was the only one of the four focus regions that showed absolutely no net accretion along any transect in the entire study region. Only net erosion occurred. Figure 48 gives the shoreline change envelope for Strand. The change ranges from 0.06 m to 182.12 m. It tends to decrease from north-west to south-east. The net shoreline movement (Figure 49) from 1944 to 2010 ranges from 122.43 m to 0.06 m erosion and averages at 39.099 m erosion.

The end point rate (Figure 50) gives the rate of change at Strand from 1944 to 2010. It ranges from 1.86 m erosion per year to 0.00 m of change per year. The average is 0.59 m erosion per year.

The linear regression rate is given in Figure 51. This is the first set of values that indicates that there was some accretion at times during the entire time period studied, even though there was net erosion. The linear regression rate ranges from 1.38 m erosion to 0.19 m accretion and with an average of 0.53 m erosion per year.

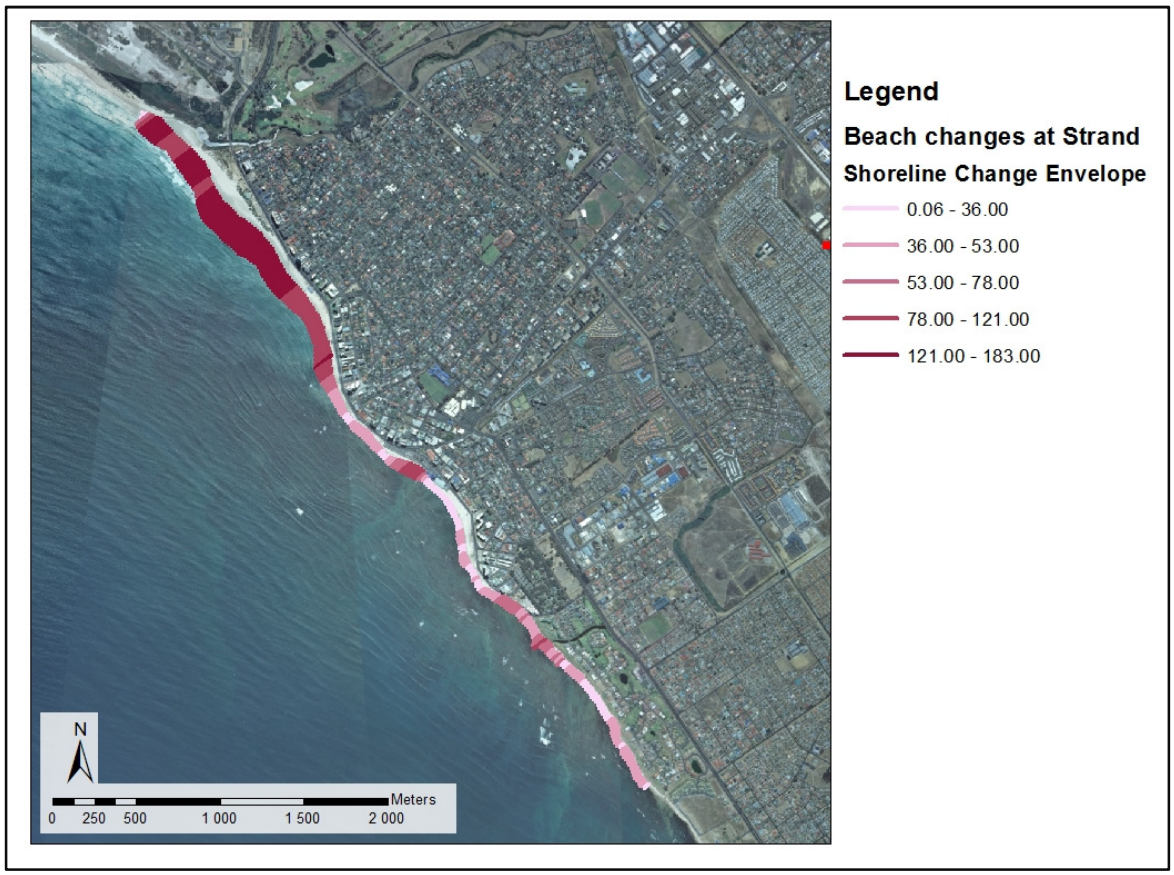

Figure 48: Shoreline change envelope at Strand.

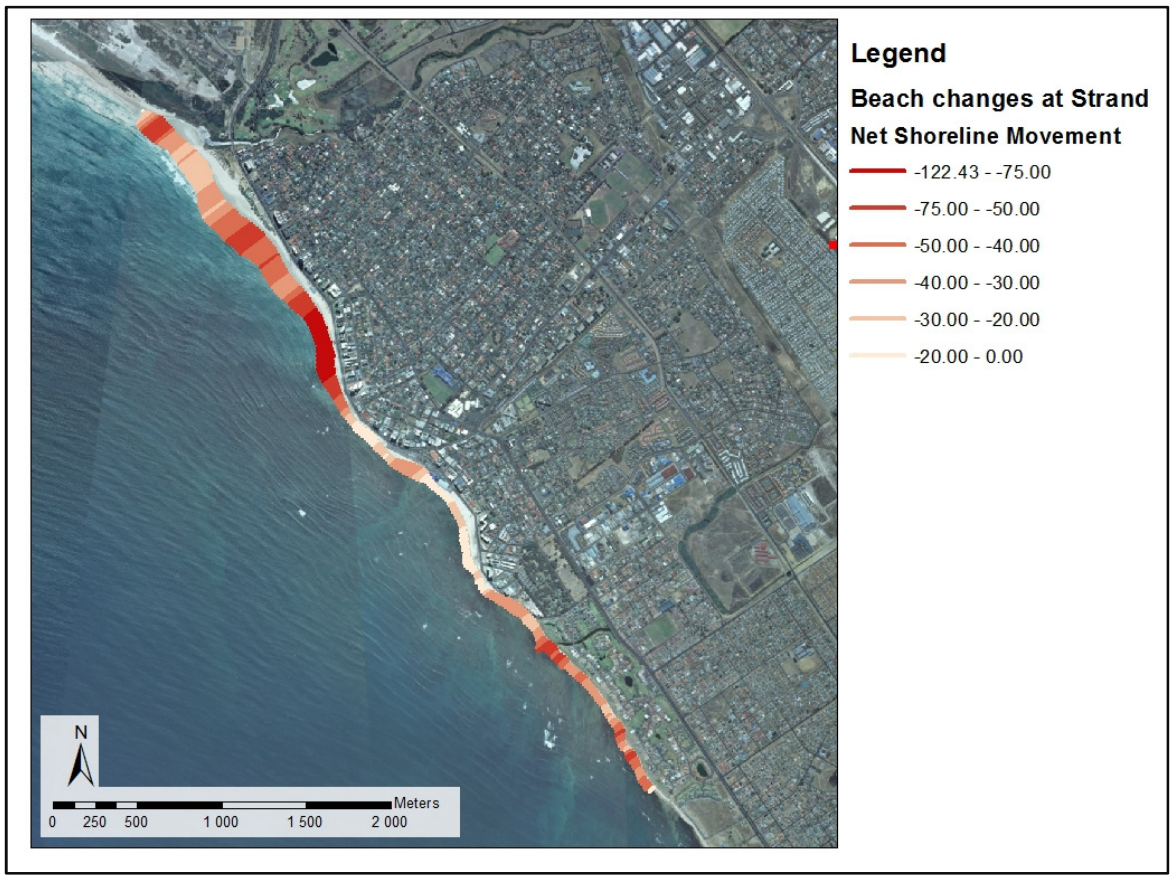

Figure 49: Net shoreline movement at Strand.

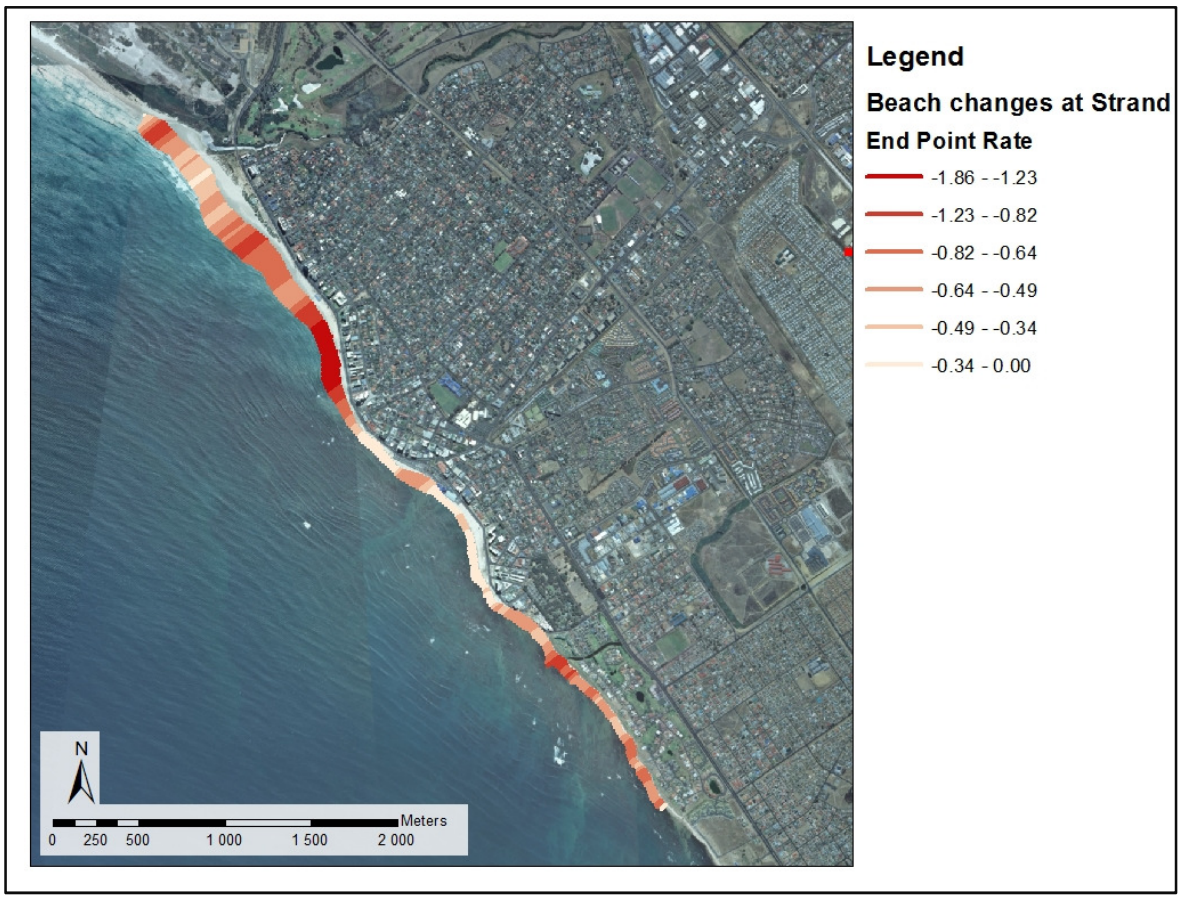

Figure 50: End point rate at Strand.

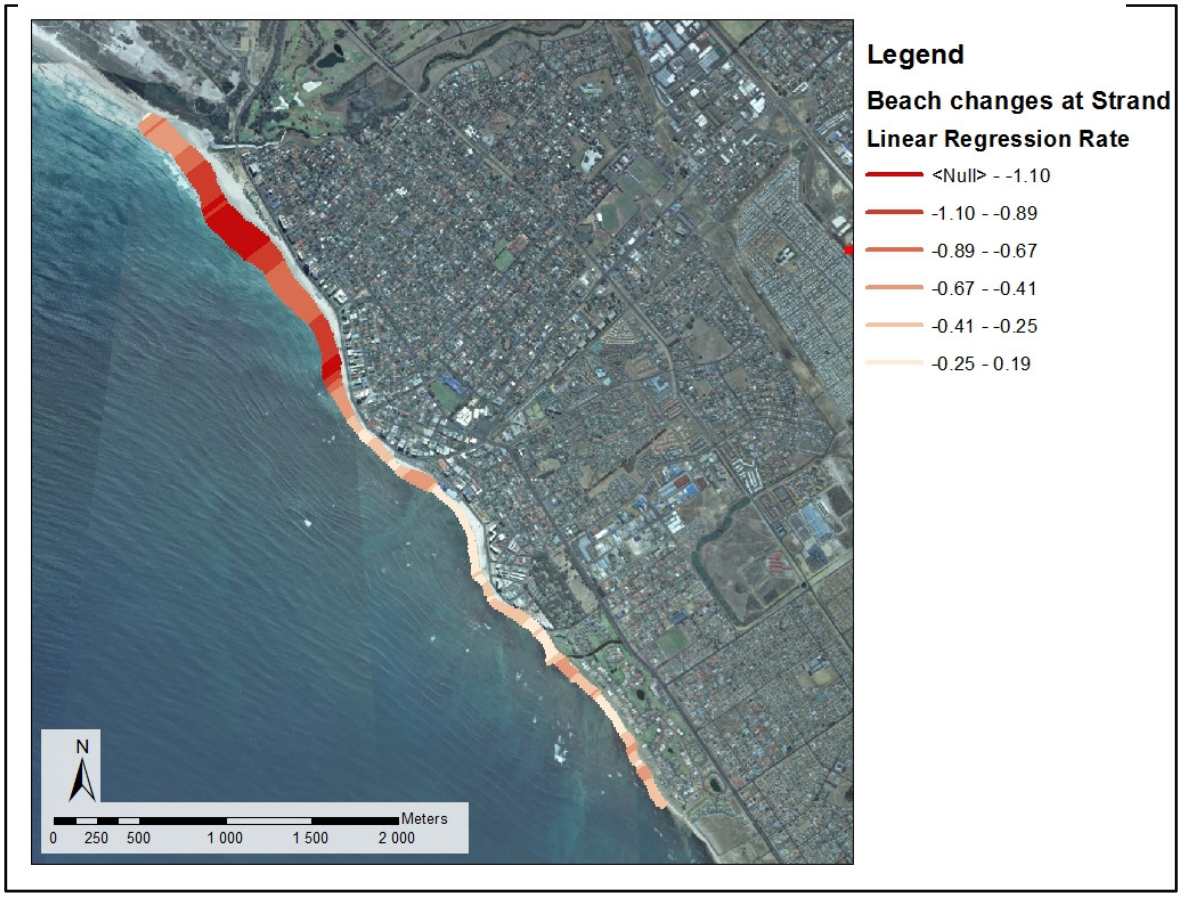

Figure 51: Linear regression rate at Strand.

The weighted linear regression rate for Strand (Figure 52) provided similar results to the linear regression rate. It ranged from 1.30 m erosion per year to 0.16 m accretion per year with an average of 0.31 m erosion per year.

The least median of squares (Figure 53) indicated higher values for both erosion and accretion, though the average also showed more erosion. The least median of squares ranged from 2.37 m erosion per year to 1.97 m accretion per year, with an average of 0.50 m erosion per year.

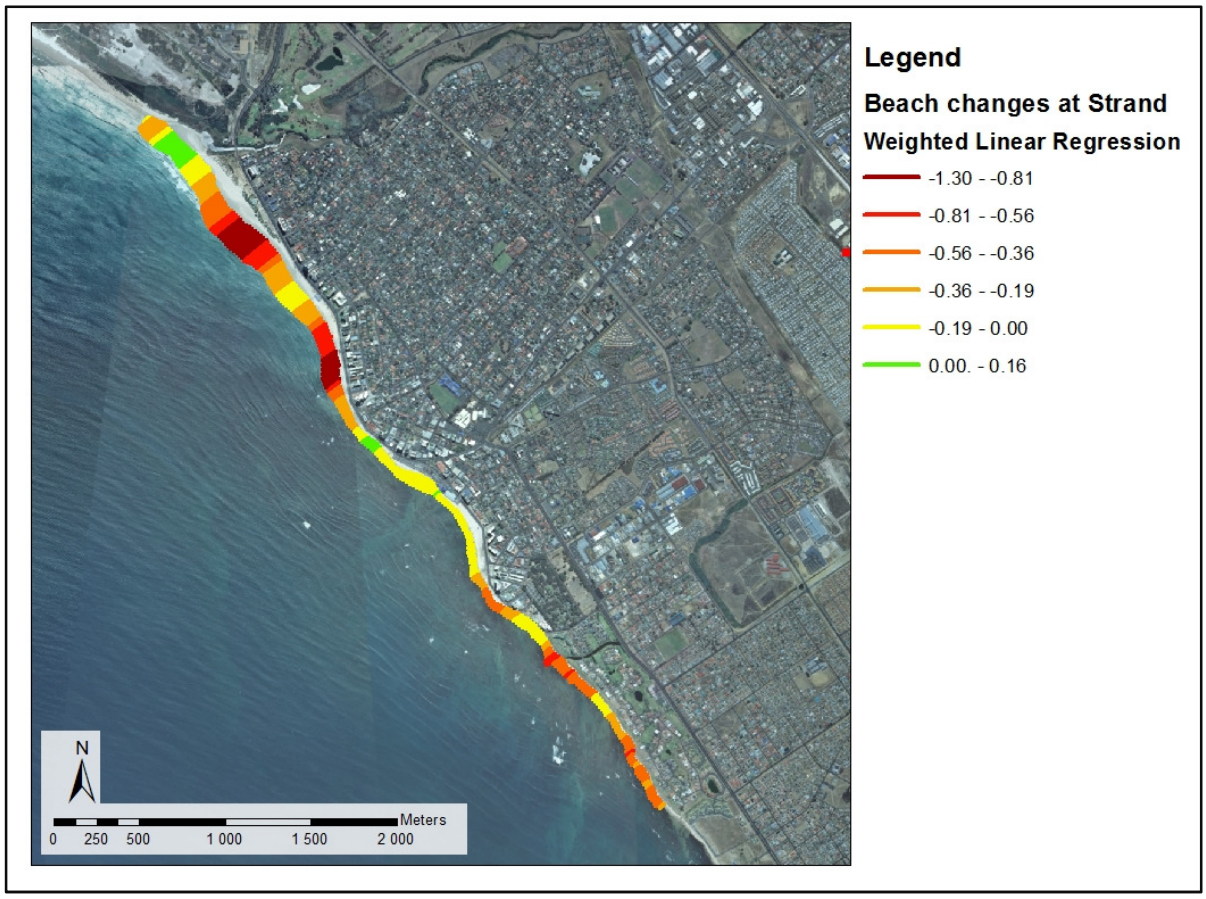

Figure 52: Weighted linear regression rate at Strand.

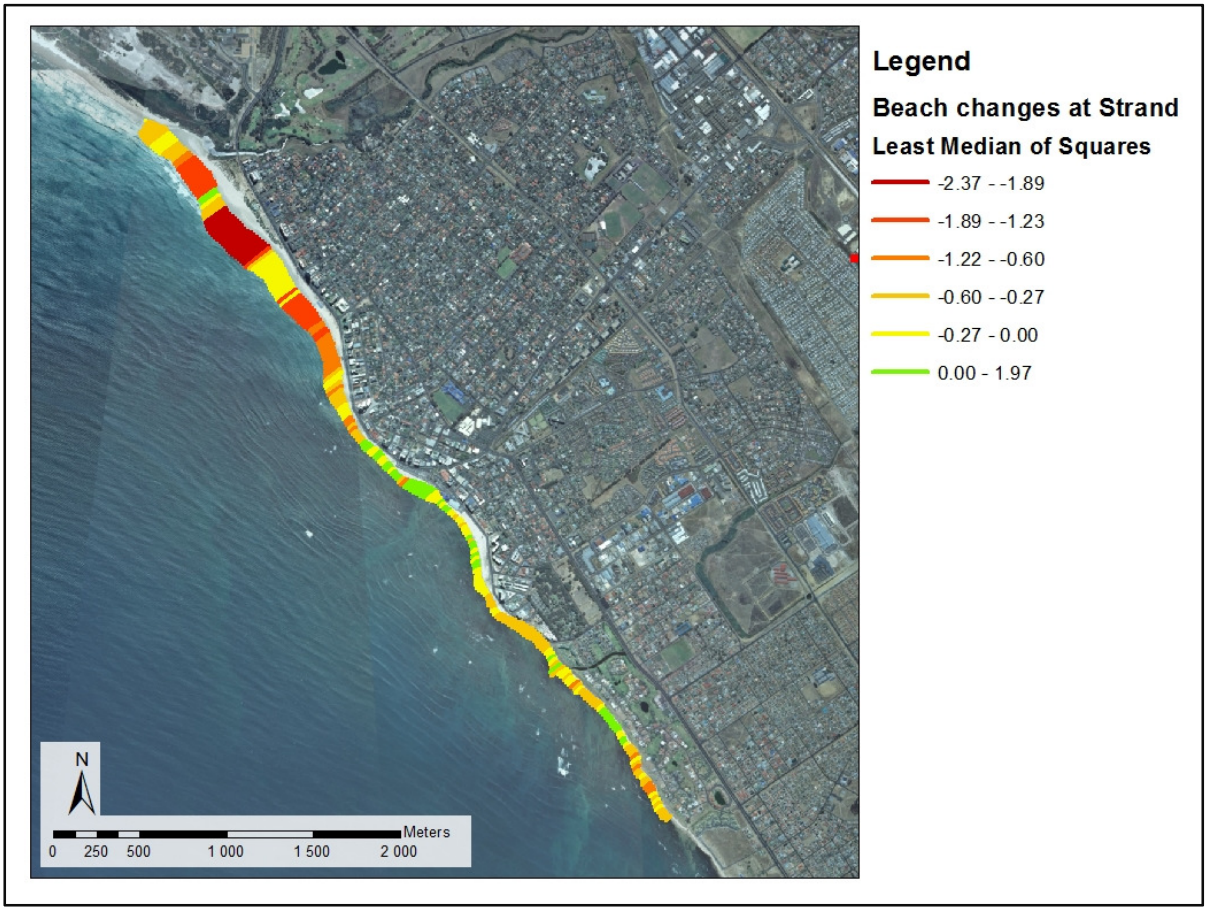

Figure 53: Least median of squares at Strand.

4.7.4. Pringle Bay

The final focus region was Pringle Bay. The shoreline change envelope for Pringle Bay is shown in Figure 54. This shows that the shoreline change ranged from 13.91 m to 141.6 m. The average change was 92.95 m.

Figure 55 shows the net shoreline movement at Pringle Bay. This ranged from 128.63 m erosion to 19.27 m accretion. The average was 65.20 m erosion. For the Pringle Bay region, some of the earlier aerial photographs did not cover the region. Therefore, the net shoreline movement is from 1961 to 2010.

The end point rate is shown in Figure 56. It ranged from 2.64 m erosion per year to 0.40 m accretion per year with an average of 1.34 m erosion per year.

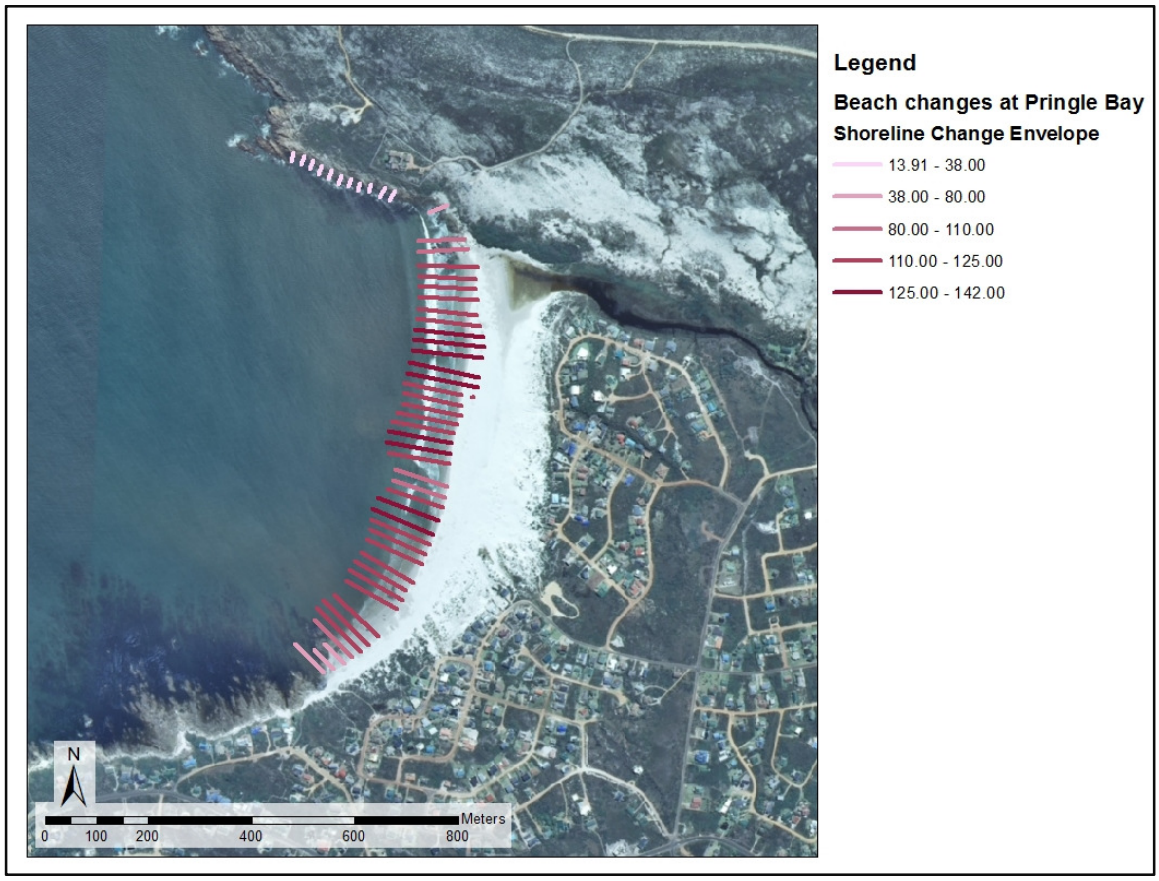

Figure 54: Shoreline change envelope at Pringle Bay.

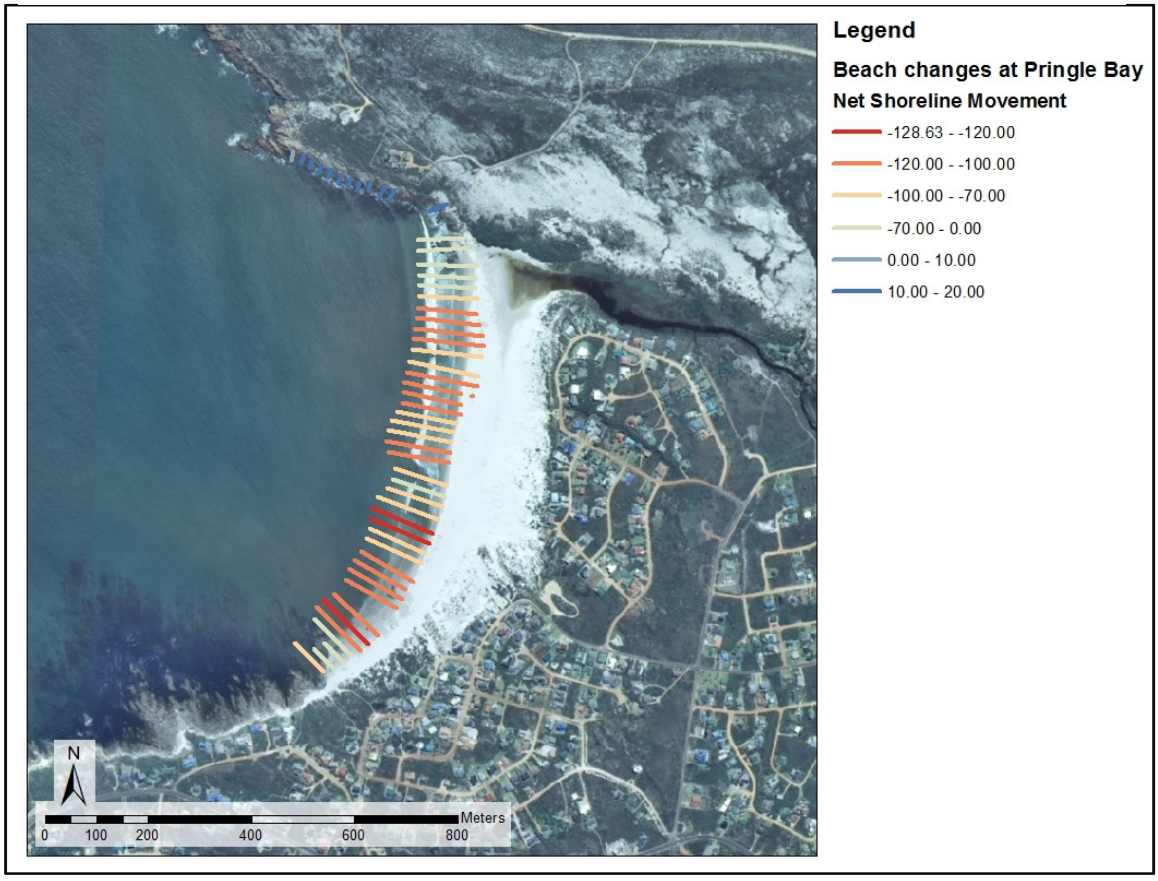

Figure 55: Net shoreline movement at Pringle Bay.

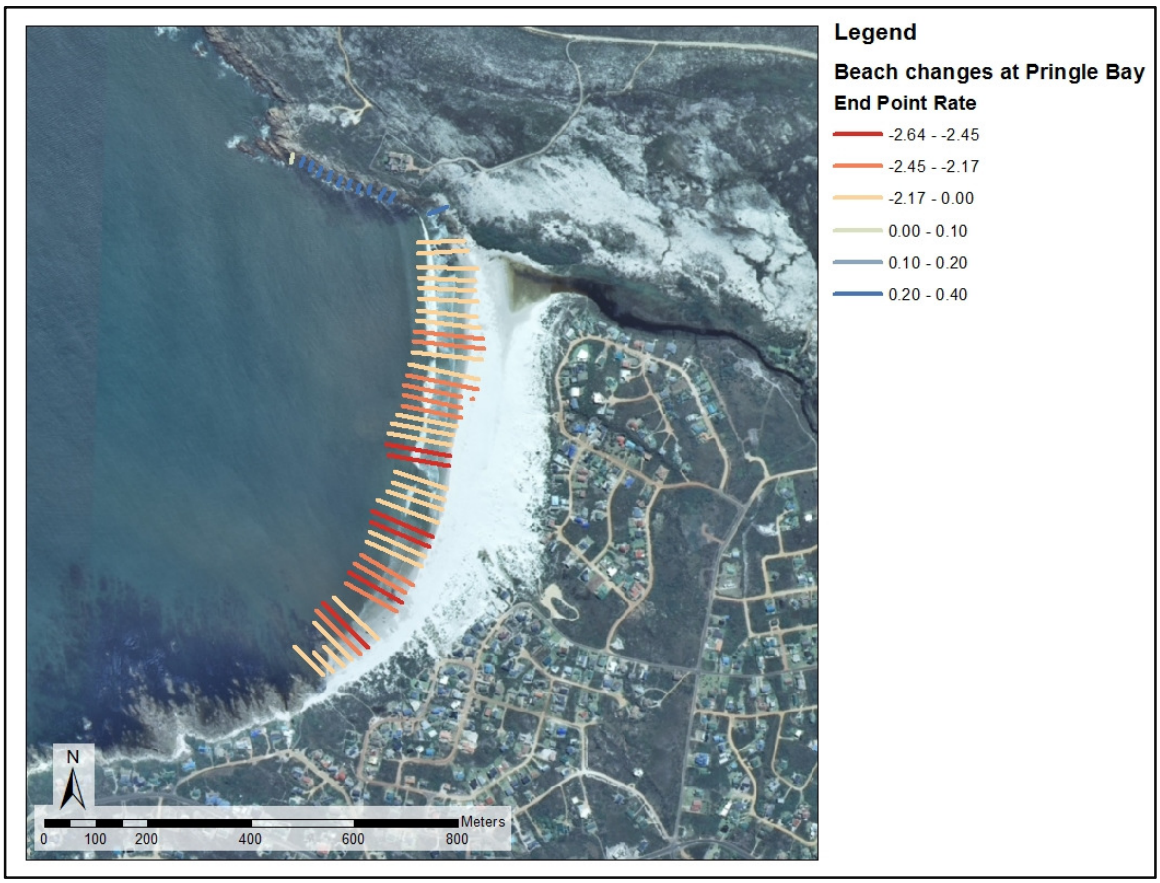

Figure 56: End point rate at Pringle Bay.

The linear regression rate for Pringle Bay is shown in Figure 57. It ranges from 2.84 m erosion per year to 0.29 m accretion per year and averages 1.64 m erosion per year.

The weighted linear regression rate (Figure 58) ranges from 2.37 m erosion per year to 0.61 m accretion per year and has an average of 1.31 m erosion per year.

Finally, the least median of squares for Pringle Bay (Figure 59) ranges from 3.25 m erosion per year to 0.32 m accretion per year and has an average of 1.46 m erosion per year.

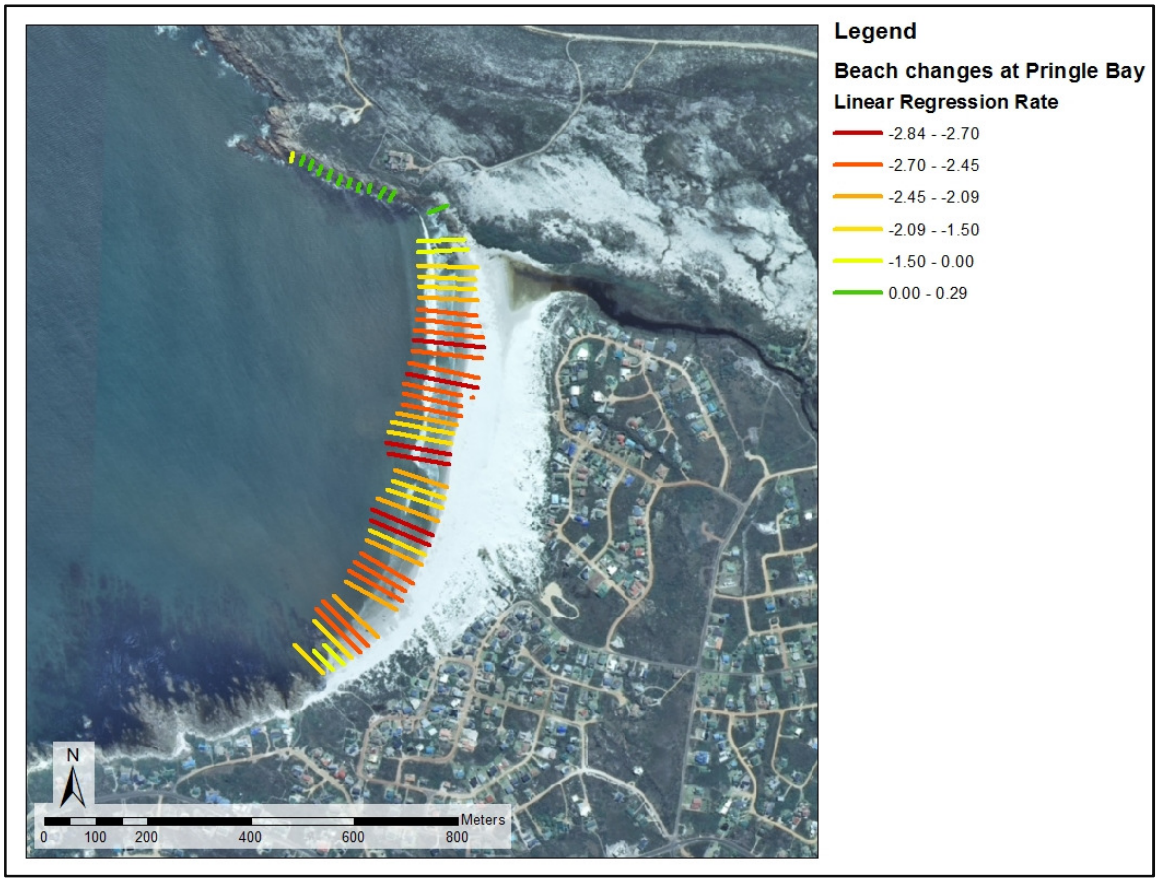

Figure 57: Linear regression rate at Pringle Bay.

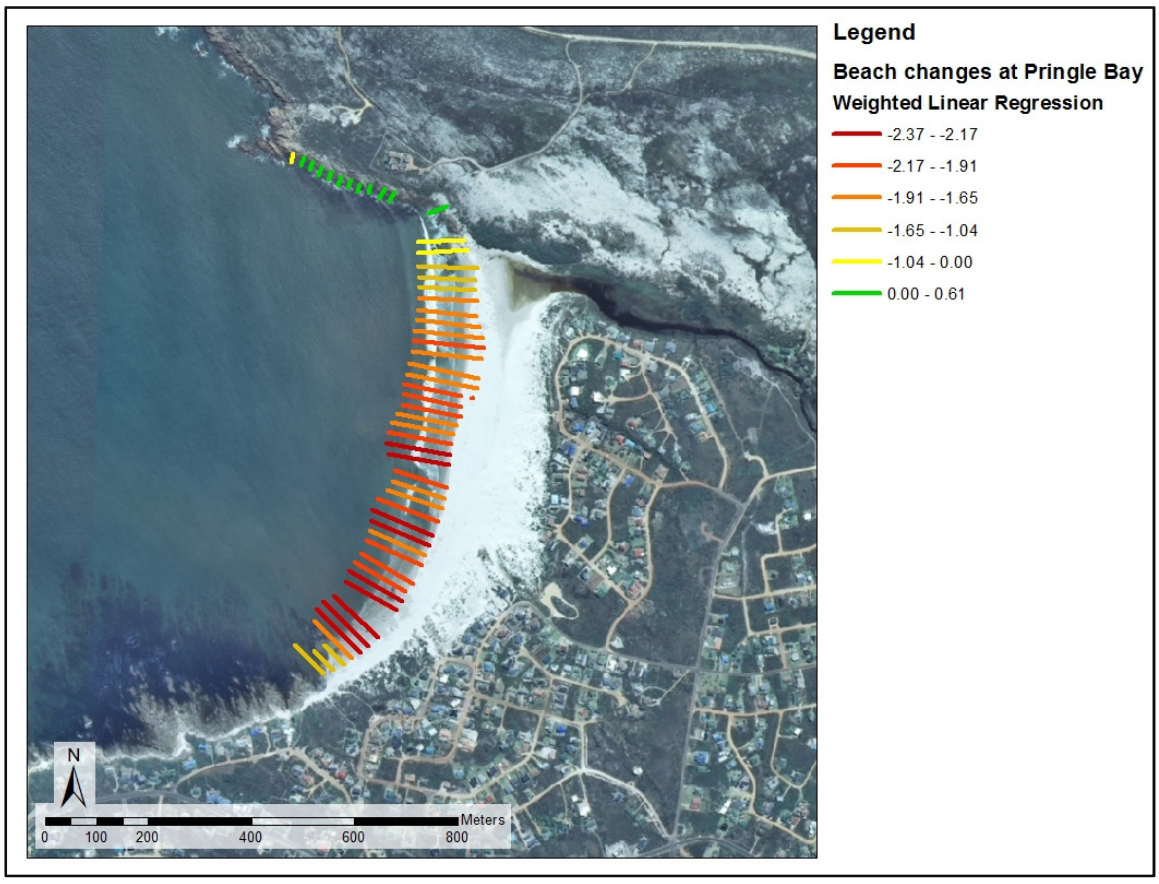

Figure 58: Weighted linear regression rate at Pringle Bay.

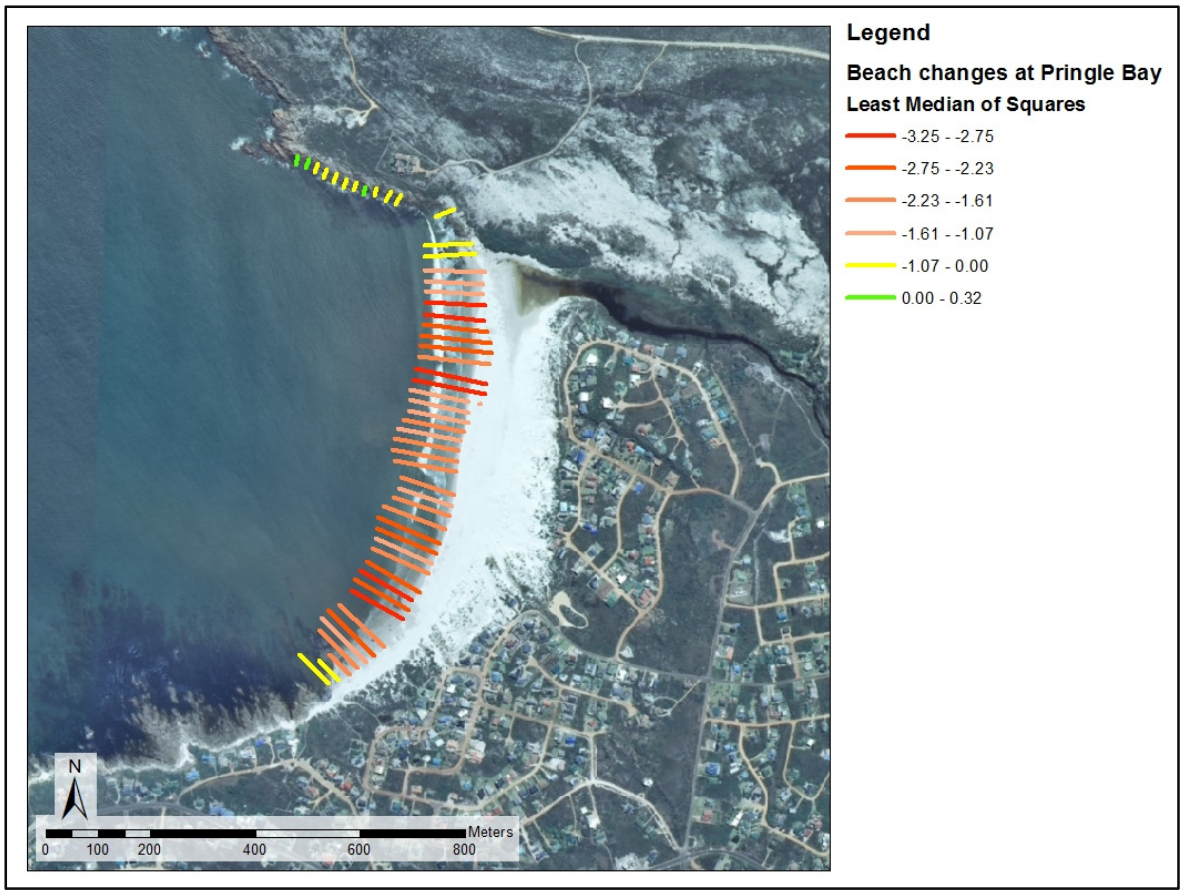

Figure 59: Least median of squares at Pringle Bay.

5. DISCUSSION

During this study, several different change detection methods were performed and compared for a beach erosion study in the False Bay region. This chapter discusses and compares the methods used, as well as the changes relating to the erosion occurring within the study area.

5.1. Coastal erosion vulnerability in False Bay

5.1.1. Vulnerability trends

Little past work has been done regarding erosion and vulnerability to erosion in False Bay. Unterner et al. (2011) did a study of erosion vulnerability for the entire South African coastline, and found that the most vulnerable region within False Bay was at Bayview Heights. Their study did not use change detection to assess actual erosion rates, but rather used factors such as beach width and wave height to create an erosion vulnerability index. The vulnerability to erosion within False Bay showed considerable variability according to their assessment.

The results of this study have shown considerable changes in erosion vulnerability over the last 30 years throughout the study area. The results show an increase in built-up regions, while sand dune regions have decreased, and NDVI has steadily decreased. Results from post-classification change detection, image differencing, and vegetation index differencing all showed increases in built-up areas and decreases in vegetation health and density. The increased urbanisation in this zone increases the risk of erosion by removing natural landcover and placing greater demand on the region through increased vehicle and pedestrian traffic in vulnerable areas, as well as the increased pollution associated with a human settlement. In addition, it makes humans more vulnerable to the effects of erosion since structures near the coast are far more vulnerable to be damaged by coastal erosion.

The results have shown a reduction in dunes as construction has occurred, but they have also shown a reduction in vegetation on the originally vegetated dunes. This can decrease dune stability, making the sand vulnerable to wind erosion. This would cause dunes which may have had little migration while vegetated to have an increased rate of dune migration. While a migrating dunefield can be stable in natural conditions, this is problematic in this region since the migration of the dunes may end in built-up regions. This may result in

further anthropogenic damage to the natural system through removal of the sand, or in damage to man-made structures through the encroachment of the sand.

Another significant change observed was an increase in the shallow coastal class. This could be an indicator of increased sediment volume from beach eroded material, however, given the dynamic nature of tides, waves, and other factors in this region, it could simply be increased turbidity from stronger ocean currents; or increased phytoplankton in the water. In combination with the factors discussed above showing increased vulnerability to erosion, it may be inferred that this is a possible indicator that erosion has occurred, however this cannot be confirmed via remote sensing alone due to the complexity of the coastal zone.

The different change detection methods used together showed similar trends in vulnerability change within the study area, however different observations were made using each method before coming to the overall conclusions.

Image differencing showed consistent decreases in band 4 and increases in the brightness band. Band 4 is the near-infrared band. Since vegetation has a high reflectance in the near-infrared range, the consistent decreases in band 4 may indicate loss of vegetation or of vegetation health. This is in line with the increase in built-up regions seen in post-classification change detection, since vegetation would have been removed for construction. Vegetation health may also have decreased in other regions.

The brightness band resulting from a tasselled cap transformation gives a weighted sum of all the non-thermal bands, hence indicating total reflectance. Differencing of this band showed both increases and decreases, but the trend was towards increases in brightness. This supports the above findings since an increase in brightness could indicate increasing amounts of artificial reflective surfaces including roads, roofs and pavements, along with open sand areas.

Within the individual focus areas, some fluctuation in increases and decreases in both band 4 and the brightness band can be seen, indicating fluctuations in vegetation levels and other factors. However, the long-term trends of increasing brightness remain the same.

The NDVI differencing method showed consistent decreases in NDVI over time, except during the period from 1991 to 1996, where the NDVI tended to increase. The general trend over time, however, is a decrease in NDVI. This is an indication of a temporary improvement in vegetation health by 1996, followed by more consistent decreases in vegetation health and density. A decrease in vegetation density and health naturally results in an increase in vulnerability to erosion within the study area. Considerable urbanisation within the study

region has resulted in removal of some of the vegetation. In other areas, the vegetation health has decreased.

Since it was thought that the NDVI would be especially useful in assessment of the sand dune class, the NDVI change from 1985 to 2011 was clipped according to the original extent of the sand dune class from 1985 and is shown in Figure 60. At this stage it is important to note that the extent of the sand dune class is subject to the accuracy of the classification as given in Section 4.2. As expected, increases in NDVI within this class are extremely minimal. Almost the entire selected region shows decreases in NDVI. Since the sand dune class refers to vegetated sand dunes, this indicates that the vegetation on the sand dunes has decreased in health and density, putting this part of the coastal zone at greater risk to erosion.

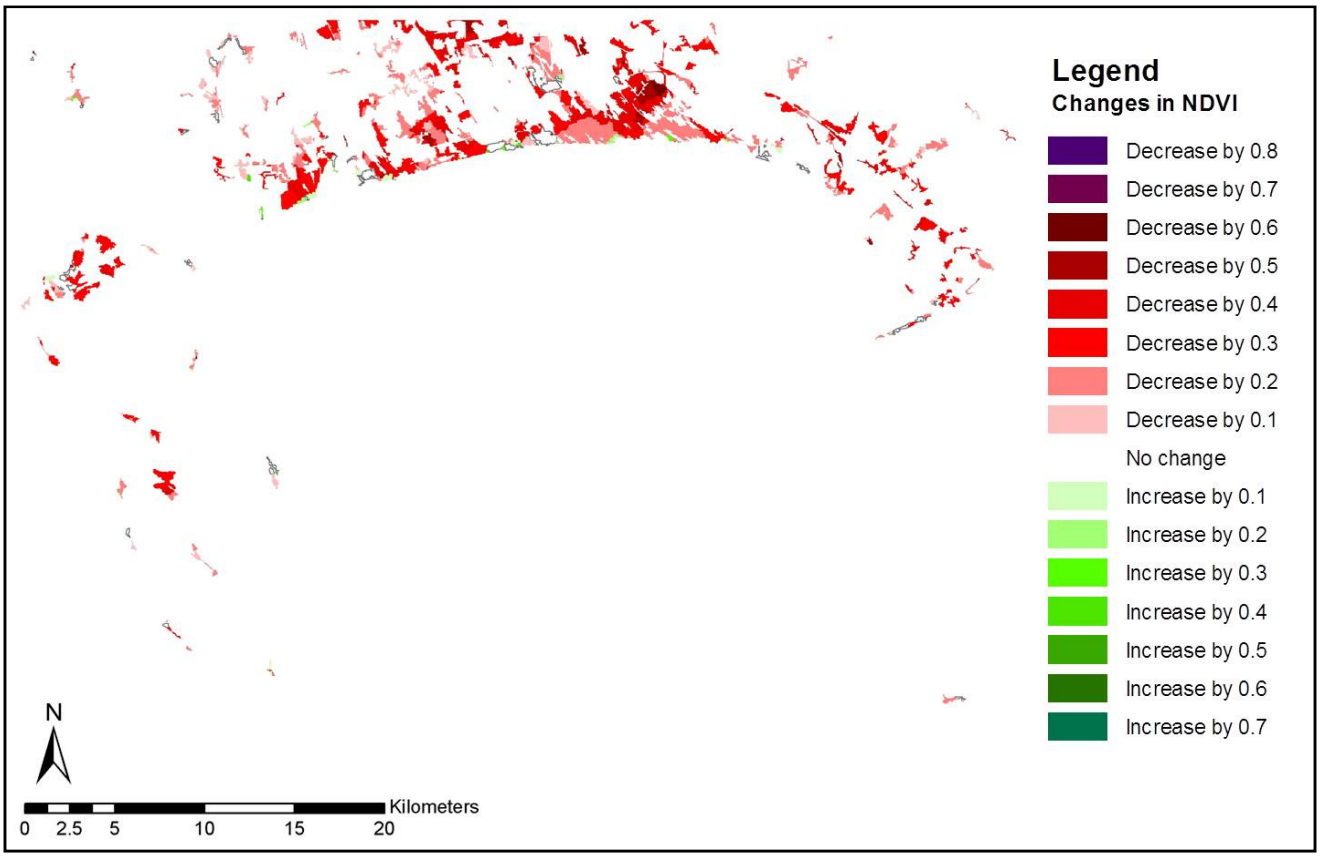

Figure 60: Changes in NDVI from 1985 to 2011 within the zones classified as sand dune in 1985.

The results of the post-classification change detection are seen in Section 4.3. Changes observed include a slight decrease in the ocean class. Since the shallow coastal class showed increases, this could be caused by more areas being classified as shallow coastal. This in itself could be a result of a build-up of sand off the beach resulting in a greater

shallow coastal area. However, it could also be caused by images being captured at different tidal levels, the wave type at the time the image was taken, increased phytoplankton, or other complex factors. The beach class showed some fluctuation in increases and decreases, although there was an overall decrease in this class. Some of this could be caused by tidal changes. However, since the Landsat imagery has a pixel size of 30 m, a change of even a single pixel could be indicative of considerable erosion. A steady increase in the built-up class is observed while sand dunes decrease overall. These results coincide with the observations from image differencing, showing that there is an increase in artificial, built-up areas, while vegetation on the sand dunes decrease. These changes increase the vulnerability of the region to erosion since the vegetation no longer protects the sand from wind erosion.

This method also allowed more detailed observations at the four focus areas.

Bayview Heights

Figure 61 shows changes in beach, ocean, and shallow coastal classes at Bayview Heights from 1985 to 2011. The most noticeable change here is that ocean has changed to shallow coastal (dark green) in an increasing amount down towards the harbour. This provides evidence that the construction of the harbour has resulted in a build-up of ocean sediments.

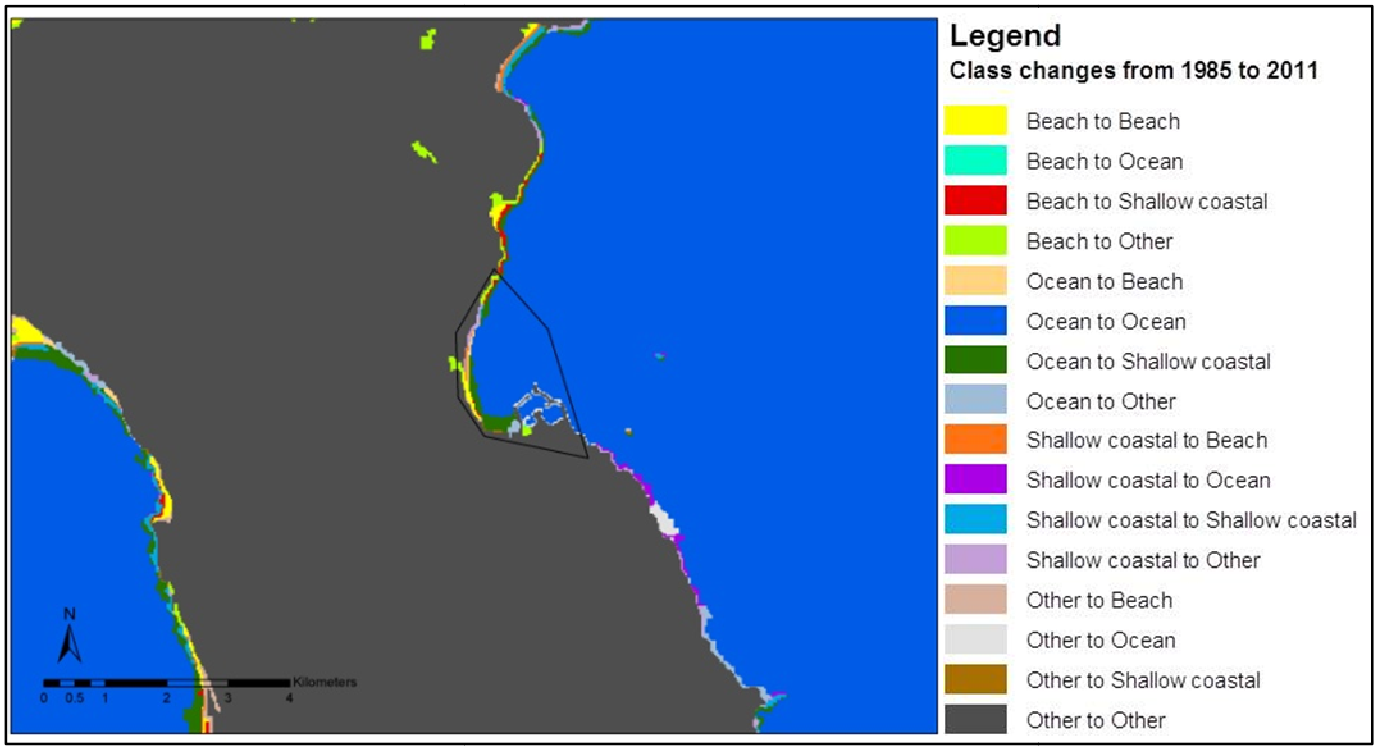

Figure 61: Changes in beach, ocean, and shallow coastal classes at Bayview Heights.

Figure 62 shows a small region of change from sand dune to built-up (red) and a few other changes in the built-up class, with little other change of interest.

The presence of the harbour is the most significant feature in this focus area. The harbour results in anthropogenic effects on the sediment movement in this area. The result is a build-up of sediments north of the harbour which would otherwise have been eroded away.

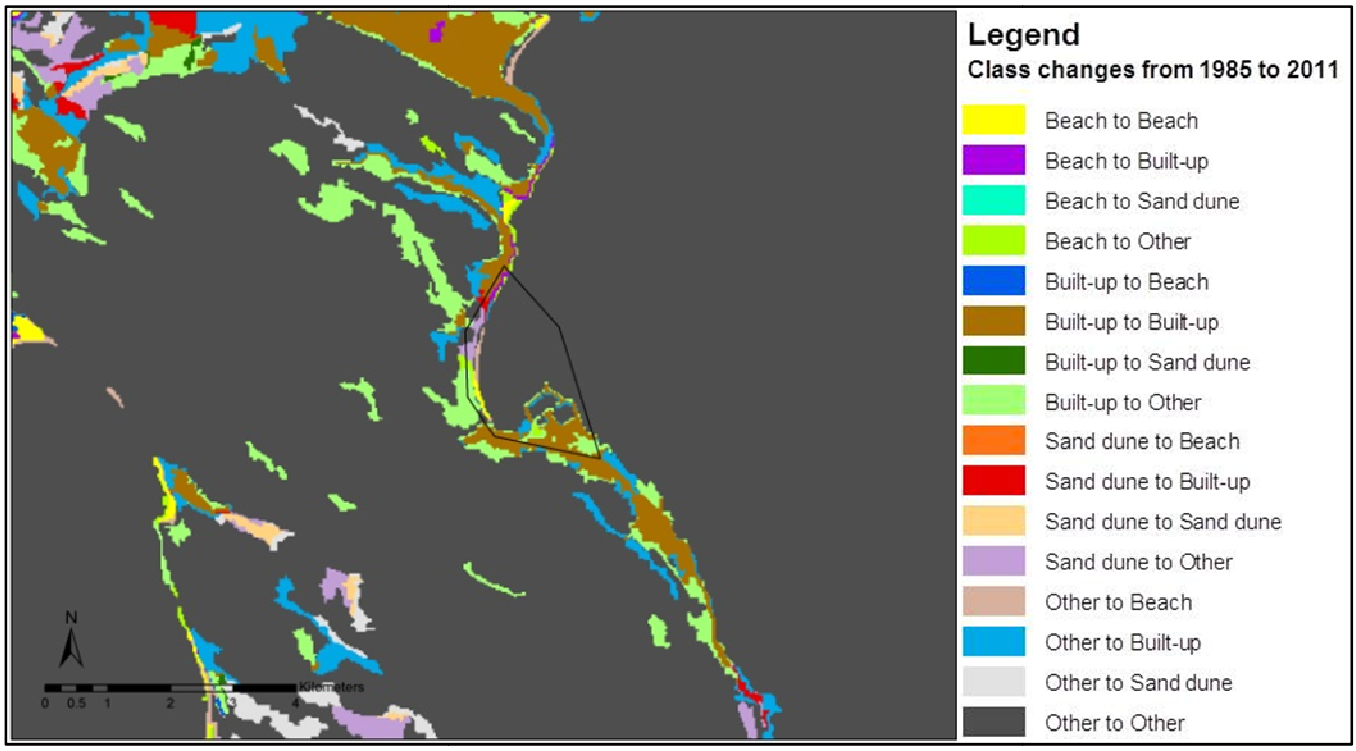

Figure 62: Changes in the beach, built-up, and sand dune classes at Bayview Heights.

Macassar Beach

Considerably more change was visible at Macassar Beach. The changes in the built-up and sand dune classes in this region were the most significant visually observable changes across the entire study region. Figure 63 shows the changes between the built-up and sand dune as well as beach classes. At the beginning of the study period, in 1985, some parts of the dune field extended over 3 km from the beach front. This has gradually been pushed back by human activity as urbanisation has taken over the region. From 1985 to 1991, a significant portion of these dunes were changed either to built-up or to sand (not beach) as preparations were made for construction. Moving in to 1996, those regions changed to built-up. These earlier years saw the most construction, although there was continued expansion

later on as well. Figure 63 also shows large portions of the 'other' class being converted to built-up (cyan). The urbanisation in this region has a drastic impact on the vulnerability to erosion in this region. While a change of sand dunes to built-up (red) does not indicate erosion in itself, it does indicate alteration to the natural system and an increased vulnerability to future erosion.

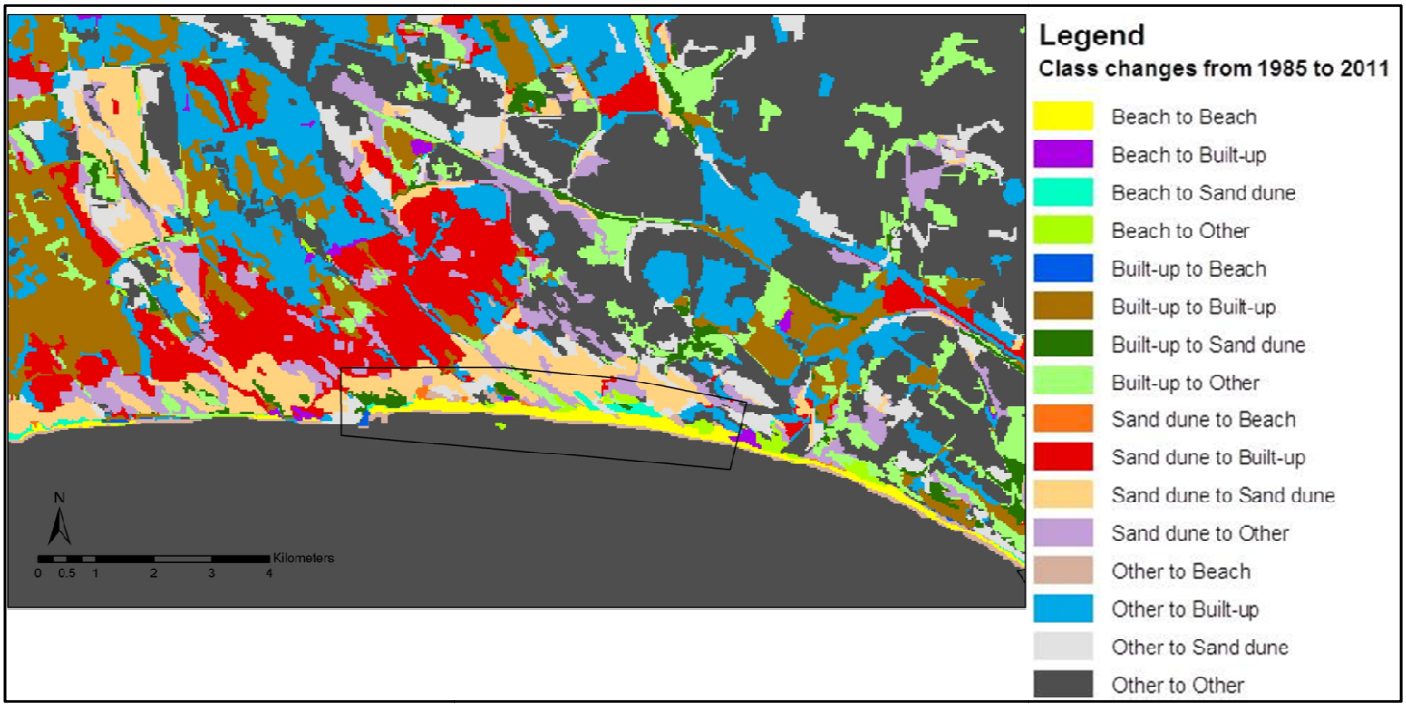

Figure 63: Changes between beach, built-up, and sand dune classes at Macassar Beach.

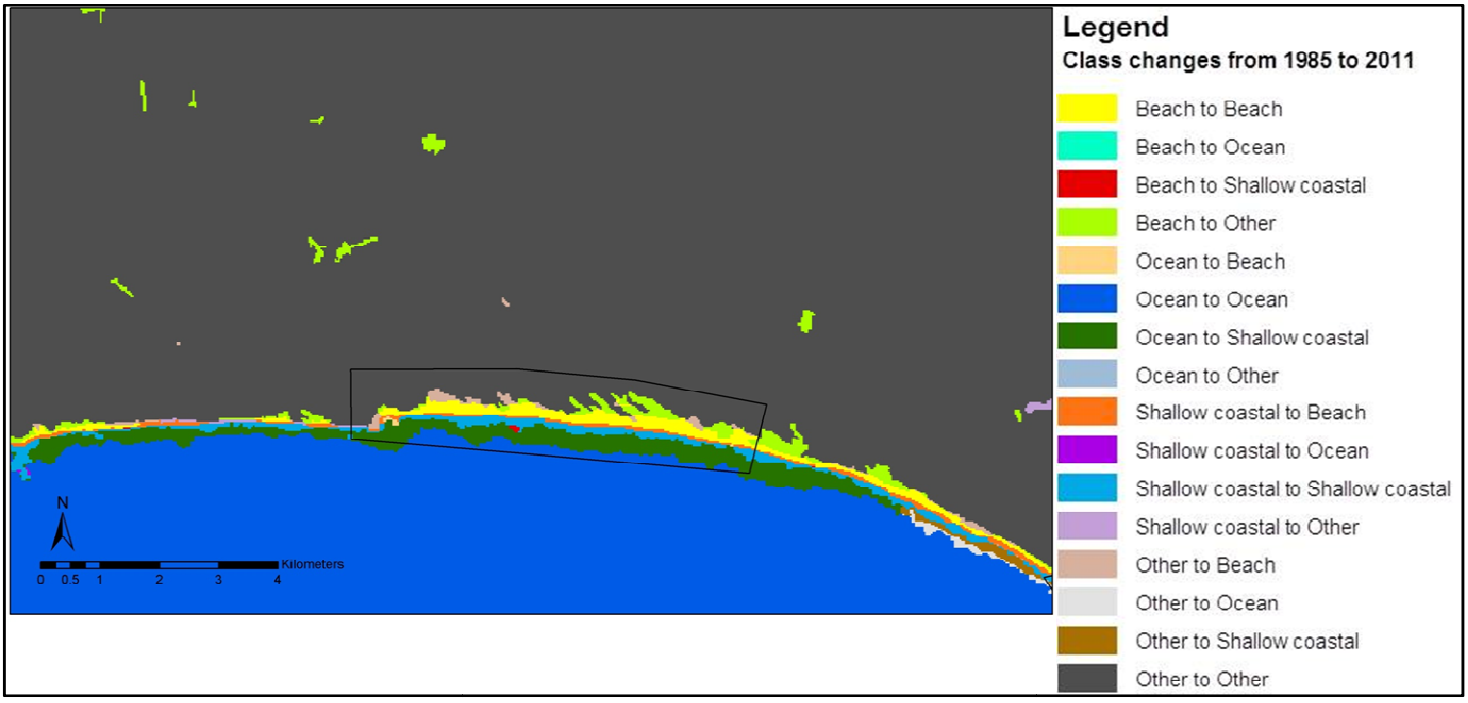

Figure 64: Changes between beach, ocean, and shallow coastal classes at Macassar Beach.

Figure 64 indicates a significant region where ocean has changed to shallow coastal (dark green). This could be an indication of increased ocean sediments in this region. The overall change zone from ocean to shallow coastal is around 100 to 300 m wide. A change this significant could clearly not be caused simply by tidal changes. A thin strip of beach change to shallow coastal is also visible, which could be a direct indicator of erosion. Different tides at the different times of image capture could also cause this change. Since the pixel size of a Landsat image is 30 m, even a single pixel wide strip of change indicates up to 30 m of beach erosion in this focus area. At this resolution, it is difficult to make conclusions about beach erosion since pixels may be mixed. Change at the level of a few pixels can therefore not be quantified. Changes seen on the aerial photographs (discussed in Section 5.1.2) were more useful for quantifying beach erosion.

Strand

In the Strand focus area, the most change is visible in the northern portion of the focus area. Figure 65 shows changes in the beach, ocean, and shallow coastal classes at Strand. This figure shows changes both from shallow coastal to beach (orange) and from shallow coastal to ocean (purple).

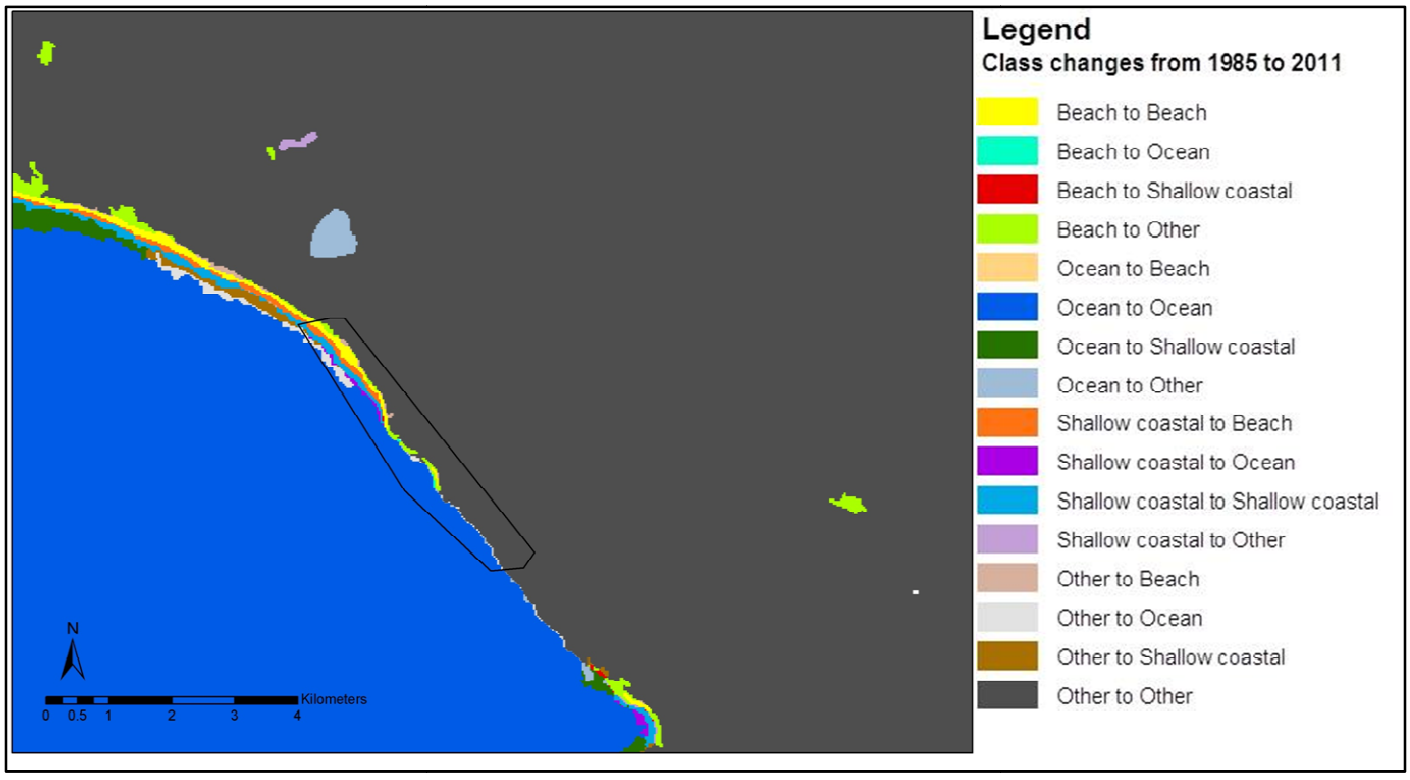

Figure 65: Changes between beach, shallow coastal, and ocean classes at Strand.

Figure 66 shows changes between beach, built-up, and sand dunes in this focus area. This shows significant areas where both sand dune and 'other' have changed to built-up (red and cyan, respectively). As with Macassar Beach, this is a definite sign of increased vulnerability in this region. Changes of built-up to other are likely the result of misclassification in some cases.

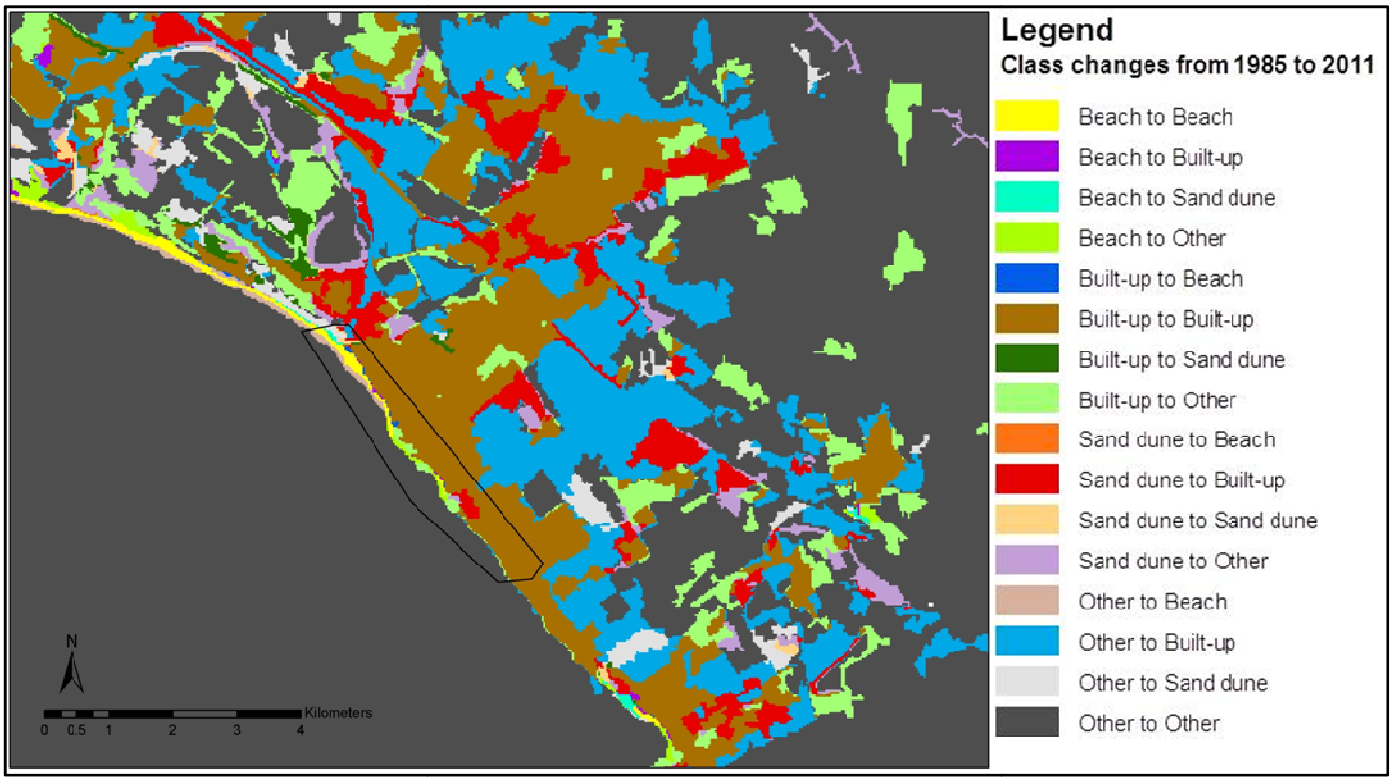

Figure 66: Changes between beach, built-up, and sand dune classes at Strand.

Pringle Bay

At Pringle Bay, few significant changes were observed by this method. The rocky areas on either side of the sandy beach here were expected to provide a degree of protection against erosion. On Figure 67, a small region which changed from beach to built-up is visible (purple). Construction on the beach leads to increased erosion vulnerability.

Figure 68 shows a change from shallow coastal to ocean (purple) along the sandy portion of the beach as well as a change from 'other' to shallow coastal (brown) along the southern rocky portion. This could indicate a higher sea level by the end of the study period, which could indicate that erosion had occurred or that there is increased vulnerability to erosion. This could be caused by sea level rise or could simply be the result of different tides at the time of image acquisition. Since the coastal area is so complex, general trends can be observed but it is often difficult to isolate specific causes since so many factors are at play.

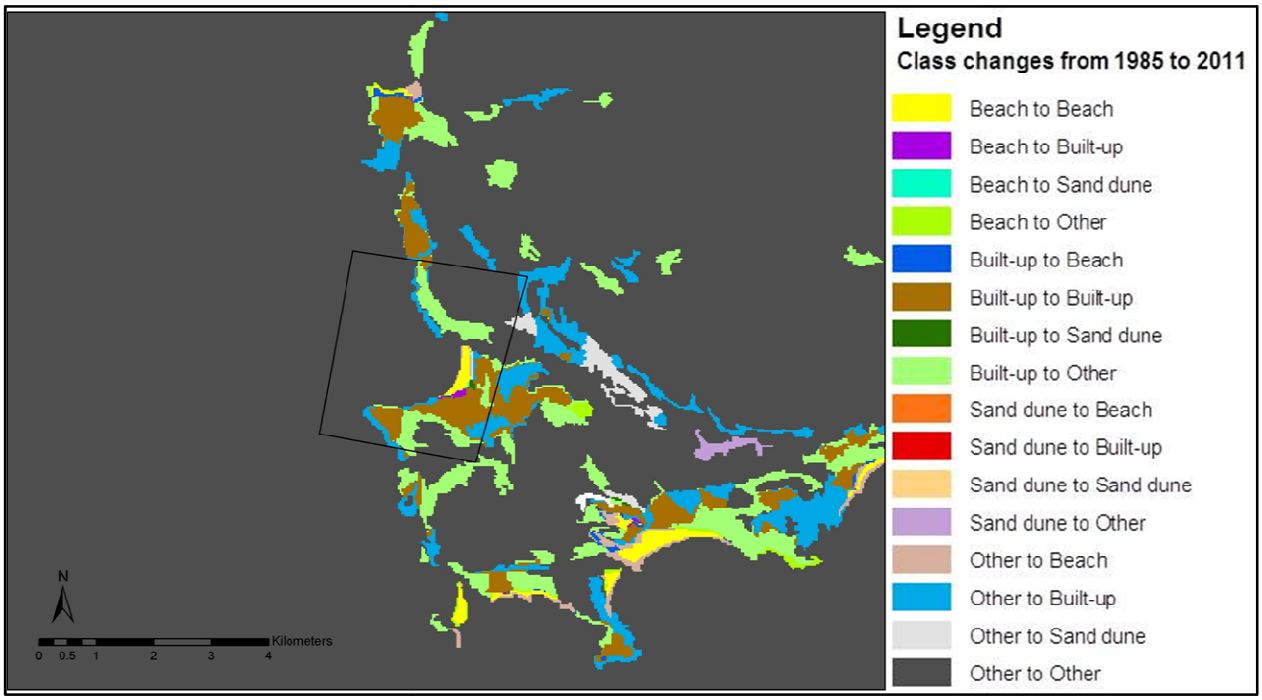

Figure 67: Changes between beach, built-up and sand dune classes at Pringle Bay.

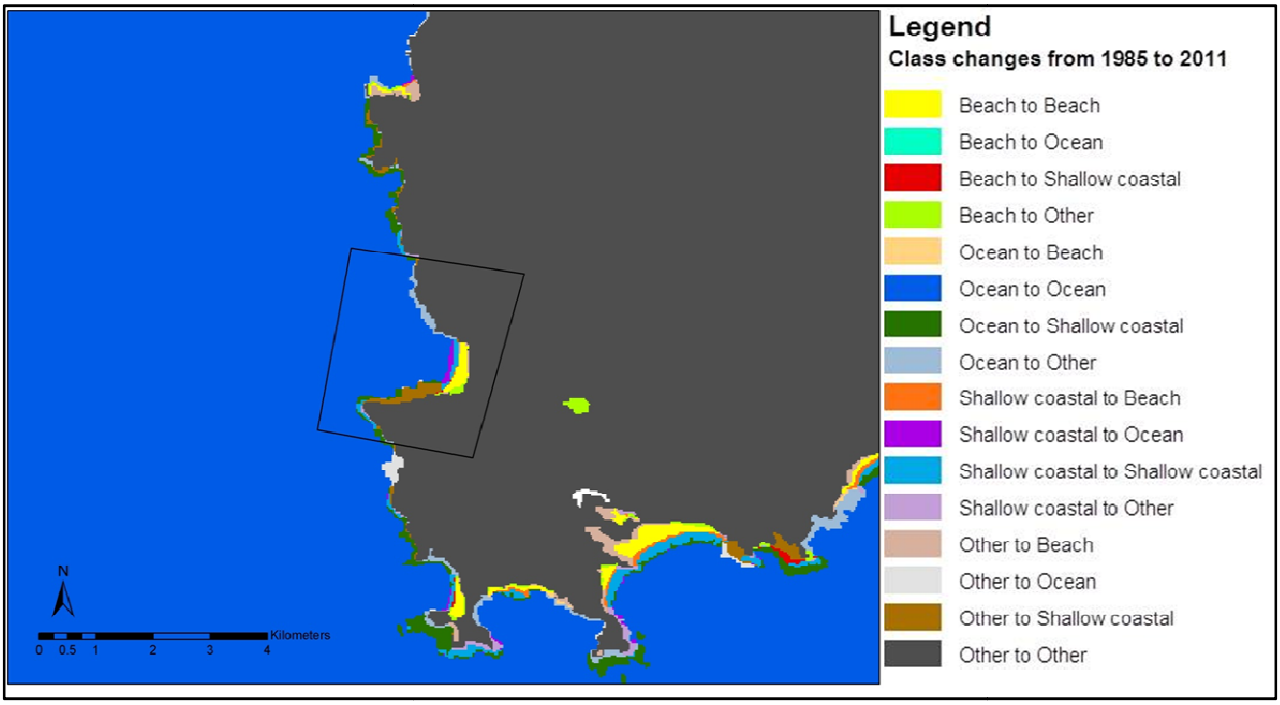

Figure 68: Changes between beach, ocean, and shallow coastal classes at Pringle Bay.

5.1.2. Erosion trends

The digital shoreline analysis system used on aerial photographs during this study provided information on erosion trends in the four focus areas. These trends are discussed in the sections below.

Bayview Heights

According to the digital shoreline analysis system, Bayview Heights showed the least change of all four focus areas. This region was identified in a study by Unterneret al. (2011) as a high-vulnerability region for erosion. Their study involved measuring various parameters such as beach width and wave height and using them together to determine an overall vulnerability. Bayview Heights was seen as the most vulnerable location in the whole of False Bay. However, their study did not incorporate change detection and changes over time. The results of the present study show that this region was not experiencing as much erosion as the other focus regions. What was seen as the most vulnerable location has actually exhibited the least coastal erosion of the four focus areas. An analysis of the discrepancy between a region thought to be vulnerable and yet experiencing low erosion may be necessary in future research. It may be that some parameter in the model by Unterneret al. (2011) was weighted more heavily than needed. The presence of the harbour in this region does make it more vulnerable to anthropogenic influence, but this does not necessarily mean that it is more vulnerable to erosion. In fact, the average end point rate of 0.008 m actually indicates that from 1944 to 2010, there was a very slight amount of accretion in this study region. However, the linear regression and least median of squares do show that on average, there was about 0.17 m of erosion per year in this region. It is significant to note that this is the region exhibiting least change and yet it still experiences an average of yearly erosion. Both in post-classification change detection and when using the digital shoreline analysis system on aerial photographs, Bayview Heights showed the least change of all four study areas.

For this region, the shoreline change envelope ranged from 8.30 m to 90.39 m, while the net shoreline movement ranged from 26.10 m erosion to 45.47 m accretion. The higher values seen in the shoreline change envelope in the northern regions of the focus area (as seen in Section 4.7.1) indicate that this region experienced considerable accretion before eroding again within the study period. This shows that, even though the overall rate of erosion/accretion is low, the region is dynamic with fluctuations between erosion and accretion. It is also important to note that the erosion is seen mostly within the northern

section of the study region while the southern section experiences accretion. This could be an indication of longshore currents depositing materials from the northern regions in the southern regions. The construction of the harbour at Bayview Heights also prevents free movement of the sediments past this point. If the harbour were not present, the erosional levels may have been much higher. The construction of the harbour has provided a major anthropogenic impact on this focus region.

As discussed in section 4.7.2, the rates of change in metres per year are generally within the error margin provided by the pixel sizes of the imagery used. This makes it difficult to come to any significant conclusions regarding erosion on a year-to-year basis. However, these values were obtained as an average over a long period of 66 years, and the total change is considerably larger than the error margin, therefore general trends in erosion can definitely be seen.

Macassar Beach

At Macassar Beach, considerable change was seen. The end point rate indicated that there was an average of 0.11 m per year of erosion from 1944 to 2010 in this focus area. One factor which influenced the results strongly in this case was the tidal pool, shown in Figure 69 (a), towards the western end of the focus area. Since the tidal pool was only constructed partway through the study period, the changes to the beach formed by the construction of the tidal pool resulted in considerable effects on the statistics. This zone shows up as accretion due to the walls built in construction of the pool. The construction of this tidal pool resulted in a stronger than usual anthropogenic influence in this focus region. Nonetheless, the linear regression and least median of squares do still indicate that there was a yearly average of erosion rather than accretion. Figure 69 (b) shows how sand moves further up the beach, covering buildings. Figure 69 (c) indicates a road which has been destroyed by erosion during a storm. Aerial photographs show that the road was already damaged severely by 2008, but the damage became considerably worse by 2009. The date of the original damage to the road is not certain.Figure 69 (d) shows how consolidated beach sand shows signs of severe erosion. Figure 70 (a) shows a small stone wall built out from the beach, which may be intended to provide some protection from erosion – though it did not protect the road from destruction. Figure 70 (b) shows a parking lot on the beach, almost within reach of the waves during a normal tidal cycle. The anthropogenic influences of construction on the beach itself can have a strong influence on erosion. Figure 70 (c) and (d) show how the sand dunes extend far into the distance at Macassar Beach.

The shoreline change envelope for Macassar Beach ranged from 24.59 m to 259.53 m while the net shoreline movement ranged from 73.49 m erosion to 90.47 m accretion.

It is important to note that in the case of Macassar Beach, the highest values both in the shoreline change envelope and in accretion are seen within the tidal pool constructed at the western end of the focus region. Since the pool was constructed during the study period, it had a considerable impact on the region. However, this does not mean that 90 m accretion occurred in this region, but rather, that the shape of the beach was changed by anthropogenic interference. In the rest of the focus area, the shoreline change envelope still shows some regions which are considerably larger than the net shoreline movement, indicating a dynamic shoreline with changes between accretion and erosion. However, the overall trends are definitely towards erosion. In this region, aside from the tidal pool, the most erosion is seen in the west while the eastern parts experience accretion. This could be the result of currents flowing west to east eroding some material and depositing it again in the east.

Figure 69: Macassar beach. a) the tidal pool; b) an abandoned building is overrun by beach sand; c) the road has been destroyed by erosion during a storm; d) the consolidated beach sand shows clear signs of strong erosive action. Photographs taken by author on 27-02-2013.

Figure 70: Macassar Beach. a) the stone wall did little to protect the road against erosion; b) a parking lot on the beach almost reaches the sea during a normal tidal cycle; c) and d) at the back of the broad beach, sand dunes extend into the distance. Photographs taken by author on 27-02-2013.

Strand

At Strand, the Digital Shoreline Analysis System showed that from 1944 to 2010, there was absolutely no net accretion over the entire focus area. The whole area experienced net erosion, ranging from 122.43 m to 0.06 m erosion. The shoreline change envelope shows even greater change, reaching 182.12 m, indicating that there was some alternation between erosion and accretion during the study period. The end point rate indicates that the average rate of erosion across the entire area was 0.59 m per year. The average erosion according to the net shoreline movement over the whole time period was 39.09 m. The other indicators provided similar rates of change, with the least median of squares averaging 0.50 m erosion per year.

Strand is the only one of the four focus areas that showed no accretion at any of the transects when looking over the entire study period. This indicates that the entire Strand beach is being gradually eroded. This could have serious implications for the structures there in coming years. The Beach Road at Strand is right next to the beach and at times, mere metres from the ocean. A stone wall intended to provide some protection for the road is shown in Figure 71 (a). During storms, waves can reach the road as well. High-rise buildings are mere metres from the beach and in some cases buildings extend over the beach itself (Figure 71 (b) and Figure 71 (c)). The road also becomes covered in beach sand which is deposited by wind or storm surges. Sand covering a portion of the road is shown in Figure 71 (d).

The shoreline change envelope and net shoreline movement are both larger in the north-western parts of the study area and decrease towards the south-east. As with Macassar Beach, this could be an indication of a longshore current eroding more material from the north-western regions. In this case, deposition further along the study region did not occur. The sandy beach was also broadest in the north-western region to begin with, supplying more material for erosion.

The erosion rate of 0.5 m per year may not seem particularly high – especially since this is within the error margin of the data used in a single year.However, the total erosion seen over the study period from 1944 to 2010 is considerably more than the error margin, showing that there is a definite trend towards erosion. Beachfront structures are therefore in danger of damage due to the erosion in the future.

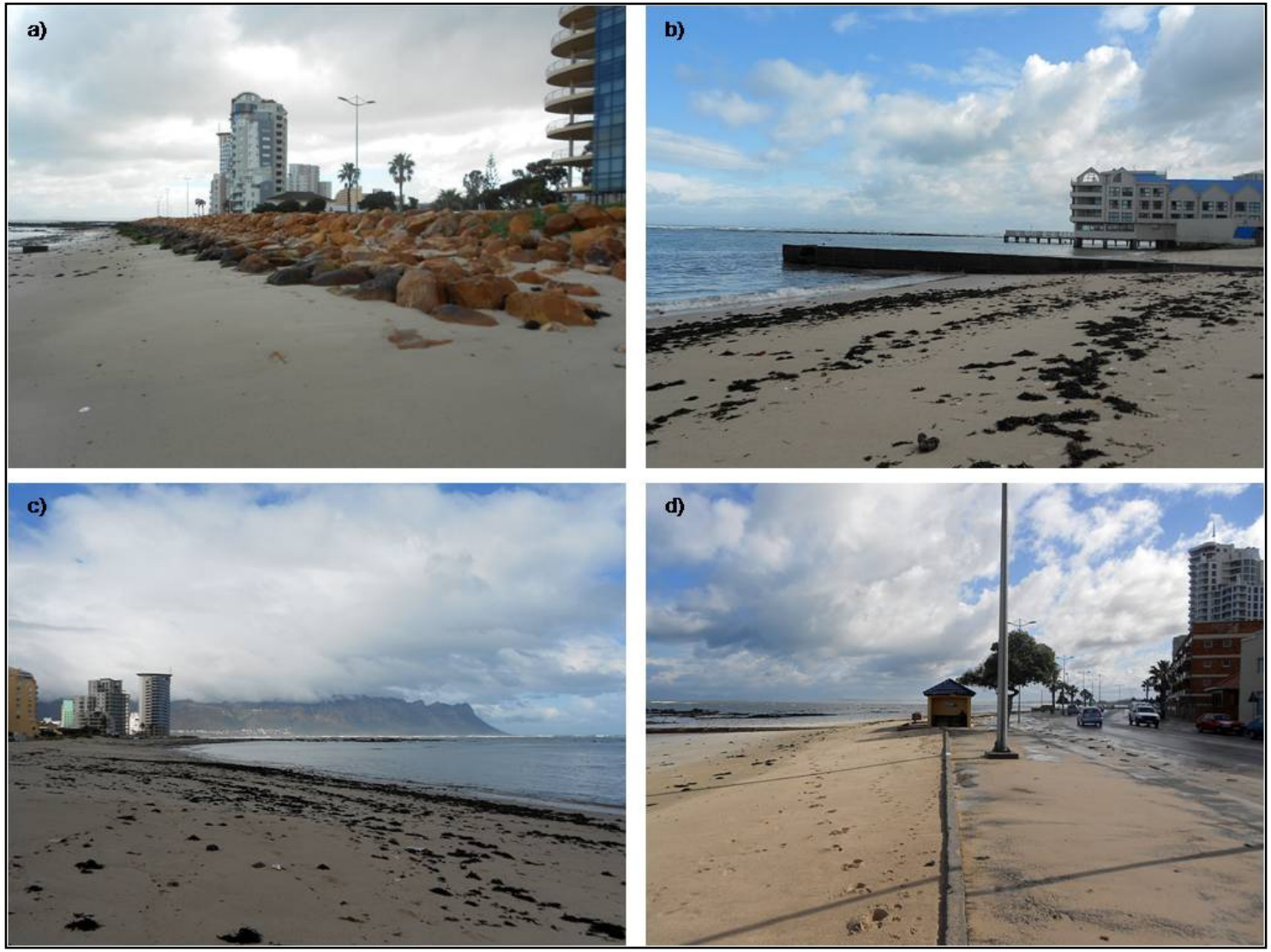

Figure 71: Strand. a) a wall of stones provides some protection for the beach road; b) a building extends right out into the water and a jetty tries to combat erosion; c) more buildings very close to the beach; d) sand washes over the road. Photographs taken by author on 28-07-2013.

Pringle Bay

The shoreline change envelope at Pringle Bay indicated greater changes in beachfront position than expected, with the change ranging from 13.91 to 142.00 m. It is possible that the surrounding protruding rocky coast may have encouraged greater tidal range at this location. As stated in Section 1.4, the region near Cape Hangklip and to a lesser degree off Gordon's Bay experiences localised wind-induced upwelling (Harrison, 1998). Pringle Bay falls within the region described and therefore experiences this upwelling. The increased swells in this region could be the cause of the high levels of erosion. However, there are many factors at play in a beach environment and the reason for the high erosion in this region is not certainly known. The small beach area surrounded by rocks and cliffs to either side is shown in Figure 72 (a) and (b). The study region extended over a part of the rocky coast at the northern end, where the net shoreline movement showed some accretion. Over the sandy beach area, however, only erosion is seen, ranging from no change to erosion of 128.63 m. The linear regression rate showed a range from 0.29 m accretion to 2.84 m erosion per year. Naturally, the sandy zone was more vulnerable to erosion, and the higher figures are seen here. These amounts could have been eroded by wave and tidal action. The accretion seen at the rocky zone could be a result of sand moving away from the sandy zone. As seen in Figure 72 (c), rocky portions on the beach may provide limited protection against erosion, although this does not explain the high erosion seen in this area.

In the case of Pringle Bay, the shoreline change envelope was only a few metres larger than the net shoreline movement. The maximum of the shoreline change envelope was 141.6 m while the highest net shoreline movement was 128.63 m erosion. This indicates that some accretion did also occur in the region, but there is a strong focus on erosion in the sandy region of this focus area. Erosion was seen throughout the sandy parts of this focus area while some accretion was seen in the rocky zone.

Figure 72: Pringle Bay. a) and b) show the extent of the small sandy beach which is surrounded by rocks and cliffs to either side; c) rocky areas on the beach provide some natural protection against erosion. Photographs taken by author on 28-07-2013.

5.2. Remote sensing methods for coastal erosion

Various remote sensing techniques were used during this study. As stated by Lu et al. (2004), there is much debate as to which change detection technique is best and no single method is the most suitable for all cases. This was also found during this study, since many of the methods used were useful for only certain aspects of the study.

Binary slicing was performed on Landsat imagery in an attempt to define the coastline position. The results of this method are shown in Section 4.6. This method was found to be unreliable at this scale and the results obtained were not useful. Since some clear errors could be seen in coastline position, results in other areas could not be trusted. In addition, at this scale, a difference of even one pixel would mean a considerable 30 m of change. The change of a few pixels seen across most of the study area may have indicated an advance in shoreline position but its unreliability prevented any conclusions being made. This is the only technique used which indicates an advance rather than a retreat in shoreline position.Without ground truth data, it cannot be conclusively said that this method provided incorrect results while the others were correct, however, the fact that this was the only method showing accretion while all the other methods indicated increased vulnerability or actual erosion suggests that the binary slicing technique was not suitable for this investigation. This method may work better when using different input data with higher resolutions or a more distinctive differentiation between land and ocean.

Image differencing was performed using both band 4 of the Landsat imagery and using the brightness band after a tasselled cap transformation. The results of these methods are shown in section 4.4. This method showed decreases in band 4 and increases in the brightness band, indicating decreases in vegetation health along with increases in artificial reflective surfaces. This method was found to be useful for providing an indication of general trends in erosion vulnerability over the whole study area. It could not provide detailed erosion information, but did suggest increasing vulnerability over time. Since this method is quick to perform, it is extremely useful for finding general trend information over a large study area. Within the smaller focus areas, it is less useful, since local fluctuations make it more difficult to assess overall trends. Image differencing is a widely used technique (e.g. Chavez and Mackinnon, 1994, in Lu et al., 2004; Jensen and Toll, 1982, in Lu et al., 2004; Nelson, 1983, in Lu et al., 2004;Pilon et al., 1988, in Lu et al., 2004; Prakash and Gupta, 1998, in Lu et al., 2004;Ridd and Liu, 1998, in Lu et al., 2004; Singh, 1989) which is simple to perform and easy to interpret (Lu et al., 2004). This study found that this method was extremely useful in observation of vulnerability trends.

The NDVI differencing method was performed using a segmented image classed from low to high NDVI. The results of this method are shown in Section 4.5. This method was found by Hayes and Sader (2001) to be more effective than simple image differencing. In this study, it is uncertain which method was more useful. NDVI differencing was only performed using the segmented method, but band 4 differencing and brightness differencing were done in the traditional pixel-by-pixel way. Use of the segmented method made image interpretation somewhat easier since it prevented any salt-and-pepper effects which may have made distinction between areas of increase and areas of decrease unclear.However, both methods led to similar conclusions about the gradual decline of vegetation health and density. NDVI has found to be effective in vegetation change studies (e.g. Huete et al., 1997; Lyon et al., 1998) although other vegetation indices may prove more useful in certain cases.

Post-classification change detection was performed using images classified by a multispectral object-based classification. The results of this method are shown in Section 4.3. The major advantage of this method is the ability to see the nature of the change – which class is changing to which class. In this case, this led to the observations that the built-up class is consistently increasing, often at the expense of the sand dune class. This type of information can be invaluable, and while the image differencing method also showed that there were trends towards increasing artificial surfaces and decreasing vegetation, the post-classification change detection method can quantify these changes, and shows exactly where which changes are occurring. However, due to the large number of classes used, it can be difficult to isolate important changes.

The main disadvantage of this method is that it is extremely time-consuming. Image classification is a slow process and high accuracies are required to make the change detection useful. Therefore, this method is extremely useful in cases where detailed or specific change information is required, but only if the requirements are sufficient to allow for the larger workload. Methods such as image differencing are useful for providing much faster change information over large areas. Post-classification change detection was found in studies by Mas (1997; 1999) to be the most accurate of six different change detection methods. This study has also found it to be more accurate and provide more detailed results than image differencing, vegetation index differencing and Boolean change detection.

The Digital Shoreline Analysis System was used for shoreline position analysis on aerial photographs. The use of aerial photographs provided the advantage of greatly enhanced detail visible in the beach region over Landsat imagery. This allowed the changing position of the shoreline to be identified with much greater accuracy. In addition, the historical archive of aerial photographs available afforded study over an increased time range, which was

useful for identification of long-term erosional trends. The DSAS tool was a very useful tool for determining changes in shoreline position. It provided quantitative values for shoreline change. This method was by far the most useful for a focussed study of shoreline position change. The main disadvantage of this method was that it did not cover as large an area as the other methods. Digitising the shoreline position is time-consuming and it is impractical to cover large areas in this way. The method also only focusses on the beach itself and therefore cannot be used to identify other vulnerability indicators such as an expansion in urban area. Another disadvantage is that digitisation of the shoreline position is done manually and therefore is subject to human error.

Each of the methods used had various advantages and disadvantages. The use of several methods together allowed the observation of both general trends in vulnerability, and of specific changes in shoreline position over time.

6. CONCLUSIONS

This research has set out to compare different sensors and techniques for the evaluation and change detection of coastal erosion in False Bay, South Africa. Referring back to Section 1.1, there is a global trend towards coastal degradation and there is a need to find the most effective methods for monitoring this. Only by monitoring these changes can we become equipped to protect coastal regions. The aim of this study was to establish the accuracy, efficacy and efficiency of various remote sensing sensors and techniques for the detection and monitoring of coastal erosion occurring in the False Bay region. In order to achieve this, both aerial photographs and Landsat imagery were used in conjunction with various methods. These were then assessed for their applicability to this study and the erosion in the study region was analysed.

The following section provides a summary of the methodology and results of the research.

6.1. Methodology and results

This study assessed the use of both Landsat imagery and aerial photographs for the study of coastal erosion over time in False Bay, South Africa. Image differencing, vegetation index differencing, Boolean change detection, and post-classification change detection were all used to detect changes over a time period of 26 years at and near the shoreline on the Landsat imagery. On the aerial photographs, shoreline positions were digitised and the Digital Shoreline Analysis System add-on for ArcMAP was used to give a quantitative analysis of changes in shoreline position at four focus areas – Bayview Heights, Macassar Beach, Strand, and Pringle Bay. On the aerial photographs the changes were assessed over a period of up to 66 years.

6.1.1. Erosion vulnerability in False Bay

The various methods used during this project indicated erosion occurred in False Bay over the study period and erosion vulnerability increased over time. Post-classification change detection indicated a decrease in the beach class of 6.17% from its original extent from 1985 to 2011. This indicates erosion of the beach causing the percentage classified as beach to become less. The greatest increase in any class was the increase in the built-up class which increased by 40.46% from its original extent from 1985 to 2011. This indicates the importance of anthropogenic influences on the study area as the already urbanised region continues to grow. The sand dune class also showed a significant decrease, decreasing by

36.06% from its original extent. This decrease was predominantly due to the built-up region extending over the sand dune fields. This change was particularly visible near Macassar Beach, indicating increased vulnerability in this region. Another interesting observation was the increase of shallow coastal by 73.93% of its original area while the ocean class decreased by 0.81%. The increase in shallow coastal appears huge since it started as a small class while the decrease in ocean appears small, however, the area of these changes are relatively similar. This could indicate increased sand banks off the beach as the beach is becoming eroded which resulted in an increase in the shallow coastal class while the ocean class decreased. However, this could also be a result of tidal change between image dates. Future research should incorporate tidal information in order to differentiate tidal change from other change.

Differencing of infra-red bands and tasselled cap brightness bands showed consistent decreases in vegetation indicators, and increases in indicators of bare or built-up surfaces. Both of these trends are in line with the results of post-classification change detection, where classes such as natural, cultivated and sand dunes all showed decreases while the built-up class increased.

NDVI differencing indicated declines in vegetation health and density within the study period. The sand dune class specifically showed significantly decreased NDVI values over nearly the entire class area during the study period. This corroborates the aforementioned findings that vegetation health is decreasing and vegetated sand dunes have disappeared. This indicates an increased vulnerability to erosion of the sand dunes as well as their associated beaches.

The binary slicing method provided few useful results. The resolution available on the Landsat imagery was not sufficient to see changes in the beach position with any clarity and the use of a single value at which to split land from sea resulted in considerable errors with this method.

The aerial photograph analysis indicated erosion to varying degrees in all four of the focus areas. The most significant erosion was seen at Strand, where there was absolutely no net accretion, and an average erosion rate of 0.53 m per year (linear regression rate). The other study regions all showed a combination of accretion and erosion, however erosion did dominate. At Macassar Beach all the measures indicated erosion with the least median of squares indicating an average of 0.14 m erosion per year. Pringle Bay showed more erosion than expected, although the rocky region within this focus area did show some accretion. The least median of squares for this study region indicated erosion of 1.46 m per year. Finally, Bayview Heights showed the least change of the four focus areas. While the end

point rate in this region actually indicated accretion of 0.008 m per year, the other measures indicated erosion with the least median of squares giving an erosion rate of 0.17 m per year. It is significant to note that this is the region exhibiting least change and yet it still experiences an average of yearly coastal erosion.

6.1.2. Remote sensing methods for erosion monitoring.

The findings of this study indicated that the resolution of the Landsat imagery (30 m) was not sufficient to detect changes in the position of the beach itself. However, these images were able to aid in the detection of various changes in the surrounding areas which have an influence on the vulnerability to coastal erosion.

Post-classification change detection highlighted various changes occurring within the coastal zone, and was capable of showing rates of growth or loss in the different classes. The ability to observe changes in classes such as built-up and sand dunes made this an invaluable tool for vulnerability assessment.

The image differencing technique provided information about general trends – decreases in vegetation health and increases in artificial and other reflective surfaces. While this technique could not provide information about specific class change or erosion at the beach itself, it did provide an indication of a general increase in erosion vulnerability. This method was also quick to perform, making it a good option for a reconnaissance of general trends within a study area.

The NDVI differencing technique was also unable to provide specific class information or detailed beach erosion information, however, viewing the change in NDVI across the study region again indicates trends in vegetation health. While changes in band 4 could also indicate vegetation health changes, the use of a vegetation index such as NDVI is more useful for this specific purpose. Again, this method is quick to perform, so it is extremely useful for identification of general trends.

The binary slicing method was intended to isolate the shoreline position, but was found not to be useful due to the size of Landsat pixels. Some areas showed clear errors, and changes would have to be in excess of 30 m to even be visible as a single pixel. Since clear errors of many pixels were visible on the 2011 image, changes of a few pixels could not be interpreted since they may also have been incorrect.

The higher resolution available on the aerial photographs allowed changes in the beach position itself to be quantified. This could be applied more efficiently to the problem of

coastal erosion itself. Erosion rates could be quantified and visualised clearly. While able to quantify beach position changes, the aerial photographs could not be used to show changes in sand dunes, built-up areas, and other inland zones. They were therefore less useful in finding indicators for vulnerability to future erosion. The DSAS method would also be highly time-consuming when used for a very large study area. The beach position changes which it supplied were easily visualised and indicated clear changes over a long time period.

6.2. Future research

It is recommended that future studies of coastal erosion utilise either aerial photographs or high resolution satellite imagery if the study aims to view changes in the beach itself since this high resolution is necessary to be able to quantify any changes. Use of high resolution satellite imagery may have an advantage over aerial photographs in being able to obtain images at a specific time of the year. However, aerial photographs will always have the advantage of being available over a longer time period. The resolution of Landsat images limits their usefulness for beach position studies, although they can be used to assess long term regional changes that will be useful for coastal studies and vulnerability studies. The advantage of Landsat, however, is that it is able to cover a larger area, enabling visualisation of changes a few kilometres inland of the beach which may influence the erosion vulnerability of the beach itself.

Other techniques and sensors may also prove useful. Alternative data sources including high-resolution satellite imagery or SAR (synthetic aperture radar) may prove useful and can be investigated to assess the information that can be extracted.

6.3. Concluding remarks

This study set out to compare the Landsat sensor with aerial photographs while using various techniques for the assessment of coastal erosion in False Bay. It has achieved this aim by finding that the higher resolution available on aerial photographs enables quantification of actual beach position change over time while the use of post-classification change detection, image differencing and NDVI differencing on Landsat imagery are all useful to indicate changing vulnerability of the region to erosion. Binary slicing on band 4 of Landsat images was unsuccessful in defining the land-ocean boundary. The erosion occurring at the four focus areas within False Bay was also assessed and discussed.

7. REFERENCES

Althausen, JD, Kendall, CGSTC, Lakshmi, V, Alsharhan, AS, & Whittle, GL, 2003. Using satellite imagery and GIS in the mapping of coastal landscapes in an arid environment: Khor Al Bazam, Western Abu Dhabi, United Arab Emirates. In Alsharhan, AS, Wood, WW, Goudie, AS, Fowler, A, and Abdellatif, EM (eds)*Desertification in the Third Millennium,* 443-449. Rotterdam: AA Balkema/Swets&Zeitlinger.

Baatz, M, &Schäpe, A, 2000.Multiresolution segmentation – an optimization approach for high quality multi-scale image segmentation.In: Strobl, J, Blaschke, T, &Griesebner, G, (eds), *AngewandteGeographischeInformationsverarbeitung XII*, 12-23. Heidelberg:Wichmann-Verlag.

Balthazar, V, Vanacker, V, &Lambin, EF, 2012.Evaluation and parameterization of ATCOR3 topographic correction method for forest cover mapping in mountain areas. *International Journal of Applied Earth Observation and Geoinformation*, 18: 436-450.

Blaschke, T, 2003. Object-based contextual image classification built on image segmentation.*Advances in Techniques for Analysis of Remotely Sensed Data, 2003 IEEE Workshop.*113-119.

Blaschke, T, 2010. Object based image analysis for remote sensing. *ISPRS Journal of Photogrammetry and Remote Sensing* 65: 2-16.

Boak, EH, & Turner, IL, 2005. Shoreline definition and detection: a review. *Journal of Coastal Research,* 21, 4: 688-703.

Boruff, BJ, Emrich, C & Cutter, SL, 2005.Erosion hazard vulnerability of US coastal counties.*Journal of Coastal Research* 21,.5: 932-942.

Byrne, GF, Crapper, PF, & Mayo, KK, 1980. Monitoring land-cover change by principal component analysis of multitemporal Landsat data.*Remote Sensing of Environment.*10: 175-184.

Carlson, TN, & Ripley, DA, 1997.On the relation between NDVI, fractional vegetation cover, and leaf area index.*RemoteSensing of Environment*, 62: 241-252.

Chen, D, & Stow, D, 2002. The effect of training strategies on supervised classification at different spatial resolutions. *Photogrammetric Engineering and Remote Sensing*.68, 11: 1155-1161.

Clark, BM, Bennet, BA, &Lamberth, SJ, 1996. Factors affecting spatial variability in seine net catches of fish in the surf zone of False Bay, South Africa. *Marine Ecology Progress Series*, 131: 17-34.

Congalton, RG, 1991. A review of assessing the accuracy of classifications of remotely sensed data.*Remote sensing of Environment,* 37:35-46.

Congalton, RG, & Green, K, 2008. *Assessing the accuracy of remotely sensed data: principles and practices*. 2nd ed. Boca Raton: CRC Press/Taylor & Francis.

Coppin, PR, & Bauer, ME, 1994.Processing of multitemporal Landsat TM imagery to optimize extraction of forest cover change features.*IEEE Transactions on Geoscience and Remote Sensing*. 32, 4: 918-927.

Darwish, A, Leukert, K, & Reinhardt, W, 2003. Image segmentation for the purpose of object-based classification.*Geoscience and Remote Sensing Symposium, 2003.IGARSS.'03. Proceedings.2003 IEEE International*.3: 2039-2041.

Department of Environmental Affairs and Tourism and Council for Scientific and Industrial Research, 2005.State of the Environment [online].Republic of South Africa.Available from http://soer.deat.gov.za/216.html [Accessed 10 December 2013].

Department of Rural Development and Land Reform, 2013. Land cover mapping of North West Province completed. *PositionIT*, September 2013, 29-31.

Drăguţ, L, Teide, D, &Levick, SR, 2010, ESP: a tool to estimate scale parameter for multiresolution image segmentation of remotely sensed data. *International Journal of Geographical Information Science.* 24,6: 859-871.

Foody, GM, 2002.Status of land cover classification accuracy assessment. *Remote Sensing of Environment*, 80: 185-201.

Foody, GM, & Arora, MK, 1997. An evaluation of some factors affecting the accuracy of classification by an artificial neural network. *International Journal of Remote Sensing*, 19,4: 799-810.

Ford, M, 2013. Shoreline changes interpreted from multi-temporal aerial photographs and high resolution satellite images: Wotje Atoll, Marshall Islands. *Remote Sensing of Environment*, 135: 130-140.

Frohn, RC, Hinkel, KM, & Eisner, WR, 2005. Satellite remote sensing classification of thaw lakes and drained thaw lake basins on the North Slope of Alaska.*Remote Sensing of Environment*, 97,1: 116-126.

Fung, T, 1990. An assessment of TM imagery for land-cover change detection. *IEEE Transactions on Geoscience and Remote Sensing*, 28, 4: 681-684.

Fung, T, &LeDrew, E, 1987.The application of principal component analysis to change detection.*Photogrammetric Engineering and Remote Sensing*, 53: 1649–1658.

Hanson, H, 1988. Genesis – a generalized shoreline change numerical model. *Journal of Coastal Research*, 5,1: 1-27.

Harrison, TD, 1998. A preliminary survey of the coastal river systems of False Bay, South-west coast of South Africa, with particular reference to the fish fauna.*Transactions of the Royal Society of South Africa*, 53, 1: 1-31.

Hayashi, RM, 1987. Beachwalls for beach erosion protection.*Proceedings of 20th Coastal Engineering Conference*, American Society of Civil Engineers, 1909-1914.

Hayes, DJ, &Sader, SA, 2001. Comparison of change-detection techniques for monitoring tropical forest clearing and vegetation regrowth in a time series.*Photogrammetric Engineering and Remote Sensing*, 67, 9: 1067-1075.

Huang, W, & Fu, B, 2002. Remote sensing for coastal area management in China.*Coastal Management*, 30,3: 271-276.

Huang, C, Wylie, B, Yang, L, Homer, C, &Zylstra, G, 2002. Derivation of a tasselled cap transformation based on Landsat 7 at-satellite reflectance. *International Journal of Remote Sensing*, 28, 8: 1741-1748.

Huete, AR, Liu, HQ, Batchily, K, & van Leeuwen, W, 1997. A comparison of vegetation indices over a global set of TM images for EOS-MODIS. *Remote Sensing of Environment*, 59: 440-451.

Jano, AP, Jefferies, RL, & Rockwell, RF, 1998. The detection of vegetational change by multitemporal analysis of LANDSAT data: the effects of goose foraging. *Journal of Ecology*, 86: 93-99.

Kamagata, N, Hara, K, Mori, M, Akamatsu, Y, Li, Y, & Hoshino, Y, 2006. A new method of vegetation mapping by object-based classification using high resolution satellite data. In

Proceedings of the first International Conference on Object-Based Image Analysis 2006, XXXVI-4/C42

Klein, RJT, & Nicholls, RJ, 1999. Assessment of coastal vulnerability to climate change.*Ambio*, 28, 2: 182-187.

Kraus, NC, 1988. The effects of seawalls on the beach: an extended literature review. (Special Issue).*Journal of Coastal Research*, 4: 1-28.

Kwarteng, AY& Al-Ajmi, D, 1996.Using Landsat Thematic Mapper data to detect and map vegetation changes in Kuwait.*International Archives of Photogrammetry and Remote Sensing,* XXXI, B7.

Livingstone, D, Raper, J, & McCarthy, T, 1999. Integrating aerial videography and digital photography with terrain modelling: an application for coastal geomorphology.*Geomorphology*, 29: 77-92.

Lu, D, Mausel, P, Brondízio, E, & Moran, E, 2004. Change detection techniques.*International Journal of Remote Sensing*, 25, 12: 2365-2401.

Lück, W, Mhangara, P, Kleyn, L, and Remas, H, 2010. Land Cover Field Guide.*CSIR Satellite Applications Centre: Earth Observation Service Centre*. Prepared for: Chief Directorate: National Geospatial Information. pp 179.

Lyon, JG, Yuan, D, Lunetta, RS, &Elvidge, CD, 1998. A change detection experiment using vegetation indices.*PhotogrammetricEngineering and Remote Sensing*, 64, 2: 143-150.

Mahendra, RS, Mohanty, PC, Bisoyi, H, Srinivasa Kumar, T, &Nayak, S, 2011. Assessment and management of coastal multi-hazard vulnerability along the Cuddalore-Villupuram, east coast of India using geospatial techniques.*Ocean and Coastal Management*, 54, 4: 302-311.

Mas, JF, 1997, Monitoring land-cover changes in the Terminos Lagoon Region, Mexico: a comparison of change detection techniques. *Proceedings of the IV International Conference on Remote Sensing for Marine and Coastal Environments, Orlando, FL, USA (Amsterdam: National Aerospace Laboratory)*, 1: 159–167.

Mas, JF, 1999, Monitoring land-cover changes: a comparison of change detection techniques. *International Journal of Remote Sensing*, 20: 139–152.

McGovern, EA, Holden, NM, Ward, SM, & Collins, JF, 2002.The radiometric normalization of multitemporal Thematic Mapper imagery of the midlands of Ireland – a case study.*International Journal of Remote Sensing*, 23, 4: 751-766.

Mouat, DA, Mahin, GG, & Lancaster, J, 1993. Remote sensing techniques in the analysis of change detection.*Geocarto International*, 8, 2: 39-50.

Myburgh, G, & Van Niekerk, A, 2013.Effect of feature dimensionality on object-based land cover classification: a comparison of three classifiers. *South African Journal of Geomatics*, 2, 1: 13-27.

Ngcofe, L, &Minnaar, H, 2012. A study on automated segmentation for object-based image analysis for geological mapping in the Northern Cape province, South Africa.*Proceedings of the 4th GEOBIA, May 7-9, 2012*. Rio de Janeiro, Brazil. pp. 129-136.

Palmer, BJ, Van der Elst, R, Mackay, F, Mather, AA, Smith, AM, Bundy, SC, Thackeray, Z, Leuci, R, &Parak, O, 2011. Preliminary coastal vulnerability assessment for KwaZulu-Natal, South Africa.*Journal of Coastal Research,* Special Issue 64: 1390-1395.

Phillips, MR, 2008. Beach erosion and marine aggregate dredging: a question of evidence.*The geographical journal*, 174, 4: 332-343.

Ramsey, RD, Wright, DL, &McGinty, C, 2004. Evaluating the use of Landsat 30 m enhanced thematic mapper to monitor vegetation cover in shrub-steppe environments. *Geocarto International*, 19,2: 39-47.

Ridd, MK, & Liu, J, 1998. A comparison of four algorithms for change detection in an urban environment.*RemoteSensing of Environment*, 63: 95-100.

Romine, BM, Fletcher, CH, Frazer, LN, Genz, AS, Barbee, MM, & Lim, SC, 2009. Historical shoreline change, southeast Oahu, Hawaii: applying polynomial models to calculate shoreline change rates. *Journal of Coastal Research*, 25, 6: 1236-1253.

Rust, IC, &Illenberger, WK, 1996. Coastal dunes: sensitive or not? *Landscape and Urban Planning,* 34: 165-169.

Ryherd, S, & Woodcock, C, 1996. Combining spectral and texture data in the segmentation of remotely sensed images.*Photogrammetric Engineering and Remote Sensing*, 62, 2: 181-194.

Segl, K, Roessner, S, Heiden, U, & Kaufmann, H, 2003. Fusion of spectral and shape features for identification of urban surface cover types using reflective and thermal hyperspectral data. *ISPRS Journal of Photogrammetry and Remote Sensing* 58, 1-2: 99-112.

Silva, TAM, &Bigg, GR, 2004.Computer-based identification and tracking of Antarctic icebergs in SAR images.*RemoteSensing of Environment*, 94, 3: 287-297.

Singh, A, 1989. Review article: digital change detection techniques using remotely sensed data. *International Journal of Remote Sensing*, 10,6: 989-1003.

Siripong, A, 2010. Detect the coastline changes in Thailand by remote sensing. *International Archives of the Photogrammetry, Remote Sensing and Spatial Information Science*, Volume XXXVIII, 8: 992-996.

Small, C, & Nicholls, RJ, 2003.A global analysis of human settlement in coastal zones.*Journal of Coastal Research*, 19, 3: 584-599.

Smith, SE, & Abdel-Kader, A, 1988.Coastal erosion along the Egyptian Delta.*Journal of Coastal Research*, 4, 2: 245-255.

Song, C, Woodcock, CE, Seto, KC, Lenney, MP, &Macomber, SA, 2001. Classification and change detection using Landsat TM data: when and how to correct atmospheric effects? *Remote Sensing of Environment*, 75: 230-244.

Stehman, SV, 1997. Selecting and interpreting measures of thematic classification accuracy. *Remote Sensing of Environment,*62: 77-89.

Sun, X, Zhang, J, & Liu, Z, 2004. An object-oriented classification method on high resolution satellite data.Conferencepaper.*Chinese academy of Surveying and Mapping Beijing (China).*Accession number: ADA437344

Thampanya, U, Vermaat, JE, Sinsakul, S, &Panapitukkul, N, 2006. Coastal erosion and mangrove progradation of Southern Thailand.*Estuarine, Coastal and Shelf Science*, 68: 75-85.

Thieler, ER, Himmelstoss, EA, Zichichi, JL, &Ergul, A, 2009.Digital Shoreline Analysis System (DSAS) version 4.0 — An ArcGIS extension for calculating shoreline change: U.S. Geological Survey Open-File Report 2008-1278. *current version 4.3

Tralli, DM, Blom, RG, Zlonicki, V, Donnellan, A, & Evans, DL, 2005.Satellite remote sensing of earthquake, volcano, flood, landslide and coastal inundation hazards.*ISPRS Journal of Photogrammetry and Remote Sensing* 59: 185-198.

Ulbricht, KA, &Heckendorff, WD, 1998. Satellite images for recognition of landscape and landuse changes. *ISPRS Journal of Photogrammetry and Remote Sensing*.53: 235-243.

Unterner, M, Wigley, R, van Zyl, W, Cawthra, H, &Machutchon, M, 2011. The vulnerability of the South African coastline to erosion.*Council for Geoscience Report* number 2011-0190.

Van der Werff, HMA, & van der Meer, FD, 2008. Shape-based classification of spectrally identical objects. *ISPRS Journal of Photogrammetry and Remote Sensing* 63: 251-258.

Van Niekerk, A, 2012.Developing a very high resolution DEM of South Africa. *PositionIT*, Nov/Dec: 55-60.

Ward, D, Phinn, SR, & Murray, AT, 2000.Monitoring growth in rapidly urbanising areas using remotely sensed data. *The Professional Geographer*, 52, 3: 371-386.

Woodcock, CE, Macomber, SA, Pax-Lenney, M, & Cohen, WB, 2001.Monitoring large areas for forest change using Landsat: Generalization across space, time and Landsat sensors. *Remote Sensing of Environment,* 78: 194-203.

Yang, X, & Lo, CP, 2002. Using a time series of satellite imagery to detect land use and land cover changes in the Atlanta, Georgia metropolitan area. *International Journal of Remote Sensing,* 23, 9: 1775-1798.

Zhang, K, Douglas, BC, & Leatherman, SP, 2001.Beach erosion potential for severe nor'easters. *Journal of Coastal Research*, 17: 309-321.

Zhang, Q, Wang, J, Peng, X, Gong, P, & Shi, P, 2002. Urban built-up land change detection with road density and spectral information from multi-temporal Landsat TM data, *International Journal of Remote Sensing*, 23,15: 3057-3078.

APPENDIX A: DSAS STATISTICS

The Digital Shoreline Analysis System (DSAS) outputs various statistics in table form. Each statistic is performed on each of a series of transects, spaced 20 m apart. The tables are given below and show both the statistical values and their related confidences. The values shown are as follows:

NSM = net shoreline movement

SCE = shoreline change envelope

EPR = end point rate

ECI = confidence of end point rate

LRR = linear regression rate

LSE = standard error of linear regression

LCI = confidence interval of linear regression

LR2 = R^2 of linear regression

WLR = weighted linear regression rate

WSE = standard error of weighted linear regression

WCI = confidence interval of weighted linear regression

WR2 = R^2 of weighted linear regression

LMS = least median of squares

Table 5: DSAS statistics for Bayview Heights.

TransectId	EPR	ECI	SCE	NSM	LMS	WLR	WR2	WSE	WCI95	LRR	LR2	LSE	LCI95
1	0.19000	0.03100	38.54000	12.24000	-0.31000	-0.04000	0.01000	5.81000	0.29900	0.03000	0.01000	11.13000	0.36500
2	-0.08000	0.03100	74.11000	-5.39000	-0.93000	-0.51000	0.29000	11.09000	0.56000	-0.20000	0.04000	21.25000	0.68200
3	-0.38000	0.03100	90.39000	-25.22000	-1.24000	-0.73000	0.64000	7.67000	0.38800	-0.52000	0.17000	25.00000	0.80300
4	-0.40000	0.03100	85.49000	-26.10000	-0.55000	-0.83000	0.61000	9.29000	0.46900	-0.62000	0.21000	26.21000	0.84200
5	-0.31000	0.03100	76.98000	-20.53000	-1.03000	-0.59000	0.62000	6.48000	0.32700	-0.47000	0.17000	22.57000	0.72500
6	0.00000	0.03100	74.13000	0.31000	-0.05000	-0.31000	0.29000	6.69000	0.33800	-0.20000	0.04000	21.48000	0.69000
7	-0.01000	0.03100	73.20000	-0.77000	-0.14000	-0.36000	0.28000	8.15000	0.41200	-0.26000	0.07000	20.96000	0.67300
8	-0.02000	0.03100	67.14000	-1.51000	-0.11000	-0.37000	0.33000	7.29000	0.36800	-0.26000	0.07000	20.58000	0.66100
9	-0.09000	0.03100	56.33000	-5.94000	-0.14000	-0.39000	0.40000	6.59000	0.33300	-0.25000	0.08000	18.38000	0.59000
10	0.05000	0.03100	65.18000	3.35000	-0.17000	-0.34000	0.16000	10.65000	0.53800	-0.21000	0.05000	20.23000	0.65000
11	-0.09000	0.03100	67.08000	-6.01000	-0.27000	-0.55000	0.37000	10.17000	0.51400	-0.38000	0.13000	20.92000	0.67200
12	-0.17000	0.03100	70.25000	-11.49000	-0.25000	-0.63000	0.26000	14.82000	0.74900	-0.37000	0.12000	21.35000	0.68600
13	-0.20000	0.03100	70.61000	-13.38000	-1.29000	-0.67000	0.29000	14.45000	0.73000	-0.41000	0.15000	21.18000	0.68000
14	-0.20000	0.03100	69.43000	-13.11000	-0.49000	-0.60000	0.31000	12.42000	0.62800	-0.35000	0.13000	20.35000	0.65400
15	-0.20000	0.03100	68.72000	-13.38000	-0.49000	-0.63000	0.28000	14.15000	0.71500	-0.36000	0.13000	20.27000	0.65100
16	-0.19000	0.03100	65.35000	-12.26000	-1.38000	-0.63000	0.31000	13.03000	0.65800	-0.36000	0.14000	20.18000	0.64800
17	-0.14000	0.03100	62.59000	-9.03000	-0.19000	-0.48000	0.53000	12.51000	0.29800	-0.28000	0.12000	18.30000	0.50900
18	-0.26000	0.03100	62.49000	-17.14000	-0.27000	-0.49000	0.63000	10.34000	0.24600	-0.30000	0.14000	18.29000	0.50800
19	-0.27000	0.03100	60.42000	-17.74000	-0.31000	-0.51000	0.71000	9.02000	0.21500	-0.35000	0.18000	17.63000	0.49000
20	-0.24000	0.03100	62.71000	-16.04000	-0.55000	-0.62000	0.64000	12.96000	0.30900	-0.39000	0.21000	18.49000	0.51400
21	-0.26000	0.03100	71.75000	-16.89000	-0.51000	-0.65000	0.54000	16.47000	0.39200	-0.40000	0.17000	20.69000	0.57500
22	-0.17000	0.03100	63.44000	-11.09000	-0.55000	-0.63000	0.67000	12.48000	0.29700	-0.38000	0.17000	20.08000	0.55800
23	-0.27000	0.03100	62.39000	-18.07000	-0.53000	-0.62000	0.70000	11.28000	0.26900	-0.39000	0.19000	19.64000	0.54600
24	-0.10000	0.03100	61.12000	-6.71000	-0.35000	-0.62000	0.62000	13.57000	0.32300	-0.36000	0.20000	17.02000	0.47300
25	-0.10000	0.03100	63.60000	-6.76000	-0.55000	-0.61000	0.65000	12.38000	0.29500	-0.38000	0.20000	18.01000	0.50000
26	-0.14000	0.03100	67.09000	-9.53000	-0.41000	-0.57000	0.62000	12.34000	0.29400	-0.38000	0.20000	18.45000	0.51300
27	-0.18000	0.03100	65.56000	-12.07000	-0.27000	-0.45000	0.63000	9.69000	0.23100	-0.33000	0.18000	17.12000	0.47600
28	-0.17000	0.03100	61.55000	-11.03000	-0.81000	-0.37000	0.69000	6.86000	0.16300	-0.30000	0.16000	16.43000	0.45700
29	-0.06000	0.03100	55.54000	-3.93000	-0.87000	-0.46000	0.62000	10.09000	0.24000	-0.29000	0.14000	17.13000	0.47600
30	-0.21000	0.03100	54.44000	-13.80000	-0.36000	-0.40000	0.67000	7.71000	0.18400	-0.30000	0.17000	15.92000	0.44200
31	-0.11000	0.03100	47.49000	-7.19000	-0.20000	-0.30000	0.69000	5.59000	0.13300	-0.22000	0.14000	13.06000	0.36300
32	-0.14000	0.03100	48.34000	-9.35000	-0.16000	-0.25000	0.73000	4.32000	0.10300	-0.21000	0.14000	12.49000	0.34700
33	-0.19000	0.03100	52.31000	-12.61000	0.00000	-0.08000	0.16000	4.91000	0.11700	-0.17000	0.10000	12.70000	0.35300
34	-0.14000	0.03100	50.56000	-9.08000	0.12000	0.03000	0.02000	6.65000	0.15800	-0.11000	0.04000	13.23000	0.36800
35	-0.06000	0.03100	45.22000	-3.76000	0.17000	0.10000	0.26000	4.76000	0.11300	0.01000	0.00000	12.39000	0.34400
36	-0.04000	0.03100	51.93000	-2.53000	-0.02000	-0.06000	0.08000	5.89000	0.14000	-0.07000	0.01000	13.91000	0.38600
37	-0.06000	0.03100	56.63000	-3.89000	-0.12000	-0.14000	0.36000	5.33000	0.12700	-0.15000	0.06000	14.52000	0.40400
38	0.15000	0.03100	40.97000	9.68000	0.58000	-0.07000	0.05000	8.05000	0.19200	0.02000	0.00000	13.59000	0.37800
39	0.18000	0.03100	49.08000	11.96000	-0.28000	-0.03000	0.01000	8.38000	0.19900	0.09000	0.02000	15.19000	0.42200
40	0.33000	0.03100	51.90000	21.89000	0.12000	-0.02000	0.00000	13.26000	0.31600	0.16000	0.05000	16.65000	0.46300

41	0.19000	0.03100	59.81000	12.49000	-0.02000	-0.01000	0.00000	9.60000	0.22900	0.13000	0.03000	18.27000	0.50800
42	0.19000	0.03100	66.39000	12.58000	-0.04000	0.01000	0.00000	4.93000	0.11700	0.10000	0.02000	19.17000	0.53300
43	0.06000	0.03100	67.39000	3.97000	0.16000	0.01000	0.00000	5.00000	0.11900	0.05000	0.00000	19.63000	0.54500
44	0.00000	0.03100	43.88000	-0.31000	-0.05000	-0.13000	0.39000	4.44000	0.10600	-0.10000	0.03000	12.87000	0.35800
45	0.00000	0.03100	37.45000	-0.04000	0.00000	-0.04000	0.09000	3.31000	0.07900	-0.06000	0.01000	11.53000	0.32000
46	0.01000	0.03100	43.96000	0.84000	0.02000	-0.07000	0.20000	3.95000	0.09400	-0.04000	0.00000	13.69000	0.38000
47	0.03000	0.03100	48.90000	1.99000	-0.07000	-0.11000	0.22000	5.82000	0.13900	-0.03000	0.00000	15.52000	0.43100
48	-0.04000	0.03100	60.08000	-2.77000	-0.14000	-0.25000	0.47000	7.39000	0.17600	-0.13000	0.04000	16.20000	0.45000
49	0.01000	0.03100	49.10000	0.71000	0.04000	-0.27000	0.71000	4.93000	0.11700	-0.08000	0.02000	15.33000	0.42600
50	0.05000	0.03100	32.36000	3.60000	0.05000	-0.20000	0.63000	4.24000	0.10100	-0.04000	0.01000	11.42000	0.31700
51	-0.01000	0.03100	34.55000	-0.37000	0.03000	-0.19000	0.65000	3.92000	0.09300	-0.09000	0.04000	11.30000	0.31400
52	0.05000	0.03100	39.11000	3.19000	0.05000	-0.27000	0.63000	5.85000	0.13900	-0.12000	0.05000	11.96000	0.33200
53	0.11000	0.03100	45.73000	7.54000	-0.05000	-0.29000	0.49000	8.43000	0.20100	-0.14000	0.06000	13.36000	0.37100
54	0.16000	0.03100	37.18000	10.39000	0.21000	-0.24000	0.59000	5.60000	0.13300	-0.09000	0.04000	11.68000	0.32500
55	0.02000	0.03100	38.52000	1.31000	0.04000	-0.36000	0.78000	5.25000	0.12500	-0.19000	0.16000	10.62000	0.29500
56	0.04000	0.03100	37.07000	2.79000	0.05000	-0.24000	0.69000	4.55000	0.10800	-0.12000	0.06000	12.20000	0.33900
57	0.11000	0.03100	40.79000	7.26000	0.04000	-0.33000	0.68000	6.19000	0.14700	-0.15000	0.08000	12.51000	0.34800
58	0.10000	0.03100	43.29000	6.51000	0.03000	-0.29000	0.65000	5.90000	0.14000	-0.14000	0.06000	13.33000	0.37000
59	-0.10000	0.03100	43.41000	-6.80000	-0.44000	-0.41000	0.87000	4.36000	0.10400	-0.30000	0.29000	11.15000	0.31000
60	-0.08000	0.03100	44.48000	-5.37000	-0.55000	-0.47000	0.87000	5.10000	0.12100	-0.34000	0.31000	11.99000	0.33300
61	-0.08000	0.03100	44.04000	-5.16000	-0.55000	-0.48000	0.88000	5.06000	0.12000	-0.35000	0.34000	11.81000	0.32800
62	-0.08000	0.03100	42.61000	-5.48000	-0.53000	-0.42000	0.86000	4.75000	0.11300	-0.32000	0.26000	12.77000	0.35500
63	-0.15000	0.03100	46.22000	-9.96000	-0.16000	-0.53000	0.87000	5.79000	0.13800	-0.40000	0.30000	14.75000	0.41000
64	-0.15000	0.03100	45.11000	-9.98000	-0.12000	-0.58000	0.87000	6.23000	0.14800	-0.41000	0.30000	14.93000	0.41500
65	-0.12000	0.03100	44.20000	-8.19000	-0.11000	-0.58000	0.88000	5.96000	0.14200	-0.39000	0.31000	14.07000	0.39100
66	-0.07000	0.03100	44.19000	-4.50000	-0.09000	-0.59000	0.85000	6.94000	0.16500	-0.38000	0.28000	14.45000	0.40200
67	-0.05000	0.03100	44.46000	-3.49000	-0.07000	-0.62000	0.83000	7.85000	0.18700	-0.40000	0.30000	14.74000	0.41000
68	-0.10000	0.03100	59.40000	-6.39000	-0.10000	-0.68000	0.81000	9.15000	0.21800	-0.49000	0.31000	17.48000	0.48600
69	-0.11000	0.03100	51.71000	-7.43000	-0.12000	-0.70000	0.83000	8.94000	0.21300	-0.50000	0.35000	16.26000	0.45200
70	-0.12000	0.03100	52.56000	-8.11000	-0.14000	-0.66000	0.84000	8.05000	0.19200	-0.48000	0.35000	15.50000	0.43100
71	-0.10000	0.03100	53.46000	-6.90000	-0.23000	-0.63000	0.88000	6.44000	0.15300	-0.45000	0.33000	15.28000	0.42500
72	-0.04000	0.03100	54.36000	-2.74000	-0.67000	-0.59000	0.83000	7.40000	0.17600	-0.40000	0.27000	15.61000	0.43400
73	-0.01000	0.03100	58.20000	-0.51000	-0.76000	-0.63000	0.77000	9.52000	0.22700	-0.38000	0.24000	16.22000	0.45100
74	-0.04000	0.03100	58.65000	-2.36000	-0.55000	-0.65000	0.80000	9.04000	0.21500	-0.42000	0.26000	16.76000	0.46600
75	-0.03000	0.03100	59.85000	-1.97000	-0.07000	-0.66000	0.78000	9.82000	0.23400	-0.42000	0.26000	16.89000	0.46900
76	-0.02000	0.03100	59.98000	-1.26000	-0.03000	-0.60000	0.78000	8.95000	0.21300	-0.37000	0.23000	16.28000	0.45200
77	-0.01000	0.03100	60.80000	-0.47000	-0.02000	-0.61000	0.78000	9.08000	0.21600	-0.38000	0.23000	16.63000	0.46200
78	-0.01000	0.03100	59.51000	-0.91000	-0.02000	-0.56000	0.79000	8.12000	0.19300	-0.34000	0.21000	15.91000	0.44200
79	0.00000	0.03100	60.09000	-0.12000	-0.53000	-0.53000	0.73000	8.99000	0.21400	-0.33000	0.20000	15.68000	0.43600
80	0.03000	0.03100	57.52000	2.14000	0.00000	-0.50000	0.72000	8.62000	0.20500	-0.32000	0.18000	16.24000	0.45100

81	0.06000	0.03100	58.70000	4.21000	-0.11000	-0.48000	0.63000	10.30000	0.24500	-0.31000	0.16000	16.97000	0.47200
82	0.06000	0.03100	58.57000	4.13000	-0.09000	-0.46000	0.63000	9.74000	0.23200	-0.28000	0.16000	15.29000	0.42500
83	0.09000	0.03100	58.01000	5.76000	-0.05000	-0.45000	0.61000	9.98000	0.23800	-0.24000	0.12000	15.12000	0.42000
84	0.11000	0.03100	58.09000	6.93000	0.03000	-0.46000	0.57000	11.07000	0.26300	-0.22000	0.10000	15.70000	0.43600
85	0.08000	0.03100	54.47000	5.43000	-0.47000	-0.40000	0.62000	8.77000	0.20900	-0.18000	0.09000	14.44000	0.40100
86	0.10000	0.03100	51.61000	6.57000	-0.41000	-0.39000	0.64000	8.06000	0.19200	-0.19000	0.09000	14.08000	0.39100
87	0.16000	0.03100	49.42000	10.83000	0.09000	-0.33000	0.58000	7.80000	0.18600	-0.13000	0.05000	14.10000	0.39200
88	0.20000	0.03100	49.47000	13.26000	0.14000	-0.33000	0.53000	8.71000	0.20700	-0.13000	0.04000	14.25000	0.39600
89	0.18000	0.03100	49.82000	11.67000	-0.14000	-0.34000	0.43000	11.10000	0.26400	-0.12000	0.04000	13.33000	0.37000
90	0.17000	0.03100	48.60000	11.05000	0.10000	-0.31000	0.35000	11.71000	0.27900	-0.07000	0.02000	12.80000	0.35600
91	0.29000	0.03100	35.62000	19.17000	0.02000	-0.06000	0.03000	9.17000	0.21800	0.17000	0.09000	12.93000	0.35900
92	0.32000	0.03100	40.09000	21.03000	0.27000	-0.10000	0.07000	9.58000	0.22800	0.17000	0.08000	13.75000	0.38200
93	0.35000	0.03100	45.12000	23.05000	0.09000	-0.01000	0.00000	9.77000	0.23300	0.23000	0.12000	14.75000	0.41000
94	0.38000	0.03100	44.16000	24.84000	0.25000	0.11000	0.11000	8.62000	0.20500	0.30000	0.21000	14.09000	0.39100
95	0.69000	0.03100	46.10000	45.47000	0.70000	0.67000	0.97000	3.43000	0.08200	0.68000	0.71000	10.37000	0.28800
96	0.13000	0.03100	28.30000	8.47000	0.03000	-0.05000	0.07000	4.96000	0.11800	0.06000	0.02000	9.70000	0.27000
97	0.05000	0.03100	33.70000	3.27000	-0.12000	-0.18000	0.55000	4.63000	0.11000	-0.05000	0.01000	11.69000	0.32500
98	0.02000	0.03100	31.14000	1.08000	-0.02000	-0.06000	0.08000	5.26000	0.12500	-0.02000	0.00000	12.34000	0.34300
99	0.02000	0.03100	30.06000	1.27000	-0.04000	-0.06000	0.13000	4.10000	0.09800	0.01000	0.00000	11.88000	0.33000
100	0.08000	0.03100	33.77000	5.19000	-0.03000	-0.07000	0.12000	5.44000	0.13000	0.02000	0.00000	13.06000	0.36300
101	0.12000	0.03100	37.18000	7.70000	0.00000	-0.08000	0.14000	5.54000	0.13200	0.03000	0.00000	13.98000	0.38800
102	0.10000	0.03100	38.69000	6.55000	-0.10000	-0.09000	0.21000	5.02000	0.12000	0.01000	0.00000	13.31000	0.37000
103	0.12000	0.03100	50.61000	7.63000	0.02000	-0.08000	0.13000	5.46000	0.13000	0.06000	0.01000	15.01000	0.41700
104	0.18000	0.03100	64.44000	12.07000	0.05000	-0.07000	0.09000	6.72000	0.16000	0.12000	0.02000	18.40000	0.51100
105	0.01000	0.03100	54.64000	0.40000	0.02000	0.12000	0.17000	7.55000	0.18000	0.03000	0.00000	16.36000	0.45500
106	0.10000	0.03100	13.31000	6.48000	0.07000	0.09000	0.54000	2.43000	0.05800	0.08000	0.19000	3.86000	0.10700
107	0.50000	0.03100	33.32000	33.12000	0.12000	0.18000	0.57000	4.33000	0.10300	0.32000	0.42000	9.08000	0.25200
108	0.20000	0.03100	30.77000	13.37000	0.02000	-0.10000	0.10000	7.91000	0.18800	0.04000	0.01000	9.85000	0.27400
109	0.20000	0.03100	27.54000	13.14000	0.00000	-0.07000	0.05000	8.08000	0.19200	0.05000	0.02000	8.32000	0.23100
110	0.09000	0.03100	24.33000	5.87000	-0.16000	-0.14000	0.40000	4.87000	0.11600	-0.03000	0.01000	7.25000	0.20100
111	0.12000	0.03100	21.58000	7.94000	0.05000	-0.07000	0.08000	6.09000	0.14500	-0.01000	0.00000	6.65000	0.18500
112	0.14000	0.03100	19.70000	9.17000	0.02000	0.04000	0.07000	4.19000	0.10000	0.09000	0.13000	5.44000	0.15100
113	0.15000	0.03100	22.26000	9.95000	0.12000	0.15000	0.69000	2.73000	0.06500	0.17000	0.42000	4.66000	0.12900
114	0.09000	0.03100	15.86000	5.75000	0.00000	0.09000	0.29000	4.01000	0.09500	0.06000	0.14000	3.83000	0.10600
115	0.20000	0.03100	14.52000	13.09000	0.19000	0.18000	0.72000	3.17000	0.07600	0.14000	0.31000	4.85000	0.13500
116	-0.03000	0.03100	31.08000	-1.89000	-0.14000	-0.17000	0.47000	5.07000	0.12100	-0.09000	0.04000	9.88000	0.27400
117	0.01000	0.03100	37.49000	0.93000	-0.09000	-0.18000	0.51000	4.85000	0.11500	-0.06000	0.02000	12.12000	0.33700
118	0.16000	0.03100	40.11000	10.57000	-0.07000	-0.08000	0.10000	6.89000	0.16400	0.06000	0.01000	12.81000	0.35600
119	0.13000	0.03100	53.32000	8.74000	-0.05000	0.02000	0.01000	6.29000	0.15000	0.13000	0.05000	13.54000	0.37600
120	-0.06000	0.03100	8.30000	-4.09000	0.04000	0.02000	0.03000	3.00000	0.07200	0.02000	0.02000	2.64000	0.07500
Minimum	-0.40000	0.03100	8.30000	-26.10000	-1.38000	-0.83000	0.00000	2.43000	0.05800	-0.62000	0.00000	2.64000	0.07500
Maximum	0.69000	0.03100	90.39000	45.47000	0.70000	0.67000	0.97000	16.47000	0.74900	0.68000	0.71000	26.21000	0.84200
Average	0.00800	0.03100	49.96908	0.50825	-0.16933	-0.30358	0.46508	7.61208	0.21662	-0.16300	0.12875	14.72867	0.42133

Table 6: DSAS statistics for Macassar Beach.

TransectId	EPR	ECI	SCE	NSM	LMS	WLR	WR2	WSE	WCI95	LRR	LR2	LSE	LCI95
2	-0.02000	0.02600	37.02000	-1.60000	-0.58000	-0.16000	0.23000	4.67000	0.20300	-0.03000	0.00000	10.57000	0.34200
3	-0.13000	0.02600	37.34000	-8.61000	-0.60000	-0.25000	0.44000	4.44000	0.19300	-0.09000	0.03000	10.89000	0.35200
4	-0.07000	0.02600	37.48000	-4.51000	-0.70000	-0.24000	0.23000	6.98000	0.30400	-0.10000	0.03000	11.83000	0.38200
5	0.06000	0.02600	35.03000	3.90000	-0.43000	-0.10000	0.07000	5.85000	0.25500	0.02000	0.00000	10.63000	0.34400
6	0.20000	0.02600	34.87000	13.16000	0.23000	-0.04000	0.00000	9.30000	0.40500	0.05000	0.01000	11.18000	0.36100
7	0.24000	0.02600	33.39000	15.55000	0.25000	0.08000	0.02000	8.93000	0.38900	0.14000	0.08000	10.30000	0.33300
8	0.37000	0.02600	39.82000	24.54000	0.40000	0.06000	0.01000	8.55000	0.37300	0.21000	0.15000	10.67000	0.34500
9	0.44000	0.02600	40.78000	29.03000	0.40000	0.15000	0.08000	8.20000	0.35700	0.24000	0.22000	9.93000	0.32100
10	0.43000	0.02600	44.58000	28.67000	0.27000	0.27000	0.23000	8.06000	0.35100	0.30000	0.30000	9.91000	0.32000
11	0.34000	0.02600	48.32000	22.59000	0.12000	0.21000	0.24000	6.14000	0.26700	0.26000	0.23000	10.35000	0.33400
12	0.30000	0.02600	52.67000	19.50000	0.16000	0.24000	0.27000	6.29000	0.27400	0.30000	0.25000	11.25000	0.36400
13	0.51000	0.02600	59.30000	33.64000	-0.07000	0.35000	0.54000	5.22000	0.22700	0.38000	0.35000	11.17000	0.36100
14	0.51000	0.02600	58.82000	33.87000	-0.10000	0.31000	0.43000	5.76000	0.25100	0.36000	0.33000	11.06000	0.35800
15	0.46000	0.02600	52.27000	30.44000	0.14000	0.31000	0.42000	5.80000	0.25300	0.34000	0.37000	9.64000	0.31200
16	0.12000	0.02600	24.59000	8.16000	0.18000	0.09000	0.24000	2.73000	0.11900	0.18000	0.29000	6.26000	0.20200
17	0.06000	0.02600	38.29000	4.04000	0.16000	0.12000	0.09000	5.96000	0.26000	0.15000	0.08000	11.02000	0.35600
18	0.40000	0.02600	46.47000	26.30000	0.39000	0.36000	0.64000	4.38000	0.19100	0.38000	0.33000	11.78000	0.38100
19	0.02000	0.02600	36.72000	1.50000	-0.02000	0.01000	0.00000	4.36000	0.19000	0.15000	0.09000	10.30000	0.33300
20	-0.14000	0.02600	57.90000	-9.17000	-0.63000	-0.16000	0.09000	8.13000	0.35400	0.02000	0.00000	17.35000	0.56100
21	0.00000	0.02600	46.55000	0.18000	-0.07000	-0.16000	0.11000	7.49000	0.32600	-0.02000	0.00000	16.81000	0.54300
22	0.10000	0.02600	46.94000	6.60000	0.12000	-0.02000	0.00000	6.82000	0.29700	0.07000	0.01000	16.24000	0.52500
23	0.04000	0.02600	52.06000	2.45000	0.14000	0.03000	0.00000	8.39000	0.36500	0.06000	0.01000	16.45000	0.53200
24	0.07000	0.02600	47.91000	4.70000	0.02000	-0.10000	0.06000	6.60000	0.28700	0.01000	0.00000	16.50000	0.53300
25	0.16000	0.02600	47.05000	10.30000	0.11000	-0.03000	0.01000	6.50000	0.28300	-0.04000	0.00000	13.91000	0.45000
26	0.03000	0.02600	49.81000	1.73000	-0.81000	-0.15000	0.11000	7.05000	0.30700	-0.19000	0.08000	14.63000	0.47300
27	0.04000	0.02600	200.03000	2.49000	0.14000	0.03000	0.00000	20.53000	0.89400	-0.59000	0.05000	53.31000	1.72300
28	-0.09000	0.02600	199.74000	-6.15000	0.16000	-0.05000	0.00000	21.10000	0.91900	-0.61000	0.06000	52.06000	1.68300
29	-0.78000	0.02600	247.33000	-51.49000	-0.18000	0.94000	0.02000	120.94000	5.26800	-0.21000	0.00000	88.33000	2.85500
30	-0.66000	0.02600	259.53000	-43.24000	2.76000	1.80000	0.07000	109.31000	4.76200	0.67000	0.03000	87.37000	2.82400
31	-0.36000	0.02600	241.59000	-23.70000	-0.94000	1.91000	0.07000	110.42000	4.81000	0.72000	0.03000	86.05000	2.78100
32	-0.25000	0.02600	247.10000	-16.81000	5.19000	2.31000	0.08000	124.14000	5.40800	0.86000	0.04000	88.01000	2.84500
33	0.61000	0.02600	247.55000	40.10000	0.04000	2.94000	0.12000	126.38000	5.50500	1.21000	0.11000	75.22000	2.43100
34	1.17000	0.02600	240.20000	76.96000	-0.73000	3.29000	0.15000	124.17000	5.40900	1.53000	0.23000	61.21000	1.97800
35	1.15000	0.02600	235.76000	75.88000	1.00000	3.08000	0.50000	50.16000	2.18500	2.26000	0.37000	64.54000	2.08600
36	1.37000	0.02600	227.76000	90.47000	4.75000	2.80000	0.67000	31.75000	1.38300	2.85000	0.52000	59.41000	1.92000
37	0.71000	0.02600	209.50000	46.72000	4.31000	2.15000	0.53000	32.93000	1.43400	2.36000	0.43000	59.28000	1.91600
38	0.59000	0.02600	197.00000	38.95000	3.10000	2.00000	0.50000	32.46000	1.41400	2.11000	0.35000	62.04000	2.00500
39	0.44000	0.02600	193.39000	28.76000	3.46000	1.94000	0.43000	36.27000	1.58000	1.99000	0.33000	61.41000	1.98500
40	0.35000	0.02600	191.14000	22.79000	2.92000	1.89000	0.30000	46.27000	2.01600	1.81000	0.31000	59.43000	1.92100

41	-0.72000	0.02600	189.50000	-47.71000	0.72000	1.70000	0.07000	97.27000	4.23700	1.15000	0.13000	63.89000	2.06500
42	-1.11000	0.02600	188.31000	-73.49000	0.25000	1.66000	0.05000	118.41000	5.15800	0.95000	0.09000	66.85000	2.16100
43	-0.90000	0.02600	186.87000	-59.66000	-1.08000	1.98000	0.05000	135.99000	5.92400	0.71000	0.06000	59.99000	1.93900
44	-0.75000	0.02600	181.40000	-49.34000	-1.03000	2.17000	0.06000	144.46000	6.29300	0.23000	0.01000	51.40000	1.66100
45	-0.69000	0.02600	58.45000	-45.39000	-0.65000	-0.35000	0.07000	20.20000	0.88000	-0.52000	0.30000	17.13000	0.55400
46	-0.27000	0.02600	52.70000	-17.70000	-0.14000	-0.15000	0.02000	16.83000	0.73300	-0.32000	0.17000	15.19000	0.49100
47	-0.25000	0.02600	49.58000	-16.20000	-0.81000	-0.35000	0.39000	6.97000	0.30400	-0.36000	0.23000	14.20000	0.45900
48	-0.27000	0.02600	50.71000	-17.53000	-0.75000	-0.24000	0.13000	10.09000	0.44000	-0.33000	0.19000	14.70000	0.47500
49	-0.44000	0.02600	53.05000	-28.79000	-0.78000	-0.28000	0.08000	15.11000	0.65800	-0.43000	0.25000	16.23000	0.52500
50	-0.44000	0.02600	57.11000	-29.09000	-1.00000	-0.46000	0.53000	6.90000	0.30000	-0.50000	0.29000	17.01000	0.55000
51	-0.65000	0.02600	64.85000	-42.60000	-0.75000	-0.59000	0.57000	8.31000	0.36200	-0.65000	0.38000	18.09000	0.58500
52	-0.59000	0.02600	64.34000	-38.96000	-0.68000	-0.51000	0.45000	9.11000	0.39700	-0.51000	0.27000	18.39000	0.59400
53	-0.38000	0.02600	69.56000	-24.92000	-0.63000	-0.04000	0.00000	17.05000	0.74300	-0.33000	0.12000	20.09000	0.64900
54	-0.68000	0.02600	75.25000	-44.66000	-0.96000	-0.65000	0.71000	6.77000	0.29500	-0.75000	0.41000	19.62000	0.63400
55	-0.75000	0.02600	79.28000	-49.50000	-0.94000	-0.75000	0.77000	6.70000	0.29200	-0.84000	0.46000	19.95000	0.64500
56	-0.77000	0.02600	82.60000	-51.11000	-0.84000	-0.67000	0.57000	9.45000	0.41200	-0.80000	0.43000	20.03000	0.64700
57	-0.75000	0.02600	80.77000	-49.22000	-0.78000	-0.71000	0.75000	6.61000	0.28800	-0.77000	0.41000	19.84000	0.64100
58	-0.72000	0.02600	76.78000	-47.63000	-0.78000	-0.76000	0.82000	5.69000	0.24800	-0.75000	0.44000	18.57000	0.60000
59	-0.56000	0.02600	63.17000	-37.22000	-0.58000	-0.60000	0.74000	5.71000	0.24900	-0.57000	0.37000	16.09000	0.52000
60	-0.20000	0.02600	43.32000	-13.11000	-0.25000	-0.07000	0.02000	7.78000	0.33900	-0.21000	0.10000	13.50000	0.43600
61	-0.32000	0.02600	38.95000	-21.44000	-0.32000	-0.24000	0.25000	6.68000	0.29100	-0.24000	0.15000	12.65000	0.40900
62	-0.29000	0.02600	38.52000	-19.30000	0.56000	-0.13000	0.07000	7.58000	0.33000	-0.20000	0.09000	13.29000	0.42900
63	-0.13000	0.02600	45.15000	-8.56000	0.81000	0.04000	0.01000	7.88000	0.34300	-0.03000	0.00000	16.63000	0.53700
64	-0.50000	0.02600	60.01000	-33.29000	-0.39000	-0.31000	0.35000	6.91000	0.30100	-0.26000	0.09000	17.69000	0.57200
65	-0.66000	0.02600	66.28000	-43.45000	-0.65000	-0.54000	0.68000	6.01000	0.26200	-0.43000	0.23000	17.33000	0.56000
66	-0.83000	0.02600	69.12000	-54.64000	-0.70000	-0.57000	0.45000	10.08000	0.43900	-0.52000	0.32000	16.77000	0.54200
67	-0.90000	0.02600	63.24000	-59.52000	-0.90000	-0.84000	0.90000	4.41000	0.19200	-0.68000	0.55000	13.59000	0.43900
68	-0.70000	0.02600	50.90000	-46.16000	-0.87000	-0.75000	0.84000	5.25000	0.22900	-0.59000	0.44000	14.47000	0.46800
69	-0.45000	0.02600	50.69000	-29.48000	-0.94000	-0.58000	0.72000	5.85000	0.25500	-0.43000	0.27000	15.14000	0.48900
70	-0.58000	0.02600	54.37000	-38.56000	-0.96000	-0.65000	0.79000	5.50000	0.24000	-0.51000	0.34000	15.50000	0.50100
71	-0.40000	0.02600	58.01000	-26.11000	-0.70000	-0.50000	0.63000	6.20000	0.27000	-0.39000	0.21000	16.32000	0.52700
72	-0.19000	0.02600	58.69000	-12.64000	-0.63000	-0.33000	0.38000	6.75000	0.29400	-0.25000	0.10000	16.26000	0.52500
73	-0.19000	0.02600	58.23000	-12.38000	-0.60000	-0.33000	0.47000	5.78000	0.25200	-0.26000	0.12000	15.26000	0.49300
74	-0.32000	0.02600	60.56000	-20.92000	-0.41000	-0.34000	0.40000	6.69000	0.29100	-0.33000	0.18000	15.65000	0.50600
75	-0.24000	0.02600	64.97000	-16.15000	-0.39000	-0.21000	0.15000	8.03000	0.35000	-0.29000	0.13000	16.57000	0.53500
76	-0.31000	0.02600	70.49000	-20.28000	-0.40000	-0.18000	0.05000	12.60000	0.54900	-0.34000	0.15000	18.05000	0.58300
77	-0.21000	0.02600	71.98000	-14.13000	-0.37000	-0.14000	0.05000	10.38000	0.45200	-0.29000	0.11000	18.06000	0.58400
78	-0.19000	0.02600	71.36000	-12.52000	-0.32000	-0.14000	0.06000	9.17000	0.39900	-0.28000	0.11000	17.36000	0.56100
79	-0.36000	0.02600	74.55000	-23.83000	-0.47000	-0.24000	0.09000	12.58000	0.54800	-0.40000	0.19000	17.66000	0.57100
80	-0.47000	0.02600	76.82000	-30.78000	-0.60000	-0.35000	0.17000	12.76000	0.55600	-0.49000	0.26000	18.08000	0.58400

81	-0.44000	0.02600	78.27000	-29.24000	-0.47000	-0.37000	0.23000	10.92000	0.47600	-0.43000	0.19000	19.08000	0.61700
82	-0.51000	0.02600	80.71000	-33.58000	0.05000	-0.42000	0.28000	10.67000	0.46500	-0.46000	0.20000	19.77000	0.63900
83	-0.57000	0.02600	83.47000	-37.94000	-0.05000	-0.53000	0.49000	8.76000	0.38100	-0.52000	0.24000	20.42000	0.66000
84	-0.57000	0.02600	84.90000	-37.59000	-0.05000	-0.51000	0.36000	10.93000	0.47600	-0.54000	0.24000	20.94000	0.67700
85	-0.68000	0.02600	84.62000	-44.87000	-0.44000	-0.52000	0.27000	13.81000	0.60200	-0.58000	0.27000	20.69000	0.66900
86	-0.78000	0.02600	84.35000	-51.39000	-1.11000	-0.68000	0.52000	10.61000	0.46200	-0.66000	0.33000	20.70000	0.66900
87	-0.75000	0.02600	83.54000	-49.21000	-1.15000	-0.66000	0.49000	10.98000	0.47800	-0.65000	0.32000	20.60000	0.66600
88	-0.58000	0.02600	82.19000	-38.34000	-0.23000	-0.69000	0.70000	7.36000	0.32100	-0.60000	0.31000	19.90000	0.64300
89	-0.50000	0.02600	80.83000	-32.75000	-0.43000	-0.73000	0.61000	9.48000	0.41300	-0.60000	0.31000	19.66000	0.63600
90	-0.46000	0.02600	80.96000	-30.27000	-1.23000	-0.74000	0.57000	10.29000	0.44800	-0.59000	0.29000	19.83000	0.64100
91	-0.47000	0.02600	81.84000	-31.25000	-0.45000	-0.69000	0.59000	9.36000	0.40800	-0.59000	0.29000	19.97000	0.64600
92	-0.49000	0.02600	82.71000	-32.13000	-0.49000	-0.64000	0.55000	9.32000	0.40600	-0.55000	0.26000	20.53000	0.66400
93	-0.50000	0.02600	83.84000	-33.08000	-0.40000	-0.64000	0.54000	9.54000	0.41500	-0.53000	0.22000	21.63000	0.69900
94	-0.51000	0.02600	85.71000	-33.81000	-0.55000	-0.74000	0.66000	8.56000	0.37300	-0.60000	0.27000	21.54000	0.69600
95	-0.67000	0.02600	85.22000	-44.49000	-1.32000	-0.87000	0.76000	7.99000	0.34800	-0.72000	0.36000	21.04000	0.68000
96	-0.72000	0.02600	83.22000	-47.65000	-1.38000	-0.89000	0.77000	7.76000	0.33800	-0.74000	0.38000	20.80000	0.67200
97	-0.69000	0.02600	81.19000	-45.23000	-1.20000	-0.84000	0.76000	7.74000	0.33700	-0.69000	0.34000	20.85000	0.67400
98	-0.77000	0.02600	79.41000	-51.01000	-1.07000	-0.81000	0.72000	8.06000	0.35100	-0.68000	0.33000	20.97000	0.67800
99	-0.81000	0.02600	78.07000	-53.35000	-0.47000	-0.76000	0.63000	9.43000	0.41100	-0.66000	0.32000	21.28000	0.68800
100	-0.74000	0.02600	76.73000	-48.66000	-0.38000	-0.67000	0.58000	9.29000	0.40500	-0.61000	0.29000	20.88000	0.67500
101	-0.73000	0.02600	75.39000	-47.90000	-0.35000	-0.66000	0.60000	8.83000	0.38500	-0.60000	0.29000	20.74000	0.67000
102	-0.67000	0.02600	73.65000	-44.21000	-0.27000	-0.62000	0.51000	9.90000	0.43100	-0.58000	0.27000	20.60000	0.66600
103	-0.62000	0.02600	72.66000	-41.20000	-0.09000	-0.61000	0.58000	8.39000	0.36600	-0.53000	0.24000	20.53000	0.66400
104	-0.61000	0.02600	72.22000	-40.09000	-0.63000	-0.57000	0.56000	8.21000	0.35800	-0.47000	0.20000	20.59000	0.66500
105	-0.52000	0.02600	71.62000	-34.58000	-0.68000	-0.58000	0.66000	6.73000	0.29300	-0.43000	0.18000	20.39000	0.65900
106	-0.49000	0.02600	70.93000	-32.23000	-0.72000	-0.59000	0.66000	6.90000	0.30100	-0.39000	0.14000	20.84000	0.67400
107	-0.50000	0.02600	71.38000	-33.16000	-0.73000	-0.55000	0.61000	7.13000	0.31000	-0.33000	0.10000	21.54000	0.69600
108	-0.46000	0.02600	71.59000	-30.47000	-0.68000	-0.49000	0.56000	6.93000	0.30200	-0.29000	0.08000	21.40000	0.69200
109	-0.45000	0.02600	70.79000	-29.73000	-0.81000	-0.46000	0.52000	7.08000	0.30900	-0.29000	0.08000	21.05000	0.68000
110	-0.37000	0.02600	67.95000	-24.53000	-0.65000	-0.38000	0.41000	7.39000	0.32200	-0.24000	0.06000	20.64000	0.66700
111	-0.37000	0.02600	65.09000	-24.61000	-0.75000	-0.46000	0.51000	7.33000	0.31900	-0.23000	0.05000	21.40000	0.69200
112	-0.39000	0.02600	63.80000	-25.98000	-0.73000	-0.43000	0.44000	7.90000	0.34400	-0.22000	0.04000	22.08000	0.71400
113	-0.43000	0.02600	64.40000	-28.25000	-0.78000	-0.40000	0.32000	9.42000	0.41000	-0.21000	0.04000	22.01000	0.71100
114	-0.48000	0.02600	65.00000	-31.91000	-0.78000	-0.53000	0.51000	8.51000	0.37100	-0.25000	0.05000	22.86000	0.73900
115	-0.41000	0.02600	67.66000	-26.94000	-0.73000	-0.46000	0.46000	8.07000	0.35200	-0.22000	0.04000	22.44000	0.72500
116	-0.41000	0.02600	70.91000	-27.29000	-0.81000	-0.37000	0.23000	11.09000	0.48300	-0.22000	0.04000	22.65000	0.73200
117	-0.38000	0.02600	74.15000	-25.03000	-0.81000	-0.45000	0.43000	8.39000	0.36600	-0.25000	0.05000	22.79000	0.73600
118	-0.35000	0.02600	77.39000	-23.18000	-0.37000	-0.43000	0.39000	8.65000	0.37700	-0.24000	0.05000	22.97000	0.74200
119	-0.35000	0.02600	79.93000	-23.04000	-0.37000	-0.46000	0.47000	7.91000	0.34400	-0.24000	0.05000	23.14000	0.74800
120	-0.38000	0.02600	75.80000	-25.17000	-0.44000	-0.42000	0.40000	8.36000	0.36400	-0.20000	0.03000	23.45000	0.75800

121	-0.39000	0.02600	72.86000	-25.82000	-0.21000	-0.38000	0.44000	6.96000	0.30300	-0.13000	0.02000	22.82000	0.73800
122	-0.44000	0.02600	69.64000	-29.34000	-0.44000	-0.25000	0.19000	8.27000	0.36000	-0.08000	0.01000	21.89000	0.70700
123	-0.51000	0.02600	66.42000	-33.83000	-0.49000	-0.31000	0.31000	7.41000	0.32300	-0.13000	0.02000	21.02000	0.67900
124	-0.49000	0.02600	64.61000	-32.29000	-0.58000	-0.34000	0.41000	6.59000	0.28700	-0.16000	0.03000	20.26000	0.65500
125	-0.49000	0.02600	64.73000	-32.03000	-0.63000	-0.32000	0.39000	6.50000	0.28300	-0.17000	0.03000	19.68000	0.63600
126	-0.42000	0.02600	64.53000	-27.60000	-0.55000	-0.28000	0.31000	6.80000	0.29600	-0.12000	0.02000	19.45000	0.62900
127	-0.46000	0.02600	64.85000	-30.20000	-0.51000	-0.29000	0.31000	6.93000	0.30200	-0.13000	0.02000	19.59000	0.63300
128	-0.46000	0.02600	66.03000	-30.05000	0.21000	-0.33000	0.36000	7.02000	0.30600	-0.15000	0.03000	19.91000	0.64300
129	-0.53000	0.02600	67.22000	-34.85000	0.16000	-0.41000	0.47000	7.01000	0.30500	-0.22000	0.06000	19.94000	0.64500
130	-0.53000	0.02600	67.33000	-34.93000	0.21000	-0.40000	0.50000	6.52000	0.28400	-0.25000	0.07000	19.72000	0.63700
131	-0.55000	0.02600	66.63000	-36.51000	-0.30000	-0.40000	0.49000	6.56000	0.28600	-0.28000	0.09000	19.51000	0.63000
132	-0.53000	0.02600	65.21000	-35.22000	-0.47000	-0.39000	0.50000	6.43000	0.28000	-0.30000	0.10000	19.03000	0.61500
133	-0.53000	0.02600	63.98000	-34.78000	-0.09000	-0.35000	0.37000	7.33000	0.31900	-0.29000	0.10000	18.87000	0.61000
134	-0.42000	0.02600	62.93000	-27.98000	-0.43000	-0.22000	0.14000	9.01000	0.39200	-0.24000	0.07000	18.85000	0.60900
135	-0.28000	0.02600	71.02000	-18.65000	-0.25000	-0.14000	0.07000	8.51000	0.37100	-0.18000	0.04000	20.87000	0.67500
136	-0.25000	0.02600	79.49000	-16.48000	-0.34000	-0.13000	0.04000	10.55000	0.45900	-0.18000	0.03000	22.40000	0.72400
137	-0.23000	0.02600	87.96000	-15.09000	-0.32000	-0.09000	0.01000	12.93000	0.56300	-0.18000	0.02000	24.48000	0.79100
138	-0.13000	0.02600	91.61000	-8.61000	-0.41000	-0.05000	0.00000	11.50000	0.50100	-0.15000	0.02000	24.87000	0.80400
139	-0.04000	0.02600	91.96000	-2.83000	-0.16000	0.09000	0.01000	13.31000	0.58000	-0.09000	0.01000	25.90000	0.83700
140	-0.04000	0.02600	92.29000	-2.41000	-0.14000	0.22000	0.04000	17.93000	0.78100	-0.04000	0.00000	26.52000	0.85700
141	-0.04000	0.02600	109.75000	-2.88000	-0.14000	0.22000	0.04000	18.57000	0.80900	-0.06000	0.00000	31.23000	1.00900
142	0.02000	0.02600	112.76000	1.11000	0.00000	0.20000	0.04000	15.22000	0.66300	-0.04000	0.00000	31.47000	1.01700
143	-0.05000	0.02600	115.55000	-3.46000	-0.09000	0.15000	0.03000	14.17000	0.61700	-0.06000	0.00000	31.68000	1.02400
144	-0.01000	0.02600	116.78000	-0.70000	-0.03000	0.14000	0.03000	12.73000	0.55500	-0.06000	0.00000	31.42000	1.01600
145	-0.05000	0.02600	119.24000	-2.98000	-0.12000	0.12000	0.02000	12.16000	0.53000	-0.10000	0.01000	31.11000	1.00600
146	-0.14000	0.02600	122.50000	-9.12000	-0.16000	0.09000	0.01000	12.85000	0.56000	-0.15000	0.01000	31.42000	1.01600
147	-0.14000	0.02600	125.86000	-9.15000	-0.18000	0.05000	0.01000	11.61000	0.50600	-0.16000	0.01000	32.24000	1.04200
148	-0.23000	0.02600	128.70000	-15.19000	-0.30000	-0.02000	0.00000	14.28000	0.62200	-0.24000	0.02000	33.26000	1.07500
149	-0.51000	0.02600	131.15000	-33.44000	-0.37000	-0.16000	0.02000	16.34000	0.71200	-0.38000	0.06000	34.06000	1.10100
150	-0.59000	0.02600	133.61000	-38.93000	-0.34000	-0.19000	0.03000	18.51000	0.80600	-0.43000	0.07000	34.64000	1.11900
151	-0.63000	0.02600	138.97000	-41.78000	-0.55000	-0.20000	0.02000	20.86000	0.90800	-0.45000	0.07000	36.36000	1.17500
152	-0.67000	0.02600	133.26000	-44.30000	-0.87000	-0.24000	0.03000	20.19000	0.87900	-0.49000	0.09000	34.52000	1.11600
153	-0.72000	0.02600	126.86000	-47.52000	-0.49000	-0.32000	0.09000	16.77000	0.73100	-0.52000	0.11000	32.78000	1.06000
154	-0.72000	0.02600	121.33000	-47.47000	-0.72000	-0.36000	0.16000	13.61000	0.59300	-0.51000	0.11000	31.38000	1.01400
155	-0.76000	0.02600	117.55000	-50.40000	-0.73000	-0.43000	0.26000	11.76000	0.51200	-0.52000	0.12000	30.45000	0.98400
156	-0.68000	0.02600	113.31000	-44.88000	-0.47000	-0.53000	0.48000	8.84000	0.38500	-0.49000	0.11000	29.55000	0.95500
157	-0.66000	0.02600	114.80000	-43.82000	-0.67000	-0.57000	0.47000	9.83000	0.42800	-0.48000	0.11000	29.91000	0.96700
158	-0.62000	0.02600	116.89000	-40.69000	-0.60000	-0.44000	0.38000	8.96000	0.39000	-0.41000	0.08000	30.41000	0.98300
159	-0.55000	0.02600	118.97000	-36.09000	-0.56000	-0.42000	0.37000	8.80000	0.38400	-0.36000	0.06000	30.81000	0.99600
160	-0.53000	0.02600	118.73000	-35.05000	-0.60000	-0.43000	0.39000	8.72000	0.38000	-0.38000	0.07000	30.35000	0.98100

161	-0.49000	0.02600	115.28000	-32.63000	-0.36000	-0.50000	0.48000	8.30000	0.36200	-0.40000	0.08000	29.35000	0.94900
162	-0.51000	0.02600	113.13000	-33.72000	-0.49000	-0.56000	0.54000	8.40000	0.36600	-0.43000	0.09000	28.96000	0.93600
163	-0.47000	0.02600	113.20000	-30.98000	-0.49000	-0.58000	0.52000	9.04000	0.39400	-0.42000	0.09000	29.13000	0.94200
164	-0.39000	0.02600	110.91000	-25.44000	-0.39000	-0.54000	0.45000	9.56000	0.41600	-0.37000	0.07000	29.07000	0.94000
165	-0.32000	0.02600	107.49000	-21.18000	-0.07000	-0.51000	0.44000	9.25000	0.40300	-0.36000	0.07000	28.38000	0.91700
166	-0.25000	0.02600	104.08000	-16.63000	-0.05000	-0.40000	0.32000	9.48000	0.41300	-0.32000	0.06000	28.15000	0.91000
167	-0.16000	0.02600	100.66000	-10.49000	-0.10000	-0.30000	0.15000	11.62000	0.50600	-0.27000	0.04000	28.22000	0.91200
168	-0.08000	0.02600	98.03000	-5.09000	-0.68000	-0.21000	0.05000	14.91000	0.65000	-0.23000	0.03000	28.45000	0.91900
169	-0.06000	0.02600	97.32000	-3.73000	0.10000	-0.16000	0.03000	13.75000	0.59900	-0.18000	0.02000	28.02000	0.90600
170	-0.02000	0.02600	96.63000	-1.51000	0.14000	-0.14000	0.03000	12.70000	0.55300	-0.17000	0.02000	27.42000	0.88600
171	-0.14000	0.02600	95.92000	-9.35000	-0.84000	-0.18000	0.04000	15.40000	0.67100	-0.21000	0.03000	27.66000	0.89400
172	-0.13000	0.02600	93.33000	-8.25000	-1.33000	-0.19000	0.04000	15.08000	0.65700	-0.23000	0.03000	27.30000	0.88200
173	-0.19000	0.02600	89.61000	-12.52000	-1.32000	-0.26000	0.08000	14.83000	0.64600	-0.28000	0.05000	26.93000	0.87000
174	-0.27000	0.02600	85.89000	-17.57000	-1.19000	-0.26000	0.06000	16.52000	0.72000	-0.31000	0.06000	26.30000	0.85000
175	-0.38000	0.02600	88.91000	-25.09000	-1.11000	-0.39000	0.15000	15.09000	0.65700	-0.40000	0.10000	25.62000	0.82800
176	-0.41000	0.02600	91.98000	-27.12000	-1.03000	-0.49000	0.31000	11.74000	0.51200	-0.43000	0.12000	25.05000	0.81000
177	-0.46000	0.02600	94.65000	-30.62000	-1.07000	-0.50000	0.28000	12.80000	0.55800	-0.50000	0.16000	24.68000	0.79800
178	-0.47000	0.02600	97.31000	-30.86000	-1.03000	-0.50000	0.31000	12.22000	0.53200	-0.51000	0.17000	25.03000	0.80900
179	-0.51000	0.02600	99.97000	-33.53000	-0.49000	-0.58000	0.41000	11.27000	0.49100	-0.57000	0.17000	26.99000	0.87200
180	-0.48000	0.02600	102.64000	-31.96000	-0.51000	-0.69000	0.55000	9.95000	0.43300	-0.63000	0.19000	28.20000	0.91100
181	-0.51000	0.02600	104.35000	-33.56000	-0.53000	-0.71000	0.57000	10.07000	0.43900	-0.68000	0.21000	28.41000	0.91800
182	-0.51000	0.02600	106.95000	-33.52000	-0.51000	-0.67000	0.52000	10.50000	0.45800	-0.63000	0.18000	29.54000	0.95500
183	-0.51000	0.02600	109.55000	-33.66000	-0.51000	-0.73000	0.53000	11.03000	0.48000	-0.63000	0.17000	30.24000	0.97800
184	-0.51000	0.02600	112.15000	-33.93000	-0.51000	-0.75000	0.54000	11.31000	0.49300	-0.64000	0.17000	30.30000	0.97900
185	-0.56000	0.02600	114.75000	-36.90000	-0.53000	-0.75000	0.52000	11.57000	0.50400	-0.64000	0.17000	30.55000	0.98700
186	-0.46000	0.02600	117.93000	-30.35000	-0.42000	-0.64000	0.39000	12.77000	0.55600	-0.58000	0.14000	30.79000	0.99500
187	-0.34000	0.02600	121.48000	-22.29000	-0.27000	-0.53000	0.27000	14.20000	0.61900	-0.50000	0.11000	31.29000	1.01100
188	-0.20000	0.02600	125.01000	-12.95000	-0.19000	-0.39000	0.12000	16.85000	0.73400	-0.42000	0.08000	31.83000	1.02900
189	-0.18000	0.02600	126.87000	-11.89000	-0.32000	-0.46000	0.18000	15.89000	0.69200	-0.45000	0.09000	31.93000	1.03200
190	-0.12000	0.02600	126.64000	-8.10000	-0.31000	-0.44000	0.17000	15.96000	0.69500	-0.41000	0.07000	32.30000	1.04400
191	-0.08000	0.02600	127.62000	-5.30000	-0.31000	-0.43000	0.16000	16.04000	0.69900	-0.39000	0.06000	32.66000	1.05500
192	-0.03000	0.02600	128.60000	-1.82000	-0.23000	-0.39000	0.13000	16.49000	0.71800	-0.34000	0.05000	32.81000	1.06000
193	-0.05000	0.02600	129.57000	-3.51000	-0.10000	-0.28000	0.06000	17.96000	0.78300	-0.27000	0.03000	33.12000	1.07000
194	-0.07000	0.02600	130.54000	-4.58000	-0.14000	-0.30000	0.08000	16.94000	0.73800	-0.28000	0.03000	32.95000	1.06500
195	-0.10000	0.02600	131.66000	-6.88000	-0.18000	-0.34000	0.10000	16.39000	0.71400	-0.30000	0.04000	32.91000	1.06400
196	-0.08000	0.02600	134.24000	-5.15000	-0.18000	-0.33000	0.09000	16.70000	0.72800	-0.31000	0.04000	33.25000	1.07500
197	-0.06000	0.02600	136.82000	-3.84000	-0.19000	-0.28000	0.06000	18.36000	0.80000	-0.30000	0.04000	33.66000	1.08800
198	-0.07000	0.02600	136.43000	-4.35000	-0.25000	-0.25000	0.04000	19.99000	0.87100	-0.31000	0.04000	33.37000	1.07800
199	-0.11000	0.02600	135.86000	-7.24000	-0.17000	-0.22000	0.03000	20.77000	0.90500	-0.31000	0.04000	33.10000	1.07000
200	-0.09000	0.02600	134.55000	-6.13000	-0.35000	-0.14000	0.01000	21.61000	0.94100	-0.27000	0.03000	32.75000	1.05800

201	-0.12000	0.02600	133.12000	-7.93000	-0.41000	-0.07000	0.00000	23.84000	1.03800	-0.26000	0.03000	32.56000	1.05200
202	-0.04000	0.02600	131.71000	-2.50000	-0.39000	0.03000	0.00000	25.36000	1.10500	-0.20000	0.02000	32.48000	1.05000
203	0.02000	0.02600	130.29000	0.99000	-0.12000	-0.13000	0.01000	17.70000	0.77100	-0.23000	0.02000	31.88000	1.03000
204	-0.01000	0.02600	128.87000	-0.36000	-0.11000	-0.09000	0.01000	19.30000	0.84100	-0.23000	0.02000	31.90000	1.03100
205	-0.01000	0.02600	127.54000	-0.53000	-0.25000	-0.22000	0.05000	15.68000	0.68300	-0.26000	0.03000	31.31000	1.01200
206	-0.07000	0.02600	126.20000	-4.46000	-0.21000	-0.26000	0.08000	13.94000	0.60700	-0.27000	0.04000	30.68000	0.99100
207	-0.04000	0.02600	124.88000	-2.84000	-0.20000	-0.18000	0.03000	15.81000	0.68900	-0.24000	0.03000	30.42000	0.98300
208	-0.09000	0.02600	123.54000	-5.65000	0.03000	-0.06000	0.00000	19.76000	0.86100	-0.21000	0.02000	30.17000	0.97500
209	-0.04000	0.02600	122.20000	-2.91000	-0.09000	-0.16000	0.03000	14.30000	0.62300	-0.20000	0.02000	29.40000	0.95000
210	-0.03000	0.02600	120.97000	-2.21000	0.03000	-0.12000	0.02000	13.88000	0.60400	-0.16000	0.01000	29.16000	0.94200
211	-0.01000	0.02600	119.82000	-0.46000	0.14000	-0.01000	0.00000	16.03000	0.69800	-0.09000	0.00000	29.51000	0.95400
212	-0.03000	0.02600	118.69000	-1.92000	-0.19000	0.02000	0.00000	18.51000	0.80600	-0.07000	0.00000	30.18000	0.97500
213	-0.20000	0.02600	117.54000	-13.21000	-0.21000	0.06000	0.00000	24.97000	1.08800	-0.10000	0.00000	30.94000	1.00000
214	-0.23000	0.02600	116.30000	-15.03000	-0.27000	0.04000	0.00000	24.58000	1.07100	-0.10000	0.00000	31.47000	1.01700
215	-0.24000	0.02600	114.88000	-15.75000	-0.19000	0.13000	0.01000	27.13000	1.18200	-0.05000	0.00000	31.79000	1.02800
216	-0.18000	0.02600	114.66000	-11.90000	0.23000	0.14000	0.01000	23.67000	1.03100	0.01000	0.00000	31.76000	1.02600
217	-0.12000	0.02600	115.11000	-7.65000	0.31000	0.08000	0.00000	18.97000	0.82600	0.02000	0.00000	31.65000	1.02300
218	-0.09000	0.02600	115.56000	-5.76000	-0.10000	-0.03000	0.00000	14.64000	0.63800	-0.01000	0.00000	31.48000	1.01700
219	0.01000	0.02600	115.63000	0.93000	0.00000	-0.13000	0.03000	11.37000	0.49500	0.00000	0.00000	31.27000	1.01100
220	-0.03000	0.02600	115.33000	-2.11000	-1.11000	-0.19000	0.07000	11.54000	0.50300	-0.04000	0.00000	30.99000	1.00200
221	-0.05000	0.02600	115.03000	-3.04000	0.09000	-0.26000	0.12000	11.52000	0.50200	-0.09000	0.00000	30.83000	0.99700
222	-0.04000	0.02600	114.86000	-2.37000	-0.04000	-0.30000	0.14000	11.81000	0.51400	-0.13000	0.01000	31.02000	1.00300
223	-0.01000	0.02600	114.70000	-0.69000	-0.05000	-0.30000	0.14000	11.91000	0.51900	-0.13000	0.01000	31.03000	1.00300
224	0.01000	0.02600	113.20000	0.86000	-1.24000	-0.32000	0.16000	11.95000	0.52100	-0.12000	0.01000	30.38000	0.98200
225	0.05000	0.02600	111.65000	3.49000	-1.11000	-0.36000	0.16000	13.30000	0.57900	-0.11000	0.01000	29.63000	0.95800
226	0.12000	0.02600	110.11000	7.66000	-0.96000	-0.34000	0.13000	14.22000	0.61900	-0.08000	0.00000	29.11000	0.94100
227	0.11000	0.02600	108.55000	7.33000	0.14000	-0.32000	0.13000	13.32000	0.58000	-0.08000	0.00000	28.84000	0.93200
228	0.11000	0.02600	108.35000	7.29000	0.07000	-0.31000	0.12000	13.56000	0.59100	-0.07000	0.00000	28.80000	0.93100
229	0.07000	0.02600	107.38000	4.59000	0.12000	-0.17000	0.05000	12.03000	0.52400	-0.03000	0.00000	28.31000	0.91500
230	0.03000	0.02600	106.23000	2.28000	0.21000	-0.11000	0.02000	13.23000	0.57600	0.00000	0.00000	28.22000	0.91200
231	0.11000	0.02600	105.09000	7.36000	0.31000	-0.07000	0.01000	12.39000	0.54000	0.04000	0.00000	27.86000	0.90000
232	0.09000	0.02600	103.94000	6.12000	0.26000	-0.12000	0.03000	12.23000	0.53300	0.02000	0.00000	27.52000	0.89000
233	0.12000	0.02600	102.79000	7.73000	0.27000	-0.12000	0.03000	11.77000	0.51300	0.02000	0.00000	27.02000	0.87300
234	0.13000	0.02600	101.66000	8.65000	0.40000	-0.12000	0.03000	11.23000	0.48900	0.04000	0.00000	26.63000	0.86100
235	0.19000	0.02600	100.78000	12.37000	-0.14000	-0.07000	0.01000	10.89000	0.47400	0.11000	0.01000	26.56000	0.85900
236	0.20000	0.02600	99.91000	13.41000	-0.14000	-0.08000	0.01000	10.96000	0.47700	0.12000	0.01000	26.53000	0.85700
237	0.24000	0.02600	97.36000	16.09000	0.10000	-0.11000	0.02000	11.68000	0.50900	0.16000	0.02000	26.52000	0.85700
238	0.26000	0.02600	94.41000	17.05000	-0.55000	-0.11000	0.02000	11.86000	0.51700	0.17000	0.02000	26.80000	0.86600
239	0.06000	0.02600	88.34000	3.91000	-0.58000	-0.22000	0.09000	10.96000	0.47800	0.09000	0.01000	27.39000	0.88500
240	0.03000	0.02600	90.81000	2.25000	-0.58000	-0.26000	0.13000	10.85000	0.47300	0.07000	0.00000	27.30000	0.88200

241	-0.02000	0.02600	92.02000	-1.28000	-0.47000	-0.17000	0.07000	9.63000	0.41900	0.10000	0.01000	26.63000	0.86100
242	-0.10000	0.02600	93.22000	-6.55000	-0.42000	-0.17000	0.07000	9.88000	0.43000	0.09000	0.01000	26.39000	0.85300
243	-0.13000	0.02600	94.42000	-8.30000	-0.37000	-0.16000	0.08000	9.12000	0.39700	0.07000	0.00000	25.87000	0.83600
244	-0.11000	0.02600	94.28000	-7.24000	-0.11000	-0.11000	0.04000	8.80000	0.38300	0.08000	0.00000	24.91000	0.80500
245	-0.11000	0.02600	94.03000	-7.04000	-0.09000	-0.15000	0.08000	8.02000	0.34900	0.06000	0.00000	23.95000	0.77400
246	-0.08000	0.02600	93.78000	-5.39000	-0.17000	-0.27000	0.15000	10.58000	0.46100	0.02000	0.00000	23.91000	0.77300
247	-0.06000	0.02600	93.53000	-4.01000	-0.20000	-0.31000	0.15000	12.05000	0.52500	0.01000	0.00000	24.33000	0.78600
248	-0.09000	0.02600	93.28000	-6.04000	-0.46000	-0.27000	0.15000	10.28000	0.44800	0.03000	0.00000	24.39000	0.78800
249	-0.01000	0.02600	92.69000	-0.65000	-0.23000	-0.13000	0.05000	8.83000	0.38500	0.10000	0.01000	24.24000	0.78400
250	0.02000	0.02600	88.92000	1.14000	-0.07000	-0.09000	0.03000	8.70000	0.37900	0.10000	0.01000	23.50000	0.76000
251	0.02000	0.02600	85.15000	1.19000	-0.12000	0.00000	0.00000	7.79000	0.34000	0.13000	0.02000	23.09000	0.74600
252	0.05000	0.02600	81.71000	3.42000	-0.36000	-0.02000	0.00000	8.09000	0.35200	0.14000	0.02000	23.19000	0.75000
253	0.00000	0.02600	82.13000	0.32000	-0.43000	0.03000	0.00000	8.60000	0.37500	0.16000	0.02000	23.69000	0.76600
254	0.02000	0.02600	82.53000	1.05000	-0.47000	-0.01000	0.00000	8.33000	0.36300	0.15000	0.02000	23.74000	0.76700
255	0.05000	0.02600	81.47000	3.40000	-0.32000	0.12000	0.02000	12.31000	0.53600	0.15000	0.02000	23.88000	0.77200
256	0.05000	0.02600	81.12000	3.27000	-0.49000	0.15000	0.03000	13.47000	0.58700	0.14000	0.02000	23.56000	0.76200
257	0.04000	0.02600	80.76000	2.53000	-0.35000	0.16000	0.03000	13.62000	0.59300	0.14000	0.02000	23.08000	0.74600
258	0.03000	0.02600	80.40000	2.07000	-0.38000	-0.06000	0.01000	8.26000	0.36000	0.08000	0.01000	22.61000	0.73100
259	0.05000	0.02600	81.33000	2.97000	-0.38000	-0.09000	0.02000	9.28000	0.40400	0.08000	0.01000	22.58000	0.73000
260	0.06000	0.02600	82.89000	3.68000	0.35000	0.02000	0.00000	9.46000	0.41200	0.12000	0.01000	22.79000	0.73700
261	0.03000	0.02600	84.45000	2.17000	0.33000	0.09000	0.01000	12.45000	0.54200	0.14000	0.02000	23.35000	0.75500
262	0.14000	0.02600	85.27000	9.49000	0.39000	0.00000	0.00000	9.10000	0.39700	0.13000	0.01000	23.47000	0.75900
263	0.21000	0.02600	85.39000	13.88000	0.28000	-0.03000	0.00000	9.87000	0.43000	0.13000	0.01000	23.61000	0.76300
264	0.29000	0.02600	84.42000	19.34000	0.30000	0.01000	0.00000	9.55000	0.41600	0.15000	0.02000	23.52000	0.76000
265	0.30000	0.02600	83.68000	19.63000	0.27000	0.07000	0.01000	9.95000	0.43400	0.14000	0.02000	23.59000	0.76200
266	0.29000	0.02600	83.34000	19.16000	0.29000	0.08000	0.02000	9.50000	0.41400	0.13000	0.01000	23.19000	0.75000
267	0.30000	0.02600	82.99000	19.86000	0.32000	0.11000	0.04000	9.14000	0.39800	0.11000	0.01000	22.75000	0.73500
268	0.34000	0.02600	86.33000	22.75000	0.34000	0.17000	0.08000	9.42000	0.41100	0.14000	0.02000	23.60000	0.76300
269	0.40000	0.02600	90.07000	26.16000	0.35000	0.16000	0.06000	10.48000	0.45700	0.14000	0.02000	24.57000	0.79400
270	0.30000	0.02600	93.82000	19.47000	0.31000	0.17000	0.04000	13.33000	0.58100	0.11000	0.01000	25.75000	0.83200
271	0.28000	0.02600	95.52000	18.44000	0.25000	0.13000	0.02000	14.40000	0.62700	0.10000	0.01000	26.78000	0.86500
272	0.26000	0.02600	95.14000	16.89000	0.17000	0.10000	0.01000	14.60000	0.63600	0.09000	0.01000	27.32000	0.88300
273	0.21000	0.02600	94.74000	13.87000	0.09000	0.00000	0.00000	15.09000	0.65700	-0.01000	0.00000	26.38000	0.85300
274	0.18000	0.02600	94.34000	11.80000	-0.04000	0.00000	0.00000	15.80000	0.68800	-0.02000	0.00000	26.07000	0.84200
275	0.21000	0.02600	93.94000	13.61000	0.44000	0.04000	0.00000	15.75000	0.68600	0.01000	0.00000	25.80000	0.83400
276	0.23000	0.02600	93.55000	15.09000	0.51000	0.09000	0.01000	16.00000	0.69700	0.06000	0.00000	25.98000	0.84000
277	0.27000	0.02600	92.49000	17.77000	-0.67000	0.11000	0.02000	12.78000	0.55700	0.14000	0.01000	26.00000	0.84000
278	0.29000	0.02600	91.20000	19.37000	-0.65000	0.10000	0.02000	12.03000	0.52400	0.16000	0.02000	26.23000	0.84800
279	0.27000	0.02600	89.60000	18.13000	-0.02000	0.04000	0.00000	14.02000	0.61100	0.12000	0.01000	27.02000	0.87300
280	0.18000	0.02600	88.21000	11.98000	-0.07000	-0.01000	0.00000	13.29000	0.57900	0.10000	0.01000	27.25000	0.88100

281	0.24000	0.02600	87.75000	15.52000	0.11000	0.08000	0.01000	12.94000	0.56400	0.18000	0.02000	26.72000	0.86400
282	0.19000	0.02600	89.31000	12.43000	0.27000	0.08000	0.01000	14.76000	0.64300	0.18000	0.02000	26.98000	0.87200
283	0.24000	0.02600	92.43000	15.53000	0.32000	0.07000	0.01000	13.48000	0.58700	0.22000	0.03000	27.45000	0.88700
284	0.20000	0.02600	94.39000	13.03000	0.36000	0.11000	0.02000	14.29000	0.62300	0.24000	0.04000	27.23000	0.88000
285	0.19000	0.02600	90.04000	12.76000	0.33000	0.13000	0.02000	14.02000	0.61100	0.23000	0.04000	26.11000	0.84400
286	0.24000	0.02600	86.23000	16.13000	0.33000	0.15000	0.04000	12.41000	0.54100	0.25000	0.04000	24.88000	0.80400
287	0.29000	0.02600	83.95000	19.03000	-0.21000	0.03000	0.00000	9.70000	0.42300	0.21000	0.04000	23.87000	0.77200
288	0.25000	0.02600	86.60000	16.19000	0.47000	0.14000	0.05000	10.25000	0.44600	0.23000	0.04000	23.38000	0.75600
289	0.20000	0.02600	90.66000	13.40000	0.21000	0.10000	0.04000	8.29000	0.36100	0.23000	0.04000	23.33000	0.75400
290	0.15000	0.02600	88.68000	9.92000	0.37000	0.09000	0.03000	8.73000	0.38000	0.18000	0.03000	22.88000	0.73900
291	0.12000	0.02600	82.85000	7.92000	0.19000	0.16000	0.03000	14.05000	0.61200	0.13000	0.02000	22.15000	0.71600
292	0.15000	0.02600	77.17000	10.00000	0.14000	0.14000	0.03000	13.43000	0.58500	0.10000	0.01000	21.30000	0.68900
293	0.17000	0.02600	75.42000	11.52000	0.18000	0.13000	0.03000	10.99000	0.47900	0.11000	0.01000	20.81000	0.67300
294	0.19000	0.02600	73.66000	12.70000	0.21000	0.05000	0.01000	8.43000	0.36700	0.10000	0.01000	20.97000	0.67800
295	0.26000	0.02600	72.04000	16.94000	0.23000	0.11000	0.04000	9.00000	0.39200	0.14000	0.02000	20.72000	0.67000
296	0.29000	0.02600	70.44000	18.99000	0.11000	0.20000	0.10000	9.52000	0.41500	0.20000	0.04000	20.84000	0.67400
297	0.31000	0.02600	70.60000	20.43000	0.16000	0.28000	0.14000	11.28000	0.49100	0.25000	0.06000	21.64000	0.69900
298	0.24000	0.02600	71.51000	15.90000	0.14000	0.26000	0.11000	11.78000	0.51300	0.24000	0.05000	22.37000	0.72300
299	0.20000	0.02600	72.43000	13.49000	0.21000	0.29000	0.12000	12.52000	0.54600	0.26000	0.06000	22.39000	0.72400
300	0.36000	0.02600	73.33000	23.83000	0.31000	0.20000	0.17000	7.07000	0.30800	0.32000	0.09000	21.88000	0.70700
301	0.38000	0.02600	76.13000	24.84000	0.37000	0.27000	0.26000	7.24000	0.31500	0.36000	0.11000	22.21000	0.71800
302	0.38000	0.02600	78.52000	24.94000	0.33000	0.32000	0.22000	9.83000	0.42800	0.37000	0.11000	22.69000	0.73300
303	0.45000	0.02600	79.47000	30.01000	0.37000	0.47000	0.24000	13.58000	0.59200	0.44000	0.15000	22.96000	0.74200
304	0.53000	0.02600	82.48000	35.01000	0.32000	0.48000	0.27000	12.81000	0.55800	0.49000	0.18000	23.20000	0.75000
305	0.51000	0.02600	87.18000	33.73000	0.33000	0.58000	0.25000	16.35000	0.71200	0.54000	0.20000	23.51000	0.76000
306	0.47000	0.02600	87.94000	31.18000	0.34000	0.66000	0.23000	19.16000	0.83500	0.58000	0.22000	23.35000	0.75500
307	0.42000	0.02600	76.09000	27.98000	0.38000	0.64000	0.24000	18.78000	0.81800	0.54000	0.23000	21.18000	0.68500
308	0.43000	0.02600	65.19000	28.08000	0.51000	0.59000	0.20000	18.78000	0.81800	0.47000	0.21000	19.67000	0.63600
309	0.43000	0.02600	65.91000	28.67000	0.40000	0.64000	0.25000	17.86000	0.77800	0.52000	0.26000	19.29000	0.62400
310	0.44000	0.02600	69.52000	29.31000	0.60000	0.78000	0.22000	24.04000	1.04700	0.58000	0.28000	20.14000	0.65100
311	0.50000	0.02600	72.05000	32.72000	0.62000	0.85000	0.22000	25.62000	1.11600	0.62000	0.31000	20.23000	0.65400
312	0.51000	0.02600	68.49000	33.81000	0.76000	0.83000	0.26000	22.77000	0.99200	0.63000	0.33000	19.52000	0.63100
313	0.54000	0.02600	67.41000	35.33000	0.40000	0.85000	0.28000	22.19000	0.96700	0.65000	0.35000	19.17000	0.62000
314	0.56000	0.02600	68.83000	36.85000	0.28000	0.87000	0.27000	22.96000	1.00000	0.66000	0.36000	19.13000	0.61800
315	0.59000	0.02600	68.59000	39.17000	0.26000	0.87000	0.29000	22.22000	0.96800	0.67000	0.38000	18.79000	0.60700
316	0.63000	0.02600	67.36000	41.71000	0.32000	0.87000	0.33000	19.92000	0.86800	0.69000	0.41000	18.24000	0.59000
317	0.62000	0.02600	64.99000	41.15000	0.26000	0.84000	0.31000	20.14000	0.87700	0.67000	0.39000	18.29000	0.59100
318	0.53000	0.02600	60.67000	34.84000	0.10000	0.62000	0.30000	15.34000	0.66800	0.59000	0.32000	18.60000	0.60100
139 319	0.49000	0.02600	66.82000	32.40000	0.09000	0.57000	0.28000	14.66000	0.63800	0.59000	0.32000	18.87000	0.61000
320	0.46000	0.02600	72.35000	30.49000	0.09000	0.56000	0.28000	14.28000	0.62200	0.61000	0.32000	19.23000	0.62200

321	0.44000	0.02600	78.67000	28.75000	0.07000	0.58000	0.24000	16.72000	0.72800	0.61000	0.31000	20.10000	0.65000
322	0.50000	0.02600	86.52000	32.71000	0.14000	0.42000	0.36000	9.06000	0.39500	0.59000	0.27000	21.18000	0.68400
323	0.46000	0.02600	81.21000	30.30000	0.07000	0.35000	0.29000	8.94000	0.38900	0.53000	0.24000	20.46000	0.66100
324	0.46000	0.02600	70.86000	30.62000	0.07000	0.33000	0.29000	8.39000	0.36500	0.49000	0.24000	19.01000	0.61400
325	0.47000	0.02600	62.21000	30.72000	-0.02000	0.28000	0.25000	7.86000	0.34300	0.43000	0.21000	18.17000	0.58700
326	0.41000	0.02600	60.52000	27.21000	-0.14000	0.18000	0.13000	7.42000	0.32300	0.37000	0.16000	18.60000	0.60100
327	0.36000	0.02600	58.61000	23.56000	0.27000	0.17000	0.09000	8.82000	0.38400	0.31000	0.12000	18.81000	0.60800
328	0.31000	0.02600	56.47000	20.43000	0.23000	0.06000	0.01000	8.13000	0.35400	0.25000	0.08000	18.76000	0.60600
329	0.22000	0.02600	55.27000	14.49000	0.12000	-0.04000	0.01000	7.95000	0.34600	0.19000	0.04000	18.86000	0.61000
330	0.12000	0.02600	54.46000	8.13000	0.07000	-0.05000	0.01000	8.78000	0.38200	0.16000	0.03000	19.06000	0.61600
331	0.10000	0.02600	55.82000	6.71000	0.05000	0.04000	0.00000	11.89000	0.51800	0.19000	0.05000	18.95000	0.61300
332	0.03000	0.02600	57.42000	1.87000	-0.07000	-0.01000	0.00000	11.91000	0.51900	0.15000	0.03000	19.29000	0.62400
333	0.14000	0.02600	55.12000	9.32000	0.00000	0.11000	0.01000	16.37000	0.71300	0.19000	0.05000	18.98000	0.61300
334	0.17000	0.02600	54.17000	11.29000	0.09000	0.16000	0.04000	13.32000	0.58000	0.27000	0.10000	17.47000	0.56500
335	0.15000	0.02600	41.79000	10.11000	0.38000	0.36000	0.12000	19.97000	1.35600	0.34000	0.29000	15.02000	0.72600
Minimum	-1.11000	0.02600	24.59000	-73.49000	-1.38000	-0.89000	0.00000	2.73000	0.11900	-0.84000	0.00000	6.26000	0.20200
Maximum	1.37000	0.02600	259.53000	90.47000	5.19000	3.29000	0.90000	144.46000	6.29300	2.85000	0.55000	88.33000	2.85500
Average	-0.10814	0.02600	91.96198	-7.13323	-0.14931	-0.04075	0.21737	15.33943	0.66966	-0.04521	0.11251	25.52883	0.82584

Table 7: DSAS statistics for Strand.

TransectId	EPR	ECI	SCE	NSM	LMS	WLR	WR2	WSE	WCI95	LRR	LR2	LSE	LCI95
1	-0.03000	0.35400	0.06000	-0.06000	-0.03000								
2	-0.39000	0.02600	33.83000	-25.48000	-0.34000	-0.10000	0.02000	11.61000	0.62700	-0.19000	0.15000	10.48000	0.41800
3	-0.45000	0.02600	75.27000	-29.76000	-0.45000	-0.23000	0.06000	13.90000	0.60300	-0.55000	0.30000	18.69000	0.55400
4	-0.53000	0.02600	120.42000	-34.91000	-0.42000	-0.28000	0.05000	18.63000	0.78400	-0.60000	0.16000	29.92000	0.87500
5	-0.66000	0.02600	129.51000	-43.25000	-0.33000	-0.26000	0.03000	23.35000	0.98300	-0.61000	0.15000	32.00000	0.93600
6	-0.96000	0.02600	136.96000	-63.05000	-0.43000	-0.27000	0.01000	34.56000	1.45500	-0.68000	0.16000	34.13000	0.99800
7	-0.90000	0.02600	135.31000	-59.38000	-0.27000	-0.23000	0.01000	35.20000	1.48200	-0.62000	0.15000	31.80000	0.93000
8	-0.86000	0.02600	134.48000	-56.53000	-0.12000	-0.14000	0.00000	37.23000	1.56800	-0.58000	0.13000	32.32000	0.94500
9	-0.82000	0.02600	133.32000	-54.26000	-0.10000	0.00000	0.00000	41.48000	1.74700	-0.55000	0.11000	32.92000	0.96300
10	-0.77000	0.02600	131.16000	-51.06000	-0.05000	0.07000	0.00000	42.89000	1.80600	-0.52000	0.10000	33.28000	0.97300
11	-0.67000	0.02600	126.28000	-44.15000	-0.12000	0.08000	0.00000	40.08000	1.68800	-0.51000	0.10000	33.01000	0.96600
12	-0.60000	0.02600	119.32000	-39.57000	-0.29000	0.10000	0.00000	39.56000	1.66600	-0.51000	0.11000	31.80000	0.93000
13	-0.57000	0.02600	111.05000	-37.46000	-0.43000	0.12000	0.00000	40.00000	1.68400	-0.52000	0.12000	30.37000	0.88800
14	-0.53000	0.02600	102.78000	-35.30000	-0.37000	0.14000	0.00000	38.89000	1.63700	-0.52000	0.13000	28.79000	0.84200
15	-0.56000	0.02600	101.23000	-36.68000	-0.42000	0.13000	0.00000	37.98000	1.59900	-0.54000	0.15000	28.19000	0.82500
16	-0.53000	0.02600	106.33000	-35.23000	-0.96000	0.11000	0.00000	36.21000	1.52400	-0.59000	0.16000	28.84000	0.84400
17	-0.45000	0.02600	112.31000	-29.98000	-1.07000	0.09000	0.00000	34.48000	1.45200	-0.67000	0.18000	30.18000	0.88300
18	-0.42000	0.02600	118.38000	-27.75000	-1.27000	0.07000	0.00000	32.68000	1.37600	-0.71000	0.19000	31.41000	0.91900
19	-0.44000	0.02600	124.45000	-29.34000	-1.59000	0.03000	0.00000	31.82000	1.34000	-0.72000	0.19000	31.85000	0.93200
20	-0.50000	0.02600	129.67000	-32.96000	-1.59000	-0.02000	0.00000	31.78000	1.33800	-0.75000	0.20000	32.49000	0.95000
21	-0.45000	0.02600	132.19000	-29.90000	-1.67000	-0.07000	0.00000	29.28000	1.23300	-0.80000	0.21000	33.12000	0.96900
22	-0.43000	0.02600	134.68000	-28.34000	-1.43000	-0.10000	0.00000	28.98000	1.22000	-0.87000	0.23000	34.46000	1.00800
23	-0.40000	0.02600	137.15000	-26.21000	-1.53000	-0.12000	0.00000	28.76000	1.21100	-0.91000	0.23000	35.79000	1.04700
24	-0.36000	0.02600	139.59000	-23.60000	-1.72000	-0.14000	0.01000	28.50000	1.20000	-0.95000	0.23000	37.25000	1.09000
25	-0.32000	0.02600	136.74000	-21.15000	-1.55000	-0.17000	0.01000	27.29000	1.14900	-0.97000	0.23000	37.70000	1.10300
26	-0.31000	0.02600	133.24000	-20.46000	-1.53000	-0.23000	0.02000	26.16000	1.10100	-1.00000	0.24000	37.93000	1.11000
27	-0.37000	0.02600	129.76000	-24.13000	-1.74000	-0.28000	0.02000	26.54000	1.11800	-1.06000	0.27000	37.81000	1.10600
28	-0.38000	0.02600	124.57000	-25.00000	-1.55000	-0.29000	0.02000	27.35000	1.15100	-1.07000	0.28000	37.16000	1.08700
29	-0.37000	0.02600	111.32000	-24.74000	0.05000	-0.32000	0.03000	26.30000	1.10700	-1.06000	0.29000	35.28000	1.03200
30	-0.40000	0.02600	111.52000	-26.43000	0.04000	-0.33000	0.03000	26.84000	1.13000	-1.04000	0.30000	34.05000	0.99600
31	-0.46000	0.02600	118.82000	-30.03000	0.00000	-0.34000	0.03000	28.46000	1.19800	-1.04000	0.29000	34.86000	1.02000
32	-0.51000	0.02600	126.05000	-33.56000	-0.53000	-0.36000	0.03000	30.84000	1.29800	-1.05000	0.28000	35.80000	1.04700
33	-0.57000	0.02600	133.72000	-37.53000	-0.41000	-0.42000	0.04000	31.85000	1.34100	-1.07000	0.28000	36.77000	1.07600
34	-0.55000	0.02600	142.54000	-36.08000	-0.53000	-0.43000	0.04000	33.08000	1.39300	-1.10000	0.27000	38.65000	1.13100
35	-0.50000	0.02600	147.74000	-33.07000	-2.04000	-0.41000	0.03000	33.98000	1.43100	-1.10000	0.25000	40.58000	1.18700
36	-0.45000	0.02600	151.21000	-30.02000	-2.06000	-0.43000	0.04000	32.91000	1.38600	-1.09000	0.24000	42.10000	1.23100
37	-0.44000	0.02600	156.48000	-28.80000	-2.25000	-0.48000	0.05000	32.10000	1.35100	-1.11000	0.23000	43.94000	1.28500
38	-0.47000	0.02600	160.79000	-31.10000	-2.37000	-0.53000	0.06000	31.78000	1.33800	-1.17000	0.24000	45.10000	1.31900
39	-0.52000	0.02600	162.25000	-34.31000	-2.37000	-0.61000	0.08000	30.21000	1.27200	-1.24000	0.26000	45.10000	1.31900
40	-0.57000	0.02600	163.24000	-37.65000	-2.23000	-0.72000	0.13000	27.32000	1.15000	-1.27000	0.28000	43.71000	1.27800

41	-0.62000	0.02600	164.20000	-40.95000	-2.34000	-0.78000	0.16000	26.43000	1.11300	-1.29000	0.30000	42.41000	1.24100
42	-0.67000	0.02600	164.03000	-44.24000	-2.34000	-0.81000	0.18000	26.23000	1.10400	-1.30000	0.32000	41.12000	1.20300
43	-0.67000	0.02600	160.06000	-44.00000	-2.34000	-0.84000	0.19000	25.54000	1.07500	-1.32000	0.33000	40.13000	1.17400
44	-0.61000	0.02600	162.86000	-40.41000	-2.15000	-0.85000	0.20000	25.13000	1.05800	-1.34000	0.34000	39.93000	1.16800
45	-0.68000	0.02600	168.99000	-44.68000	-2.15000	-0.89000	0.20000	26.92000	1.13300	-1.38000	0.35000	40.62000	1.18800
46	-0.74000	0.02600	175.11000	-48.96000	-2.16000	-0.90000	0.18000	28.67000	1.20700	-1.38000	0.34000	41.06000	1.20100
47	-0.80000	0.02600	181.24000	-52.63000	-2.14000	-0.89000	0.15000	31.10000	1.30900	-1.37000	0.33000	41.69000	1.21900
48	-0.83000	0.02600	178.20000	-54.72000	-2.06000	-0.86000	0.14000	32.26000	1.35800	-1.34000	0.33000	40.70000	1.19000
49	-0.86000	0.02600	174.29000	-56.53000	-2.06000	-0.84000	0.13000	32.56000	1.37100	-1.31000	0.33000	39.63000	1.15900
50	-0.85000	0.02600	177.44000	-56.12000	-2.04000	-0.83000	0.13000	32.45000	1.36600	-1.27000	0.32000	40.03000	1.17100
51	-0.82000	0.02600	182.12000	-54.16000	-1.89000	-0.82000	0.14000	31.17000	1.31200	-1.23000	0.29000	40.99000	1.19900
52	-0.79000	0.02600	181.68000	-52.20000	-1.81000	-0.74000	0.11000	31.89000	1.34300	-1.15000	0.27000	41.16000	1.20400
53	-0.75000	0.02600	171.17000	-49.46000	-0.31000	-0.66000	0.09000	32.07000	1.35000	-1.07000	0.26000	39.08000	1.14300
54	-0.68000	0.02600	160.59000	-44.67000	-0.23000	-0.58000	0.07000	31.45000	1.32400	-0.99000	0.25000	36.80000	1.07700
55	-0.70000	0.02600	151.71000	-45.87000	-0.25000	-0.59000	0.08000	30.62000	1.28900	-0.99000	0.27000	34.67000	1.01400
56	-0.71000	0.02600	145.06000	-47.08000	-0.25000	-0.56000	0.07000	31.33000	1.31900	-0.99000	0.29000	33.24000	0.97200
57	-0.73000	0.02600	138.41000	-48.44000	-0.23000	-0.54000	0.06000	32.18000	1.35500	-0.98000	0.30000	32.38000	0.94700
58	-0.75000	0.02600	128.44000	-49.79000	-0.21000	-0.44000	0.03000	35.09000	1.47800	-0.94000	0.29000	31.57000	0.92300
59	-0.77000	0.02600	126.82000	-50.89000	-0.12000	-0.33000	0.02000	38.50000	1.62100	-0.89000	0.26000	32.41000	0.94800
60	-0.75000	0.02600	125.87000	-49.44000	-0.10000	-0.32000	0.02000	37.36000	1.57300	-0.85000	0.24000	32.32000	0.94500
61	-0.73000	0.02600	127.30000	-47.99000	-0.07000	-0.30000	0.01000	37.11000	1.56200	-0.83000	0.23000	32.36000	0.94700
62	-0.71000	0.02600	128.59000	-46.96000	-0.12000	-0.27000	0.01000	38.10000	1.60400	-0.82000	0.23000	32.56000	0.95200
63	-0.70000	0.02600	127.29000	-46.42000	-0.16000	-0.24000	0.01000	38.37000	1.61500	-0.81000	0.23000	32.23000	0.94300
64	-0.69000	0.02600	125.30000	-45.48000	-0.19000	-0.23000	0.01000	36.77000	1.54800	-0.80000	0.23000	31.54000	0.92300
65	-0.63000	0.02600	124.13000	-41.54000	-0.12000	-0.20000	0.01000	34.79000	1.46500	-0.76000	0.22000	31.05000	0.90800
66	-0.56000	0.02600	123.30000	-37.26000	-1.49000	-0.17000	0.01000	34.26000	1.44200	-0.75000	0.21000	31.07000	0.90900
67	-0.51000	0.02600	123.73000	-33.35000	-0.14000	-0.13000	0.00000	35.10000	1.47800	-0.76000	0.21000	31.49000	0.92100
68	-0.51000	0.02600	125.76000	-33.91000	-1.32000	-0.09000	0.00000	36.23000	1.52500	-0.78000	0.21000	32.24000	0.94300
69	-0.53000	0.02600	124.62000	-35.11000	-1.23000	-0.09000	0.00000	34.80000	1.46500	-0.76000	0.21000	31.53000	0.92200
70	-0.56000	0.02600	122.72000	-37.07000	-1.43000	-0.08000	0.00000	34.22000	1.44100	-0.74000	0.21000	30.84000	0.90200
71	-0.63000	0.02600	120.80000	-41.89000	-1.42000	-0.10000	0.00000	34.34000	1.44600	-0.74000	0.22000	30.39000	0.88900
72	-0.71000	0.02600	118.93000	-46.76000	-1.54000	-0.14000	0.00000	33.90000	1.42700	-0.75000	0.22000	30.00000	0.87700
73	-0.77000	0.02600	115.15000	-51.10000	-1.49000	-0.19000	0.01000	33.35000	1.40400	-0.77000	0.25000	29.14000	0.85200
74	-0.83000	0.02600	111.39000	-54.57000	-1.43000	-0.23000	0.01000	33.75000	1.42100	-0.79000	0.26000	28.37000	0.83000
75	-0.88000	0.02600	107.35000	-58.01000	-1.43000	-0.24000	0.01000	34.72000	1.46200	-0.80000	0.28000	27.73000	0.81100
76	-0.93000	0.02600	99.76000	-61.22000	-1.23000	-0.26000	0.01000	35.53000	1.49600	-0.80000	0.30000	26.48000	0.77400
77	-0.94000	0.02600	92.01000	-62.06000	-1.29000	-0.28000	0.01000	35.14000	1.48000	-0.80000	0.32000	24.87000	0.72700
78	-0.98000	0.02600	86.23000	-64.53000	-0.75000	-0.33000	0.02000	33.89000	1.42700	-0.84000	0.37000	23.54000	0.68800
79	-1.14000	0.02600	83.82000	-75.24000	-0.81000	-0.44000	0.04000	34.24000	1.44200	-0.92000	0.42000	23.12000	0.67600
80	-1.23000	0.02600	82.51000	-81.41000	-1.23000	-0.53000	0.05000	32.79000	1.38100	-0.97000	0.45000	22.76000	0.66600

81	-1.29000	0.02600	85.36000	-85.36000	-1.29000	-0.61000	0.08000	30.78000	1.29600	-1.01000	0.49000	22.19000	0.64900
82	-1.32000	0.02600	86.84000	-86.84000	-0.90000	-0.68000	0.12000	27.74000	1.16800	-1.01000	0.51000	21.47000	0.62800
83	-1.28000	0.02600	84.83000	-84.58000	-0.87000	-0.76000	0.19000	23.03000	0.97000	-1.01000	0.51000	21.39000	0.62600
84	-1.27000	0.02600	83.57000	-83.57000	-0.87000	-0.77000	0.21000	22.17000	0.93400	-1.00000	0.51000	21.23000	0.62100
85	-1.30000	0.02600	85.91000	-85.91000	-0.87000	-0.77000	0.20000	23.10000	0.97200	-0.99000	0.50000	21.31000	0.62300
86	-1.23000	0.02600	81.29000	-81.14000	-0.84000	-0.73000	0.19000	22.41000	0.94400	-0.94000	0.48000	21.05000	0.61600
87	-1.25000	0.02600	84.35000	-82.63000	-0.87000	-0.74000	0.19000	23.27000	0.98000	-0.93000	0.46000	21.60000	0.63200
88	-1.31000	0.02600	86.89000	-86.65000	-0.76000	-0.76000	0.17000	25.15000	1.05900	-0.94000	0.45000	22.50000	0.65800
89	-1.45000	0.02600	95.93000	-95.93000	-0.97000	-0.85000	0.19000	26.22000	1.10400	-1.01000	0.47000	23.15000	0.67700
90	-1.55000	0.02600	103.38000	-102.11000	-0.84000	-0.94000	0.24000	25.04000	1.05400	-1.06000	0.48000	23.79000	0.69600
91	-1.69000	0.02600	111.49000	-111.49000	-0.84000	-1.07000	0.29000	24.97000	1.05100	-1.17000	0.51000	24.85000	0.72700
92	-1.82000	0.02600	119.79000	-119.79000	-0.28000	-1.19000	0.35000	24.51000	1.03200	-1.23000	0.50000	26.34000	0.77100
93	-1.86000	0.02600	122.43000	-122.43000	-0.21000	-1.30000	0.43000	22.25000	0.93700	-1.22000	0.46000	28.27000	0.82700
94	-1.65000	0.02600	109.12000	-109.12000	-0.07000	-1.26000	0.49000	19.32000	0.81400	-1.16000	0.44000	28.38000	0.83000
95	-1.48000	0.02600	97.85000	-97.78000	-0.47000	-1.14000	0.44000	19.30000	0.81300	-1.09000	0.42000	27.22000	0.79600
96	-1.39000	0.02600	91.77000	-91.77000	-0.62000	-0.88000	0.22000	24.44000	1.02900	-0.96000	0.39000	25.47000	0.74500
97	-1.32000	0.02600	87.06000	-87.06000	-0.47000	-0.62000	0.08000	31.20000	1.31300	-0.82000	0.35000	23.97000	0.70100
98	-1.13000	0.02600	77.15000	-74.87000	-0.51000	-0.53000	0.08000	26.98000	1.13600	-0.70000	0.34000	20.88000	0.61100
99	-1.02000	0.02600	70.69000	-67.15000	-0.36000	-0.43000	0.06000	24.59000	1.03500	-0.61000	0.33000	18.66000	0.54600
100	-0.92000	0.02600	64.24000	-60.79000	-0.33000	-0.37000	0.06000	21.83000	0.91900	-0.52000	0.30000	16.99000	0.49700
101	-0.84000	0.02600	57.78000	-55.37000	-0.23000	-0.32000	0.06000	19.72000	0.83000	-0.47000	0.30000	15.45000	0.45200
102	-0.80000	0.02600	52.98000	-52.71000	-0.21000	-0.30000	0.05000	19.20000	0.80800	-0.46000	0.32000	14.47000	0.42300
103	-0.77000	0.02600	50.54000	-50.54000	-0.21000	-0.28000	0.05000	18.45000	0.77700	-0.45000	0.32000	14.17000	0.41500
104	-0.73000	0.02600	48.25000	-48.25000	-0.19000	-0.27000	0.05000	17.47000	0.73600	-0.44000	0.34000	13.38000	0.39100
105	-0.70000	0.02600	45.95000	-45.95000	-0.65000	-0.27000	0.06000	16.87000	0.71000	-0.44000	0.35000	12.72000	0.37200
106	-0.66000	0.02600	43.62000	-43.62000	-0.68000	-0.26000	0.05000	16.76000	0.70600	-0.43000	0.36000	12.33000	0.36100
107	-0.63000	0.02600	41.38000	-41.38000	-0.57000	-0.24000	0.04000	16.63000	0.70000	-0.41000	0.35000	11.86000	0.34700
108	-0.59000	0.02600	44.32000	-39.15000	-0.65000	-0.24000	0.05000	15.25000	0.64200	-0.38000	0.29000	12.54000	0.36700
109	-0.51000	0.02600	40.04000	-33.40000	-0.56000	-0.23000	0.08000	12.07000	0.50800	-0.33000	0.25000	12.25000	0.35800
110	-0.41000	0.02600	33.17000	-27.38000	-0.45000	-0.19000	0.07000	10.49000	0.44200	-0.29000	0.24000	10.94000	0.32000
111	-0.35000	0.02600	30.90000	-22.82000	-0.39000	-0.16000	0.06000	9.54000	0.40200	-0.27000	0.26000	9.80000	0.28700
112	-0.38000	0.02600	34.45000	-24.93000	-0.39000	-0.15000	0.04000	10.57000	0.44500	-0.29000	0.31000	9.33000	0.27300
113	-0.12000	0.02600	38.98000	-7.67000	0.05000	-0.07000	0.04000	4.57000	0.19200	-0.17000	0.12000	9.67000	0.28300
114	-0.23000	0.02600	45.03000	-15.04000	0.16000	-0.04000	0.01000	6.81000	0.28700	-0.21000	0.16000	10.37000	0.30300
115	-0.26000	0.02600	49.54000	-17.13000	0.14000	0.02000	0.00000	10.67000	0.44900	-0.23000	0.16000	11.26000	0.33000
116	-0.29000	0.02600	50.18000	-18.94000	-0.21000	0.09000	0.01000	14.47000	0.60900	-0.24000	0.16000	11.81000	0.34500
117	-0.28000	0.02600	50.36000	-18.75000	-0.19000	0.09000	0.01000	14.51000	0.61100	-0.26000	0.18000	11.90000	0.34800
118	-0.27000	0.02600	50.54000	-17.96000	0.02000	0.03000	0.00000	11.71000	0.49300	-0.27000	0.22000	11.21000	0.32800
119	-0.27000	0.02600	47.20000	-17.56000	0.04000	0.01000	0.00000	10.56000	0.44500	-0.27000	0.24000	10.38000	0.30400
120	-0.28000	0.02600	42.00000	-18.57000	-0.16000	-0.01000	0.00000	11.08000	0.46700	-0.26000	0.25000	9.87000	0.28900

121	-0.30000	0.02600	39.08000	-19.50000	-0.05000	-0.02000	0.00000	11.72000	0.49300	-0.27000	0.27000	9.61000	0.28100
122	-0.31000	0.02600	39.41000	-20.43000	0.02000	-0.03000	0.00000	11.83000	0.49800	-0.28000	0.29000	9.25000	0.27000
123	-0.33000	0.02600	39.14000	-21.45000	0.07000	-0.06000	0.01000	11.28000	0.47500	-0.28000	0.31000	8.95000	0.26200
124	-0.33000	0.02600	36.77000	-21.55000	-0.12000	-0.08000	0.01000	9.66000	0.40700	-0.26000	0.32000	8.31000	0.24300
125	-0.31000	0.02600	32.75000	-20.65000	0.19000	-0.11000	0.05000	7.50000	0.31600	-0.23000	0.32000	7.29000	0.21300
126	-0.26000	0.02600	25.69000	-16.85000	0.02000	-0.08000	0.03000	6.96000	0.29300	-0.19000	0.25000	7.26000	0.21200
127	-0.33000	0.02600	31.28000	-21.59000	0.12000	-0.10000	0.02000	9.56000	0.40200	-0.23000	0.18000	10.36000	0.30300
128	-0.45000	0.02600	39.57000	-29.53000	-0.45000	-0.08000	0.01000	13.78000	0.58000	-0.29000	0.22000	11.94000	0.34900
129	-0.52000	0.02600	51.46000	-34.40000	-0.62000	-0.11000	0.01000	15.53000	0.65400	-0.37000	0.24000	13.86000	0.40500
130	-0.51000	0.02600	59.35000	-33.46000	0.21000	-0.08000	0.01000	16.32000	0.68700	-0.38000	0.21000	15.67000	0.45800
131	-0.49000	0.02600	66.31000	-32.64000	0.04000	-0.05000	0.00000	16.80000	0.70700	-0.41000	0.21000	17.17000	0.50200
132	-0.51000	0.02600	74.40000	-33.52000	0.17000	-0.03000	0.00000	17.26000	0.72700	-0.44000	0.21000	18.46000	0.54000
133	-0.52000	0.02600	81.02000	-34.05000	0.34000	-0.05000	0.00000	16.31000	0.68700	-0.45000	0.19000	19.59000	0.57300
134	-0.52000	0.02600	82.94000	-34.14000	0.21000	-0.12000	0.02000	13.64000	0.57400	-0.47000	0.21000	19.38000	0.56700
135	-0.50000	0.02600	84.67000	-32.76000	0.21000	-0.18000	0.05000	11.57000	0.48700	-0.47000	0.23000	18.55000	0.54300
136	-0.45000	0.02600	83.13000	-29.50000	0.18000	-0.18000	0.06000	10.44000	0.44000	-0.45000	0.22000	18.13000	0.53000
137	-0.38000	0.02600	78.02000	-25.12000	-0.03000	-0.18000	0.08000	9.17000	0.38600	-0.48000	0.29000	16.23000	0.47500
138	-0.25000	0.02600	55.83000	-16.42000	-0.07000	-0.12000	0.06000	7.01000	0.29500	-0.36000	0.29000	12.17000	0.35600
139	-0.26000	0.02600	36.87000	-17.31000	-0.12000	-0.15000	0.41000	2.64000	0.11100	-0.13000	0.13000	7.57000	0.22100
140	0.00000	0.02600	35.74000	-0.16000	0.23000	0.16000	0.26000	4.08000	0.17200	0.19000	0.12000	11.05000	0.32300
141	-0.04000	0.02600	31.10000	-2.73000	0.00000	-0.08000	0.02000	8.57000	0.36100	-0.02000	0.00000	8.98000	0.26300
142	-0.27000	0.02600	23.58000	-17.94000	0.21000	-0.12000	0.24000	3.17000	0.13400	-0.10000	0.08000	7.21000	0.21100
143	-0.28000	0.02600	25.59000	-18.36000	0.21000	-0.12000	0.19000	3.71000	0.15600	-0.12000	0.10000	7.62000	0.22300
144	-0.27000	0.02600	24.43000	-17.66000	-0.18000	-0.12000	0.16000	3.96000	0.16700	-0.12000	0.10000	7.74000	0.22600
145	-0.28000	0.02600	23.38000	-18.58000	-0.16000	-0.09000	0.05000	5.91000	0.24900	-0.12000	0.10000	8.13000	0.23800
146	-0.27000	0.02600	23.60000	-17.55000	-0.27000	-0.06000	0.02000	6.58000	0.27700	-0.11000	0.07000	8.51000	0.24900
147	-0.24000	0.02600	23.88000	-16.13000	-0.23000	-0.01000	0.00000	7.90000	0.33200	-0.09000	0.05000	8.44000	0.24700
148	-0.28000	0.02600	25.69000	-18.44000	-0.14000	-0.01000	0.00000	9.57000	0.40300	-0.13000	0.11000	7.76000	0.22700
149	-0.34000	0.02600	29.26000	-22.40000	-0.27000	-0.04000	0.00000	10.20000	0.42900	-0.17000	0.17000	8.14000	0.23800
150	-0.36000	0.02600	30.73000	-23.91000	-0.05000	-0.09000	0.02000	9.54000	0.40200	-0.20000	0.21000	8.15000	0.23800
151	-0.35000	0.02600	28.92000	-22.99000	-0.09000	-0.11000	0.04000	8.27000	0.34800	-0.20000	0.25000	7.51000	0.22000
152	-0.35000	0.02600	27.08000	-23.31000	-0.25000	-0.11000	0.03000	8.84000	0.37200	-0.20000	0.27000	7.23000	0.21200
153	-0.34000	0.02600	24.32000	-22.73000	0.16000	-0.10000	0.03000	9.00000	0.37900	-0.19000	0.26000	7.00000	0.20500
154	-0.32000	0.02600	21.85000	-21.07000	-0.34000	-0.08000	0.01000	9.50000	0.40000	-0.16000	0.20000	6.96000	0.20400
155	-0.31000	0.02600	24.28000	-20.33000	0.16000	-0.06000	0.01000	10.10000	0.42500	-0.17000	0.19000	7.32000	0.21400
156	-0.31000	0.02600	26.88000	-20.61000	0.17000	-0.06000	0.01000	10.91000	0.46000	-0.18000	0.20000	7.66000	0.22400
157	-0.27000	0.02600	32.17000	-18.02000	-0.19000	-0.04000	0.00000	10.75000	0.45200	-0.19000	0.19000	8.37000	0.24500
158	-0.21000	0.02600	37.31000	-14.17000	0.05000	-0.03000	0.00000	10.48000	0.44100	-0.20000	0.18000	9.27000	0.27100
159	-0.15000	0.02600	42.82000	-10.07000	-0.05000	-0.03000	0.00000	9.83000	0.41400	-0.19000	0.12000	10.62000	0.31100
160	-0.14000	0.02600	43.34000	-9.21000	0.02000	-0.05000	0.01000	9.35000	0.39400	-0.18000	0.10000	11.05000	0.32300

161	-0.24000	0.02600	39.85000	-15.67000	0.12000	-0.10000	0.03000	9.06000	0.38200	-0.19000	0.13000	10.52000	0.30800
162	-0.25000	0.02600	35.45000	-16.45000	-0.02000	-0.13000	0.06000	7.94000	0.33400	-0.19000	0.15000	9.78000	0.28600
163	-0.26000	0.02600	35.41000	-17.47000	-0.07000	-0.12000	0.06000	7.38000	0.31100	-0.19000	0.16000	9.22000	0.27000
164	-0.29000	0.02600	37.52000	-19.36000	-0.11000	-0.14000	0.08000	6.95000	0.29300	-0.22000	0.24000	8.55000	0.25000
165	-0.29000	0.02600	42.84000	-18.92000	-0.07000	-0.14000	0.06000	8.06000	0.33900	-0.24000	0.26000	8.79000	0.25700
166	-0.28000	0.02600	45.00000	-18.43000	-0.09000	-0.25000	0.28000	6.03000	0.25400	-0.26000	0.25000	9.88000	0.28900
167	-0.26000	0.02600	40.72000	-17.44000	-0.16000	-0.26000	0.40000	4.80000	0.20200	-0.23000	0.19000	10.17000	0.29700
168	-0.28000	0.02600	34.61000	-18.21000	-0.14000	-0.24000	0.46000	3.93000	0.16500	-0.18000	0.13000	9.77000	0.28600
169	-0.29000	0.02600	27.67000	-18.92000	-0.21000	-0.25000	0.67000	2.61000	0.11000	-0.21000	0.32000	6.66000	0.19500
170	-0.32000	0.02600	26.39000	-21.19000	-0.28000	-0.31000	0.80000	2.28000	0.09600	-0.26000	0.43000	6.36000	0.18600
171	-0.36000	0.02600	30.04000	-23.81000	-0.37000	-0.39000	0.83000	2.66000	0.11200	-0.32000	0.47000	7.35000	0.21500
172	-0.27000	0.02600	37.33000	-17.75000	-0.32000	-0.43000	0.48000	6.68000	0.28100	-0.36000	0.41000	9.17000	0.26800
173	-0.28000	0.02600	26.22000	-18.37000	-0.55000	-0.39000	0.65000	4.27000	0.18000	-0.29000	0.45000	6.92000	0.20200
174	-0.24000	0.02600	31.95000	-15.60000	-0.25000	-0.37000	0.59000	4.60000	0.19400	-0.21000	0.22000	8.44000	0.24700
175	-0.28000	0.02600	32.65000	-18.57000	-0.25000	-0.45000	0.48000	6.96000	0.29300	-0.26000	0.34000	7.65000	0.22400
176	-0.44000	0.02600	36.14000	-28.98000	-0.44000	-0.47000	0.73000	4.33000	0.18200	-0.31000	0.37000	8.66000	0.25300
177	-0.52000	0.02600	47.64000	-34.20000	-0.30000	-0.47000	0.80000	3.50000	0.14700	-0.32000	0.34000	9.56000	0.28000
178	-0.48000	0.02600	43.49000	-31.49000	-0.43000	-0.36000	0.73000	3.28000	0.13800	-0.29000	0.32000	9.03000	0.26400
179	-0.48000	0.02600	42.56000	-31.98000	-0.42000	-0.29000	0.34000	6.14000	0.25800	-0.31000	0.33000	9.39000	0.27500
180	-0.55000	0.02600	49.02000	-36.17000	-0.53000	-0.33000	0.34000	6.85000	0.28800	-0.36000	0.32000	11.23000	0.32800
181	-0.56000	0.02600	55.72000	-37.21000	-0.55000	-0.33000	0.31000	7.27000	0.30600	-0.38000	0.29000	12.55000	0.36700
182	-0.55000	0.02600	59.67000	-36.49000	-0.56000	-0.23000	0.10000	10.23000	0.43100	-0.32000	0.23000	12.70000	0.37100
183	-0.56000	0.02600	60.78000	-36.64000	-0.29000	-0.15000	0.03000	13.03000	0.54900	-0.28000	0.17000	13.02000	0.38100
184	-0.56000	0.02600	61.73000	-36.80000	-0.31000	-0.16000	0.03000	12.64000	0.53200	-0.26000	0.15000	13.27000	0.38800
185	-0.55000	0.02600	60.80000	-36.25000	-0.32000	-0.18000	0.06000	10.68000	0.45000	-0.25000	0.14000	13.11000	0.38400
186	-0.53000	0.02600	59.60000	-35.18000	-0.32000	-0.14000	0.03000	11.19000	0.47100	-0.24000	0.13000	12.98000	0.38000
187	-0.52000	0.02600	55.93000	-34.11000	-0.29000	-0.10000	0.02000	11.91000	0.50200	-0.22000	0.12000	12.33000	0.36100
188	-0.50000	0.02600	51.54000	-33.05000	-0.35000	-0.08000	0.01000	12.47000	0.52500	-0.21000	0.13000	11.58000	0.33900
189	-0.42000	0.02600	48.27000	-27.67000	-0.51000	-0.07000	0.01000	11.43000	0.48100	-0.23000	0.15000	11.74000	0.34400
190	-0.40000	0.02600	54.02000	-26.14000	-0.55000	-0.11000	0.02000	10.60000	0.44600	-0.29000	0.20000	12.63000	0.36900
191	-0.41000	0.02600	45.38000	-27.21000	-0.46000	-0.10000	0.02000	10.40000	0.43800	-0.24000	0.18000	11.11000	0.32500
192	-0.43000	0.02600	43.03000	-28.36000	-0.35000	-0.10000	0.02000	10.35000	0.43600	-0.19000	0.15000	9.93000	0.29000
193	-0.45000	0.02600	39.48000	-29.50000	-0.12000	-0.12000	0.03000	10.06000	0.42400	-0.17000	0.14000	9.33000	0.27300
194	-0.51000	0.02600	39.69000	-33.59000	-0.05000	-0.19000	0.10000	8.73000	0.36700	-0.20000	0.18000	9.38000	0.27400
195	-0.56000	0.02600	40.77000	-36.89000	0.07000	-0.31000	0.29000	7.14000	0.30100	-0.19000	0.13000	10.87000	0.31800
196	-0.60000	0.02600	48.30000	-39.57000	0.00000	-0.43000	0.34000	8.96000	0.37700	-0.22000	0.08000	15.59000	0.45600
197	-0.67000	0.02600	53.92000	-43.99000	-0.41000	-0.45000	0.21000	13.19000	0.55500	-0.21000	0.05000	20.69000	0.60500
198	-0.74000	0.02600	73.12000	-48.59000	1.97000	-0.58000	0.27000	14.11000	0.59400	-0.21000	0.03000	25.46000	0.74500
199	-0.87000	0.02600	91.83000	-57.21000	-0.27000	-0.69000	0.24000	18.29000	0.77000	-0.25000	0.03000	29.83000	0.87300
200	-0.92000	0.02600	60.96000	-60.96000	-0.14000	-0.54000	0.17000	18.21000	0.76700	-0.40000	0.31000	12.61000	0.36900

201	-0.90000	0.02600	59.30000	-59.30000	-0.20000	-0.51000	0.18000	16.66000	0.70200	-0.45000	0.43000	11.15000	0.32600
202	-0.83000	0.02600	54.76000	-54.76000	-0.31000	-0.49000	0.22000	13.81000	0.58100	-0.49000	0.55000	9.54000	0.27900
203	-0.70000	0.02600	46.33000	-46.33000	-0.21000	-0.46000	0.28000	10.84000	0.45600	-0.48000	0.56000	9.13000	0.26700
204	-0.77000	0.02600	50.61000	-50.61000	-0.16000	-0.50000	0.29000	11.62000	0.48900	-0.53000	0.56000	9.99000	0.29200
205	-0.83000	0.02600	54.46000	-54.46000	-0.68000	-0.60000	0.51000	8.77000	0.36900	-0.62000	0.59000	11.10000	0.32500
206	-0.73000	0.02600	48.47000	-48.09000	-0.30000	-0.50000	0.49000	7.75000	0.32600	-0.47000	0.35000	13.82000	0.40400
207	-0.62000	0.02600	56.41000	-41.12000	-0.23000	-0.43000	0.41000	7.70000	0.32400	-0.37000	0.25000	13.98000	0.40900
208	-0.53000	0.02600	34.74000	-34.74000	-0.27000	-0.37000	0.52000	5.37000	0.22600	-0.32000	0.42000	8.10000	0.23700
209	-0.54000	0.02600	35.85000	-35.85000	-0.35000	-0.41000	0.60000	5.06000	0.21300	-0.35000	0.45000	8.25000	0.24100
210	-0.56000	0.02600	37.32000	-36.97000	-0.39000	-0.44000	0.64000	4.94000	0.20800	-0.36000	0.44000	8.88000	0.26000
211	-0.59000	0.02600	40.18000	-38.64000	-0.29000	-0.44000	0.60000	5.39000	0.22700	-0.38000	0.46000	8.81000	0.25800
212	-0.64000	0.02600	42.50000	-42.12000	-0.38000	-0.43000	0.43000	7.33000	0.30900	-0.38000	0.43000	9.45000	0.27600
213	-0.67000	0.02600	44.37000	-44.37000	-0.49000	-0.40000	0.29000	9.40000	0.39600	-0.39000	0.38000	10.56000	0.30900
214	-0.70000	0.02600	46.46000	-46.46000	-0.40000	-0.37000	0.15000	13.11000	0.55200	-0.44000	0.46000	10.41000	0.30400
215	-0.56000	0.02600	37.02000	-37.02000	-0.23000	-0.17000	0.03000	13.93000	0.58700	-0.27000	0.35000	7.93000	0.23200
216	-0.47000	0.02600	31.31000	-31.31000	0.04000	-0.06000	0.00000	14.90000	0.62700	-0.15000	0.14000	7.95000	0.23200
217	-0.50000	0.02600	33.28000	-33.28000	0.07000	-0.07000	0.00000	15.54000	0.65400	-0.13000	0.09000	8.73000	0.25500
218	-0.52000	0.02600	34.09000	-34.09000	0.07000	-0.09000	0.01000	15.47000	0.65100	-0.13000	0.09000	8.90000	0.26000
219	-0.50000	0.02600	33.11000	-33.11000	0.10000	-0.08000	0.01000	15.33000	0.64500	-0.13000	0.10000	8.46000	0.24800
220	-0.49000	0.02600	32.16000	-32.16000	0.12000	-0.10000	0.01000	14.17000	0.59700	-0.15000	0.13000	8.21000	0.24000
221	-0.49000	0.02600	32.24000	-32.24000	0.18000	-0.14000	0.03000	12.84000	0.54100	-0.17000	0.16000	8.19000	0.24000
222	-0.53000	0.02600	34.76000	-34.76000	0.16000	-0.21000	0.07000	11.53000	0.48500	-0.21000	0.23000	8.14000	0.23800
223	-0.47000	0.02600	31.07000	-31.07000	0.12000	-0.25000	0.18000	7.99000	0.33600	-0.20000	0.24000	7.56000	0.22100
224	-0.40000	0.02600	26.43000	-26.15000	-0.07000	-0.23000	0.27000	5.69000	0.23900	-0.16000	0.20000	6.94000	0.20300
225	-0.41000	0.02600	26.96000	-26.96000	-0.04000	-0.23000	0.27000	5.59000	0.23500	-0.17000	0.23000	6.70000	0.19600
226	-0.43000	0.02600	28.39000	-28.39000	0.09000	-0.23000	0.23000	6.26000	0.26400	-0.18000	0.25000	6.84000	0.20000
227	-0.46000	0.02600	30.29000	-30.29000	0.09000	-0.24000	0.25000	6.27000	0.26400	-0.18000	0.22000	7.54000	0.22100
228	-0.44000	0.02600	29.01000	-29.01000	-0.02000	-0.29000	0.58000	3.68000	0.15500	-0.19000	0.25000	7.07000	0.20700
229	-0.53000	0.02600	34.89000	-34.89000	-0.47000	-0.34000	0.45000	5.64000	0.23700	-0.27000	0.35000	7.86000	0.23000
230	-0.61000	0.02600	40.46000	-39.94000	-0.32000	-0.43000	0.52000	6.23000	0.26200	-0.37000	0.43000	9.10000	0.26600
231	-0.65000	0.02600	42.90000	-42.90000	-0.30000	-0.47000	0.72000	4.38000	0.18400	-0.39000	0.49000	8.55000	0.25000
232	-0.67000	0.02600	44.16000	-44.16000	-0.68000	-0.48000	0.74000	4.25000	0.17900	-0.40000	0.52000	8.27000	0.24200
233	-0.77000	0.02600	50.94000	-50.94000	-0.18000	-0.53000	0.65000	5.79000	0.24400	-0.44000	0.56000	8.50000	0.24900
234	-0.74000	0.02600	48.91000	-48.91000	-0.37000	-0.57000	0.76000	4.77000	0.20100	-0.45000	0.57000	8.43000	0.24700
235	-0.64000	0.02600	42.33000	-42.33000	-0.65000	-0.47000	0.65000	5.17000	0.21800	-0.35000	0.47000	8.18000	0.23900
236	-0.58000	0.02600	38.49000	-38.49000	-0.51000	-0.41000	0.64000	4.56000	0.19200	-0.32000	0.41000	8.18000	0.23900
237	-0.56000	0.02600	36.83000	-36.83000	-0.49000	-0.38000	0.61000	4.52000	0.19000	-0.30000	0.38000	8.17000	0.23900
238	-0.42000	0.02600	27.73000	-27.73000	-0.09000	-0.27000	0.41000	4.83000	0.20300	-0.24000	0.36000	6.74000	0.19700
239	-0.62000	0.02600	41.18000	-41.18000	-0.58000	-0.40000	0.56000	5.23000	0.22000	-0.36000	0.51000	7.55000	0.22100
240	-0.77000	0.02600	50.80000	-50.80000	-0.37000	-0.51000	0.66000	5.54000	0.23300	-0.51000	0.66000	7.87000	0.23000

241	-0.80000	0.02600	52.67000	-52.67000	-0.65000	-0.50000	0.48000	7.89000	0.33200	-0.57000	0.64000	9.17000	0.26800
242	-0.76000	0.02600	49.93000	-49.93000	-0.81000	-0.47000	0.42000	8.25000	0.34700	-0.54000	0.71000	7.37000	0.21500
243	-0.71000	0.02600	46.76000	-46.76000	-0.60000	-0.37000	0.16000	12.90000	0.54300	-0.42000	0.51000	8.83000	0.25800
244	-0.62000	0.02600	40.71000	-40.71000	-0.14000	-0.33000	0.28000	8.03000	0.33800	-0.29000	0.27000	10.20000	0.29800
245	-0.59000	0.02600	38.62000	-38.62000	-0.58000	-0.34000	0.39000	6.24000	0.26300	-0.25000	0.25000	9.22000	0.27000
246	-0.57000	0.02600	37.86000	-37.86000	-0.10000	-0.36000	0.58000	4.58000	0.19300	-0.29000	0.36000	8.22000	0.24000
247	-0.59000	0.02600	38.86000	-38.86000	-0.51000	-0.39000	0.67000	4.08000	0.17200	-0.34000	0.52000	7.02000	0.20500
248	-0.62000	0.02600	40.91000	-40.91000	-0.18000	-0.42000	0.68000	4.23000	0.17800	-0.36000	0.56000	6.75000	0.19800
249	-0.63000	0.02600	41.65000	-41.65000	-0.58000	-0.37000	0.41000	6.64000	0.28000	-0.26000	0.27000	9.23000	0.27000
250	-0.64000	0.02600	41.91000	-41.91000	-0.34000	-0.40000	0.52000	5.76000	0.24300	-0.30000	0.34000	8.84000	0.25900
251	-0.66000	0.02600	43.87000	-43.87000	-0.53000	-0.44000	0.47000	6.99000	0.29400	-0.30000	0.32000	9.41000	0.27500
252	-0.30000	0.07200	16.18000	-11.51000	-0.30000	-0.29000	0.87000	1.57000	1.41500	-0.37000	0.77000	5.60000	2.53100
Minimum	-1.86000	0.02600	0.06000	-122.43000	-2.37000	-1.30000	0.00000	1.57000	0.09600	-1.38000	0.00000	5.60000	0.18600
Maximum	0.00000	0.35400	182.12000	-0.06000	1.97000	0.16000	0.87000	42.89000	1.80600	0.19000	0.77000	45.10000	2.53100
Average	-0.59337	0.02748	74.30143	-39.09972	-0.50163	-0.31020	0.16888	17.65068	0.74913	-0.53315	0.27952	18.73773	0.55798

Table 8: DSAS statistics for Pringle Bay.

TransectId	EPR	ECI	SCE	NSM	LMS	WLR	WR2	WSE	WCI95	LRR	LR2	LSE	LCI95
1	0.07000	0.08300	17.82000	3.43000	0.07000	-0.07000	0.09000	1.65000	0.24700	-0.05000	0.02000	6.14000	0.40400
2	0.32000	0.08300	18.94000	15.61000	0.32000	0.31000	0.67000	1.68000	0.25200	0.16000	0.16000	6.45000	0.42400
3	0.34000	0.08300	18.55000	16.54000	-0.05000	0.37000	0.77000	1.56000	0.23400	0.19000	0.24000	6.06000	0.39800
4	0.24000	0.08300	17.99000	11.53000	-0.23000	0.30000	0.64000	1.70000	0.25600	0.11000	0.07000	6.91000	0.45400
5	0.21000	0.08300	18.23000	10.24000	-0.02000	0.24000	0.69000	1.23000	0.18500	0.13000	0.11000	6.19000	0.40700
6	0.31000	0.08300	20.24000	14.93000	-0.02000	0.36000	0.70000	1.79000	0.27000	0.20000	0.17000	7.49000	0.49200
7	0.23000	0.08300	13.91000	11.08000	0.00000	0.19000	0.45000	1.61000	0.24300	0.12000	0.10000	6.07000	0.39900
8	0.26000	0.08300	15.86000	12.87000	0.05000	0.26000	0.58000	1.68000	0.25300	0.15000	0.14000	6.72000	0.44200
9	0.26000	0.08300	14.95000	12.75000	-0.70000	0.17000	0.38000	1.62000	0.24300	0.07000	0.03000	6.73000	0.44200
10	0.40000	0.08300	20.81000	19.27000	-0.02000	0.54000	0.84000	1.81000	0.27200	0.29000	0.39000	6.22000	0.40900
11	0.26000	0.08300	21.62000	12.50000	-0.23000	0.47000	0.71000	2.27000	0.34100	0.16000	0.12000	7.47000	0.49100
12	0.23000	0.08300	38.51000	11.06000	-0.70000	0.61000	0.55000	4.22000	0.63500	0.03000	0.00000	14.15000	0.93000
13	-0.06000	0.08300	92.17000	-2.81000	-0.05000	-0.14000	0.03000	6.40000	0.96100	-0.54000	0.09000	30.99000	2.03700
14	-0.42000	0.08300	97.23000	-20.24000	-0.53000	-0.68000	0.45000	5.82000	0.87500	-0.97000	0.24000	29.89000	1.96500
15	-1.01000	0.08300	115.32000	-49.11000	-1.29000	-1.48000	0.75000	6.47000	0.97200	-1.67000	0.43000	33.83000	2.22400
16	-0.86000	0.08300	111.07000	-41.75000	-1.07000	-1.37000	0.72000	6.58000	0.98800	-1.50000	0.38000	33.55000	2.20600
17	-0.89000	0.08300	110.12000	-43.26000	-1.15000	-1.33000	0.71000	6.44000	0.96700	-1.55000	0.42000	31.83000	2.09200
18	-1.82000	0.08300	114.18000	-88.59000	-2.76000	-1.69000	0.82000	6.01000	0.90300	-2.32000	0.70000	26.50000	1.74200
19	-2.06000	0.08300	114.91000	-100.08000	-2.75000	-1.75000	0.81000	6.49000	0.97500	-2.45000	0.76000	24.39000	1.60300
20	-2.10000	0.08300	123.10000	-102.00000	-2.46000	-1.76000	0.81000	6.52000	0.98000	-2.50000	0.77000	23.88000	1.57000
21	-2.22000	0.08300	134.32000	-108.23000	-2.59000	-1.86000	0.84000	6.14000	0.92200	-2.60000	0.81000	22.34000	1.46800
22	-2.30000	0.08300	139.64000	-112.00000	-2.23000	-2.02000	0.83000	7.04000	1.05700	-2.81000	0.77000	27.23000	1.79000
23	-1.93000	0.08300	136.26000	-93.74000	-1.89000	-1.83000	0.80000	6.95000	1.04400	-2.54000	0.71000	28.51000	1.87400
24	-1.89000	0.08300	138.28000	-92.09000	-2.76000	-1.74000	0.76000	7.50000	1.12800	-2.57000	0.66000	32.06000	2.10800
25	-2.17000	0.08300	141.60000	-105.43000	-2.75000	-1.84000	0.75000	8.17000	1.22700	-2.80000	0.69000	33.11000	2.17600
26	-2.28000	0.08300	115.15000	-110.85000	-1.33000	-1.96000	0.81000	7.19000	1.08100	-2.64000	0.69000	30.82000	2.02600
27	-2.28000	0.08300	115.61000	-111.19000	-1.43000	-1.93000	0.83000	6.60000	0.99200	-2.63000	0.73000	27.69000	1.82000
28	-2.17000	0.08300	117.30000	-105.66000	-1.33000	-1.93000	0.83000	6.66000	1.00100	-2.60000	0.71000	28.82000	1.89500
29	-1.53000	0.08300	118.21000	-74.36000	-1.97000	-1.65000	0.78000	6.67000	1.00200	-2.09000	0.57000	31.43000	2.06600
30	-1.52000	0.08300	122.18000	-73.87000	-1.53000	-1.84000	0.81000	6.72000	1.01000	-1.92000	0.41000	40.11000	2.63700
31	-1.58000	0.08300	125.56000	-76.74000	-1.67000	-1.91000	0.82000	6.73000	1.01100	-1.96000	0.45000	37.58000	2.47000
32	-2.45000	0.08300	127.55000	-119.15000	-1.81000	-2.31000	0.89000	6.34000	0.95300	-2.82000	0.76000	27.60000	1.81400
33	-2.46000	0.08300	119.85000	-119.85000	-1.74000	-2.25000	0.90000	5.83000	0.87700	-2.80000	0.80000	24.36000	1.60100
34	-1.88000	0.08300	106.48000	-91.29000	-1.74000	-1.91000	0.90000	4.83000	0.72600	-2.23000	0.78000	20.95000	1.37700
35	-1.21000	0.08300	108.66000	-58.81000	-1.38000	-1.68000	0.83000	5.76000	0.86500	-1.69000	0.55000	26.89000	1.76800

36	-1.45000	0.08300	114.22000	-70.47000	-1.67000	-1.83000	0.85000	5.76000	0.86500	-1.89000	0.57000	28.35000	1.86300
37	-1.97000	0.08300	127.36000	-95.86000	-1.87000	-2.09000	0.86000	6.54000	0.98300	-2.33000	0.62000	31.95000	2.10000
38	-2.64000	0.08300	128.63000	-128.63000	-2.62000	-2.37000	0.87000	7.15000	1.07400	-2.84000	0.71000	32.07000	2.10800
39	-2.53000	0.08300	123.23000	-123.23000	-2.49000	-2.28000	0.87000	6.69000	1.00500	-2.70000	0.68000	32.53000	2.13800
40	-1.54000	0.08300	118.23000	-74.88000	-1.43000	-1.79000	0.81000	6.53000	0.98100	-1.86000	0.44000	36.98000	2.43100
41	-2.04000	0.08300	118.26000	-99.15000	-2.04000	-2.04000	0.86000	6.27000	0.94200	-2.33000	0.58000	34.43000	2.26300
42	-2.36000	0.08300	117.45000	-114.76000	-2.36000	-2.10000	0.86000	6.51000	0.97800	-2.58000	0.67000	31.79000	2.09000
43	-2.38000	0.08300	116.06000	-116.06000	-2.92000	-2.08000	0.87000	6.08000	0.91300	-2.49000	0.73000	26.80000	1.76100
44	-2.45000	0.08300	119.03000	-119.03000	-2.46000	-2.23000	0.91000	5.43000	0.81600	-2.51000	0.79000	22.91000	1.50600
45	-2.33000	0.08300	113.46000	-113.46000	-3.25000	-2.19000	0.90000	5.53000	0.83100	-2.39000	0.76000	23.28000	1.53000
46	-2.06000	0.08300	117.98000	-100.05000	-1.89000	-2.17000	0.90000	5.42000	0.81500	-2.24000	0.72000	24.29000	1.59600
47	-2.54000	0.08300	123.66000	-123.66000	-2.59000	-2.35000	0.90000	5.98000	0.89800	-2.63000	0.75000	26.61000	1.74900
48	-2.36000	0.08300	120.82000	-114.86000	-1.55000	-2.24000	0.89000	6.04000	0.90700	-2.48000	0.73000	26.56000	1.74600
49	-1.37000	0.08300	103.38000	-66.66000	-1.61000	-1.73000	0.87000	5.19000	0.78000	-1.55000	0.56000	24.05000	1.58100
50	-1.12000	0.08300	55.72000	-54.61000	-1.67000	-1.38000	0.93000	2.90000	0.43600	-1.04000	0.73000	10.95000	0.72000
51	-0.95000	0.08300	54.44000	-46.30000	-0.81000	-1.04000	0.91000	2.42000	0.36300	-0.97000	0.74000	10.04000	0.66000
52	-1.63000	0.08300	79.49000	-79.49000	-0.70000	-1.20000	0.81000	4.37000	0.65700	-1.66000	0.79000	14.89000	0.97800
Minimum	-2.64000	0.08300	13.91000	-128.63000	-3.25000	-2.37000	0.03000	1.23000	0.18500	-2.84000	0.00000	6.06000	0.39800
Maximum	0.40000	0.08300	141.60000	19.27000	0.32000	0.61000	0.93000	8.17000	1.22700	0.29000	0.81000	40.11000	2.63700
Average	-1.34000	0.08300	92.95385	-65.20096	-1.45519	-1.31192	0.75808	5.14404	0.77292	-1.63712	0.51923	23.06615	1.51617

APPENDIX B: ERROR MATRICES

The six Landsat 5 TM and Landsat 7 ETM+ images were classified using an object-based classification. An accuracy assessment was then performed. The error matrices describing the accuracy of each classification are given in this appendix.

Table 9: The error matrix based on the classification for 1985.

User/reference class	Ocean	Mountain	Mountain shadow	Beach	Sand (not beach)	Natural	Shallow coastal	Dams	Cultivated	Built-up	Sand dunes	Sum
Confusion Matrix												0
Ocean	108437	0	59	0	0	0	9	0	0	0	0	108505
Mountain	0	13537	476	0	48	0	0	0	1277	164	0	15502
Mountain shadow	138	658	8266	0	0	410	0	0	1282	0	0	10754
Beach	0	0	0	4256	417	378	304	0	0	244	88	5687
Sand (not beach)	0	141	0	123	3329	74	0	0	55	740	431	4893
Natural	16	0	542	21	0	13632	8	158	928	738	1557	17600
Shallow coastal	51	0	0	0	0	57	7050	0	0	0	0	7158
Dams	306	0	239	0	20	0	0	13668	46	0	0	14279
Cultivated	0	879	187	0	49	1324	0	0	12864	1000	0	16303
Built-up	0	215	0	212	37	2024	0	0	1727	12853	745	17813
Sand dune	0	0	0	0	222	2813	0	0	1416	1493	9570	15514
Unclassified	0	0	0	0	0	0	0	0	0	0	0	0
Sum	108948	15430	9769	4612	4122	20712	7371	13826	19595	17232	12391	
Accuracy												
Producer	0.99531	0.87732	0.84615	0.92281	0.8076177	0.65817	0.95645	0.98857	0.656494	0.74588	0.77233	
User	0.99937	0.87324	0.76864	0.74837	0.6803597	0.77455	0.98491	0.95721	0.789057	0.72155	0.61686	
KIA per class	0.99125	0.86861	0.83873	0.92089	0.8035091	0.63037	0.955	0.98783	0.63077	0.725	0.75617	
Totals												
Overall Accuracy	**0.88656**											
KIA	**0.849**											

Table 10: The error matrix based on the classification for 1991.

User/reference class	Ocean	Mountain	Mountain shadow	Beach	Sand (not beach)	Natural	Shallow coastal	Dams	Cultivated	Built-up	Sand dunes	Sum
Confusion Matrix												
Ocean	81594	0	0	0	0	0	0	0	0	0	0	81594
Mountain	0	9870	1263	0	0	0	0	0	1088	301	0	12522
Mountain shadow	22	166	11226	0	0	447	0	0	520	0	475	12856
Beach	0	0	0	3578	741	0	208	0	0	135	50	4712
Sand (not beach)	0	263	0	356	4331	32	218	0	292	477	87	6056
Natural	61	0	0	0	0	13497	205	0	861	1059	634	16317
Shallow coastal	0	0	0	261	0	0	4898	0	0	0	0	5159
Dams	993	84	2350	126	0	34	132	8326	87	16	160	12308
Cultivated	0	970	72	0	0	2305	0	0	13620	2163	325	19455
Built-up	0	221	0	52	347	1127	0	0	2205	16308	840	21100
Sand dunes	0	575	0	88	62	307	0	0	1967	2888	8078	13965
Unclassified	0	0	0	0	0	0	0	0	0	0	0	0
Sum	82670	12149	14911	4461	5481	17749	5661	8326	20640	23347	10649	
Accuracy												
Producer	0.98698	0.81241	0.75287	0.80206	0.7901843	0.76044	0.86522	1	0.659884	0.69851	0.75857	
User	1	0.78821	0.87321	0.75934	0.7151585	0.82717	0.94941	0.67647	0.700077	0.77289	0.57845	
KIA per class	0.97845	0.80027	0.73642	0.79743	0.7838307	0.73983	0.86176	1	0.624421	0.66411	0.741	
Totals												
Overall Accuracy	**0.851**											
KIA	**0.813**											

Table 11: The error matrix based on the classification for 1996.

User/reference class	Ocean	Mountain	Mountain shadow	Beach	Sand (not beach)	Natural	Shallow coastal	Dams	Cultivated	Built-up	Sand dune	Sum
Confusion Matrix												
Ocean	107486	0	47	0	0	0	147	144	0	0	0	107824
Mountain	0	9200	1343	0	0	0	0	0	1060	141	0	11744
Mountain shadow	52	1798	10565	0	0	168	0	0	329	162	149	13223
Beach	0	0	0	3717	386	0	26	0	0	172	55	4356
Sand (not beach)	0	255	0	133	4501	0	6	0	284	810	0	5989
Natural	0	0	160	0	0	16231	0	13	2608	2269	200	21481
Shallow coastal	510	0	0	0	0	0	7730	0	0	22	0	8262
Dams	411	0	1701	0	0	203	0	8862	860	1	0	12038
Cultivated	0	1303	924	0	0	2055	0	0	9849	904	38	15073
Built-up	0	582	20	44	422	862	260	0	823	17531	446	20990
Sand dune	0	731	588	0	0	2476	0	0	1773	1771	7473	14812
Unclassified	0	0	0	0	0	0	0	0	0	0	0	0
Sum	108459	13869	15348	3894	5309	21995	8169	9019	17586	23783	8361	
Accuracy												
Producer	0.99103	0.66335	0.68836	0.95455	0.8478056	0.73794	0.94626	0.98259	0.560048	0.73712	0.89379	
User	0.99687	0.783379	0.79899	0.85331	0.7515445	0.7556	0.93561	0.73617	0.65342	0.83521	0.50452	
KIA per class	0.98347	0.645704	0.66985	0.95369	0.8438392	0.71167	0.94431	0.98166	0.53	0.71144	0.88667	
Totals												
Overall Accuracy	**0.86154**											
KIA	**0.81651**											

Table 12: The error matrix based on the classification for 2001.

User/reference class	Ocean	Mountain	Mountain shadow	Beach	Sand (not beach)	Natural	Shallow coastal	Dams	Cultivated	Built-up	Sand dune	Sum
Confusion Matrix												
Ocean	102073	0	266	0	0	0	0	0	0	0	0	102339
Mountain	0	12295	255	0	0	0	0	0	672	0	0	13222
Mountain shadow	163	613	8382	0	0	879	0	0	471	166	0	10674
Beach	0	32	0	4771	371	280	151	0	0	125	0	5730
Sand (not beach)	0	46	0	165	5056	218	0	0	36	328	185	6034
Natural	18	0	0	0	0	16411	57	0	417	295	685	17883
Shallow coastal	2504	0	0	0	0	0	4288	0	0	0	0	6792
Dams	28	0	806	0	0	643	94	8387	243	416	215	10832
Cultivated	0	488	0	0	62	1136	0	0	13989	205	637	16517
Built-up	0	345	0	41	306	1652	0	0	916	18169	1079	22508
Sand dune	0	1145	155	0	90	2861	0	0	2700	2855	9141	18947
Unclassified	0	0	0	0	0	0	0	0	0	0	0	0
Sum	104786	14964	9864	4977	5885	24080	4590	8387	19444	22559	11942	
Accuracy												
Producer	0.97411	0.82164	0.849757	0.95861	0.8591334	0.68152	0.9342	1	0.719451	0.8054	0.76545	
User	0.9974	0.92989	0.785273	0.83264	0.8379185	0.91769	0.63133	0.77428	0.846946	0.80722	0.48245	
KIA per class	0.95359	0.81083	0.842494	0.95756	0.8553631	0.65486	0.93222	1	0.697894	0.78444	0.74454	
Totals												
Overall Accuracy	**0.87681**											
KIA	**0.83855**											

Table 13: The error matrix based on the classification for 2006.

User/reference class	Ocean	Mountain	Mountain shadow	Beach	Sand (not beach)	Natural	Shallow coastal	Dams	Cultivated	Built-up	Sand dune	Sum
Confusion Matrix												
Ocean	88902	0	303	0	0	0	0	0	0	0	0	89205
Mountain	0	13438	291	0	0	0	0	0	1254	0	0	14983
Mountain shadow	173	682	8500	0	0	497	0	141	1474	0	0	11467
Beach	0	0	0	3169	190	29	354	0	0	183	0	3925
Sand (not beach)	0	0	0	233	2928	89	0	0	0	1559	478	5287
Natural	0	0	0	0	38	17118	0	34	1064	1677	1373	21304
Shallow coastal	147	0	0	37	0	208	6072	0	0	43	0	6507
Dams	258	0	1459	0	0	376	204	9228	390	0	0	11915
Cultivated	0	1347	0	0	159	1050	0	0	10388	1806	604	15354
Built-up	0	66	0	195	305	1279	0	0	582	19310	1706	23443
Sand dune	0	821	0	0	275	3133	0	95	1208	517	8195	14244
Unclassified	0	0	0	0	0	0	0	0	0	0	0	0
Sum	89480	16354	10553	3634	3895	23779	6630	9498	16360	25095	12356	
Accuracy												
Producer	0.99354	0.82169	0.80546	0.87204	0.751733	0.71988	0.91584	0.97157	0.634963	0.76948	0.66324	
User	0.9966	0.89688	0.74126	0.80739	0.5538112	0.80351	0.93315	0.77449	0.676566	0.8237	0.57533	
KIA per class	0.989	0.80851	0.79464	0.86969	0.7455517	0.68948	0.91324	0.97	0.607255	0.74165	0.63966	
Totals												
Overall Accuracy	**0.86038**											
KIA	**0.82272**											

Table 14: The error matrix based on the classification for 2011.

User/reference class	Ocean	Mountain	Mountain Shadow	Beach	Sand (not beach)	Natural	Shallow coastal	Dams	Cultivated	Built-up	Sand dune	Sum
Confusion Matrix												
Ocean	92278	0	0	0	0	0	0	0	0	0	0	92278
Mountain	0	15028	103	0	26	0	0	0	889	437	0	16483
Mountain Shadow	0	1495	8489	0	0	226	0	0	212	0	68	10490
Beach	0	0	0	5042	356	38	156	0	0	0	152	5744
Sand (not beach)	0	111	0	82	3634	0	0	0	279	248	143	4497
Natural	0	0	215	0	0	13714	33	87	2313	1594	655	18611
Shallow coastal	841	0	104	227	0	0	9819	0	0	190	0	11181
Dams	0	0	971	0	0	216	0	9192	179	558	0	11116
Cultivated	0	1114	0	0	0	2670	0	0	10744	2106	178	16812
Built-up	168	0	0	0	250	1648	0	49	1726	20061	397	24299
Sand dune	0	150	0	0	103	3264	0	0	1158	2134	6582	13391
Unclassified	0	0	0	0	0	0	0	0	0	0	0	0
Sum	93287	17898	9882	5351	4369	21776	10008	9328	17500	27328	8175	
Accuracy												
Producer	0.98918	0.83965	0.85904	0.94225	0.8317693	0.62978	0.98112	0.98542	0.613943	0.73408	0.80514	
User	1	0.91173	0.80925	0.87779	0.8080943	0.73688	0.87819	0.82692	0.639067	0.82559	0.49152	
KIA per class	0.98166	0.827	0.85214	0.94074	0.8283368	0.59638	0.98013	0.98466	0.582753	0.70187	0.7928	
Totals												
Overall Accuracy	**0.86519**											
KIA	**0.82882**											

APPENDIX C: TASSELLED CAP TRANSFORMATIONS

The six Landsat 5 TM and Landsat 7 ETM+ images were all transformed using a tasselled cap transformation in order to concentrate more of the important data from all the bands into fewer bands. The tasselled cap transformation results in 3 bands, representing brightness, greenness, and wetness. The brightness bands obtained were used for image differencing, as shown in the as explained in Section 3.6.2 and shown in Section 4.4. This appendix shows the tasselled cap transformed images both as RGB representations of the brightness, greenness, and wetness bands (RGB = brightness, greenness, wetness), and greyscale representations of the brightness band only.

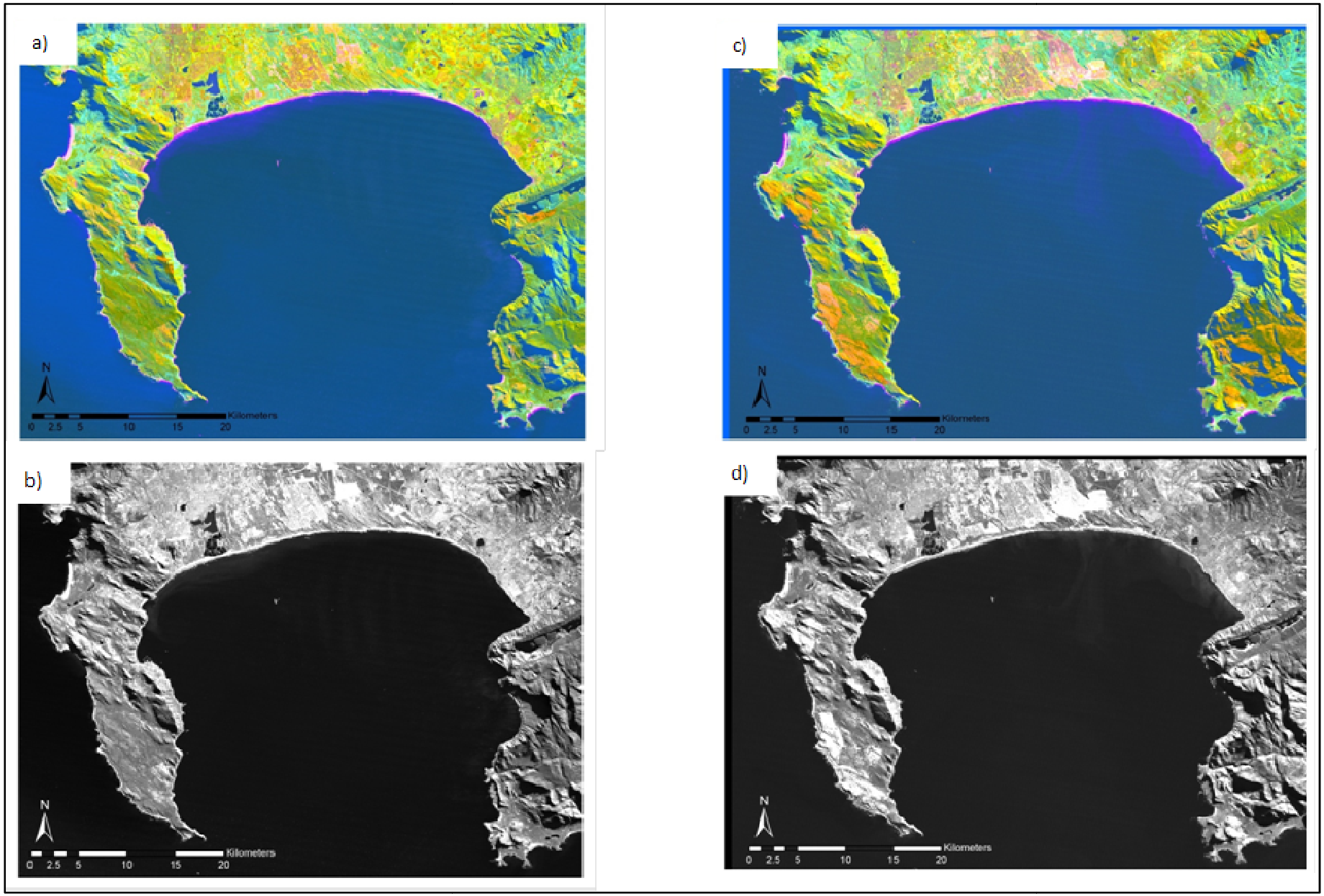

Figure 73: Tasselled cap transformations. a) RGB image showing the three bands of the tasselled cap transformation for 1985 (RGB = brightness, greenness, wetness); b) Greyscale image showing the brightness band for 1985; c) RGB image showing the three bands of the tasselled cap transformation for 1991 (RGB = brightness, greenness, wetness); d) Greyscale image showing just the brightness band for 1991.

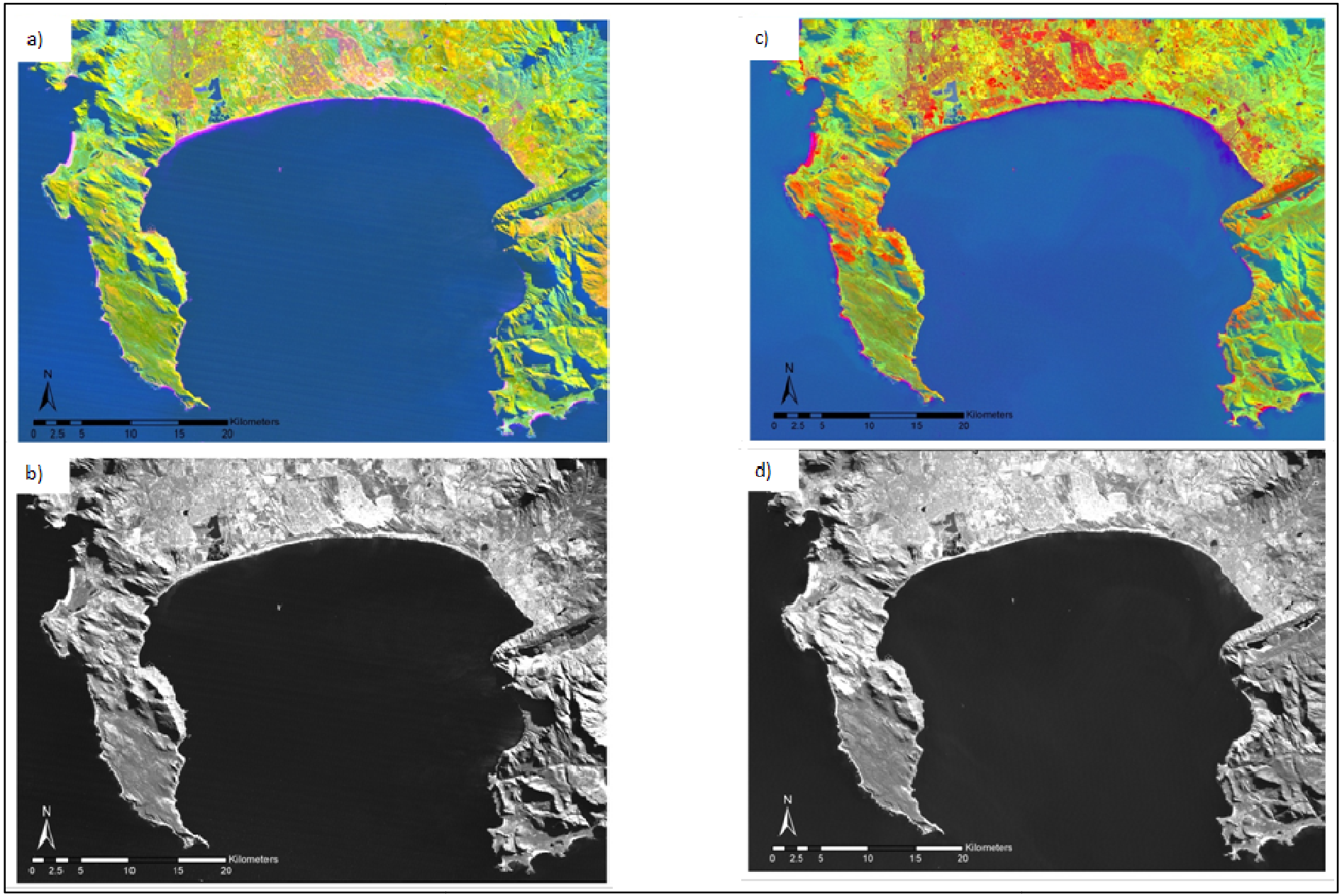

Figure 74: Tasselled cap transformations. a) RGB image showing the three bands of the tasselled cap transformation for 1996 (RGB = brightness, greenness, wetness); b) Greyscale image showing the brightness band for 1996; c) RGB image showing the three bands of the tasselled cap transformation for 2001 (RGB = brightness, greenness, wetness); d) Greyscale image showing just the brightness band for 2001.

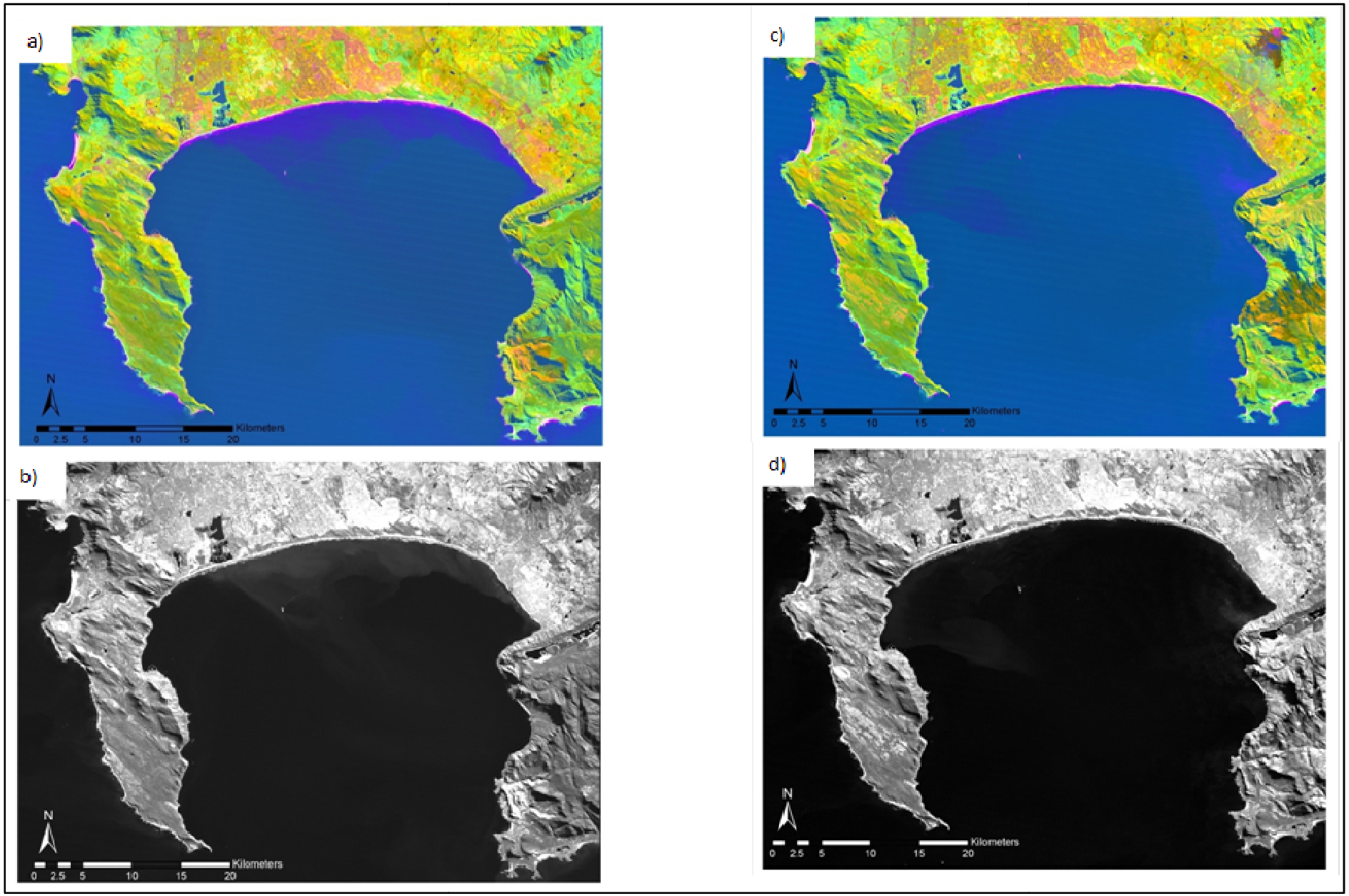

Figure 75:Tasselled cap transformations. a) RGB image showing the three bands of the tasselled cap transformation for 2006 (RGB = brightness, greenness, wetness); b) Greyscale image showing the brightness band for 2006; c) RGB image showing the three bands of the tasselled cap transformation for 2011 (RGB = brightness, greenness, wetness); d) Greyscale image showing just the brightness band for 2011.

APPENDIX D: POST-CLASSIFICATION CHANGE DETECTION

The six classified images given in Section 4.1 were used for post-classification change detection. Use of all 11 classes when performing the post-classification change detection made images overly busy and difficult to interpret. These images using all 11 classes are given below. The colours used indicate only to which class the segment had changed at the final date. Images using only a few of the more significant classes are given in Section 4.3, and are easier to interpret.

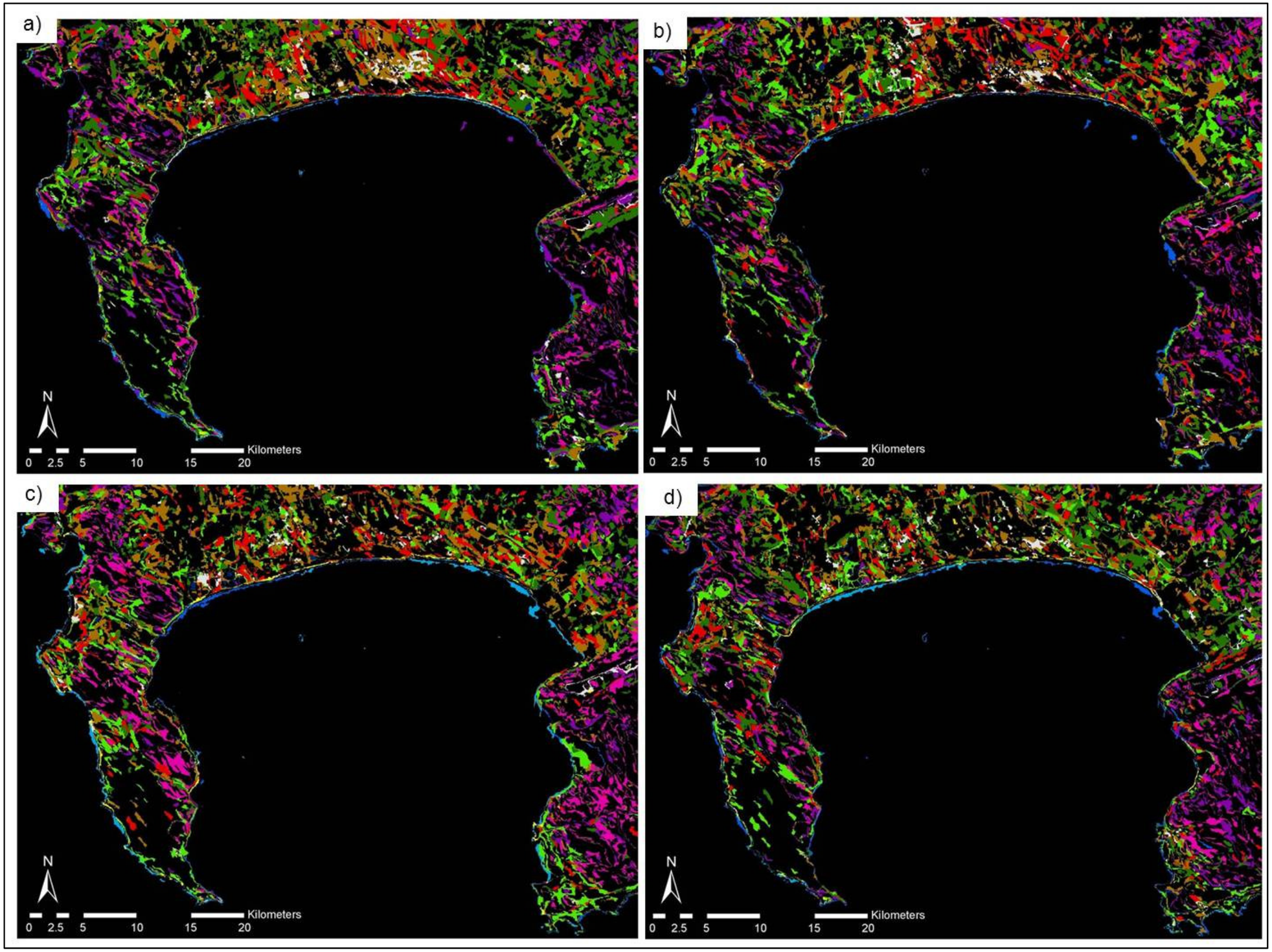

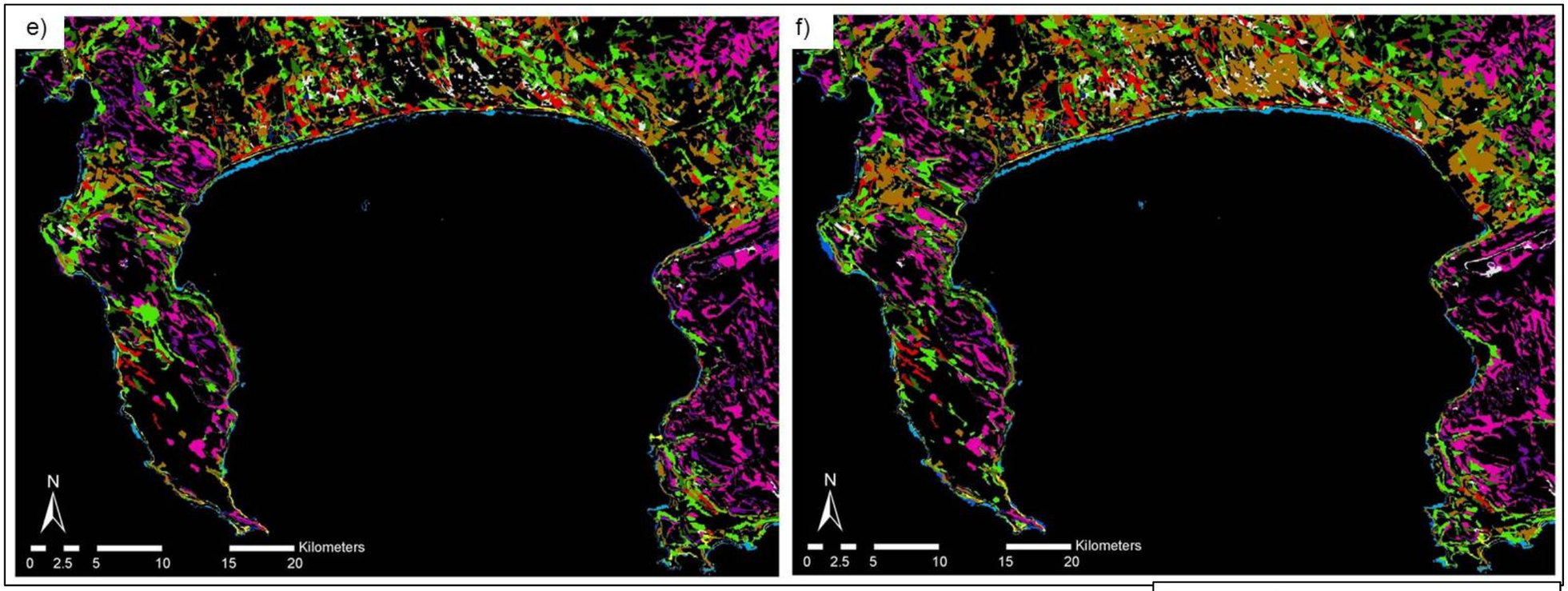

Figure 76: The total change for all classes present between the classified images from a) 1985 to 1991; b) 1991 to 1996; c) 1996 to 2001; d) 2001 to 2006; e) 2006 to 2011; and f) 1985 to 2011. The colours used indicate the class to which the regions have changed at the second date.

APPENDIX E: NDVI IMAGES

As discussed in Section 3.5.1, NDVI images were created for use in this study in order to assess vegetation changes. These images were segmented according to a method followed by Hayes and Sader (2001), who classified segmented NDVI images from low to high prior to change detection. The images in this appendix show the classified NDVI images for each date. They were used for change detection, the results of which are shown in Section 4.5.

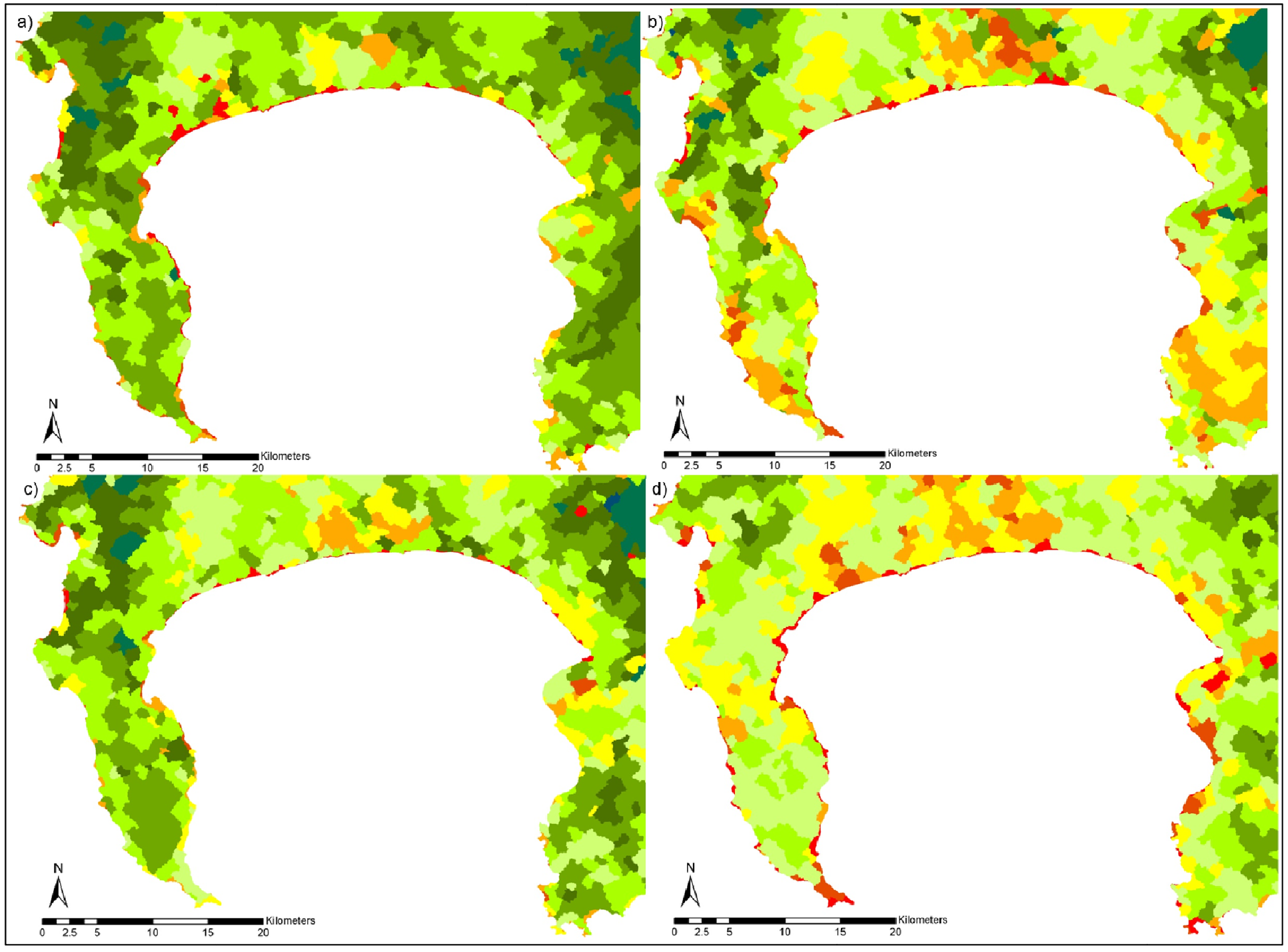

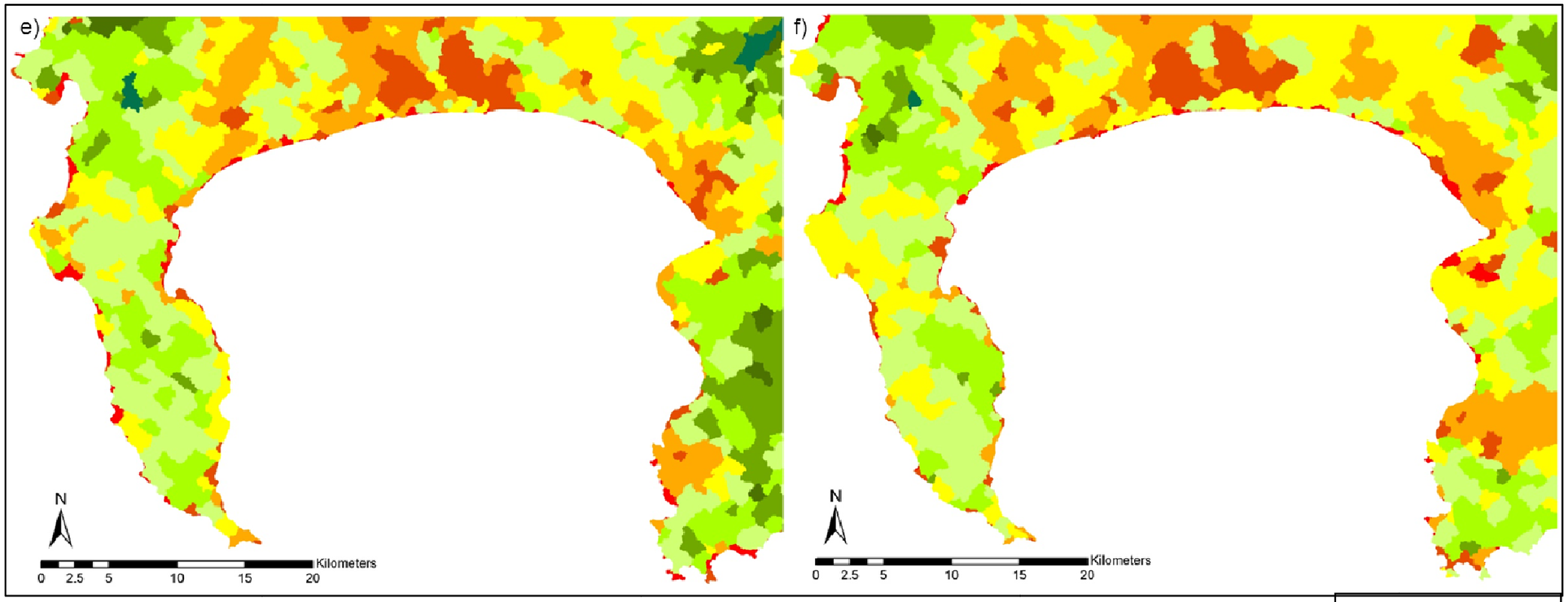

Figure 77: The NDVI shown from low (red) to high (green) as calculated for each study date: a) 1985; b) 1991; c) 1996; d) 2001; e) 2006; f) 2011.

APPENDIX F: RASTER COLOUR SLICES

As discussed in Section 3.5.3, raster colour slices were created in an attempt to define the coastline through binary slicing. This appendix shows the resulting images, with one slice representing land and the other representing ocean. The image for 2011 indicates a 'land' area extending into actual ocean just to the south-east of Strand. Such an error provides uncertainty as to how precisely the coastline is defined in other areas. These images were used for change detection, the results of which are shown in Section 4.6.

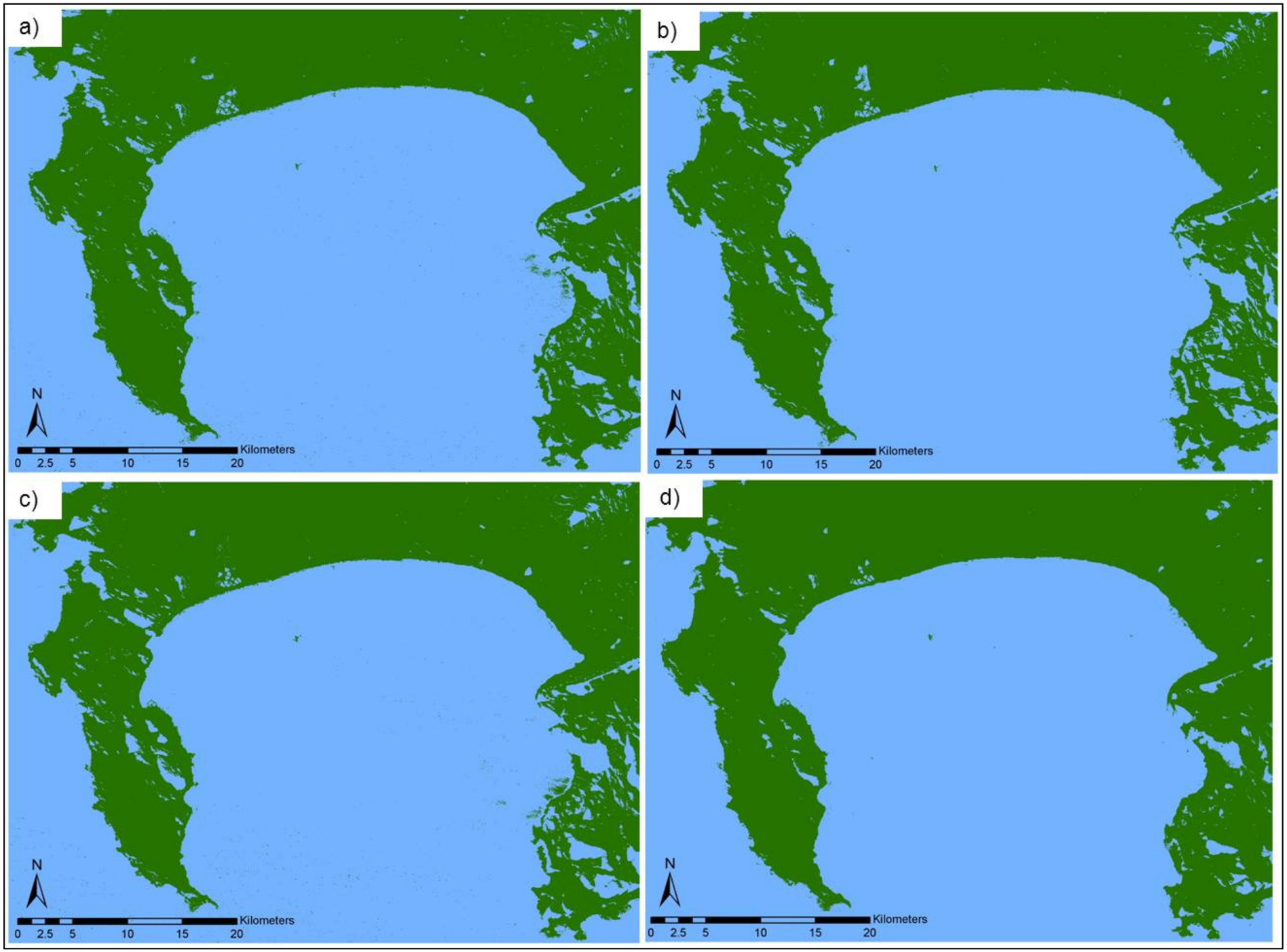

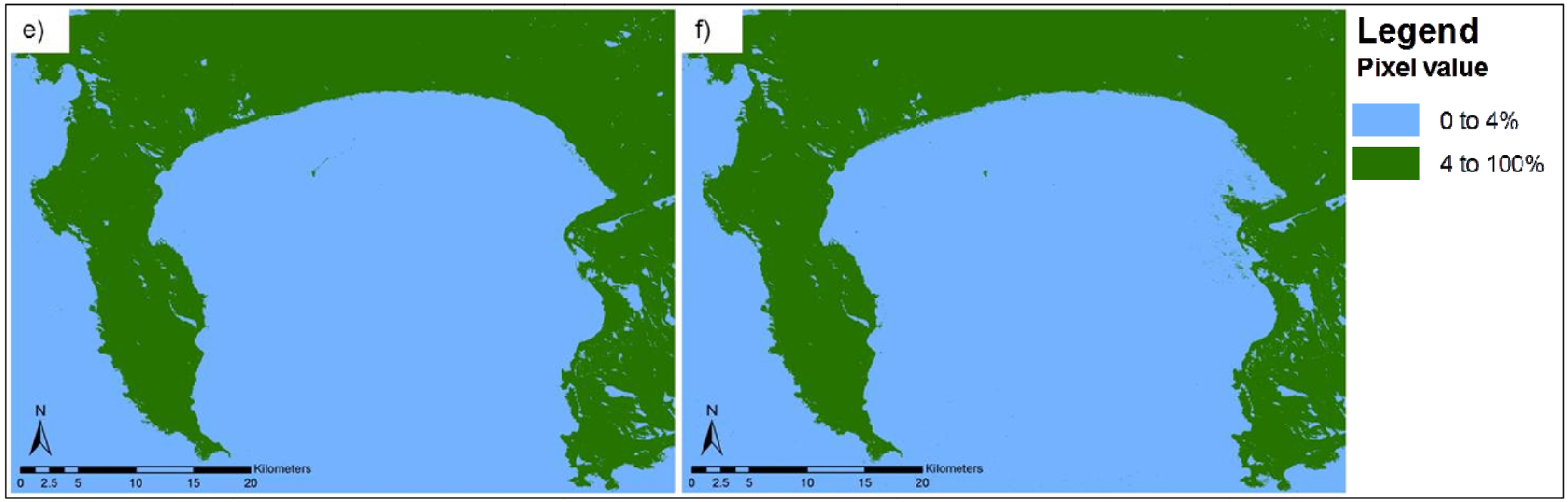

Figure 78: The binary slicing images for a) 1985, b) 1991, c) 1996, d) 2001, e) 2006, and f) 2011.